2001

The use of conducting polymer sensors for environmental monitoring

Roderick L. Shepherd
University of Wollongong

THE USE OF CONDUCTING POLYMER SENSORS FOR ENVIRONMENTAL MONITORING

A thesis submitted in fulfilment of the requirements
for the award of the degree

DOCTOR OF PHILOSOPHY

from

UNIVERSITY OF WOLLONGONG

by

Roderick L. Shepherd
BEnvSc(Hons)

Department of Chemistry
2001

DECLARATION

I, Roderick L. Shepherd, declare that this thesis, submitted in fulfilment of the requirements for the award of Doctor of Philosophy, in the Department of Chemistry, University of Wollongong, is wholly my own work unless otherwise referenced or acknowledged. The document has not been submitted for qualifications at any other academic institution.

Roderick L. Shepherd

15 October 2001

PUBLICATIONS

Shepherd, R.L., Barisci, J.N., Collier, W.A., Hart, A.L., Partridge, A.C., and Wallace, G.G., **Development of Conducting Polymer Coated Screen-Printed Sensors for Measurement of Volatile Compounds**, *Electroanalysis* (In Press).

ACKNOWLEDGEMENTS

First and foremost I must thank Professor Gordon Wallace for making this PhD an experience I will never forget, and one that I will reminisce over for the rest of my life. Through good times and bad, he was always there to help, and treated me more like a friend than a supervisor. It really made all the difference. Thanks mate, for everything, it is greatly appreciated. It has been a privilege to work under your guidance and I am sure we will continue to 'work' together in the coming years.

I would also like to thank Dr Norman Barisci, for his much needed advice and assistance throughout the project. Again, I really appreciated your friendship during my time at IPRI, and for me your sense of humour in the lab always helped to keep things in perspective.

Dr Ashton Partridge. The word 'Legend' springs to mind. I cannot thank you enough for the time you spent helping me out in NZ. I learned so much from you in such a short period. I think that without my trips over to Lower Hutt I would have been lost. I would also like to thank all those at Industrial Research Limited who helped make my time in NZ so enjoyable.

I would also like to thank Dr Alan Hart and Wendy Collier of AgResearch, Palmerston North, NZ, for their help and advice with screen-printing. Your hospitality during my visits, and subsequent supply of electrodes is greatly appreciated.

Thanks go to Megan Ash of Tecra Diagnostics, Sydney, for her assistance with the PMAS *Listeria* work and for supply of cultures over the course of the project.

A wealth of much needed advice and supervision in the areas of robotics and odour plume tracking has been provided by Assoc. Prof. Andy Russell, of the Intelligent Robotics Research Centre, Monash University, Melbourne. Please accept my sincere thanks for all the time and effort you have invested in someone with little background knowledge of the area. I have thoroughly enjoyed this aspect of the work and as a consequence continue to conduct research in this area.

To all at and associated with the Intelligent Polymer Research Institute, University of Wollongong, I had a fantastic time both working and socialising with you. The experience would have been much less rich without the amazing group of people at IPRI, which is more like a family than a research team.

I have to take this opportunity to thank Prof. Leon Kane-Maguire, who through his incredible passion for science and life in general continues to inspire all of those around him.

To my parents, Linette, and Peter, thankyou both for all your support over the years, and in particular during my PhD. I couldn't have done this without you.

Finally, I have to thank my kelpie, Buster, for keeping things in focus during the last few months in the lab.

DEDICATION

This thesis is dedicated to my mother, Linette, whose determination and optimism in times of incredible personal hardship inspired me to keep going.

TABLE OF CONTENTS

LIST OF FIGURES

LIST OF TABLES

List of Abbreviations

AFM	Atomic Force Microscopy
CP	Conducting Polymer
CV	Cyclic Voltammetry
Da	Daltons
DPV	Differential Pulse Voltammetry
HBS	4-hydroxybenzenesulfonic acid
ICP	Inherently Conducting Polymer
i.d.	Internal Diameter
ISE	Ion Selective Electrode
LOD	Limit of Detection
MAS	Methoxyaniline sulfonate
Mo	Microorganism
MS	Methanesulfonic acid
Mw	Molecular Weight
NBS	3-nitrobenzenesulfonic acid
NDS	1,5 napthalenedisulfonic
o.d.	Outer Diameter
Pani	Polyaniline
PCA	Principal Component Analysis
PMAS	Poly-methoxyaniline sulfonate
PPy	Polypyrrole
PPy/Cl	Polypyrrole Chloride
PSS	Polysodium-4-styrenesulfonate
PT	Polythiophene
pTS	*p*-toluene sulfonic acid
QCM	Quartz Crystal Microbalance
R.S.D.	Relative Standard Deviation
SB	4-sulfobenzoic acid
SEM	Scanning Electron Microscopy
S/N	Signal to Noise ratio
T.I.T.	Tube In Tube Sensor
UV-vis	UV Visible Spectroscopy
XPS	X-ray Photoelectron Spectroscopy

ABSTRACT

This thesis details the development of conducting polymer (CP) sensors, and associated devices for monitoring chemical species of environmental significance. A key aspect of this work was the fabrication and testing of novel CP gas sensors, based on inexpensive polymer substrates with screen-printed carbon electrodes. These devices were used in electronic nose systems for the identification and discrimination of organic vapours, and on a small autonomous robot to detect, track and locate the source of ammonia vapour plumes. The possibility of modifying chemically deposited Polypyrrole (PPy) thin films post-polymerisation using solution based anion exchange methods was evaluated, in an attempt to alter chemical selectivity whilst retaining the sensitivity of such devices. Approaches to reducing the humidity response of PPy gas sensors, a significant interferant when sensing many sample matrices, were also examined with the view to developing vapour detection systems for organic volatiles in water. A comprehensive study of the electrochemistry and spectral properties of a water soluble conducting polymer, Polymethoxyaniline sulfonate (PMAS), and the effect of molecular weight on these properties was undertaken. This work was carried out in order to better understand the mechanism of interaction between PMAS and the microorganism *Listeria Monocytogenes*, which is under development at IPRI as a detection system for this species.

Chapter 1

Properties of Conducting Polymers and Application to Environmental Sensing

1.1 Conducting Polymers (CPs)

Inherently conducting polymers (ICPs) are a relatively new group of materials that possess electrical conductivities of up to 10^5 s cm^{-1}. The development of these materials began in the 1970s when Shirakawa and co-workers found that the conductivity of polyacetylene increased dramatically in the presence of iodine vapour [1]. The most common materials investigated since include polypyrrole (PPy), polyaniline (Pani), polythiophene (PT), poly (*p*-phenylene) and poly (phenylene vinylene). The term conducting polymer (CP) has also been used to describe loaded polymers, which consist of an insulating polymer matrix containing conductive particles such as carbon black [2-4] or an ICP such as PPy [5, 6]. These materials rely mainly on swelling of the insulating polymer matrix to give varied changes in conductivity for different vapours, rather than on changes in the intrinsic conductivity of the polymer network as is the case with ICPs. The term conducting polymer (CP) will be used in this thesis to refer exclusively to ICPs.

While conjugated polymers in their neutral state are usually insulating, CPs are made conductive by the presence of mobile charge carriers along the polymer backbone, known as polarons and bipolarons. The process of rendering a CP conductive is known as doping and involves the oxidation or reduction of the polymer backbone. These materials can be doped either during polymerisation, as is the case with electrochemical oxidation of pyrrole to give the corresponding polymer (Figure 1.1), or after formation of the polymer as is the case with polyacetylene doped by iodine vapour. CPs can either be p-type conductors, for example polypyrrole and polythiophene, where electrons are removed by oxidation leaving positive charges, or n-type conductors such as polyacetylene doped with iodine where the charge carriers are negative. The formation of charge carriers in CPs leads to significant changes in the structural and electronic

arrangement of the polymer. As is shown for polypyrrole in Figure 1.1, these structural defects are delocalised over approximately four repeat units [7]. In the case of electrochemical oxidation of CPs a stoichiometry of 2.07 to 2.60 faraday/mol of monomer is involved, but it is known that only 2 faradays/mol are used for polymer formation. The remaining charge, which is usually between 0.25 and 0.4 electrons, is involved in doping the forming polymer.

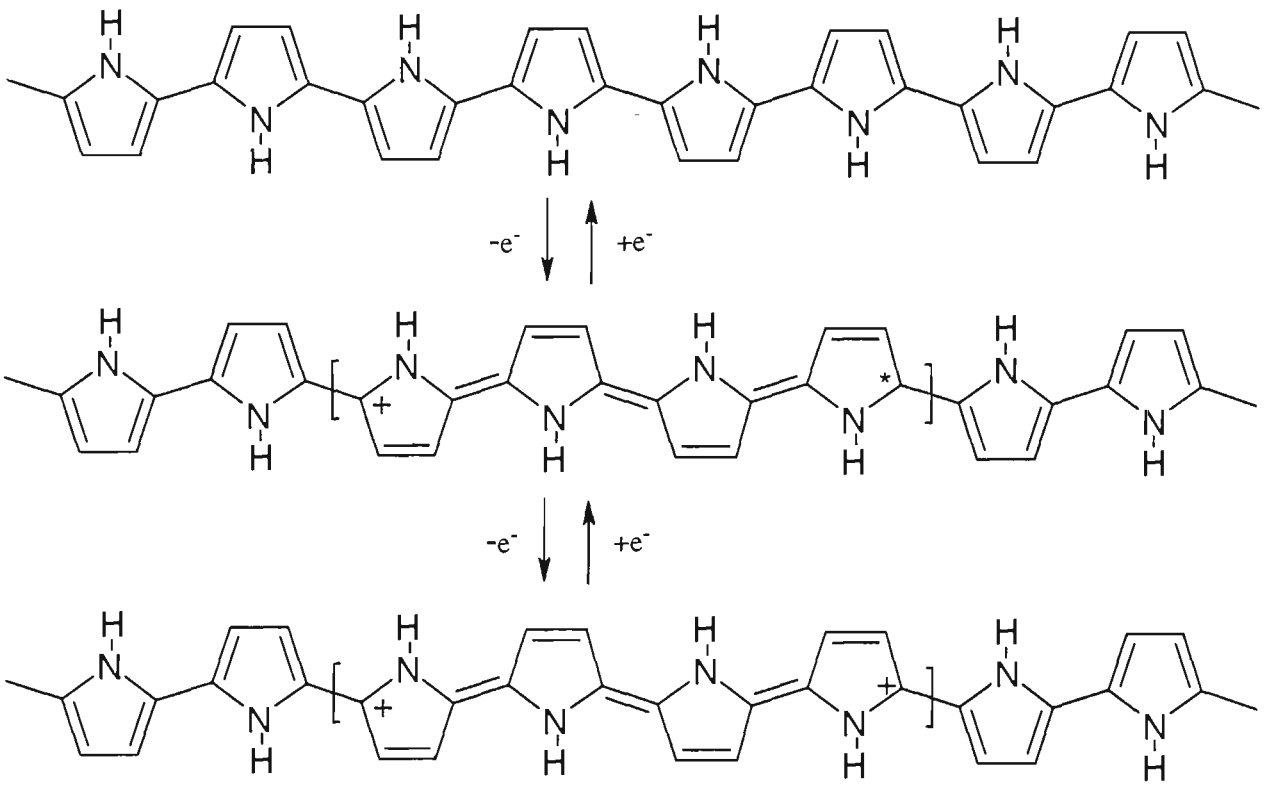

Figure 1.1 Formation of positive charge carriers in polypyrrole: (1) neutral, (2) polaron, (3) bipolaron.

The magnitude of this charge is directly related to the extent of doping along the polymer backbone and explains why every 3rd or 4th monomer unit is charged [8]. Charge carrier mobility within CPs is thought to involve both movement along polymer chains and interchain hoping [9]. While interchain hoping is involved in the movement of polarons/bipolarons, CPs generally behave as one-dimensional conductors as these

charge carriers predominantly travel through the linear conjugated chains. These materials possess a gap between the valance and conduction bands at room temperature and hence the conduction mechanism is electrical rather than metallic (conductivity is dependent on the temperature) [10].

1.2 Preparation of CPs

CPs can be prepared by chemical or electrochemical means that most commonly involve oxidation of the monomer. In both cases a radical monomer cation is first formed which then combines with a second cation to form a dimeric species. Further coupling with individual monomeric cations continues until the oligomers formed are large enough to be insoluble. At this stage the polymer deposits as a solid on an electrode or precipitates into solution. During the process of anodic oxidation a counter-ion from the electrolyte solution used for polymerisation is incorporated into the polymer to maintain charge neutrality. In the case of chemical oxidation the number of counter-anions available is limited to those associated with the oxidant used, which is most commonly $FeCl_3$ or ammonium persulfate. The electrochemical route gives a much wider range of dopant anions, as the reaction is driven by an applied potential or current in the presence of an appropriate electrolyte rather than by a chemical oxidant. Other advantages include better control of film properties, which is achieved by modifying the electrochemical conditions, and the ability to produce CP films on electrodes that can be used as prepared for subsequent chemical sensing. For these reasons the electrochemical method of CP preparation is most commonly employed, particularly in the field of sensor fabrication. The most common approaches used for electrochemical polymerisation are galvanostatic and potentiostatic. The galvanostatic approach, which involves applying a constant current between the working and auxiliary electrodes, gives

the best control over film thickness and is more reproducible than the potentiostatic (constant potential) method [11]. The other widely used method is potentiodynamic electropolymerisation in which case the potential is cycled between two limits which include the oxidation potential of the monomer. The plot of current response versus potential, a cyclic voltammogram, shows clearly the formation of polymer, and hence this technique is often employed in preliminary investigations of the electrodeposition process [12].

1.3 Factors Influencing CP Formation

One of the most attractive features of CPs for use in chemical sensing is the ability to carefully tailor the materials produced by varying deposition conditions. While chemical routes to polymer formation are more limited in this regard, some aspects can be controlled reasonably well.

1.3.1 Chemical Polymerisation

The most important parameters associated with chemical deposition of CPs are the concentration of oxidant used and the oxidising power of this species. It is possible to vary the rate of deposition and level of doping by varying these, provided that the concentration of monomer present in solution is sufficient to avoid diffusion controlled deposition occurring [13]. If the monomer concentration is too low this will significantly affect the rate of polymerisation. Some variation in the final properties of chemically prepared CPs can be achieved by varying the nature of the anion in the oxidising salt employed. However, in doing so the oxidising power differs and hence the rate of polymerisation and extent of oxidation will be affected.

1.3.2 Electrochemical Polymerisation

The primary factor affecting polymer deposition when using electrochemical methods is the applied potential or current. Constant current (galvanostatic) deposition is most commonly employed as this approach allows for exact control over the rate of polymerisation, whereas potentiostatic growth does not unless solution and electrode parameters are carefully controlled [13]. The applied current density is known to affect the final morphology obtained [14], with faster growth rates leading to more porous films [15], and the conductivity [16]. The amount of polymer deposited is directly related to the total amount of charge passed during growth, and while some charge is lost forming oligomers, film thickness can be controlled carefully by growing films to a desired charge value.

The nature of counter-ions present in the polymerisation solution can also affect the polymerisation process. In some cases, interactions between the monomer or monomer radicals and counter-ions occurs, as is the case when dodecylsulfate anions are employed, which have a significant effect on the growth process. When Tiron, an electrocatalyst, is employed as a counter-ion the growth rate of polypyrrole is enhanced dramatically [17]. Again, as for chemical polymerisation, the concentration of monomer must be sufficient that diffusion controlled growth does not dominate, and the same applies to the concentration of counter-ion, which if too low will control the reaction rate.

1.4 CPs for Chemical Sensing

CPs have been employed in a wide range of sensing applications, due to the unique electrical and physical properties that these materials possess, and the ease with which polymer characteristics can be tailored during sensor production. The main areas of

application to date have been gas sensing, anion/cation detection, and biosensing. Some of the general properties associated with CPs will be discussed in order to illustrate the suitability of these materials for such applications.

1.4.1 General CP Properties

As was mentioned earlier, the electrochemical route to CP preparation enables specific control over physical properties of the polymers produced such as film thickness and morphology. This is of utmost importance when fabricating devices as these factors significantly affect the chemical sensing performance. Of particular interest is the ability to tailor film properties by varying the dopant or counter-ion incorporated during polymerisation. This parameter not only controls the physical properties of the film, but also provides a means to impart specificity into the material. By judicious selection of the dopant it may be possible to target a particular analyte, which interacts specifically with the counter-ion incorporated into the CP layer. This feature can also be used to build up arrays of CP sensors, each with a different dopant ion, giving rise to patterns of responses for a particular analyte. This approach is employed in the area of electronic nose based gas sensing where odour fingerprints, rather than highly specific interactions, are utilised to discriminate between different samples.

1.4.1.1 Ion Exchange

The necessary incorporation of a counter-ion, in most cases negatively charged, into the CP structure for charge balance is a particularly useful feature of these materials when employed for chemical sensing of ions. Once a polymer film has been formed the oxidation state can be switched electrochemically from oxidised to neutral. When in the neutral state, charge compensation by a counter-ion is not required and the species is

expelled from the polymer backbone. Once re-oxidised the polymer possesses positive charges that are balanced by re-incorporation of ions. The ion reincorporated is not necessarily the same species that was present in the as prepared polymer, but in fact may be a different ion present in a 'sample matrix that selectively associates with the CP. This process is controlled to a significant extent by the size, and hence the mobility, of the ions involved. A significant change in conductivity is associated with the change in CP oxidation state, and the change in ion concentrations in the polymer, giving rise to variations in current flow. Measurement of film resistance (resistometry) in solution has been demonstrated by monitoring the resistance in an electrochemical cell between the CP working electrode and a reference electrode. The changes in CP oxidation state from oxidised to reduced, or neutral, were clearly observed when using this technique, and while CPs such as PPy are doped with anions, cations are also thought to play a significant part in controlling film resistance properties [18, 19]. As a result cation selective transport can also be achieved by selecting large immobile anions during film preparation, which are difficult to remove from the polymer matrix during electrochemical cycling [20, 21].

1.4.1.2 Incorporation of Biological Components

CPs are extremely flexible materials as they can be prepared in a variety of ways. As many of these polymers can be produced electrochemically from aqueous solutions, and under mild conditions of pH, it is possible to incorporate a broad range of biological species such as enzymes [22-25] antibodies [26, 27] and whole cells [28] into CP films without compromising the integrity of these components. This can be done without limiting the control over film properties that is available by employing electrochemical deposition.

1.4.1.3 Flexible Substrate Range

Conducting polymers can be deposited onto a wide range of substrate materials, including glass, insulating polymers, fabrics and conducting electrode structures such as metals and carbon. This is due to the varied methods of polymerisation/deposition available. It is possible to prepare coatings using purely physical means such as casting, spin or dip coating, which are commonly used with more conventional polymer systems. Chemical deposition of CPs is not limited to solution but extends to such techniques as vapour phase oxidative polymerisation, which allows very thin uniform films to be formed on both planar and three dimensional objects. Electrodeposition of CPs allows the controllable formation of films on metal electrodes, and it is possible to form bridge structures across gaps between sets of parallel electrodes across an insulating substrate. A good example of the flexibility described above is the fabrication of CP chemical sensors based on quartz crystal microbalances (QCM). CP sensing films can be cast, or for a more uniform film spun from solution onto the metal electrodes of a QCM. Chemical oxidative polymerisation can also be employed to prepare sensors, but in this case perhaps the most useful approach is electrodeposition onto the metal electrode surface of a QCM device. All the advantages of electrodeposition are available, but of particular importance is the ability to grow uniform films of precise thickness.

1.4.2 General Application Areas

CPs have been applied for a broad range of sensing tasks, due to the properties outlined above, particularly for gas sensing, biosensing and ion sensing. CPs have been used widely in the field of gas sensing due to the ease of device fabrication, rapid and reversible response to range of organic and polar analytes, room temperature operation and the range of polymers available. In general these sensors are not highly specific to a

particular analyte but rather respond to some degree to a wide range of chemically similar species. As a result CP gas sensors have commonly been employed in array based devices, referred to as electronic noses, where the pattern of responses from a set of sensors to a particular analyte is used for discrimination purposes. These systems are used more for qualitative analysis of samples with the advantage of providing rapid results without the need for lengthy sample pre-processing before analysis.

The ion exchange properties of CPs, mentioned above and discussed in more detail in section 1.5.1 and Chapter 3, have seen these materials employed in a diverse range of solution based chemical sensors. These devices function on the basis of variations in the ion populations associated with CP films that cause changes in electrical properties. These processes can be carefully selected by the nature of counter-ion incorporated in the CP and by the electrochemical conditions employed during sensing.

The other main area to which CPs have been employed widely is biosensing due to the possibility of incorporating biomolecules into CP films with ease. CP biosensors have been developed for a broad range of analytes, for example glucose [29], amino acids [30], uric acid [31] and DNA [32].

The remainder of this chapter will focus on examining the application of CP chemical sensors to environmental monitoring. Solution based sensors for a range ions, including heavy metals, surfactants, nitrates and sulfates will be discussed first before the focus moves to gas sensing.

1.5 Environmental Monitoring with CPs

The field of environmental monitoring has become a multi-million dollar industry due to the pressure placed upon the earth by current industrial practice and the 'consumer' nature of modern society. We are now at a point in history where the only way to ensure

the health of our surroundings, and ultimately ourselves, is to take steps to protect it from further damage. Governments have sought to ensure this occurs by introducing legislation that incurs financial costs to the polluter. As a result there is a huge demand for reliable low-cost environmental sensors in a broad range of different application areas, both from industry, and government enforcement bodies. Conducting polymers have been employed in a wide variety of these areas for monitoring environmental systems due to the flexibility of this class of materials as outlined above. A significant amount of development in the area of solution phase sampling with CPs has been carried out, and many of the electrochemical principles associated with such devices were used in this thesis for the preparation and post-fabrication of CP gas sensors. Hence the main CP solution sensor types will be examined, but as a large number of examples are available in the literature, only a selection will be reviewed. The discussion will then examine CPs for environmental monitoring of vapour phase samples, as the main focus of this thesis is on gas sensing. However, CPs have not been applied in this area to the same extent, which is one of the reasons we sought to develop the sensors described herein.

1.5.1 Solution Based Sensors

CP sensors for monitoring ions and solution phase species of environmental interest generally fall into two broad classes, amperometric and potentiometric. Amperometric sensors are based on measurement of the current flowing when the device is held at a constant potential with respect to a reference electrode. Changes in current in response to exposure to chemical species of interest are monitored over time. Potentiometric sensors are based on measurement of the potential between a chemical sensor and a reference electrode. A less common type of sensor is based on voltammetry, which

involves sweeping the potential between two limits and monitoring the current responses relative to applied potential over time. The electrochemical principles of operation of these devices are employed in Chapter 3, to modify the sensing properties of CP vapour sensors, and in Chapter 6 for the study of a water soluble Pani and it use in detection of the microorganism *Listeria monocytogenes*.

Other types of solution based CP sensors that have found some application in environmental monitoring include resistometric devices, which are based on measurement of resistance in the presence of analyte species, optical sensors, which rely on changes in the spectral properties of CP films, and QCM devices that employ mass change for detection of analytes.

1.5.1.1 Amperometric Sensors

Trace chlorocarbons have been detected in aqueous solutions using poly(N-methylpyrrole) amperometric sensors. Responses to dichloromethane were observed over a wide range of concentrations, from 10 ng/mL to 1 mg/mL, without the need for sample preconcentration or dilution. Other chlorinated compounds including chloroform, 1,2-dichloroethane, and carbon tetrachloride gave rise to similar sensor responses, while small non-chlorinated compounds gave rise to much smaller signals indicating potential selectivity to small chlorinated species [33]. An amperometric potassium ion-selective electrode was reported based on a PPy/$Fe(CN)_6$ film with a PVC-K over layer. [20]. The sensor responded to K^+ over a very wide concentration range (10^{-7} to 3 M) and was not susceptible to interference from solution redox species. As a result of the later, the same current response was observed in KCl and $K_4Fe(CN)_6$ solutions with the same K^+ concentration. Barnett *et al* [34] reported on the development of a PPy biosensor for the detection of p-cresol and other phenolics. The

sensing layer incorporated antibodies to a p-cresol bovine serum albumin conjugate, and gave to responses to both p-cresol and phenol at a concentration of 0.1mg/L when interrogated by a pulsed potential waveform. The detection of cyanide, chlorophenols, atrazine, dithiocarbamate, and carbamate pesticides has been achieved using an amperometric biosensor based on a pyrrole amphiphilic monomer/tyrosinase coating [35]. A Pani-dispersed mercury electrode has been developed for the detection of chloramines by depositing a Pani film over a thin mercury film electrode. The presence of chloramines, in particular dichloramine, has a dramatic effect on taste and odour problems in drinking water, and hence detection of this species is extremely important. Detection limits of 0.1 and 0.8 μM were observed for monochloramine and dichloramine respectively [36]. An amperometric sensor based on a PPy/horseradish peroxidase membrane has been described for the simultaneous detection of superoxide and hydrogen peroxide at concentrations in the low micromole to high nanomole range [37]. Nguyen *et al* have reported on the use of PPy amperometric sensors for flow injection analysis of potassium and methylamine [38]. These cations, which are difficult to separate using conventional cation exchange columns, were successfully discriminated using PCA of the sensor responses.

1.5.1.2 Potentiometric Sensors

Potentiometric CP sensors have been used extensively for detecting ions in solution. These devices rely upon either ion-exchange properties of CPs, as discussed above, or changes in the redox state of the polymer. CPs have been used as exchange membranes in ion selective electrodes (ISEs), which are in direct contact with the analyte solution, or can be used as an internal electrical contact between an electrode surface and conventional ion selective materials. Potentiomettry is employed in Chapter 3 in order

to exchange the chloride anion of PPy/Cl vapour sensing films for a different anion, in theory altering selectivity to various vapours.

When used as the direct interface to solution, the basic process involves reversible movement of ions in and out of the CP sensing film. Substituted phenols, aromatic amines and pyrrole have been detected using PPy, Pani, and a Pani/*para*aminophenol composite polymer using potentiometry. The interactions giving rise to signals were said to be closely related to the monomer-polymer potentiometric equilibrium [39]. Electrochemically prepared poly(ortho-methoxyaniline) and poly(ortho-methylaniline) sensors have been used successfully to monitor pH [40]. In this case the movement of H^+ ions causes changes in the oxidation potentials of the Pani. The poly(ortho-methylaniline) sensor performed best with a Nernstian like response over a pH range of 1 – 12 and a slope of 63.8 mV/decade. The poly(ortho-methoxaniline) exhibited linear responses in the range of 2 - 11 pH with a slope of 62.0 mV/decade. No interference was observed from Cl^- anions, and the presence of F^- only caused minor shifts in electrode potentials without any erosion of the electrode. The sensors responded to Li^+, however, with significant shifts in potentials observed in the presence of this cation. Therefore, the sensors are applicable for pH sensing in the absence of Li^+ ions, and are also suitable for monitoring pH in acid-base titrations of solutions containing HF. Pei and Qian also noted the pH sensing potential of PPy films on platinum electrodes, with responses of -40 mV/pH unit, but these changes were rather slow [41]. PPy doped with bisulfate has also been employed for potentiometric sensing of pH [42]. After a suitable conditioning period in $NaHSO_4$, near Nernstian responses of 54 mV/pH were obtained with response times of between 1 and 3 minutes depending on the solution pH.

A Br^- sensor, based on a copolymer of methyl-PT and methyl-PPy, was prepared on a graphite working electrode and doped electrochemically with Br^-. The sensor

functioned well in pH 4 to 7, had a linear range of 10^{-1} to 10^{-4}, and a LOD of 6×10^{-5} M. The electrode also showed a rapid potential response making it superior to other Br^- electrodes. The performance of homopolymer electrodes based on both methyl-PPy and methyl-PT, were evaluated and it was found that the copolymer showed better stability and better sensitivity. The electrode was also used for end-point detection in potentiometric titrations of Br^- with $AgNO_3$, and due to the rapid response times of the sensor the $AgNO_3$ titrant could be added drop wise without pausing [43].

Galal *et al* used the CPs poly(3-methylthiophene), poly(N-methylpyrrole) and Pani for the detection of iodide, bromide, chloride, and sulfite [44]. The sensors were prepared by potentiostatic deposition of the CP onto graphite electrodes, followed by a dedoping step which involved holding the potential at – 0.2 V to completely remove the counter-ions present after preparation. The sensors were then activated for ion sensing by either immersion in a 0.1M aqueous solution of the anion of interest (e.g. KBr, KI) with a potential applied, or where exposed to the corresponding of interest (e.g. I_2, Br_2).

Alizadeh and Mahmodian [45, 46] have developed dodecylsulfate ion selective sensors as a means of detecting the presence of harmful surfactant molecules in environmental water samples. The sensors are based on a PPy/PVC/DS copolymer plasticised with 2-nitro-phenyloctlyether, and showed Nernstian behaviour with a response of 57.5 mV per decade over a DS^- concentration range of 10^{-5} to 10^{-7} M. The LOD for DS^- was determined to be 5×10^{-6} M, and excellent selectivity was observed in the presence of a wide range of inorganic ions, suggesting that this sensor would also be very useful in detecting end-points of potentiometric titrations.

Potentiometric biosensors based on self-doped Pani have been reported for the detection of organophosphates, which are found in pesticides and chemical weapons. The Pani

films incorporated an enzyme, organophosphate hydrolase, which hydrolyses organophosphate molecules such as the pesticide paraoxon into sub-units. The LOD of this sensor was 10^{-7} M paraoxon, which although lower than for other potentiometric devices is not sufficient for environmental control monitoring. Despite this it was suggested that the sensor could be used for the detection of such species by flow-injection analysis, where the sample is first pre-concentrated before detection [47].

CPs have also been used for potentiometric sensing of dissolved oxygen in aqueous media. Shim *et al* [48] described an electrodeposited Pani film on a platinum electrode, which was oxidised in the presence of dissolved oxygen, giving rise to a detectable potential change. The sensor gave a change of 97 mV/decade of oxygen concentration, and had a wide linear range of approximately 400 mV allowing for oxygen detection over more than 3 orders of magnitude. The LOD for dissolved oxygen was determined to be 5×10^{-7} M.

Hutchins and Bachas [49] used PPy doped with NO_3^- for the potentiometric detection of nitrate. Near Nernstian responses of approximately -56 mV/decade were observed over a linear range of 5.0×10^{-5} – 0.50 M nitrate. Detection limits of 2×10^{-5} M nitrate were demonstrated, and selectivity to nitrate in the presence of common interfering lipophilic anions such as perchlorate and iodide were improved substantially. An ISE based on CPs for sulfide has also been described which employed poly(3-methylthiophene) derivatised with poly(dibenzo-18-crown-6) on an alloy electrode [50]. The linear dynamic range for total sulfide in solution was 1.0×10^{-7} – 1.0×10^{-2} M, and the electrode functioned over a wide range of pH from 1 to 13. Excellent selectivity to sulfide was demonstrated in the presence of common interfering anions such as NO_3^-, NO_2^-, halogen ions, and sulfate.

CPs have also been used as internal contact layers in ISEs for a range of ions in solution. Lindfors *et al* [51] described an all-solid-state ISE for lithium, which employed a soluble conducting Pani contact layer. The CP provided a path for electron transfer between a platinum electrode and lithium-selective PVC membrane in contact with solution. It was found that the presence of Pani improved the potential stability and reproducibility due to better charge transfer at the electrode-membrane interface. In a similar device using PPy as an electron transfer contact, potassium ions were selectively detected by a bis-crown ether ligand based plasticised PVC membrane [52]. Ca^{2+} and Li^{+} ISEs have also been prepared with a CP component to mediate electron transfer from the sensing membrane to the substrate. Soluble poly(3-octylthiophene and Pani were incorporated into PVC membranes for this purpose, improving the standard potential stability of the sensors [53]. An all-solid state electrode based on a calixarene ionophore in a PVC membrane that employed PPy as a solid contact has been used for selective detection of sodium [54]. The presence of a PPy/$NaBF_4$ contact layer between the PVC ion-selective membrane and platinum electrode improved stability and performance compared to an electrode without the CP. Near Nernstian responses were observed of approximately 58 mV/decade and a LOD of 1×10^{-5} was determined.

CPs can also be employed as an electron transfer matrix for ISE sensing, in addition to the contact role described above. The CP is combined with an ion selective polymer and acts to transfer electrons to the electrode. A calcium ISE has been prepared by this approach using Pani functionalised with bis [4-(1,1,3,3-tetramethylbutyl) phenyl]phosphate. Sensitivity to Ca^{2+} was 27.8 mV/log[Ca^{2+}] and a limit of detection of 8×10^{-4} M was observed [55]. Plasticiser-free all-solid state K^{+} selective electrodes have been prepared using the CP poly(3-octylthiophene) as the conducting matrix in

combination with a potassium ionophore, valinomycin, and a lipophilic additive, potassium tetrakis[3,5-bis(triflouromethyl)phenyl]borate [56]. The lipophilic additive is included to induce permselectivity to cations and hence exclude anions. The electrodes were selective towards potassium in the presence of sodium cations, and were able to detect K^+ over a concentration range of 10^{-8} to 10^{-1} M KCl. Sensitivity to pH was also observed for these ISEs, most significantly when pure poly(3-octylthiophene) films were used, and hence was attributed to the changes in the CP. Calcium ISEs have also been prepared by combining a CP, ionophore, and cationic additive. A soluble PANI was mixed with di(ethylhexyl)phosphate, a Ca^{2+} complexing agent, and tetraoctylammonium chloride, the cationic additive. Ca^{2+} sensitivity was 27.0 mV/log[Ca^{2+}] over a concentration range of 10^{-1} to 10^{-3} $CaCl_2$. The LOD observed was 10^{-4} M, and good selectivity towards Na^+, K^+, and Li^+ was achieved. However, major interference was noted in the presence of Mg^{2+}. Responses to pH were observed in the range 4.5 – 9.7 with a sensitivity of 5mV/pH [57].

Sjoberg *et al* [58] have also developed an all-solid-state chloride-selective electrode based on poly(3-octylthiophene). The CP was mixed with tridodecylmethylammonium chloride in chloroform and solution cast onto a glassy carbon electrode. Optimised sensors showed virtually no redox or pH sensitivity, with responses of approximately 50mV/decade of chloride even after periods of 6 months testing in solution. The linear range of these electrodes under ideal conditions was 10^{-1} to 10^{-4} for which the slope was 57 mV/decade, and the observed LOD was 10^{-6} M.

1.5.1.3 Voltammetric Sensors

Cyclic voltammetry (CV) with PPy films has been used for the preconcentration and detection of silver species in solution, using both PPy doped with chemically active

counterions [59] and PPy films with normal (non-active) dopants [60]. In the later case a linear concentration dependence was observed in the range of 2 – 150 μM silver, and an LOD of about 2 μM was determined.

Nguyen *et al* have reported on the use of PPy sensors for CV based detection of potassium and methylamine, which are difficult to separate using conventional cation exchange columns. These species were successfully discriminated using PCA of the sensor responses [61]. Voltammetric responses of a boronic ester-functionalised PPy have been reported for the selective detection of fluoride and chloride [62, 63]. Shifts in potential of the doping/undoping processes were induced by binding of the analyte to the boron atom, as these changes were not observed for the unfunctionalised PPy.

CPs have also been used in more conventional chemical analyses. PPy coated mercury film electrodes have been employed for sono-anodic stripping voltammetry of cadmium and lead in the presence of surfactant molecules [64]. Pani and PT mercury coated films have also been employed for the detection of these heavy metals in the presence of interfering surfactant molecules, but sensor performance was significantly affected under the conditions [65]. Recently Poly(*o*-ethoxyaniline) sensors were used to detect heavy metal ions including Fe^{3+}, $Hg2^{+}$, Cu^{2+}, Pb^{2+} and Cd^{2+} in solution using differential pulse voltammetry (DPV). Lead was detected by this approach over the concentration range 0.1 to 5 ppm [66].

1.5.1.4 Resistometric Sensors

Koul *et al* [67] reported on the development of a Pani/acrylonitrile-butadiene-styrene composite film for sensing ammonia in solution. The film resistance was monitored upon exposure to aqueous ammonia, and showed well-defined responses in the

concentration range 10^{-4}N to 10^{-5}N. These changes in conductivity were confirmed spectrally by UV-vis.

PPy films have been used to prepare simple resistometric based pH sensors on PVC substrates with carbon conductors. The sensors gave linear responses in the pH range 2 to 6, were selective to H^+ and were not significantly affected by variations in ionic strength of the supporting electrolyte [68]. Talie [69] reported on the use of PPy, Pani and PPy/Pani composite films for pH sensing. In this case changes in film resistance were monitored as a function of solution pH. Resistance measurements made on PPy films in solution have been used as a basis for the detection of DS^-, SO_4^{2-}, and Cl^-, and in combination with artificial neural network training this system was able to discriminate between different electrolyte solutions [70].

PPy films have also been used to develop simple detectors for microbial metabolism based on measurement of dc resistance. In the presence of toxic substances, the metabolism of yeast cells incorporated into the PPy is inhibited, providing a means of detection. Exposure of this device to 1000 ppm Hg^{2+} ions led to complete inhibition [71]

1.5.1.5 Optical Sensors

Changes in the oxidation state of CPs upon exposure to chemical species lead in some cases to spectral changes of the material, and this has also been used as a means of sensing. Composite films of Prussian Blue and N-substituted pyrroles have been employed for the optical determination of pH [72]. The composites were polymerised onto nonconducting plastic supports by chemical oxidation of Prussian Blue in the presence of pyrrole acids such as 4-(pyrrol-1-yl)benzoic acid and 3-(pyrrol-1-yl) propanoic acid. These films have an absorption maxima at 720 nm, the magnitude of

which is affected by pH. The sensors gave reversible responses in the pH 5 –9 range with good reproducibility. At pH > 9 the films underwent irreversible spectral changes due to the decomposition of Prussian Blue by hydroxide ions. There were no interferences from common cations such as lithium, sodium, potassium, magnesium, calcium and ammonium. Such devices could prove very useful in monitoring pH within the bounds of the operating range. A PPy/chloride optical sensing system for pH determination has also been developed by chemically oxidising pyrrole in polystyrene cuvettes leading to the formation of a thin (< 1 μm) film on the walls of the vessel. The dynamic range of this device was pH 6 to 12, with optimal changes in the spectral absorbance of the PPy film at 650 nm. Response time was of the order of 10 to 20 seconds, but measurements were taken after 2 minutes to ensure reproducibility. At pH > 6 the PPy dedopes and spectral shifts to lower wavelengths were observed, however, re-conditioning with dilute HCl returned the films to their original state. Although ionic strength had little effect of performance of the system, some spectral interference was noted in the presence of mercury and silver ions [73]. In related studies, Pani and substituted Panis were employed in the same type of pH sensing system, with spectral measurements taken at 600 and 840 nm. In this case the dynamic range was found to be wider, from pH 2 to 10, and the effect of ring substituents on the pH sensing performance was notable [74]. Sotomayor *et al* [75] used a Pani-porous Vycor glass nanocomposite optical sensor for pH monitoring. Sensor responses were reversible over a pH range 5 to 12, and linear from pH 7.4 to 9.5. Response times of 4 to more than 16 minutes were noted for sensing films of different thickness. A Pani based optical sensor has been developed for a wider testing range of pH 2 to 12, with rapid response times of the order of 1 second. Optical changes in the Pani film were monitored in the near infrared region of the spectrum, at a wavelength of 910 nm, which has the advantage of

eliminating interference from naturally occurring organic absorbers as they do not exist [76].

1.5.1.6 Other Applications

CPs have also been employed for extraction of species in environmental samples in combination with subsequent instrumental analysis for detection. PPy coated capillary systems were used for in-tube solid-phase microextraction of both polar and non-polar aromatics in aqueous samples. The analytes, which were thought to adsorb onto the PPy coating, were analysed by HPLC after extraction. A range of highly toxic aromatics, including benzene, toluene, phenol, naphthalene, and amine substituted species were successfully detected at low ng/mL levels. The PPy capillary system was found to possess a higher extraction efficiency for these aromatics compared to commercial coatings such as poly(dimethylsiloxane) and poly(ethylene glycol) [77]. These workers also reported on the use of this extraction technique coupled with liquid chromatography-electrospray ionisation mass spectrometry for the successful detection of organoarsenic compounds in water. Using the PPy coated capillaries led to more efficient extraction for most of the compounds analysed, which included monomethylarsonic acid, dimethylarsenic acid, arsenobetaine and arsenocholine [78]. Ion chromatography in concert with PPy SPE capillaries for a range of inorganic anions including fluoride, chloride, bromide, nitrate, phosphate, sulfate, selenite, selenate, and arsenate, has also been reported by this group [79]

PPy coated reticulated vitreous carbon has also been employed for toxic chromate remediation in aqueous media. PPy films reduced to a neutral state by imposition of a negative potential, and then are able to donate electrons to the oxidised Cr (VI) species converting it to the less toxic Cr (III) form [80]. *N*-n-octylaniline has also been used for the recovery platinum (IV) from organic solvents containing iron (III), cobalt (II), nickel

(II) and copper (II) [81]. PPy coated QCMs, which rely on changes in mass of the coated quartz crystal, were used by Desimoni and Bassani [82] for the detection of chromate and ascorbic acid.

1.5.1.7 Water Soluble CPs

In recent years a growing interest in the development of water soluble CPs has led to the realisation of a new class of materials. As this form of CPs are relatively new, the majority of work to date has been on preparation and characterisation of the polymers themselves, however, they have been applied to a limited extent for solution based chemical sensing. The development of PT water soluble materials, which exhibit counter-cation dependent chromic properties, have been reported as potential materials for chemical sensing. In the presence of ammonium hydroxide the CP changes colour from purple to red, and upon subsequent exposure to NaCl the purple colour is restored. This behaviour is also noted for $MgCl_2$ and $ZnCl_2$, and is thought to be due to a combination of cation size dependant twisting of the polymer backbone and aggregational ordering [83].

Water soluble CPs have also been employed for biosensing and the detection of important microorganisms. Polyacetylenes have been used for colorimetric determination of the Cholera toxin [84], which was detectable in the mg/L range. Sergeyeva *et al* [85] described the use of a water soluble Pani solution in combination with the same water soluble CP cast on interdigitated planar electrodes as a immunoelectrochemical assay for IgG. A range of Pani molecular weights were examined, and it was found that the detection of IgG was significantly affected by this parameter. The Pani molecules were used as a label for one of the components of the

binding pair, and IgG presence measured by monitoring conductance upon binding. The LOD of this method was 500ng/mL of unlabelled IgG.

Such detection systems are of interest in the analysis of samples contaminated with microorgansisms, an area of extreme importance in water supply management, waste water treatment, and the food industry. It was due to the importance of these areas, and the potential of water soluble CPs for chemical sensing, that we sought to detect the microorganism *Listeria Monocytogenes* using water soluble Poly-methoxyaniline sulfonate (PMAS). Chapter 6 reports on an electrochemical investigation of PMAS in relation to molecular weight fraction, and various electrochemical properties. CPs have also been used in the vapour phase for detection of microorganisms, which will be mentioned later in the electronic nose section of this review.

1.5.2 Gas Sensors

As the main focus of this thesis is on the development of CP gas/vapour sensors for environmental monitoring, some time will now be spent examining proposed explanations for the detection mechanism of such devices, after which actual examples of application will be discussed.

1.5.2.1 Detection Mechanism

When exposed to molecules in the vapour phase, conducting polymers undergo changes in resistance, which for many species are linear over a wide concentration range. The mechanism of this interaction has been investigated by a number of different workers over the last decade, and still some controversy exists over the actual processes involved. Early studies on CP/vapour interactions suggested that in the presence of nucleophilic vapours or gases such as NH_3, the polymer is reduced causing a marked

increase in resistance due to a lower number of positive charges along the backbone [86-88]. Similarly, in the presence of electrophilic vapours such as NO_2 the polymer is oxidised, the number of positive charges increases and hence decreases in resistance are observed [89, 90]. However, Li *et al* [88] found that for Pani gas sensors based on emeraldine salt, an increase in resistance was observed upon exposure to NO_2. They suggest that as this form of Pani is in the highest oxidation state obtainable, further removal of electrons by the NO_2 leads to an increase in film resistance, or in other words, over-oxidation. Agbor *et al* [89] used the emeraldine base form, which is at a lower level of oxidation than the salt, and hence oxidation by NO_2 leads to a decrease in resistance rather than over-oxidation. Another exception to the proposed redox-type mechanism of CP/vapour interaction was noted for PPy exposed to H_2S. While this species is a nucleophile, and hence would be expected to cause decreases in PPy conductivity much in the same way as NH_3, this was not the case. Increases in conductivity were noted, which has been suggested were due to the dissociation of H_2S into HS^- and H^+. While the HS^- acts to reduce the PPy film, the presence of protons which have high mobility along the chains induce ionic conductivity leading to an overall decrease in resistance of the polymer film [91].

Kukla *et al* [92] suggest that the interaction between NH_3 and Pani involves protonation/deprotonation reactions between the ammonia and N-H adsorption centres on the polymer. Both the Pani and NH_3 compete for protonation in this mechanism, which is said to involve both physical adsorption and chemisorption. Tan and Blackwood studied the interaction between Pani and methanol for both the emeraldine salt and emeraldine base forms. An increase in conductivity was observed for the Pani salt in the presence of methanol, while the opposite effect was noted for the emeraldine base. In both cases methanol molecules hydrogen bond to N-H groups on the polymer

affecting the spacing between polymer chains. As the quinoid moieties' nitrogen is protonated in the case of the emeraldine salt, methanol molecules cannot form bridges between the chains, instead forcing them further apart, which leads to uncoiling and increases in conductivity. The corresponding species in the emeraldine base is not protonated, and hence bridges can be formed between chains causing more coiling and localisation of charge carriers (decrease in conductivity). It is also thought that in both cases electron density is drawn from the Pani by the methanol as a result of the hydrogen bonds formed, which in the case of the salt leads to increased conductivity, but for the emeraldine base is localised in specific areas of the polymer leading to decreases in conductivity [93].

The electron affinity of an electrophilic gas or vapour relative to that of the dopant within a CP is also known to affect the interaction. It has been shown using chemically doped PPy films that if the dopant is less electrophilic in nature than the analyte, a decrease in resistance will be observed upon exposure [94].

Changes in the thickness of PPy films have been observed in parallel with variation in conductivity upon exposure to methanol vapours. It was suggested that during this swelling, conducting cross-links between chains in the CP are lengthened causing increases in film resistance. This infers that the response of CPs to vapours has a dual nature comprising both redox interactions, which modify the oxidation state of the polymer, and swelling which increases the distance electrons are required to hop between chains. As a result apolar vapours also induce conductivity changes in CP sensing layers, and hence can be detected [95]. It has been suggested that this swelling effect is not uniform for thicker CP films, and by measuring the resistance at different points across a single PPy layer, discrimination between methanol, ethanol and propanol was possible [96]. The effect of pyrrole ring substituents on vapour responses has been

examined with the view to utilising the swelling process for improved detection of non-polar volatile organic compounds. [97]. It was suggested that by attaching non-polar alkyl side-chains to the polymer, vapours of this nature would be more likely to interact via van der Waals forces and H-bonding, leading to stronger swelling-type responses. Much higher sensitivities to non-polar vapours such as hexane and toluene were observed for 3-alkyl PPys compared to PPy alone, which did not respond to these analytes. From this it was also postulated that the presence of the alkyl substituents limits cross-linking during polymerisation. As the chain length of the substituent is increased, the extent of cross-linking decreases and the influence of swelling interactions becomes greater. Josowicz *et al* [98] improved the selectivity of PPy potentiometric gas sensors toward toluene vapours by electrochemically incorporating nitrotoluenes into the CP matrix. Responses to toluene increased substantially when these species were present, which is thought to be due to an increase in electron affinity in the presence of the nitrotoluyl radical.

Vapour molecules are thought to also interact with dopant ions incorporated in CP films [96, 99], which may explain some of the selectivity obtainable by simply varying this factor. For example, Topart and Josowicz noted that the nature of the counter anion in PPy films significantly affected the surface density of states, which in turn had a substantial effect on interactions with methanol vapours [100]. Interactions between organic vapours, the polymer, and incorporated dopant anion have also been said to cause small but significant changes in conformation of the CP. This leads to changes in the degree of π conjugation along the CP backbone, and hence conductivity is affected [101]. Selampinar *et al* [90] suggested that the hopping process involved in electron transfer in CPs is can be enhanced by grafting or copolymerisation with other polymers, and hence responses due to the redox interactions described above are more

pronounced. They showed that PPy-polyamide copolymer films possessed better gas sensitivities to both NH_3 and CO_2 in terms of response speed and reversibility.

This process is widely accepted as one possible mechanism occurring between CPs and vapours, however, not all species that affect the resistance of CP films fall into this class. Polar organic molecules such as methanol, ethanol and acetone cause significant changes to CP film resistance. It has been suggested that these species also donate electron density into CP sensing films leading to a increase in resistance [102]. Blackwood and Josowicz [103] employed work function and spectroscopic studies to elucidate the mechanism of interaction between PPy and organic vapours. By incorporating an electron accepting dye into a PPy film, they showed that electron density was transferred from methanol vapour into the CP film. The mechanism they proposed involves movement of electron density into/out of the π backbone of the CP from/into the organic vapour. Vapour-induced shifts in the work function of a CP were found to be related to the size and electronegativity of the vapour.

1.5.2.2 Resistometric Gas Sensors

These devices rely solely on changes in resistance occurring within a CP layer on exposure to a gas or vapour due to the processes outlined above. The parameter measured is usually either voltage or current across the resistive element, which will change relative to the conductivity of the sensor.

Feng and MacDiarmid discuss examples of the potential application of CPs for detection of toxic gases released in subways, in the field by military personnel, or at old military waste dumps. A gas sensor based on octaaniline is reported for the detection of toluene that showed remarkable sensitivity to this species. Changes in resistance of 1% were noted upon exposure to 35 ppm of toluene in air, and interferences from water

vapour were not as significant as for most CP gas sensors [104]. Thin films of electropolymerised PPy have been reported for the detection of BTEX vapours. Resistance changes in the presence of ethylbenzene were most significant (8.3 Mohm/ppm), with reasonable sensitivities observed for benzene (2.3 Mohm/ppm), toluene (0.4 Mohm/ppm) and xylene (2.9 Mohm/ppm) [105].

Misra *et al* [106] reported on the development of sensors for toxic gases in the environment, such as trimethylamine, using semiconducting polymers. Toxic gas and vapour sensors based on PPy have also been reported for the detection of hydrogenhalides, hydrogen cyanide, halogenes, hexachloroacetone (HCA), 1,3,5-trichloro-methylbenzene (TCMB), methylbenzyl bromide (MBB), bromoacetone (BA) and cyanogen bromide [107]. Pani has also been used for the detection of hydrogen cyanide at very low levels in a suspended gate field-effect transistor device. The Pani film, which had clusters of mercury incorporated within, responded to HCN in the concentration range 0 to 19.3 ppm. Pani films without the mercury clusters did not respond to HCN [108].

de Souza *et al* [109] employed different PPy sensors for the detection and discrimination of methanol, ethanol, carbon tetrachloride and benzene. They found using PCA that not only could these vapours be successfully identified, but that more general data grouping was observed based on polarity.

Humidity sensing has also been successfully demonstrated using PPy in combination with different anion-exchange membranes [110]. Composite membranes were prepared using commercial anion-exchange membranes, with quaternary ammonium groups, and polypyrrole coatings deposited by chemical oxidation using ferric salt solutions. Humidity sensitivity varied according to the anion incorporated during PPy formation, and was thought to depend upon the hydration force of the anion. Sensors with Cl^- and

NO_3^- ions responded well, with maximum potential shifts of 330 mV and 200 mV respectively at 90% humidity, but these changes were irreversible due to strong interactions between the anion and water molecules. Sensors with SO_4^- ions showed good reversible potential changes in response to changes in humidity (260 mV change at 90% humidity), while ClO_4 doped films displayed lower sensitivity to humidity with reversible changes in potential of 140 mV at 90%. Composite films containing the conducting polymer poly(*o*-phenylenediamine) and PVA have also been employed for humidity sensing, with linear changes in conductivity in the range $2.5 * 10^{-5}$ to $1.5 * 10^{-2}$ S/cm from wet to dry state [111].

As discussed earlier, CP films are known for their sensitivity to ammonia, and this property has been exploited in the development of devices for the detection of this species. A Pani gas sensor prepared by emulsion polymerisation has been described, which was able to detect ammonia at levels as low as 10 ppm. The sensor performed reliably over a period of 80 days, and the effect of humidity on sensor response was much smaller when compared with that of ammonia gas [112].

Hirata and Sun [113] employed a chemically deposited Pani film for selective detection of ammonia in the presence of interfering gases including H_2, CO_2 and O_2. Decreases in sensor resistance were observed at 5 ppm NH_3, and detection at this low level was not affected by the presence of 1000 ppm H_2, CO_2 or O_2. The sensor was also responsive to Cl_2 gas at 5 ppm, but the resistance change was in the opposite direction to that observed for ammonia. Gas sensors based on poly-beta-bromothiophene have been developed to respond selectively to bromine vapours [114]. Chabukswar *et al* [115] recently reported an acrylic acid doped Pani sensor for the detection of ammonia over a broad range of concentrations (1 to 600 ppm), for which the resistance decreased upon exposure to ammonia. This trend is in complete contrast to the normal behaviour of Pani when

exposed to ammonia, and is thought to relate to interaction between the acrylic acid and ammonia leading to the formation of COO^- within the Pani film.

PPy also exhibits sensitivity to ammonia, as was first noted by Nylander *et al* [116] who observed 30% changes in conductivity of a pyrrole black impregnated filter-paper when exposed to 1% NH_3. However, the sensitivity and reversibility of this and other early devices was not good [117, 118]. More recently PPy gas sensors with improved sensitivity to ammonia have been reported [119]. Free standing films of PPy/perchlorate were used to detect 10 ppm ammonia, with changes in resistance of 150% observed at this concentration inferring a much lower limit of detection could be obtained. These responses were stable over a period of 60 days, and in fact the sensitivity to ammonia increased after a period of 80 days. PPy/*p*-toluenesulphonate films were also evaluated, and while responses were also observed to 10 ppm ammonia, the sensitivity was considerably lower. This highlights the importance of the incorporated counter-ion on CP gas sensing performance.

PPy films have also been used for the detection of ammonia gas in the presence of interfering gases such as CO, CH_4, H_2, N_2 and O_2. The films, which were prepared by the Langmuir-Blodgett technique, could detect 100 ppm NH_3 with only negligible responses to the interfering gases. The performance of this sensor was compared to an electrochemically deposited device and found to be two-three times more sensitive at low concentrations [120]. PPy sensors based on acrylic substrates for the detection of ammonia and hydrazine have also been investigated. The importance of detecting hydrazine relates to the fact that the human olfactory threshold for this species is above the threshold at which permanent damage can be caused. Both ammonia, and hydrazine

were detected at very low levels, 0.00001% in the case of ammonia and 0.0025% for hydrazine [87].

Poly(3-octylthiophene) Schottky barrier diodes have been used for the detection of ammonia and nitric oxide at concentrations of 100 ppm, with minor responses observed for ethanol, and virtually no responses for water vapour [121].

Domansky *et al* [122] reported a field-effect transistor based sensor array that used Pani/palladium films for the detection of hydrogen and ammonia gas mixtures in humid air. The sensing array, which was exposed to such mixtures in humid air over a concentration range of 0 to 10 000 ppm, gave very good responses to ammonia, and showed high sensitivity to hydrogen in spite of less stability in the presence of this gas. A Pani/poly(bisphenol-A carbonate) composite sensor was reported for the detection of ammonia at levels of 0.025% v/v, and gave better defined, more reproducible responses than pristine Pani films [123]. PPy has also been used in a composite sensing film for ammonia, combined with thermoplastic binders and a proprietary glass-fibre paper. The response of PPy to non-polar vapours was enhanced by the presence of the thermoplastic binder. Volatile amines including ammonia, methylamine, dimethylamine and trimethylamine were successfully detected at 1 ppm, with good responses shown over a range of 50 to 1000 ppm [124]. Gangopadhyay and De [125] used a PPy/PVA composite for the detection of ammonia that showed large increases in resistance at low concentrations (1 to 4%) of the test vapour.

Common atmospheric pollutants, such as NO_x and SO_2, have also been monitored using CP gas sensors. Barker *et al* [126] developed a Pani charge-flow transistor for the detection of NO_x and SO_2. The advantage of this approach to sensing is that larger currents are measured, which reduces problems with noise. Responses were observed upon exposure to NO_x at concentrations of 1 ppm, however, these could not be

differentiated from responses to 2 ppm NO_x. In the case of SO_2, the sensitivity was lower with a LOD of 2 ppm. These workers also reported on a Pani/Silicone hybrid field-effect transistor for detection of NO_2 at a concentration of 8 ppm [127]. SO_2 gas sensing has also been carried out using PPy/dodecylbenzene sulfonic acid films, which gave responses in the concentration range 500 to 2500 ppm that were influenced by dopant levels in the films [128].

Pani thin films for CO_2 sensing have been prepared by plasma polymerisation, and were reported to respond rapidly and reversibly to this analyte [129]. The detection of CO using PPy electrodeposited on an inderdigital-capacitor was reported by Liu *et al* [130]. CO was successfully detected using this device at 100 ppm, and maximal sensitivity was observed at 500 ppm. CO_2 detection with PPy-polyamide composite films has also been reported [90]. Metallophthalocyanine-doped PPy/silicon heterojunctions have been described for the detection of NOx at ppm levels [131, 132]. Torsi *et al* [133] describe CP sensors based on PPy and poly-3-methylthiophene doped with copper and palladium inclusions for the detection of NH_3, H_2, and CO gases. Highly reversible and reproducible responses to CO and H_2 were observed for the Pd doped PPy, but these were of the opposite direction to those of the Cu doped PPy and normal PPy. A Pani film doped with nickel-containing anions has also been reported for the detection of ammonia in the range 1 – 10000 ppm [134]. Composite films of Pani/polyethyleneoxide doped with copper chloride were found to show enhanced sensitivity to alcoholic vapours, and in particular to methanol [135].

Lin *et al* developed an ethanol vapour sensor based on electrochemically codeposited PPy/polyvinylalcohol(PVA) thin films. Sensitivity of this device to ethanol increased as the amount of PVA increased to a point at which no further addition of PVA improved

responses. In spite of enhanced sensitivity to the alcohol, some lose of response speed and sensor stability was noted [136].

de Souza *et al* reported on the use of PPy gas sensing arrays for the detection and discrimination of methanol, ethanol, and carbon tetrachloride [137]. Micro-bridge type resistive sensors based on PPy and Pani have been reported for the detection of ethanol in the presence of varying temperature and humidity levels. These devices were able to detect 5% ethanol in air under varying condition of humidity and temperature, and showed good responses to ethanol at less than 3000 ppm under fixed conditions [138]. Pani chemoresistor gas sensors have also been pre-treated by dipping in solvents such as methanol and ethanol to modify responses to vapours. These devices were used to successfully discriminate between water, methanol, ethanol, acetone, and isopropanol at concentrations of 20% saturation [139]. In other work carried out by this group, the effect of varying the dopant anion on sensing properties of a PPy gas-dependent field effect transistor was demonstrated. The responses of PPy/butane sulfonic acid and PPy/tetraethylammonium tetraflouroborate devices to isopropanol were of opposite sign, and of differing magnitude [140].

PPy gas sensors have also been evaluated for potential use in portable monitoring of health and safety, for example exposure of house painters to dangerous vapours. Responses of these sensors to toluene, butanon and ethanol were obtained, but the significant effects of water and ageing were such that further work continues to address these issues [141].

The concept of competitive doping, where a mix of different dopants are present in the same polymer film, was shown by Cabala *et al* to effect the vapour sensing properties of PPy. Using PPy films doped with either tetraflouroborate or perchlorate, and tetrasulfonated metallophthalocyanines, the Kelvin probe responses to

dimethylmethylphosphonate, tetrachloroethane and NO_x were better than those of pristine PPy. The detection range of the mixed dopant films for NO_x in air was 0.4 to 40 ppm, and 2 – 40 ppm for dimethylmethylphosphonate [142].

1.5.2.3 CP Mass Sensors

The main advantage of using CPs as the chemically sensitive layer on a QCM mass sensitive device is that the sensing film can be electrodeposited to give a very uniform coating of desired thickness, rather than requiring other less controllable methods of deposition such as casting or chemical oxidation. Changes in the oscillation frequency of the coated QCM are directly related to variations in mass, proving an accurate means of measuring adsorbed chemical species. These devices can and have been used both in the gas phase and in solution for chemical sensing, although the later is often a more complex problem due to solution viscosity effects.

A decade ago Slater and Watt [143] demonstrated the use of polypyrrole coated QCMs for the detection of ammonia vapours. Electrodeposited layers of PPy doped with common inorganic anions such as Br^-, NO_3^-, and SO_4^{2-} were employed to detect ammonia at between 0.5 and 1.0%. Simultaneous mass and conductivity measurements were carried out, by employing a second type of electrode that enabled film resistance to be monitored, and it was found that the two signals corresponded. What was also illustrated in this work is the careful control over film thickness achievable when electrochemical layers of CPs are grown onto QCM devices. Syritski *et al* [144] employed electrodeposited PPy doped with *p*-toluenesulphonate on QCM devices for the development of environmental SO_2 and humidity sensors. Linear responses were observed for ammonia over a range 0 – 100%, and 0 – 76% in the case of humidity. PPy coated QCM sensors have also been employed to detect NO_2 and other noxious

vapours including H_2S. PPy/tosylate and PPy/silicon phthalocyanine sensors exhibited linear responses to NO_2 over a concentration range of 10 to 100 ppm, and gave signals in the presence of 25 ppm H_2S [145]. Kunugi *et al* [102] employed specially designed QCMs that allowed for simultaneous measurement of frequency and resistance on the one crystal device. Coatings of PPy doped with tetraethylammonium tetraflouroborate were deposited electrochemically and then used to detect primary alcohols (methanol, ethanol, propanol, butanol), acetone and water. It was shown that by measuring only conductivity similar responses were obtained for the four alcohols, while when frequency changes were included in the analysis, discrimination between all four species was possible. Cui *et al* [146] used a range of electrodeposited polypyrroles, doped with sulfonated organic salts, on both QCMs and separate interdigitated microelectrodes for sensing a variety of organic vapours including methanol, ethanol, propanol and butanol, acetone and toluene. By combining the QCM and resistance data, better discrimination between compounds was achieved, and it was possible to reduce the total number of sensors required. Hwang *et al* [147] used PPy, as well as PPy/ PEO and PPy/PAN composite polymer coatings, on QCMs to monitor alcohol vapours such as methanol and ethanol. Specially designed QCMs allowed both mass and resistance changes to be monitored simultaneously on the same polymer film. Better odour identification was achieved using the $\Delta R/\Delta F$ ratio rather than each property alone, whilst quantitative information could be taken from either measure. All three sensing films gave good responses to both methanol and ethanol at the lowest test concentration of 14 mg/L.

CPs have also been used as the chemically sensitive layer in surface acoustic wave (SAW) devices, which employ surface waves rather than oscillations through the bulk as is the case with QCM devices. Milella and Penza [148] reported on the use of Langmiur-Blodgett (LB) PPy films for a SAW ammonia sensor. The device exhibited

an excellent dynamic range to NH_3 (100 – 10000 ppm) and a LOD of 18 ppm from calibration data in the 0 – 200 ppm range. This is much lower than the LOD determined for the same polymer film in a resistive type sensor, which was 100 ppm [120]. These workers also reported on the responses of a resistive type sensor based on a LB PPy film exposed to organic vapours. Good reversible responses were noted to methanol and ethanol, smaller responses were observed for ethyl acetate and acetone, while toluene had a only minor effect on film conductivity [149].

1.5.2.4 Optical Sensors

CPs have also been employed in optical gas sensors. Pani has also been used to develop and optical sensor for ammonia that relies upon spectral changes in the film caused by vapour exposure. The interior surface of clear polyethylene tubes was coated by chemical oxidation of aniline, and spectral changes in the resulting Pani film were monitored during exposure to a flowing stream of ammonia vapour in nitrogen. It was possible to detect NH_3 at 1 ppm, and the sensor had a linear dynamic range of 180 – 18000 ppm. Also, the sensor exhibited a rapid response time of only 15 seconds, and recovered within 2 minutes after exposure [150]. In a variation on this approach, the optical properties of Pani and Pani/polymethyl methacrylate composite films were monitored by using a 632 nm laser (He-Ne) source to detect ammonia vapours in the concentration range 10 to 4000 ppm [151]. An optical Pani gas sensor has also been developed, based on surface plasmon resonance, for the detection of H_2S and NO_2, with LODs of approximately 50 ppm [152].

1.5.2.5 CP Electronic Noses

CPs have been used extensively in electronic nose systems for the detection and discrimination of a range of different volatile substances. An electronic nose generally consists of a group or array of vapour sensors, a sample delivery system, onboard electronics for both system control and monitoring of the sensors, and a computer equipped with appropriate data acquisition and analysis software. The distinguishing feature of an electronic nose is the manner in which samples are analysed. The pattern of responses from an array of non-specific sensors is obtained to give a unique fingerprint for a particular vapour or sample. In the case of CP electronic noses, the sensor array comprises a group of chemoresistor detectors, usually based on PPy, Pani and PT, which undergo changes in resistance upon exposure to vapour molecules. The magnitude, and in some cases the direction of response, varies depending on the CPs used to build the array and the nature of the sample analysed. The pattern of responses generated upon exposure to a volatile substance or mixture of vapours is analysed by recognition software, typically using Principal Component Analysis (PCA), allowing for both identification and quantification of unknown samples. CP based electronic noses have found application mainly in the areas of food and beverage analysis and quality control, with examples in the literature describing olive oil classification [153, 154], discrimination of wines [155], quality control of beers [156], determination of boar taint odour intensity in pork [157], discrimination of odours arising from 'La France' pears [158], and the assessment of wheat degradation by mite infestation [159] to name but a few. CP electronic nose systems have to date not been used widely for environmental sensing, but some examples have been reported and these will now be discussed.

An electronic nose was employed to monitor air quality of the MIR space station on the EuroMir '95 and DARA Mir '97 missions. The system, which employed a 20 element CP sensing array, was able to distinguish different activities such as meal times and sleep periods based on changes in the station atmosphere. Of more importance was the ability to analyse the composition of the onboard drinking water supply, and the detection of a contamination event that occurred when a cooling system leak led to the introduction of ethylene glycol. To test the system for detection of atmospheric contaminants ethanol vapour was deliberately released into the station air supply. The electronic nose successfully discriminated between this event and ambient baseline conditions. After an operational period of 1.5 years aboard the space station, the system was still functioning reliably with little drift or degradation in response [160].

Stuetz *et al* [161-163] have used an electronic nose based around an array of 12 PPy sensors to characterise wastewater samples. In one study [161], raw sewage, settled sewage, and final effluent samples from three different treatment works were analysed by the system to provide feedback on processes occurring within each plant, and between them. The nose successfully differentiated between the three types of sample, raw, settled, and final within each treatment works. The system was also able to detect differences in each type of sample over time within a plant. Differentiation between each sample type from the three plants was possible, and a correlation was found to exist between actual BOD_5 values and response patterns from the nose. This infers that with appropriate calibration the system could be used to provide real-time feedback on variations in the biochemistry of the treatment process. This would be of great benefit for optimal operation of such facilities, which currently rely on length BOD_5 testing for data. In other work carried out by this group, the CP electronic nose was used to successfully identify water samples tainted with various organic contaminants including

phenol, 2-chlorophenol, 2-chloro-6-methylphenol, diesel, methylisoborneol, and geosmin. Tainted and untainted samples were discriminated, and different taint concentrations were clearly separated using multiple discriminant analysis of the data [162].

Analysis of waste water treatment plant samples has also been carried out with a CP electronic nose for atmospheric odour annoyance analysis [164]. An array of alkoxy substituted PTs were employed to monitor the odour profiles of untreated industrial waste water, partially treated industrial waste water, and untreated municipal waste water. Dilutions of the three sample classes were also analysed by the system to simulate different sampling distances from the effluent source. After sufficient training the system was able to recognise undiluted samples with a 95% success rate. The diluted samples were recognised 83.3% of the time, which suggests such a system could be used to monitor odours at more diluted concentrations as would encountered at increased distance from the source.

CP electronic noses based on PPy have been used by others to successfully detect taints such as diacetyl, DMS, and laa in water samples at levels as low as 500 ppb [165].

CP electronic noses have also found application in the area of agricultural malodour assessment. Byun *et al* [166] reported on measuring the odour of fresh faeces from pigs that have been fed different diets in order to determine which produced the least obnoxious odour for humans. Cluster analysis on the data gathered for odours arising from a normal diet and protein reduced diet showed that the two were successfully discriminated by the system. Malodour concentrations have also been assessed by an ICP electronic nose after cattle slurry was applied to grassland [167]. The responses of a CP sensing array to a range of eight volatile and semi-volatile halogenated organic compounds of environmental significance have been reported [168]. 2,4-dinitrophenol,

which continues to be important in the production of chlorinated phenoxyacetic acid herbicides, 2,4,5-trichlorophenol, pentachlorophenol, 1,1-bis(4-chlorophenyl)-2,2,2-trichloroethane (DDT), and 2,2-bis(4-chlorophenyl)-1,1-dichloroethylene (DDE) were some of the more important substances detected successfully by the system. The compounds were discriminated on the basis of differences in size, polarity, vapour pressure, and the type and position of functional groups present.

Hudon *et al* [169] compared the performance of a CP based electronic nose with another system based on metal oxide sensors for the detection of n-butanol, CH_3COCH_3, C_2H_5SH and mixtures of n-butanol and CH_3COCH_3. They reported that the CP system detected these vapours most effectively, with a linear correlation between odour intensity and average sensor response.

Using an array of PPy/plasticizer composite sensors, Freund and Lewis [5] report on the detection and discrimination of organic vapours of environmental interest, such as benzene, chloroform, acetone and tetrahydrofuran, in air at parts per thousand concentrations. PT has also been used in a similar composite sensor, which consisted of poly(3,4ethylenedioxyl)thiophene-poly(styrene sulfonate) films, for sensing both polar and non-polar organic vapours [170]. Sotzing *et al* [171] have also employed Pani/carbon black composite sensors for detection of biogenic amines such as butylamine at levels of 1 – 10 ppt. These sensors were tested with water, acetone, methanol, ethyl acetate, and butanol, but gave much smaller responses in comparison to the highly sensitive response to butylamine. Composite Pani/PVA sensors, containing the base form of Pani, have also been reported for the detection of CO_2 [172]. Conn *et al* [173] described a Pani/platinum oxide chemosresistor and response to combustible gases including hydrogen, methane, ethylene, acetylene and CO. The devices showed

sensitivity for hydrogen in the concentration range 1000 to 5400 ppm, with only minor responses to hydrocarbons and CO.

An array based CP system has been reported for the discrimination of CO_2, methanol and acetone, for which responses to CO_2 were opposite in polarity to those observed for the other vapours examined [174]

CP electronic noses have also been employed for the detection of microorganisms by sampling the headspace produced by the cultures. The volatiles produced are to some extent specific to a particular microorganism, and hence can be used to discriminate between different cultures. Such a system, based on an array of 12 PPy gas sensors, was used to detect microbial contamination in a bioprocess and monitor growth during cultivation of microorganisms for inoculum and antibiotic production [175]. In other applications, CP electronic noses have been used to detect pneumonia and other lung infections in hospital patients [176]. Gibson *et al* used a 16 sensor CP array to successfully discrimination between a range of yeasts and bacteria including *E. coli*, *Salmonella Virchow* and *Staphylococcus Aureus* [177]. Analysis of a more complex sample matrix, milk, contaminated with microorganisms has also been demonstrated [178]. Using an array of 14 CP sensors, it was possible to discriminate between unspoilt milk and samples containing bacteria (*Pseudomonas aureofaciens, P. fluorescens, Bacillus cereus*) and yeasts (*Candida pseudotropicalis, Kluyveromyces lactis*).

1.6 Thesis Outline

Chapter 2 describes the development of PPy gas sensors based on clear polyester polymer film substrates with screen-printed carbon electrodes. Optimisation of the fabrication process was investigated before sensor performance was evaluated using

methanol. The use of these sensors in place of lithographically prepared electrodes for organic vapour detection and discrimination was examined. Chapter 3 describes various chemical-electrochemical solution based treatments used to alter the vapour phase sensing properties of chemically deposited PPy films. The affect of these on sensor properties and response to some organic vapours was examined. Approaches to reducing the humidity response of PPy vapour sensors are reported in Chapter 4. The use of cast hydrophobic silicone membranes, and polymer diffusion sampling tubes were considered to enable detection of organic volatiles in water. Chapter 5 reports on the application of PPy/Cl screen-printed sensors, and solution modified sensors as described in Chapter 3, with a small autonomous mobile robot to detect, track and locate the source of ammonia vapour plumes. Such a system could prove invaluable for the detection of dangerous or environmentally hazardous gas and vapour leaks. Chapter 6 details a study of the water soluble CP Poly(methoxyaniline sulfonic acid) (PMAS), and in particular the effect of molecular weight on electrochemical and spectral properties. The influence of MW on the performance of a PMAS voltammetric solution based *Listeria* detection system is reported. Conclusions about the work presented herein, and recommendations for future work arising from this thesis are given in Chapter 7.

Chapter 2

Development of Conducting Polymer Coated Screen-Printed Gas Sensors for Measurement of Volatiles

2.1 INTRODUCTION

Conducting polymers (CPs) have been used in a wide variety of gas sensing applications for a number of years, including commercial electronic nose systems such as Bloodhound [177], AromaScan [179] and eNOSE [175]. Gas sensors based on CPs make use of the fact that these materials undergo resistance changes in the presence of volatile compounds. The CP polypyrrole (PPy) is an attractive material for use as a gas sensitive layer due to its environmental stability, and the ease with which it is prepared. Electrochemical fabrication of PPy sensors allows a wide range of dopants to be incorporated into the polymer giving greater control over film morphology and chemistry.

CP gas sensors have been prepared on a range of substrates including silicon [180], alumina ceramic [177, 181], quartz [100] and modified commercial ceramic capacitors [5]. CP sensor development in our laboratories has focused on the use of lithographically defined gold tracks on silicon as the base substrate [180]. The advantages of silicon include the narrow inter-track gaps achievable and the stability of the substrate. Disadvantages include the high cost and the lengthy production times associated with the manufacture of these electrodes.

Screen-printing techniques have been used extensively in the preparation of electrodes for solution based electrochemical analysis [e.g. 182-187], particularly for the production of disposable devices where the issue of fabrication cost is paramount. While screen-printing has been used extensively to print metal oxide gas sensing layers over interdigitated electrode structures [188-193], the use of the technique for printing the electrode support structures of gas sensors is not common [e.g. 194-196]. An extensive literature search revealed only one example of a conducting polymer chemoresistive gas sensor, for which the film was deposited electrochemically to bridge screen-printed

electrodes. However, in this case a single thick film electrode layer of Pd-Pt-Ag was screen-printed on alumina ceramic, after which laser engraving was employed to cut a gap (10 – 60 •m) in the structure forming two separate electrodes [197]. To our knowledge, there are no reports on the use of conducting polymer gas sensors deposited electrochemically on inexpensive polymer substrates with electrode tracks formed by screen-printing alone. This may be due to limitations in the resolution of the structures produced by screen-printing which are of the order of 100 - 200 •m [198, 199].

2.1.1 Aims and Approach

This chapter details an investigation into the use of polymer substrates, upon which carbon electrode tracks were deposited by screen-printing, for the development of novel PPy gas sensors.

Initially, direct galvanostatic growth onto the carbon tracks and over the polymer substrate was employed in an attempt to electrodeposit eight different PPy sensing films. The influence of the underlying substrate on this process was investigated by using Melinex (polyester), polyvinylchloride, polypropylene and polycarbonate for screen-printing carbon tracks. In order to facilitate electrodeposition and obtain more uniform conducting polymer films the effect of depositing a PPy/Cl layer by vapour phase polymerisation was examined. Optimisation of this approach was carried out using PPy/Tiron, a polymer that is known to electrodeposit efficiently due to the catalytic effect of Tiron [200].

Having established the most suitable approach to sensor preparation, a comparison was made between the performance of PPy sensors fabricated on polymer substrates with screen-printed carbon tracks, and on gold electrodes deposited lithographically on silicon. Limit of detection (LOD), and linearity of response to methanol were

examined. Responses of both sensor types to a variety of other common organic compounds in the gas phase were compared, and principal component analysis was used to establish the utility of the new sensor design for vapour discrimination.

2.2 EXPERIMENTAL

2.2.1 Chemicals and Materials

Pyrrole (Merck) was distilled prior to use *p*-Toluenesulfonate (pTS) was obtained from Merck and used as supplied. All other dopants [4-hydroxybenzenesulfonic acid (HBS), 4,5-dihydroxy-1,3-benzenedisulfonic acid (Tiron), 4-sulfobenzoic acid (SB), methanesulfonic acid (MS), 3-nitrobenzenesulfonic acid (NBS), 1,5 napthalenedisulfonic acid (NDS) and Polysodium-4-styrenesulfonate (PSS)] were obtained from Aldrich and used as received. $FeCl_3$ was obtained from BDH. $NaNO_3$ was obtained from Ajax and $K_3Fe(CN)_6$ from BDH. All solutions were prepared in deionised Milli-Q water (18MΩ/cm). All solvents used for testing were obtained from BDH and were of AR grade. For preparation of screen-printed electrodes on polymer substrates Electrodag 423SS carbon ink was obtained from Acheson. Melinex™ ST725 polyester film was obtained from Industrial Group, ICI New Zealand Ltd. Other polymer substrates were obtained from Goodfellow.

2.2.2 Instruments

All screen-printing was carried out using a DEK 245 semi-automatic printer (DEK Printing Machines Ltd., UK). An in-house galvanostat (Science Faculty Workshop, University of Wollongong, Australia) was used for electrochemical deposition of polymers onto the screen-printed sensors. Silicon chip sensors were prepared using an in-house potentiostat (Industrial Research Limited, Lower Hutt, New Zealand). Cyclic voltammetry of the polymers was carried out using an ADI Maclab potentiostat and EChem software. Scanning electron microscopy (SEM) was carried out using a LEO440 Scanning Electron Microscope. Atomic force microscopy (AFM) was carried

out on a Jeol 2000 Multimode instrument operating in contact mode. Video images were taken using a National WV-CD black and white camera and captured using Video Pro software.

2.2.3 Screen-printing

Commercial screen-printing carbon ink (Electrodag 423SS, Acheson) was used to print four parallel carbon electrodes (0.8 mm in width separated by a 0.5 mm gap, and 17 mm in length) onto various polymer films (Figure 2.1). Each track included a 3 mm x 1.5 mm contact pad for electrical connection. The total track length including the contact was 20 mm, and the track resistance from the contact pad to the end was in the range 5 - 10 kΩ After printing, the electrodes were dried in an oven at 50°C for two hours to cure the ink.

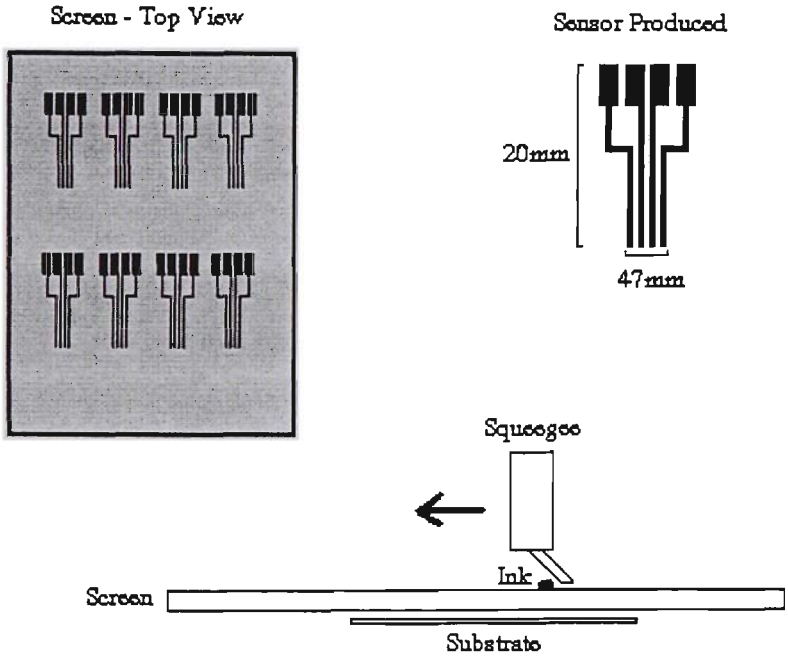

Figure 2.1 The screen-printing process involved in preparation of carbon track electrodes on polymer substrates.

2.2.4 Polymer Deposition

2.2.4.1 Direct Growth on Screen-printed Polymer Substrates

Conducting polymers were deposited galvanostatically, using a standard three electrode cell, directly onto the carbon tracks and over the bare polymer film between them. The four carbon tracks were shorted and used as the working electrode in conjunction with a platinum mesh auxiliary and a Ag/AgCl reference (BAS) electrode. Connection to the screen-printed substrates was made using a modified edgeway connector (RS-components). Polymers were grown at a current density of 2 mA/cm^2, from a 0.1 M pyrrole/0.1 M dopant solution, until the 4 tracks were bridged. PSS was prepared on the basis of monomer weight to give a concentration of 0.1 M. The sensing area was defined by masking with cellulose tape to give a sensing polymer film of dimensions 2 mm x 5 mm.

2.2.4.2 PPy/Cl Coated Melinex

Before electrodepositing the desired conducting polymer, a thin layer of polypyrrole chloride (PPy/Cl) was vapour deposited onto the melinex substrate. The desired sensing area was masked with tape and a drop of 0.5 M $FeCl_3$ in methanol spread over the electrode surface. The resulting film was then suspended above neat pyrrole for one minute to form the PPy/Cl layer. The sensor was washed with Milli-Q water to remove excess methanol solution and monomer before being placed in the monomer/dopant solution for electrodeposition. A range of PPys were deposited galvanostatically, using the conditions employed for deposition onto bare polymer substrates, over the PPy/Cl layer for periods ranging from 4 to 12 minutes. Resistance values of the base PPy/Cl

layer and final electrodeposited film were measured by 2-point probe between the outer tracks with a digital voltmeter.

2.2.4.3 Silicon Sensor Fabrication

The silicon substrate consisted of a silicon chip 5 mm square, coated with 100 nm of silicon dioxide. Four parallel gold electrodes, 10 μm wide with 10 μm spacing, each 2000 μm long were deposited onto the chip using conventional microlithography, and the area of tracks exposed to solution was defined by a glass window (1 μm thick) which was 500 μm long. Deposition of the polymer onto the silicon chip was achieved using a pulsed current technique. The four tracks were shorted *via* a relay and a current pulse of 1-10 mA/cm^2 applied. The resulting voltage was measured relative to a Ag/AgCl reference electrode using the sensor as a working electrode in a standard 3-electrode cell. After each pulse the inter-track resistance was measured in order to determine when the tracks had bridged with conducting polymer. Once contact between the tracks was made both resistance and potential could be monitored simultaneously enabling careful control over the final film resistance [180]. This approach was not used for deposition of PPy onto screen-printed polymer substrates as the large track gap (500 μm) would necessitate extremely long growth times, and the larger size enabled visual monitoring of track bridging.

2.2.5 Vapour Generation

The vapour generation apparatus consisted of a series of solenoid valves, mass flow controllers and gas bubblers containing test solvents [180]. Figure 2.2 depicts a simplified version of this system schematically. The solenoid valves and mass flow controllers were interfaced to a computer and controlled by a series of macros written in Visual Basic (Microsoft Excel). Sample and purge streams were turned on and off using

the solenoids while the total flow rate to the sensors was maintained at 200 mL/min by the mass controllers. Target vapours were produced by bubbling a nitrogen carrier gas stream through an appropriate solvent (A), and diluting this with a second stream of nitrogen (B). The pneumatically actuated rotating 4-way valve, which was also interfaced to and controlled by the PC, was used to switch between the diluted gas stream (A + B) and the nitrogen purge stream (C). This setup allowed a constant gas flow to be maintained over the sensors, which for the majority of time consisted of pure nitrogen (C) when the 4-way valve was in the normal (OFF) position. The test protocol typically comprised a 100 second purge of the test gas (A + B to waste) to allow the plumbing to become saturated, a 10 second 'ON' time during which the sensors were exposed to the test gas (A + B), and a 40 second 'OFF' time during which the sensors were purged with nitrogen (C). The ON / OFF cycles were repeated 4 times for each gas, after which pure nitrogen was purged through both gas lines to remove any residual solvent from the sensing cell and plumbing. The sensors were then purged continually for 100 seconds before testing a new solvent.

2.2.6 Resistance Measurement

Responses of both the silicon and polymer film (usually Melinex) based sensors were recorded by monitoring the resistance using a 4-terminal measurement, to avoid any effect of contact resistance. A 1 kHz constant current set at 1 - 100 μA was passed between the outer pair of tracks and the implied voltage on the inner two tracks measured. This signal was amplified and filtered before being sent to the PC for final output in the form dR/R, the fractional resistance change [180].

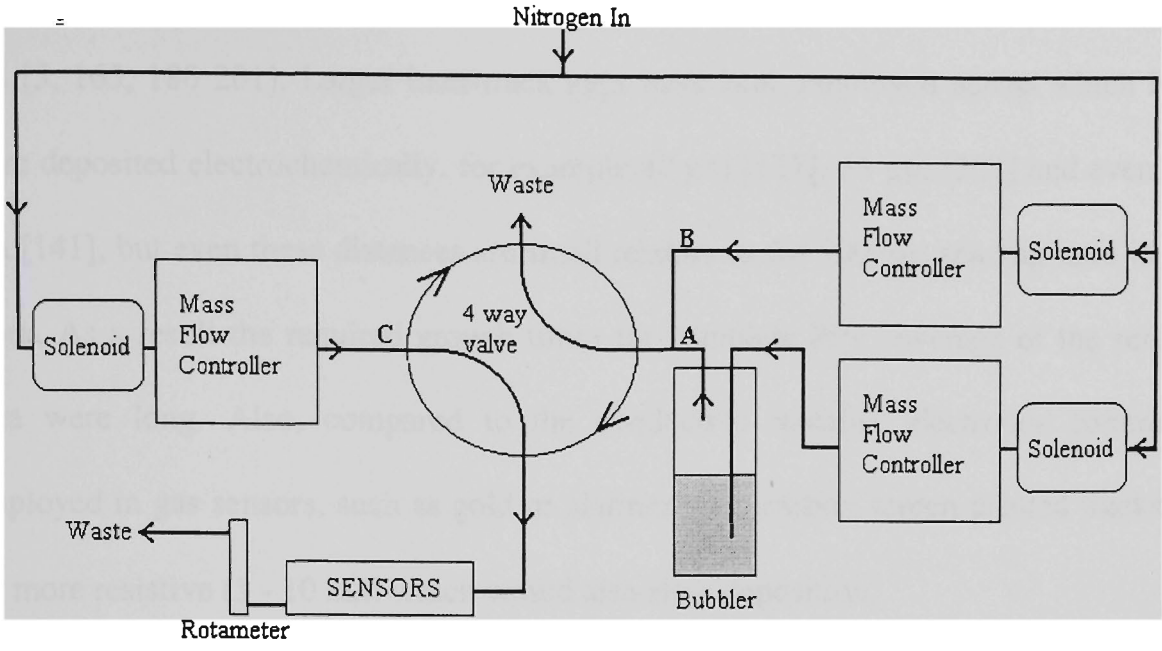

Figure 2.2 Schematic of the gas rig used for generation and delivery of solvent vapours. The rotating 4-way valve was used to switch between solvent vapours diluted with a second stream of nitrogen (A + B) and a pure stream of nitrogen for purging the sensors (C).

2.3 RESULTS AND DISCUSSION

2.3.1 Polypyrrole Deposition

2.3.1.1 Melinex

The polymers deposited onto bare Melinex substrates are listed in Table 2.1, as are the growth times required for bridging and the final resistance value for each sensor. Times for the polymers to completely bridge the inter-track gaps were determined by both visual inspection and measurement of the resistance between the outer pair of electrodes. These times ranged from 20 to 50 minutes, after which the entire sensing area was coated with conducting polymer. Often the tracks bridged before this time was reached but small holes in the polymer coating remained. Growth was continued until these gaps were bridged and complete coverage of the sensing area was obtained. Conducting polymers are known to grow laterally in order to bridge between electrodes

on insulating substrates, but the distances involved commonly range between 10 – 15 μm [5, 165, 180 201]. Larger inter-track gaps have been employed across which PPys were deposited electrochemically, for example 40 μm [137], 55 μm [202] and even 100 μm [141], but even these distances are small relative to the 500 μm spacing used in this work. As a result the required growth times for complete PPy coverage of the sensing area were long. Also, compared to the conductive metallic electrodes commonly employed in gas sensors, such as gold or platinum, the carbon screen-printed tracks are far more resistive (5 - 10 kΩ) which would also slow deposition.

The growth of PPy on the screen-printed carbon electrodes involved the formation of thick, dendritic polymer structures directly over the tracks, which gradually spread laterally to form much thinner bridges in between the electrodes. This process is illustrated in Figure 2.3, which shows a series of video images of PPy/Tiron growth over the carbon tracks. Only six of the eight PPys employed successfully bridged on the bare Melinex substrates. PPy/MS and PPy/PSS films were not close to bridging even after a 60 minute deposition period. Resistance measurements were made using a digital voltmeter between the outer pair of tracks at various stages during deposition to check for bridging, and once growth was completed. The final resistance values given in Table 2.1 were recorded in this manner.

Table 2.1 Growth times for complete coverage of the sensing area and R_0 values for eight PPys deposited on Melinex screen-printed substrates. PPy/MS and PPy/PSS failed to bridge the inter-track gaps after 60 minutes of deposition as indicated by 'X'.

Sensor	Dopant	Growth Time (mins)	R_0 (kΩ)
1	Tiron	20	29.9
2	HBS	30	23.6
3	pTS	40	32.5
4	SB	40	22.4
5	NBS	45	24.0
6	NDS	50	21.6
7	MS	60	X
8	PSS	60	X

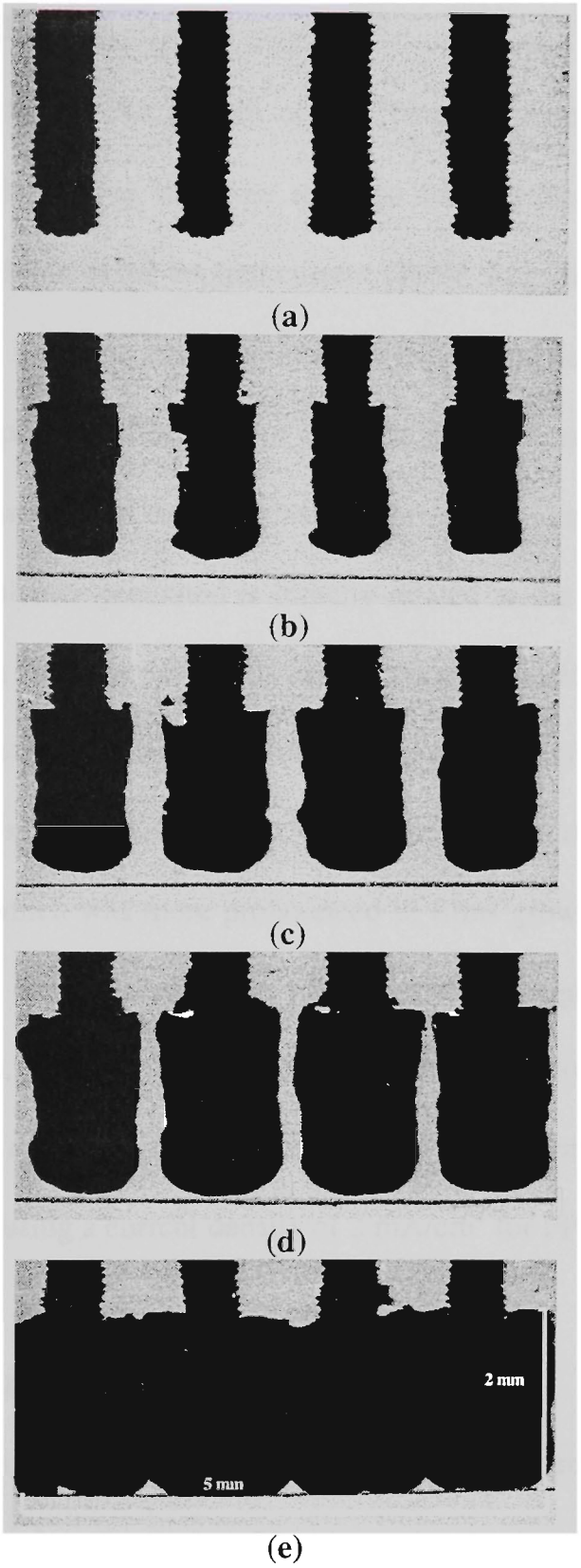

Figure 2.3 Video images of PPy/Tiron sensing films deposited onto carbon tracks on Melinex (a) for periods of 5 (b), 10 (c) 15 (d) and 20 (e) minutes. Note that each image shown corresponds to an individual sensor.

2.3.1.2 Effect of Current Density

The effect of current density on the growth of PPy/Tiron on untreated Melinex was investigated and it was found that the time required for complete coverage of the sensing area decreased with increased applied current (Table 2.2). In order to halve the PPy/Tiron deposition time it was necessary to increase the current density by a factor of five (10 mA/cm^2). As deposition time did not decrease proportionally with increasing current, the total charge passed at all current densities above 2 mA/cm^2 was significantly larger. The amount of polymer generated is directly related to the charge passed and hence while growth times were improved at higher current densities, the PPy/Tiron films formed were found to be thicker. After the films had been left to dry in air for a period of 30 minutes, visual inspection at 15 × magnification revealed significant cracking in each sample which was more pronounced in films grown at higher current densities. This would be due to increases in film thickness brought about by higher amounts of charge passed, and may also be related to the flexibility of the substrate. These defects would have a detrimental effect on the film sensing properties and hence it was decided to continue using a current density of 2 mA/cm^2 for PPy deposition.

2.3.1.3 Other Polymer Substrates

In addition to Melinex, which is a polyester, carbon tracks were also screen-printed on polyvinylchloride (PVC), polycarbonate, and polypropylene polymer sheets. PPy/pTS did deposit onto polypropylene but unfortunately the resulting film was easily peeled from the substrate and hence polypropylene electrodes were not investigated further.

Table 2.2 Properties of PPy/Tiron sensing films deposited at various current densities on untreated Melinex with screen-printed carbon tracks.

Current (mA)	Current density (mA/cm^2)	Potential (V)	Time (mins)	Charge (mC)	R_0 (kΩ)
0.2	2	0.8	20	240	29.9
0.4	4	1.19	15	360	19.5
0.6	6	1.53	14	508	26.4
0.8	8	2.29	13	624	22.3
1.0	10	2.15	10	600	19.1

This poor adhesion to polypropylene may relate to the ability of PPy/pTS to form freestanding films, a characteristic which relates to the high mechanical strength of this polymer [203]. Attempts were made to bridge the inter-track gaps by galvanostatically depositing PPy/Tiron, PPy/pTS and PPy/HBS onto electrodes prepared from PVC and polycarbonate. Growth times required for complete coverage of the sensing area and the final resistance value for sensors produced on these two substrates are listed in Table 2.3.

PPy growth times were reduced most significantly on the polycarbonate substrate when compared to the growth periods required on screen-printed Melinex substrates. A 50% improvement in bridging time was observed for PPy/pTS, and substantial reductions in time for deposition of both PPy/HBS and PPy/Tiron were noted. Growth times on PVC for both PPy/Tiron and PPy/pTS were the same as on Melinex, but PPy/HBS was deposited most efficiently on this substrate. A comparison of base resistance (R_0) values reveals that PPy films deposited onto PVC were more conductive than those on

the other two substrates which may be due to better contact between the film and carbon electrodes at the track/substrate interface.

Table 2.3 Comparison of growth times for complete coverage of the sensing area on polycarbonate and PVC substrates by PPy/Tiron, PPy/pTS and PPy/HBS. Final resistance values were measured between the outer tracks.

Sensor	Substrate	Polymer	Growth Time (mins)	R_0 (kΩ)
1	Polycarbonate	PPy/pTS	20	25.7
2	PVC	PPy/pTS	40	13.8
3	Polycarbonate	PPy/HBS	22	21.2
4	PVC	PPy/HBS	20	12.5
5	Polycarbonate	PPy/Tiron	14	30.6
6	PVC	PPy/Tiron	20	22.1

The importance of polymer substrate surface chemistry on PPy deposition is highlighted by the results obtained, and although growth times were generally much shorter on polycarbonate, the fact that PPy/HBS grew even faster on PVC illustrates the specificity of these surface interactions. While deposition times were reduced on substrates other than Melinex, bridging of the tracks by the conducting polymer still led to the formation of rather thick films with irregular morphologies as illustrated in Figure 2.3. These types of structures are not ideal for gas sensing where the issues of sensitivity and rapid response times are of interest [180]. In order for these requirements to be met sensing films are kept relatively thin (submicron to micrometer thickness) with more uniform morphologies to ensure reproducibility [202]. In an attempt to achieve these sensor characteristics, and further reduce bridging times, another approach was investigated which involved surface modification of the polymer substrate prior to electrodeposition

of PPy. As this process minimises the effect of the base polymer substrate on PPy deposition, Melinex was used exclusively for the remainder of this work.

2.3.1.4 PPy/Cl Modified Melinex

To promote electrodeposition of PPy sensing films, Melinex screen-printed substrates were modified with a PPy/Cl layer deposited by vapour phase polymerisation (Scheme 2.1). The resistance of the PPy/Cl base layer varied, usually between 50 and 200 kΩ, and was difficult to control precisely. However, by utilising galvanostatic deposition to form the final PPy sensing layer, the amount of charge passed was kept constant and therefore the amount of polymer deposited could be controlled. As a result the final R_0 values of all sensors were in the range 20-30 kΩ, and it would be expected from this that the effect of variations in the R_0 of the base PPy/Cl layer from one sensor to the next should be minimised. Such variations in conductivity of the PPy/Cl substrates would possibly effect the final morphology of the electrodeposited layer, which would modify the sensing characteristics of these films. However, as the resistance of the PPy/Cl was relatively high (>50 kΩ), the current path and hence the characteristics of the sensors would be dominated by the more conductive electrodeposited film.

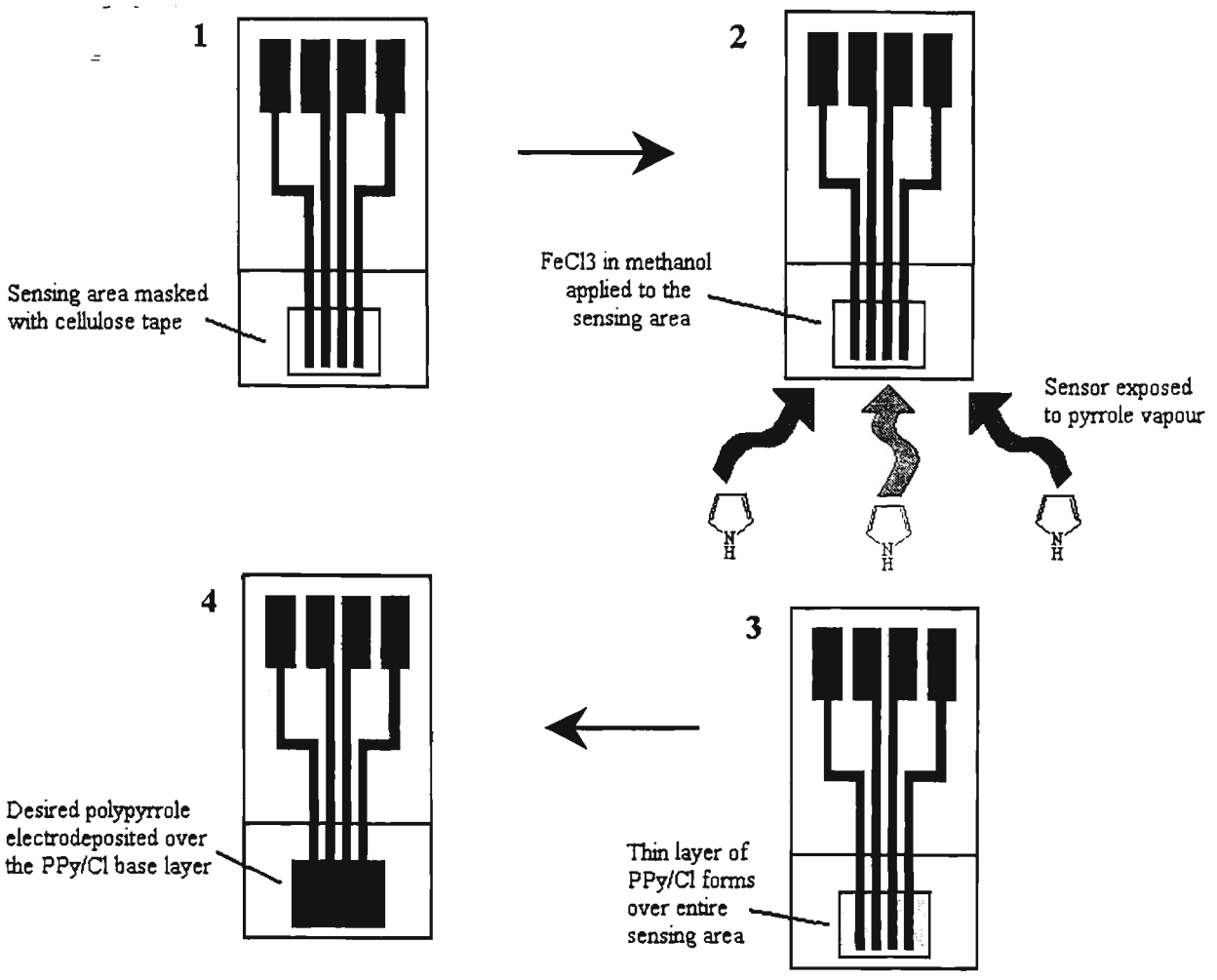

Scheme 2.1 Production of PPy gas sensors on Melinex screen-printed substrates *via* PPy/Cl surface modification

Electrodeposition of the PPys onto the PPy/Cl adhesion layer resulted in a significant reduction in the times taken for the polymers to reach their final resistance values. The PPy/Cl coating also provided a means of successfully fabricating sensors from dopants, such as MS and PSS, which would not bridge otherwise (Table 2.1). Table 2.4 details the growth times, resistances of the PPy/Cl adhesion layer and final resistances of the electrodeposited PPy films for the eight sensors fabricated by this method. Most of the polymers only required four minutes before a uniform coating had deposited over the PPy/Cl as determined by visual inspection of the sensing layer and by checking the final resistance. In some cases (PPy/MS and PPy/NDS) the film formed after four minutes had not completely coated the PPy/Cl surface, and hence deposition was continued (six

minutes) until the PPy/Cl was completely covered. It is interesting to note that only one of the polymers that would not bridge on untreated Melinex (PPy/MS) required this extended growth time on PPy/Cl, which further emphasises the importance of substrate chemistry on deposition. PPy/NDS and PPy/MS have less of an affinity for the PPy/Cl modified surface than the other electrodeposited polymers.

Table 2.4 Growth times and resistances for PPy/Cl coated Melinex sensors.

Dopant	Growth Time (mins)	R_0 after PPy/Cl Coating (kΩ)	Final Growth R_0 (kΩ)
pTS	4	55.6	26.7
Tiron	4	90.8	35.9
SB	4	70	25.2
NDS	6	84.3	28.6
NBS	4	73	28.3
HBS	4	65.6	22.9
MS	6	136	27.4
PSS	4	45.9	27.6

While the opposite must be true for PPy/PSS deposition as this polymer would not bridge on untreated Melinex but only required four minutes growth over PPy/Cl. It should be noted that some of the PPys used may not have needed four minutes growth, but that this time was chosen based upon optimisation studies of PPy/Tiron deposition on PPy/Cl.

2.3.1.5 Optimisation of PPy/Tiron Growth Time

PPy/Tiron was used to ensure the electrodeposition times employed for preparation of PPy coated screen-printed sensors were optimised. A range of PPy/Tiron sensors were prepared, as detailed above (Scheme 2.1), on PPy/Cl coated Melinex substrates with screen-printed carbon tracks. To establish the effect of PPy/Cl base resistance on the final sensing layer R_0, the statistical variation in R_0 of 6 individual PPy/Tiron sensors was determined at both stages of production. For each sensor the R_0 of the PPy/Cl layer was measured between the outer tracks, then a PPy/Tiron film was deposited over this layer galvanostatically for 4 minutes after which the final resistance was measured in the same manner. The results (Table 2.5) show that the average resistance of the PPy/Cl layer (15.7 kΩ) was significantly lower than previously observed (50 - 200 kΩ). The reason for this is not clear as attempts were made to keep the resistance of this base layer above 50 kΩ, and this again highlights the difficulties associated with controlling the resistance of PPy/Cl films by vapour phase polymerisation. As a result of the lower resistances obtained for the PPy/Cl layer, much smaller decreases in sensor resistance after PPy/Tiron deposition were observed, however, the results clearly show that variations in the PPy/Cl resistance have a significant effect on the final sensor resistance (R_0).

Sensor irreproducibility can be attributed to variation in the resistance of the PPy/Cl base, as indicated by similar relative standard deviations of the PPy/Cl layer (17.9%) and PPy/Tiron layer (18.9%) average resistance values. While the use of galvanostatic deposition allows for careful control over the amount of polymer deposited, if films are grown in this manner for set periods of time the effect of the underlying PPy/Cl layer on

final sensor resistance will still predominate. In order to reduce the variation in final sensor resistance values, growth time would have to be specifically tailored for each individual sensor relative to the base PPy/Cl resistance.

Table 2.5 Properties of 6 different PPy/Tiron sensors prepared using PPy/Cl modified Melinex substrates. PPy/Tiron films were electrodeposited over PPy/Cl for a period of 4 minutes.

Polymer	Mean R (kΩ)	R.S.D (%)	Min. R (kΩ)	Max. R (kΩ)
PPy/Cl	15.75	17.90	13.80	21.00
PPy/Cl + PPy/Tiron	14.23	18.86	9.80	17.80

The relationship between final sensor resistance and responses to methanol were examined in order to establish whether or not the variation discussed above is important. Responses of five PPy/Tiron sensors to 50% methanol, and R_0 values of each sensor, are shown in Figure 2.4. There was no clear correlation between sensor R_0 values, arranged in ascending order, and the corresponding responses to methanol. This trend would only be observed if both morphology and the amount of polymer deposited were constant. Clearly this is not the case, which suggests that even if R_0 is carefully controlled, the fabrication method significantly affects morphology and film thickness. The standard deviations for each sensor response, which were small, show good reproducibility in all cases.

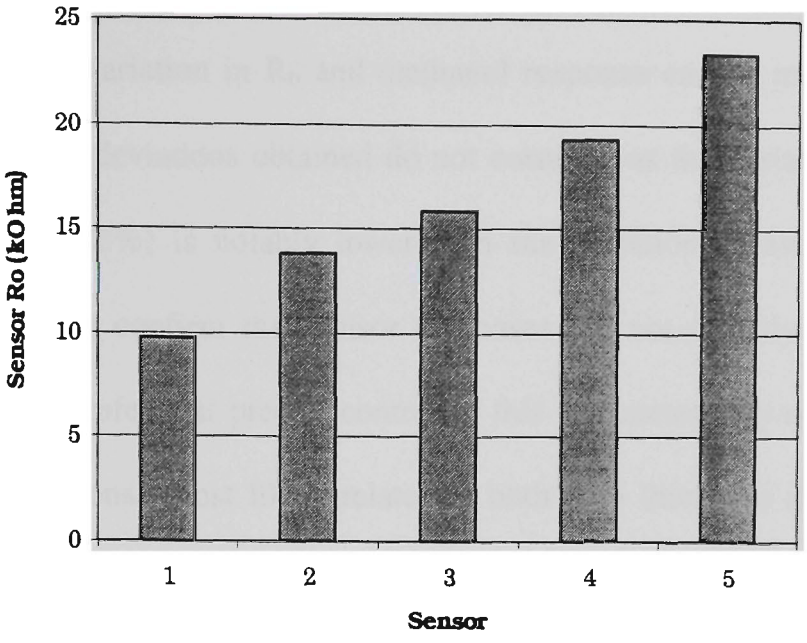

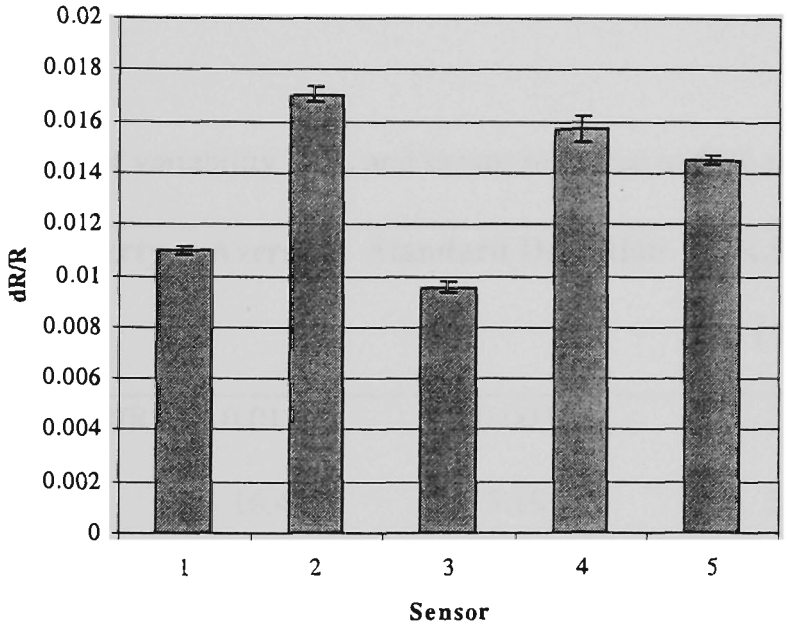

Figure 2.4 Five PPy/Cl/PPy/Tiron sensors arranged in ascending order of R_0 values, and corresponding average responses of these sensors to 50% methanol calculated from 3 exposures. Error bars indicate standard deviation.

If sensor properties are combined, by averaging the R_0 values and methanol responses, a comparison of the variation in R_0 and methanol response can be made (Table 2.6). The relative standard deviations obtained do not correlate as the variability in average methanol response (23%) is notably lower than the variation in average sensor R_0 (32%). These results confirm that sensor responses are not directly related to final sensor R_0 and hence infer that precise control of this parameter may not be necessary. The variation in response most likely relates to both film thickness and variations in morphology. The amount of polymer, and distribution across the sensing area would be affected by the underlying PPy/Cl layer. While the vapour deposition time of PPy/Cl films is controlled, it is difficult to control the exact film thickness using this method.

Table 2.6 Comparison of variability in R_0 and sensor response to 50% methanol.

Sensor Property	**Average**	**Standard Deviation**	**R.S.D. (%)**
Response (dR/R)	0.0135	0.003	23
R_0 (kΩ)	16.44	5.19	32

To investigate the effect of electrochemical growth time and hence film thickness further, a range of PPy/Tiron sensors were prepared on PPy/Cl coated Melinex, with growth times of 1, 4 and 8 minutes. For each time a set of 4 sensors was prepared and the response of these to 50% methanol in nitrogen compared to establish the effect on sensitivity and reproducibility. The term sensitivity will be used to describe the magnitude of sensor response (dR/R) to solvent vapours at one given concentration

rather than the IUPAC accepted calibration sensitivity obtained from the calibration curve slope [207]. Figure 2.5 shows the set of average responses observed for the PPy/Tiron sensors when exposed to 50% methanol and highlights the lack of reproducibility between those prepared using a 1 minute deposition period. The standard deviation of each is small indicating that the response reproducibility to methanol for individual sensors is good. However, the range of responses observed for the set of one minute sensors is large (76% R.S.D.). The average response and associated standard deviation of these sensors, and the other two sets are shown in Table 2.7. The average response to methanol of the 1 minute sensors was quite high relative to films prepared with longer growth times, as would be expected with a thinner sensing layer. However, the variability in response observed infers one minute of PPy/Tiron deposition is not sufficient for uniform, reproducible, coverage of the PPy/Cl layer. This was confirmed by observations made upon visual inspection during PPy/Tiron deposition, and may be due to variation in the thickness of the PPy/Cl coating. While vapour deposition of this polymer on a planar substrate should be uniform, the presence of the carbon tracks on Melinex may interfere with the process causing localised variations in film thickness.

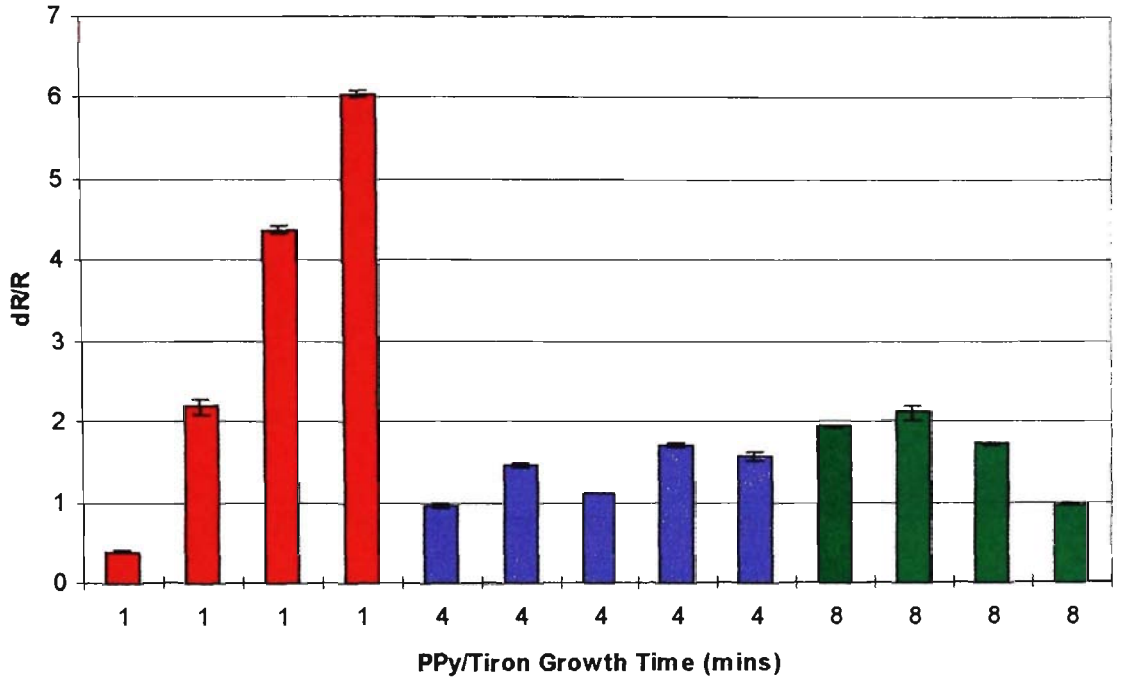

Figure 2.5 Average responses of PPy/Tiron sensors to triplicate exposures of 50% methanol in nitrogen. Error bars indicate standard deviations obtained on individual sensors.

Figure 2.5 and Table 2.7 show that as PPy/Tiron growth time increased, responses to methanol decreased but reproducibility between sensors improved. While the average response of sensors grown for 4 minutes was smaller, the improvement in sensor reproducibility (18% R.S.D.) offset this loss of response. The eight minute sensors actually showed a larger average response to methanol when compared to the 4 minute sensors, but the associated standard deviation also increased (30% R.S.D). This result is interesting as a further decrease in methanol response would be expected after doubling the growth period from 4 to 8 minutes. Also, it would be expected that the variation between sensor responses would be similar or smaller than that observed for the 4 minute set. This again suggests that the underlying PPy/Cl layer significantly affects the final sensing characteristics obtained for electrodeposited films.

Table 2.7 Averaged responses and associated standard deviations of PPy/Tiron sensors to 50% methanol.

PPy/Tiron growth time (mins)	Mean Response (dR/R)	St. Dev.	R.S.D. (%)
1	0.03248	0.02473	76
4	0.01456	0.00259	18
8	0.01683	0.00505	30

Substrate effects on PPy film characteristics have been shown to be significant [204], and in the case of growth over a PPy base layer the R_0 is said to effect characteristics of the final sensing film [205]. As was mentioned earlier, controlling the R_0 of the PPy/Cl is difficult and as a result there is substantial variation in the base resistance obtained. This is clearly the factor that dictates reproducibility between sensors, but in spite of this the approach significantly reduced growth times and enabled the successful deposition of all eight PPys of interest. Also, the use of PPy/Cl as a surface modification produced very smooth sensing films with more uniform morphology. The thickness of these films, which were in the range of 15 - 30 μm (Section 2.3.1.7.) was reduced relative to those on the bare polymer substrates due to the shorter deposition times required. For these reasons this approach was selected exclusively for use in all future development of conducting polymer coated screen-printed sensors, and based on the above set of results for PPy/Tiron, deposition times of 4 and 8 minutes were employed.

2.3.1.6 Silicon Sensors

Table 2.8 lists the 8 CP sensors deposited by a pulsed current technique onto silicon and their final growth resistances. This approach to deposition allows resistance to be monitored to the point at which the electrode tracks are bridged, after which the

resistance is continually monitored to allow careful control over the final sensor R_0. In spite of this, the final growth resistances are quite varied as a result of the different dopants employed, variation of which is known to affect the conductivity of PPy films [15]. Due to the small track spacing of these electrodes (10 μm), the total growth times employed were much shorter than for the Melinex screen-printed electrodes. The pulsed current method was not employed for deposition of PPy on Melinex screen-printed electrodes as it would not offer any improvement in deposition time. Growth times for PPy on Melinex may actually be longer using a pulsed current as the driving force behind polymerisation is continually being turned on and off.

Table 2.8 Growth details of silicon sensors.

Dopant	Final Growth R_0 (kΩ)
pTS	4.00
Tiron	8.00
SB	0.15
NDS	0.07
NBS	4.00
HBS	5.00
MS	100.00
PSS	2.50

While the approach allows the exact time of bridging to be determined, the growth times employed for PPy deposition on Melinex using galvanostatic polymerisation were chosen to ensure complete coverage of the inter-track region, a process that was easily monitored visually due to the larger dimensions of these electrodes. Although PPy/pTS was not deposited by pulsed current onto Melinex a comparison can be made between

the times taken to completely cover the sensing areas of these and the silicon electrodes. Results presented by Partridge *et al* [180] show that a deposition time of approximately 50 seconds was required for PPy/pTS to bridge the 10 μm inter electrode spaces. The time taken for PPy/pTS to completely cover the 0.1 cm^2 sensing area on a Melinex substrate was 40 minutes (2400 seconds), using a deposition current density double that applied to the silicon sensor. The area of the inter-track gap of the Melinex sensor (1.0 mm^2) is significantly larger than the corresponding area on the silicon substrate (0.02 mm^2) which explains the difference in growth times.

2.3.1.7 Estimate of Film Thickness

The thickness of PPy films produced by pulsed current deposition on silicon substrates was estimated from SEM images to be sub-micron [180]. Unfortunately, due to the relatively large electrode dimensions of the Melinex sensors, SEM and AFM images did not allow for thickness estimates to be made. However, a comparison of the total charge passed for deposition of PPy/pTS onto both substrates, which relates to the total amount of polymer formed, enables an estimate of film thickness of PPy films on Melinex. The applied current used for PPy/pTS deposition on silicon was 1 mA/cm^2 and the sensing area exposed to the polymerisation solution was approximately 0.0014/cm^2 (as estimated from track dimensions and spacing). The actual current passed would therefore be of the order of 0.0014 mA, and assuming a deposition time of 120 seconds, the total charge passed can be approximated as 0.168 mC. If this calculation is made for the deposition of PPy/pTS onto Melinex, which required 40 minutes and an applied current of 0.2 mA, the total charged passed is 480 mC. If these figures are normalised on the basis of area coated, the values are 120 mC/cm^2 and 4800 mC/cm^2 respectively. The charged passed during deposition of PPy/pTS on Melinex is

approximately forty times greater than the charge passed for deposition of this polymer on silicon. Not all of this charge will be involved in polymer deposition, as a significant proportion would be consumed forming oligomers. Assuming a current efficiency of between 0.5 and 1.0, and the thickness of PPy/pTS on silicon to be 1 μm, the estimated thickness on Melinex after 40 minutes growth is between 20 and 40 μm. Hence the estimated thickness of PPy/Tiron on Melinex, which required a growth time of 20 minutes, should lie in the range 10 - 20 μm.

To confirm these estimates a range of PPy/Tiron sensors, deposited on Melinex and PPy/Cl coated Melinex, were measured using a micrometer (Table 2.9). The Melinex substrate was measured to be 250 μm thick, and the carbon tracks were approximately 10 μm in height. PPy film thickness was measured relative to the combined thickness of the Melinex and track for each individual sensor.

Table 2.9 Comparison of estimated and measured thickness of PPy/Tiron films on both Melinex and PPy/Cl coated Melinex substrates. Thickness measurements were made over the carbon track.

Substrate	Growth Time (mins)	Charge Passed (mC)	Estimated Thickness (μm)	Measured Thickness over Track (μm)
PPy/Cl	1	12	1	10
PPy/Cl	2	24	2	13
PPy/Cl	4	48	4	15
PPy/Cl	8	96	8	30
Melinex	20	240	20	40

Estimates of thickness assume that a uniform polymer layer forms over the entire area coated. In reality this is not the case with thicker deposits being formed directly over the electrode tracks. Hence the estimated and measured thickness values do not agree exactly, but suggest that the thickness of PPy films on Melinex should lie in the range 1 - 50 μm. Also, more porous films may form on the screen-printed electrodes, which are less dense than those on silicon and hence thicker than estimated.

2.3.2 Characterisation

2.3.2.1 Scanning Electron Microscopy

The screen-printed substrates and sensors were characterised by SEM at each stage of development. Figure 2.6a shows the bare carbon track on Melinex, and highlights the limitation in the edge resolution of the screen-printing technique which can be estimated as approximately 50 μm from this image. Figure 2.6b shows the carbon track coated by a thin layer of vapour deposited PPy/Cl, which appears to have a flakey morphology. Figures 2.6c and d depict electrochemically deposited films of PPy/Tiron grown on both

PPy/Cl coated (2.6c) and untreated (2.6d) carbon tracks on Melinex. In both cases cracks appeared in the polymer, the extent of which are much more significant for the thicker PPy/Tiron layer deposited on untreated melinex (2.6d). The effect of cracking on sensor responses would be significant as this would lead to interruptions in the conducting network and hence reduce electron flow. Figure 2.6d also highlights the irregular morphology obtained by directly depositing PPys onto untreated polymer substrates, as a result of the growth pattern depicted earlier in Figure 2.3. The majority of PPy/Tiron has been deposited over the carbon track as indicated by much larger nodules of polymer in this region, the size of which are related to polymer thickness [202]. The PPy/Cl coating appeared to give the PPy/Tiron polymer film a more even texture when compared to the irregular growth pattern observed for PPy/Tiron onto bare carbon tracks. Figure 2.6e shows a PPy/Tiron film deposited on a silicon substrate with gold tracks. The track structure under the polymer layer is well defined indicating that the PPy/Tiron film is thin. Also, while the nodule size is larger over the tracks, on the whole the morphology is more uniform across the area shown as a result of the short bridging times required on these electrodes.

2.3.2.2 Atomic Force Microscopy

Atomic force microscopy (AFM) of the bare carbon track on Melinex revealed that the surface was rough (Figure 2.7a). The morphology of a PPy/Tiron film deposited over a carbon track (Figure 2.7b) showed characteristic nodule structures commonly associated with PPy films, some of which had joined due to the thickness of the film. The rough surface morphology of the underlying track clearly influenced the structure of the deposited film. The morphology of this PPy/Tiron film in the inter-track region (Figure 2.7c) was significantly different with a smoother surface as indicated by the more

uniform distribution of nodules. Also, the diameter of the nodules was smaller (ca 1 - 5 μm) when compared to those deposited over the track (ca 1 - 10 μm) indicating a clear variation in film thickness.

The morphology of a vapour deposited PPy/Cl layer on Melinex (Figure 2.8a) was irregular with a very jagged appearance. In contrast was the very uniform nodule distribution of PPy/Tiron deposited for 8 minutes over PPy/Cl in the inter-track region (Figure 2.8b), indicating a smooth morphology. While the nodule size ranged from approximately 0.5 to 2 μm, the diameter of most was less then 1 μm indicating that the film was relatively thin. The roughness of the carbon track surface influenced the morphology of PPy/Tiron even after coating with PPy/Cl (Figure 2.8c), which confirms that the vapour polymerised PPy/Cl layer is thin (a few nanometres).

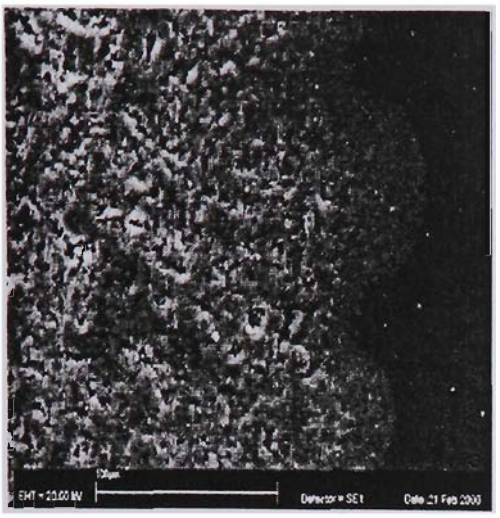

(a)

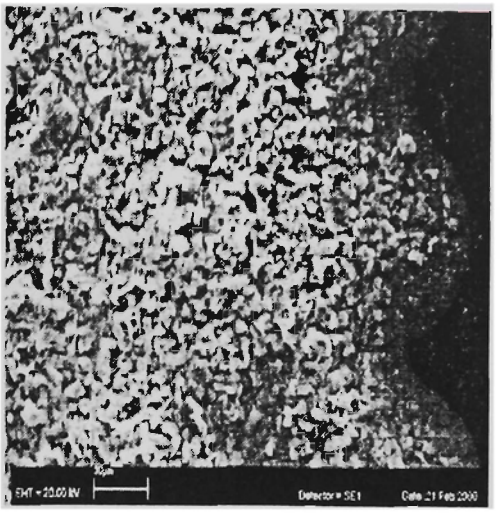

(b)

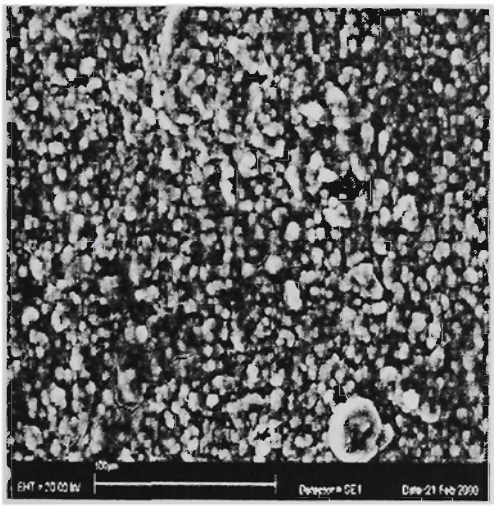

(c)

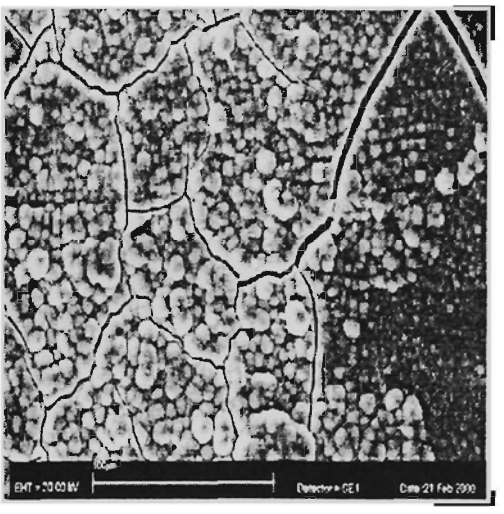

(d)

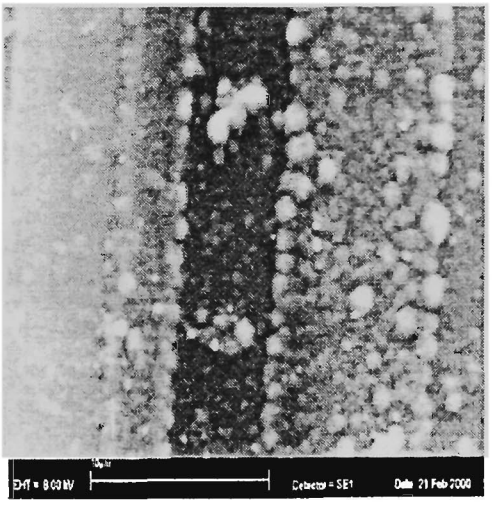

(e)

Figure 2.6 SEMs of substrates and PPy/Tiron sensors: (a) Bare carbon track on Melinex, (b) vapour deposited PPy/Cl on carbon track, (c) PPy/Tiron on PPy/Cl, (d) PPy/Tiron on bare Melinex, PPy/Tiron on silicon.

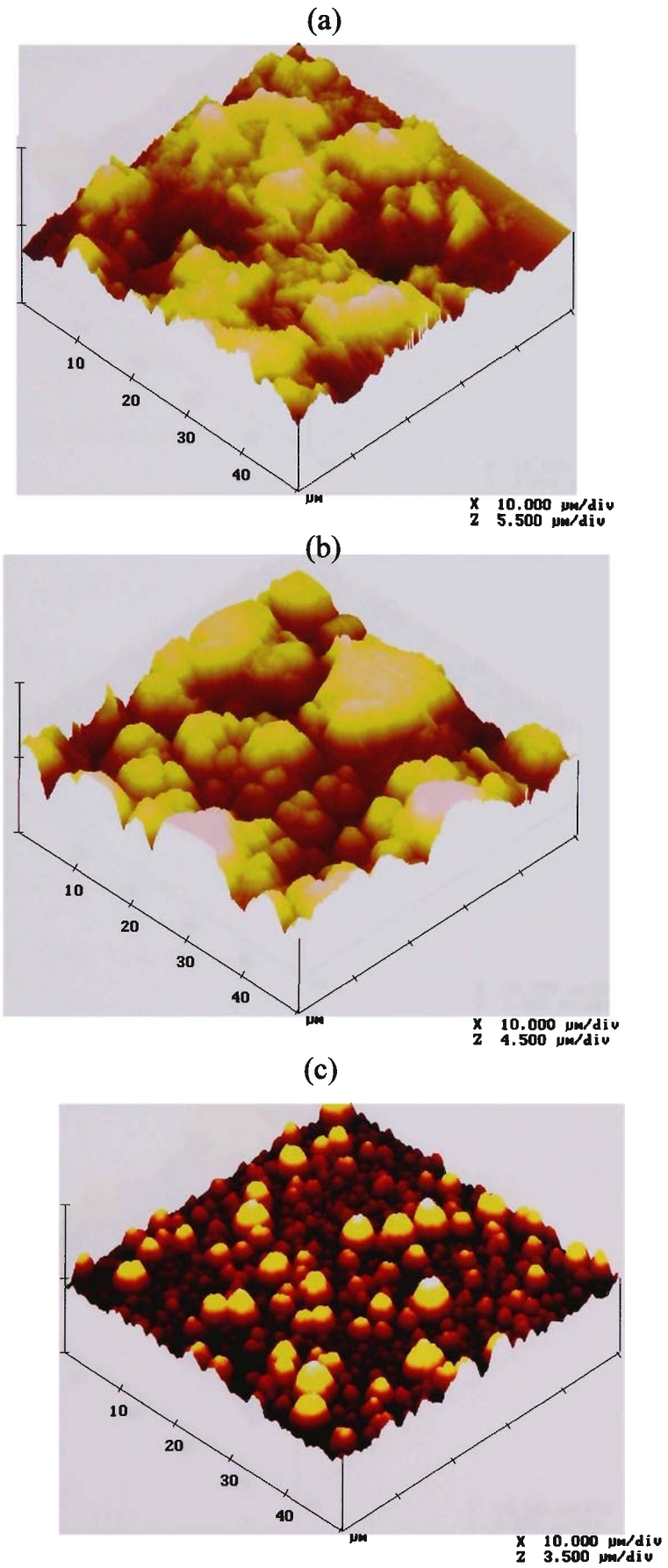

Figure 2.7 AFM images of a bare carbon electrode (a), a PPy/Tiron film grown for 20 minutes (b) over the electrode and (c) between the electrodes.

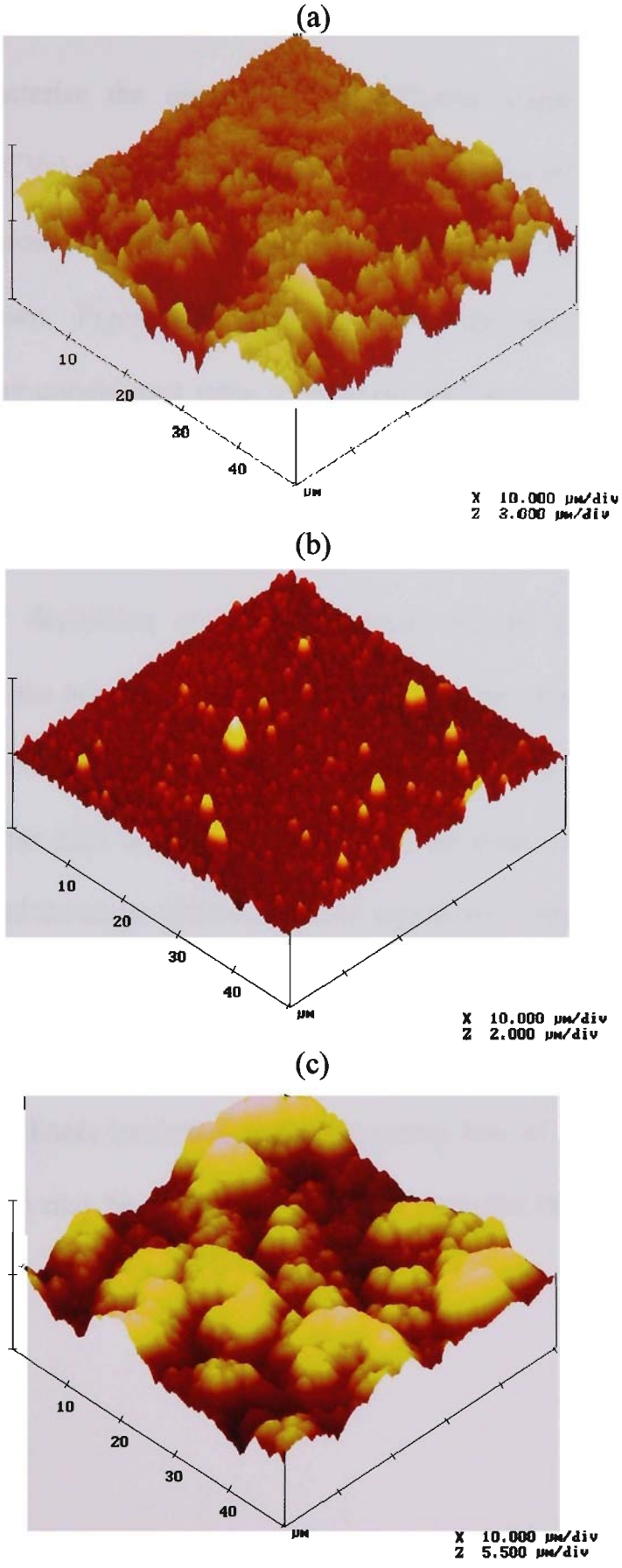

Figure 2.8 AFM images of (a) PPy/Cl coating on Melinex between the carbon tracks, (b) PPy/Tiron film grown for 8 minutes over (a), and (c) PPy/Tiron grown on PPy/Cl on a carbon track for 8 minutes.

2.3.2.3 Cyclic Voltammetry

To further characterise the sensors at the different stages of preparation, cyclic voltammograms (CVs) were run in 0.1M $NaNO_3$/0.01M $K_3Fe(CN)_6$. CVs were also run in 0.1M $NaNO_3$ alone, but the redox responses observed in most cases were small and hence are not shown. Figure 2.9a shows the CV of the four bare carbon tracks. The sensor was not pre-conditioned prior to characterisation as no interfering peaks were observed in CVs of electrodes used as received. The responses of the bare carbon electrodes were poor, possibly due to the resistive nature of the tracks (5 - 10 kΩ). The CV after vapour deposition of a PPy/Cl layer (Figure 2.9b) showed significant differences due to the presence of the conducting polymer. Figures 2.9c and 2.9d show CVs of a PPy/Tiron film grown for one minute (c) and two minutes (d) on top of a PPy/Cl layer. After each addition of PPy/Tiron, the peak currents were observed to increase further and the shape of the CVs were significantly different from that observed for PPy/Cl alone. This was further evidence that the PPy/Tiron layer dominated the electrical characteristics, and hence the sensing characteristics of the film. As the PPy/Tiron film thickness increased, a corresponding loss of $Fe(CN)_6^{3-}$ peak response was observed which may be due to slower electron transfer through the composite PPy film.

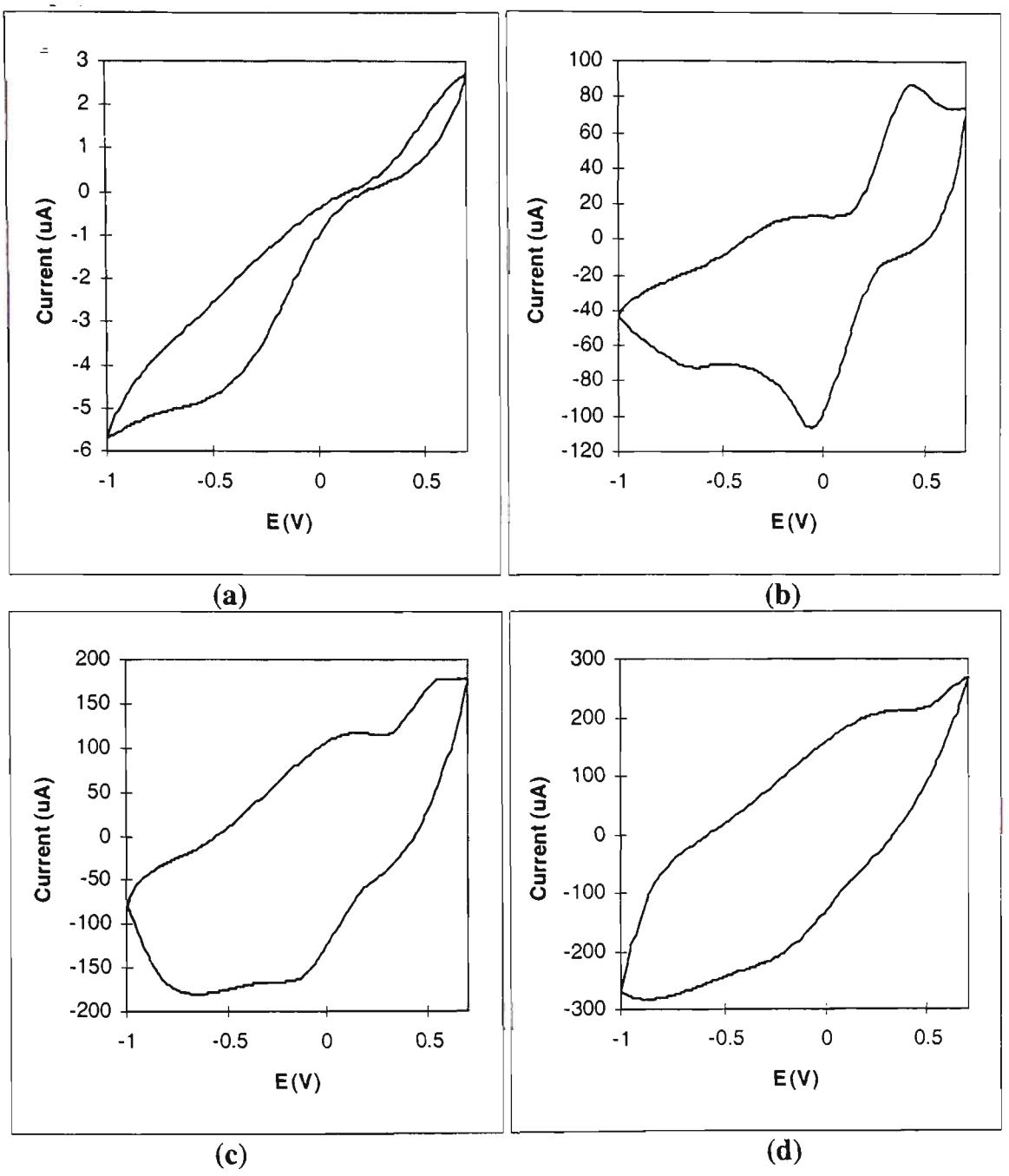

Figure 2.9 Cyclic voltammograms of various sensors in 0.1M $NaNO_3$/0.01M $K_3(FeCN)_6$: a) 4 track bare screen-printed electrode, b) PPy/Cl coated sensor on (a), c) PPy/Tiron grown on (b) for 1 minute, d) PPy/Tiron grown on (b) for 2 minutes.

2.3.3 Sensor Responses

PPy gas sensors are known to respond well to polar vapours [179, 206], particularly alcohols [137], and hence methanol was chosen as a test case for examining the general responses of various sensors, the limits of detection, and linear range.

2.3.3.1 Responses to Methanol

Figure 2.10 shows the responses of the different sensor types to 10 second exposures of 50% methanol vapour. Figure 2.10ashows the response of a PPy/Cl film on screen-printed carbon tracks, Figure 2.10b shows responses of the 8 PPys deposited onto PPy/Cl modified Melinex electrodes, and Figure 2.10c shows the responses of the 8 PPy sensors deposited onto silicon. Note that in Figure 2.10c the PPy/pTS response is not included as this sensor failed during testing. The response of the PPy/C1 layer (average $dR/R = 0.0276 \pm 0.0001$) was of a similar magnitude to those of the most sensitive composite sensors comprising a PPy/CI layer covered with a second PPy layer (average $dR/R = 0.0408 \pm 0.0005$). However, the array of electrochemically deposited PPys gave a range of responses which appeared to depend on the overlying polymer layer rather than on the PPy/Cl. A detailed comparison between the responses of the two sets of PPy sensors shows that although the CPs employed were nominally the same, the shapes (Figure 2.10b and c) and magnitudes of the responses (Table 2.10 and Figure 2.11) were significantly different. The PPy sensors on silicon (Figure 2.10c, Figure 2.11c) gave larger responses on the whole to 50% methanol, with responses of the screen-printed sensors often an order of magnitude smaller. There were marked differences between the patterns of responses observed for the silicon array (Figure 2.11c) and the SP

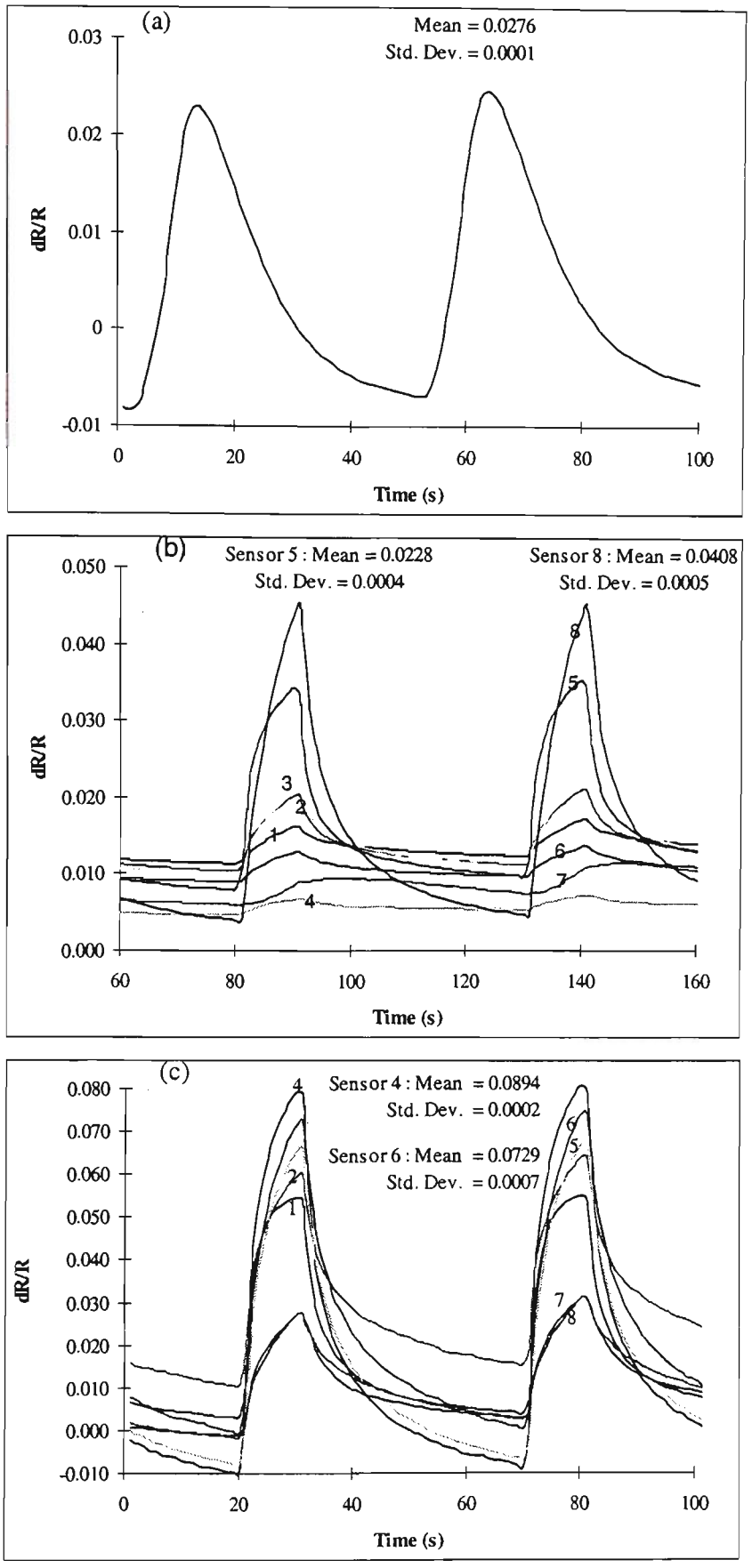

Figure 2.10 General response profiles of (a) PPy/Cl vapour deposited layer on Melinex, (b) 8 electrochemically deposited PPys on PPy/Cl modified Melinex, (c) 8 electrochemically deposited PPys on silicon substrates, to 50% methanol vapour in nitrogen. (1)PPy/SB, (2) PPy/NDS, (3)*PPy/pTS, (4)PPy/HBS, (5)PPy/MS, (6)PPy/NBS, (7)PPy/Tiron, (8)PPy/PSS.

array (Figure 2.11a and b) and also variations in responses (σ) were slightly higher for the screen-printed sensors. These differences must result from the deposition of identical polymers under different growing regimes giving polymer films with varied morphologies and hence sensing characteristics. Also, the PPy/Cl vapour deposition step was not completely controllable, with significant variation (Rel. σ = 18%) in the conductivity of resulting films. This would affect the rate of deposition of the final sensing polymer film, causing variation in the sensing properties obtained. Also differences between the two substrates may play a significant role in modifying the morphology and therefore sensing characteristics of the films produced. Also note that the screen-printed sensors are much larger than the silicon based electrodes and that the films produced on the former substrates are much thicker, factors that would influence both the sensitivity and response speed. Figure 2.11 includes the response patterns obtained for two different screen-printed sensing arrays, one for which growth times were between 8 and 12 minutes (Figure 2.11a), and the other for which growth times ranged between 4 and 6 minutes (2.11b). Comparison of the two response patterns and magnitudes of these responses reveals that the overall patterns were similar, with major differences observed for only a couple of the sensors. In general, only slight decreases in sensitivity were observed for PPy/NDS, PPy/HBS, PPy/PSS and PPy/Tiron after doubling the growth time. The response of PPy/MS was much higher for the 12 minute film (2.11a) than the 6 minute film (2.11b). The only response that was significantly reduced after a longer growth time was that for PPy/NBS. The fact that these response patterns are not exactly the same is not surprising, as the nature of PPy deposition is subject to variability, a factor that can lead to variation of final sensor resistance even if all growth conditions are kept constant [180].

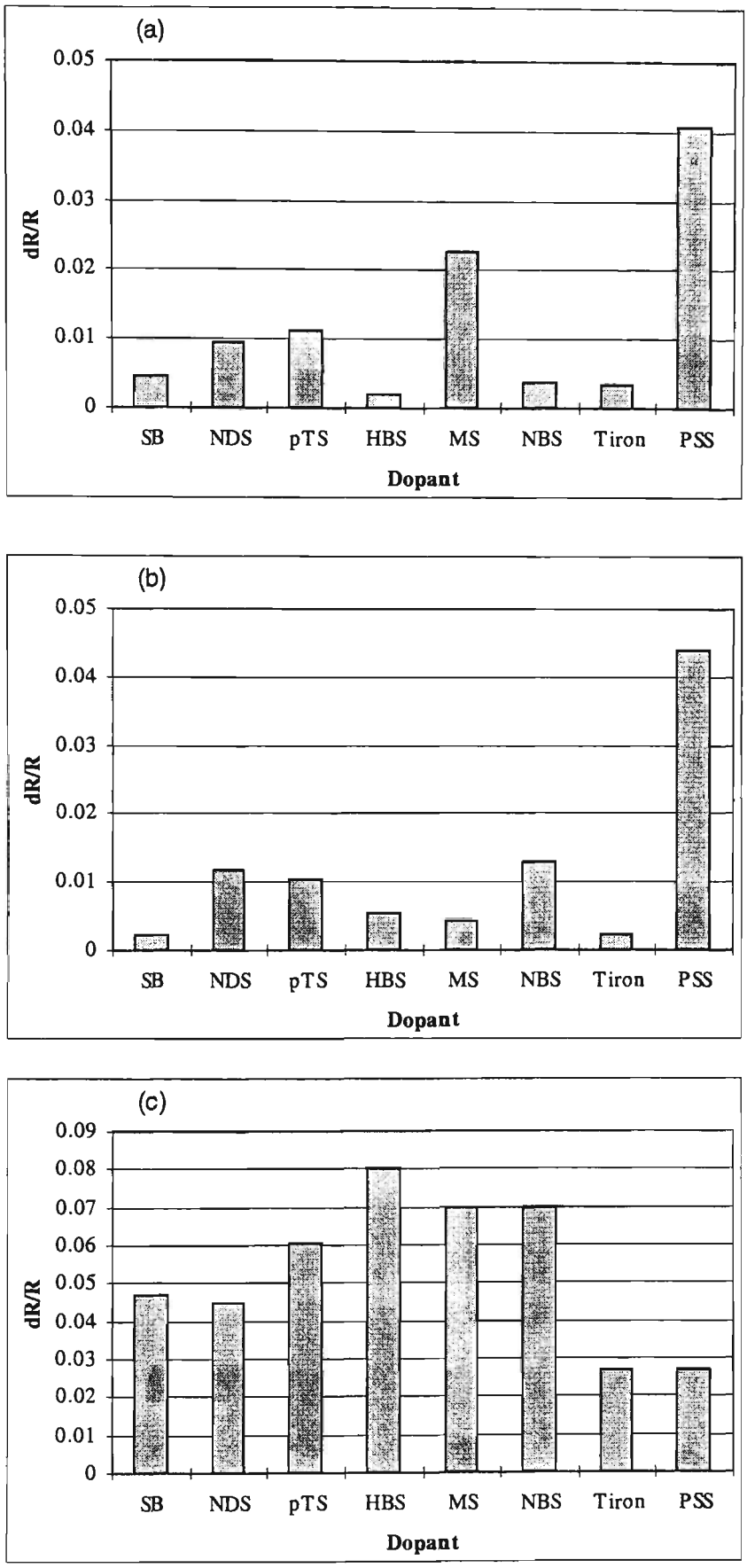

Figure 2.11 Response patterns obtained for 50% methanol in nitrogen from 8 PPys on (a) PPy/Cl modified Melinex with growth time of 8 - 12 minutes, (b) PPy/Cl modified Melinex with growth times of 4 - 6 minutes, (c) silicon chips.

Table 2.10 Mean responses to 50% methanol and associated standard deviations of screen-printed and silicon based PPy sensing arrays.

	Screen-printed		Silicon	
Dopant	**Mean dR/R**	**St. Dev.**	**Mean dR/R**	**St. Dev.**
SB	0.00465	0.00003	0.05111	0.00032
NDS	0.00955	0.00008	0.04837	0.00050
pTS	0.01129	0.00014	-	-
HBS	0.00198	0.00012	0.08937	0.00017
MS	0.02282	0.00050	0.07343	0.00035
NBS	0.00384	0.00007	0.07288	0.00067
TIR	0.00335	0.00031	0.02788	0.00020
PSS	0.04081	0.00050	0.02821	0.00029

Variations in the resistance, morphology and thickness of the underlying PPy/Cl layer may also be responsible for the different patterns obtained between the arrays. In terms of sensitivity there appears to be little difference between the two arrays for most sensors, which infers the longer growth times can be employed to ensure better sensor reproducibility without major loss of sensitivity. For this reason the array prepared using longer growth times (8 - 12 minutes) was used in subsequent solvent discrimination work.

2.3.3.2 Linearity of Response and Limit of Detection

Figure 2.12 shows the average responses for (a) the 8 - 12 minute screen-printed array and (b) the silicon array to methanol (1 - 50%). These plots were prepared by averaging the sensor responses to three pulses of methanol in nitrogen. The responses of both arrays are not linear but the methanol concentration range examined is extremely large.

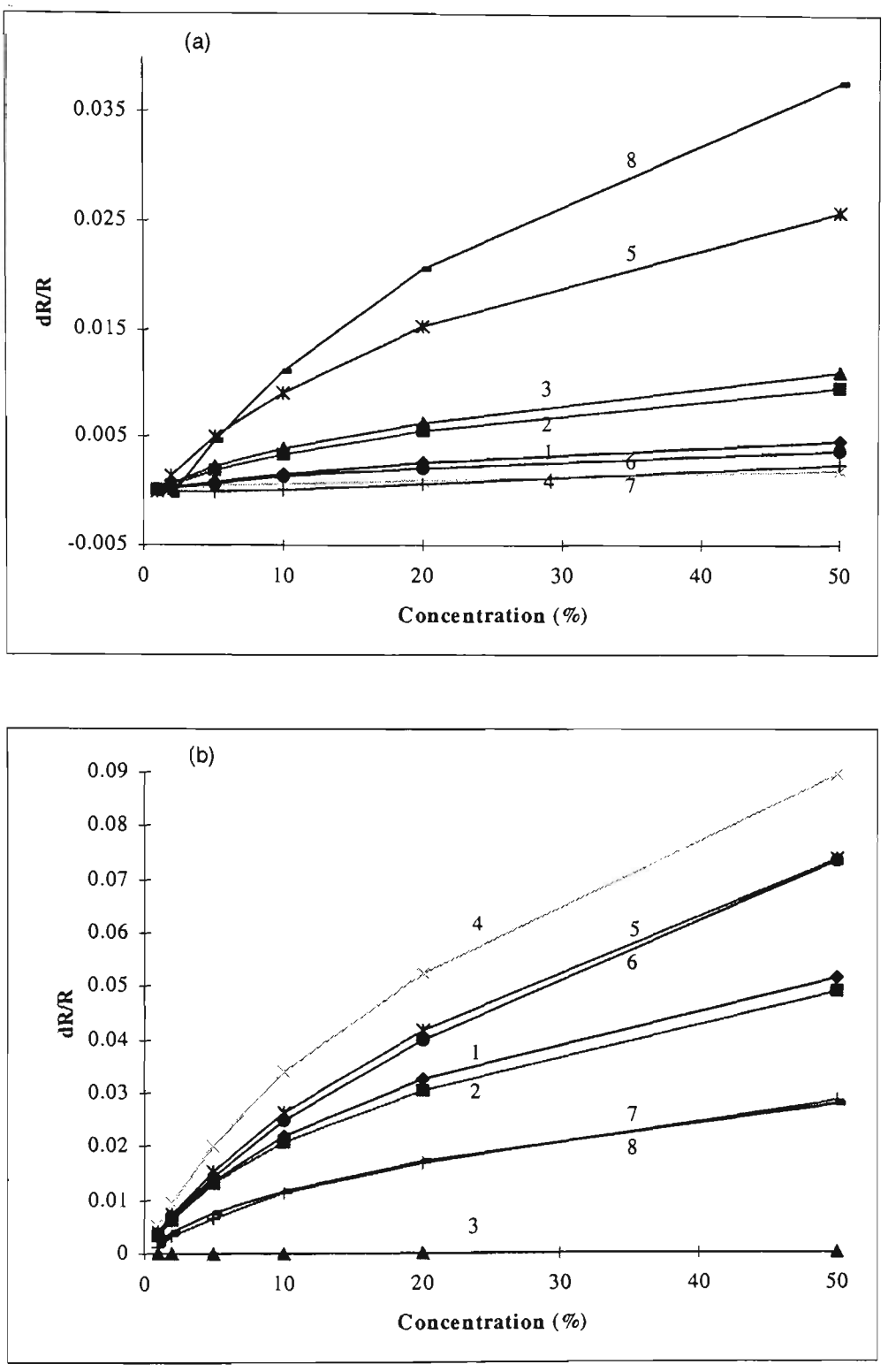

Figure 2.12 Average responses of 8 different PPys [PPy : SB (1), NDS (2), pTS (3), HBS (4), MS (5), NBS (6), Tiron (7), PSS (8)] on (a) PPy/Cl coated Melinex screen-printed electrodes with growth time of 8 - 12 mins, and (b) silicon chips to methanol vapour in nitrogen over a range of concentrations (1- 50%). Each line represents the response of an individual sensor.

For both types of sensors there is a clear departure from linearity as the methanol concentration increases beyond 10%. A complete comparison of linearity is given in Table 2.11, which shows R^2 co-efficients obtained by fitting linear trend-lines to the data from each sensor. For each sensor three different R^2 values are shown corresponding to lines of best fit for 1 - 10%, 1 - 20%, and 1 - 50% methanol responses. Note that the PPy/pTS sensor in the silicon array failed during this work and hence gave no responses to methanol. With the exception of the PPy/Tiron screen-printed sensor, which did not respond well at low methanol levels, R^2 values for response curves increase as the methanol concentration range is decreased. Although the silicon sensors generally display slightly more linear responses, the linear range of both sensing arrays for methanol was the same (1 - 10%).

Table 2.11 Least squares regression R^2 values from lines of best fit for responses of both silicon and screen-printed PPy sensors to 1 - 10%, 1 - 20%, and 1 - 50% methanol in nitrogen.

	1 - 10% Methanol		**1 -20% Methanol**		**1 - 50% Methanol**	
Dopant	**Silicon**	**Screen-printed**	**Silicon**	**Screen-printed**	**Silicon**	**Screen-printed**
SB	0.991	0.987	0.966	0.979	0.935	0.967
NDS	0.985	0.985	0.960	0.971	0.939	0.950
pTS	-	0.983	-	0.967	-	0.951
HBS	0.993	0.962	0.976	0.960	0.960	0.950
MS	0.995	0.987	0.983	0.977	0.968	0.948
NBS	0.997	0.988	0.985	0.974	0.976	0.954
Tiron	0.984	0.002	0.965	0.610	0.951	0.945
PSS	0.974	0.981	0.961	0.988	0.943	0.964

The most commonly used definition for limit of detection (LOD) in analytical chemistry is the minimum concentration or mass of an analyte that can be detected at a known confidence level. Normally replicate measurements are made on a blank and the standard deviation of the average blank signal is multiplied by a factor to give the LOD. The LOD is usually estimated to be 3 times the standard deviation of the blank signal [207]. For this work the LOD for was defined as the analyte concentration at which the signal was three times the background noise level (S/N = 3). Figure 2.13 depicts responses of the screen-printed array (a) with PPys grown for between 8 and 12 minutes, (b) a second screen-printed array with growth times of 4 to 6 minutes, and (c) the silicon array to methanol at concentrations ranging from 1% to 50%. Generally the magnitude of responses associated with the silicon array were greater than for those of the screen-printed arrays, and the entire silicon array responded well at the lowest methanol concentration tested (1%). In comparison, only the most sensitive sensors in both screen-printed arrays responded to 1% methanol.

For all three arrays the noise associated with each sensor was estimated graphically from the baseline response during nitrogen purging, and from this methanol LODs were calculated (Table 2.12, 2.13). This approach estimates peak to peak noise deviations of a sensor baseline signal, which is effectively a measure of the standard deviation about the mean baseline signal. An estimate of the LOD signal was obtained by multiplying the noise value of each sensor by three. For each sensor the response to 1% methanol was then divided by the LOD signal value to give a ratio S_{MeOH}/S_{LOD}. LODs for methanol (% saturation) were obtained by dividing the minimum test concentration (1%) by S_{MeOH}/S_{LOD}. Responses of the silicon array to 1% methanol and calculated LODs (Table 2.12) highlight that the overall sensitivity is better than that of the screen-printed arrays. The calculated methanol LODs for all silicon sensors, with the exception

of PPy/pTS which had been damaged and gave no responses, were in the range 0.07 - 0.49%. When the responses and estimated methanol LODs for the two screen-printed arrays (Table 2.13) are compared to those of the silicon array (Table 2.12), the issue of reproducibility is clear. For both screen-printed arrays there is significant variation in response at low methanol levels between sensors, and a range of estimated LODs were calculated. If the two screen-printed arrays are compared, selected sensors from the 8 - 12 minute array showed better sensitivity to 1% methanol but only 3 of the eight sensors responded (Table 2.13a). Estimated methanol LODs for these sensors were in the range 0.13 - 0.25%, however, 3 of the other sensors in this array had calculated LODs of approximately 26 - 48%. It should be noted that this array, responses of which are also shown in Figure 2.13a, had already been used for a number of experiments and some of the sensors were not functioning well even in the presence of 50% methanol. This may have been due to sensor decay but is more likely a result of damage to the carbon contacts from repeated installation and removal from the sensor connectors. The 4 - 6 minute array gave a better range of responses at low methanol concentrations with more sensors giving signals (Table 2.13b). In all six of the eight sensors gave responses to 1% methanol that were greater than the estimated LOD signal. Calculated methanol LODs for these sensors were in the range 0.18 - 1.15%.

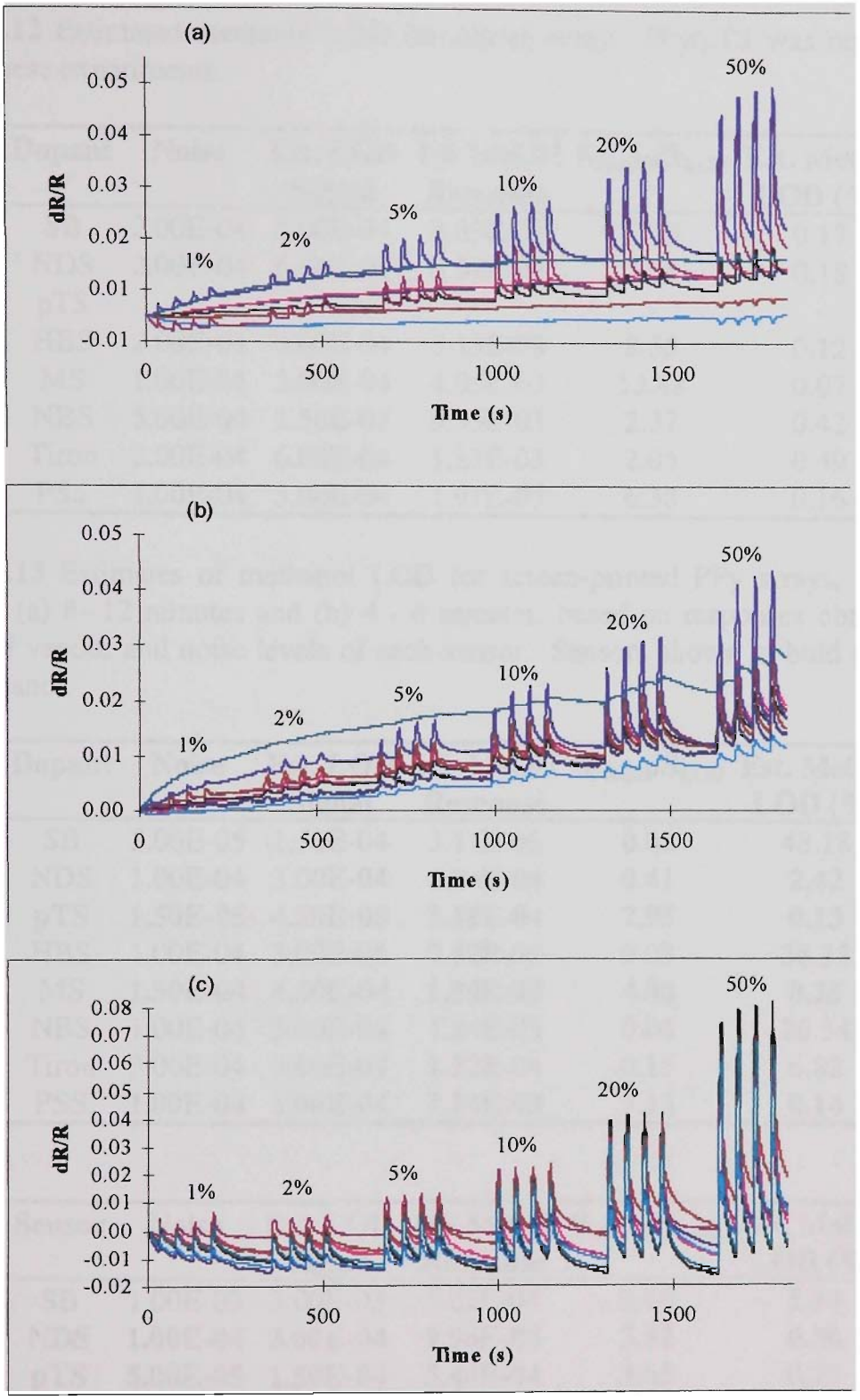

Figure 2.13 Comparison of the responses of (a) a screen-printed array of 8 PPys (pTS, PSS, SB, NDS, NBS, MS, Tiron, HBS) grown for 8 - 12 mins over PPy/Cl, (b) an array of the same PPys grown on PPy/Cl for 4 - 6 mins, and (c) these 8 PPys on silicon electrodes to a range of concentrations of methanol in nitrogen. The concentrations given are as percentages of saturated vapour.

Table 2.12 Estimated methanol LOD for silicon array. PPy/pTS was not responding during these experiments.

Dopant	Noise	Est. LOD Signal	1% MeOH Response	S_{MeOH}/S_{LOD}	Est. MeOH LOD (%)
SB	2.00E-04	6.00E-04	3.53E-03	5.89	0.17
NDS	2.00E-04	6.00E-04	3.39E-03	5.66	0.18
pTS	-	-	-	-	-
HBS	2.00E-04	6.00E-04	5.13E-03	8.56	0.12
MS	1.00E-04	3.00E-04	4.05E-03	13.48	0.07
NBS	5.00E-04	1.50E-03	3.55E-03	2.37	0.42
Tiron	2.00E-04	6.00E-04	1.23E-03	2.05	0.49
PSS	1.00E-04	3.00E-04	1.91E-03	6.38	0.16

Table 2.13 Estimates of methanol LOD for screen-printed PPy arrays, with growth times of (a) 8- 12 minutes and (b) 4 - 6 minutes, based on responses obtained to 1% methanol vapour and noise levels of each sensor. Sensors shown in bold responded to 1% methanol.

(a)

Dopant	Noise	Est. LOD Signal	1% MeOH Response	S_{MeOH}/S_{LOD}	Est. MeOH LOD (%)
SB	5.00E-05	1.50E-04	3.11E-06	0.02	48.18
NDS	1.00E-04	3.00E-04	1.24E-04	0.41	2.42
pTS	**1.50E-05**	**4.50E-05**	**3.58E-04**	**7.95**	**0.13**
HBS	1.00E-04	3.00E-04	7.82E-06	0.03	38.35
MS	**1.50E-04**	**4.50E-04**	**1.80E-03**	**4.00**	**0.25**
NBS	1.00E-04	3.00E-04	1.14E-05	0.04	26.34
Tiron	3.00E-04	9.00E-04	1.32E-04	0.15	6.82
PSS	**1.00E-04**	**3.00E-04**	**2.14E-03**	**7.13**	**0.14**

(b)

Sensor	Noise	Est. LOD Signal	1% MeOH Response	S_{MeOH}/S_{LOD}	Est. MeOH LOD (%)
SB	1.00E-03	3.00E-03	5.62E-04	0.19	5.34
NDS	**1.00E-04**	**3.00E-04**	**9.96E-04**	**3.32**	**0.30**
pTS	**5.00E-05**	**1.50E-04**	**5.48E-04**	**3.65**	**0.27**
HBS	**1.00E-04**	**3.00E-04**	**2.61E-04**	**0.87**	**1.15**
MS	**1.00E-04**	**3.00E-04**	**1.65E-03**	**5.50**	**0.18**
NBS	**1.50E-04**	**4.50E-04**	**1.67E-03**	**3.70**	**0.27**
Tiron	2.00E-04	6.00E-04	1.30E-04	0.22	4.63
PSS	**2.00E-04**	**6.00E-04**	**8.69E-04**	**1.45**	**0.69**

Shorter PPy growth times gave rise to a much better range of responses at low concentrations, as would be expected with thinner sensing films. However, the fact that some of the sensors with longer growth times (thicker films) gave more sensitive responses to 1% methanol suggests the sensor production process requires further study to ensure reproducibility. While the above results demonstrate that comparative sensitivity to methanol is obtainable using screen-printed sensors in place of silicon chips, in order to successfully discriminate different odours at low concentrations the overall sensitivity of screen-printed sensors arrays needs to be improved in a reproducible manner. The difference between the silicon and screen-printed arrays in terms of sensitivity is most likely a result of the much thicker sensing films obtained on the PPy/Cl modified Melinex. While the larger surface area of the screen-printed electrode films may assist in reducing this difference, clearly film thickness is the key.

2.3.3.3 Discrimination of Vapours

In addition to low limits of detection, a very important feature of sensors organised in an array is the ability to discriminate between different compounds. In order to test the two sensor types, both the screen-printed and silicon arrays were exposed to 50% concentrations of methanol, ethanol, propanol, and acetone. Principal component analysis (PCA) of the screen-printed sensor responses showed very good separation between the compounds (Figure 2.14). The silicon array also discriminated between these vapours, but the data were slightly more spread (Figure 2.15). The two PCAs are not identical in terms of the vapour cluster positions, but both show that the arrays successfully discriminated between the four compounds. These differences result from different response patterns observed for the two arrays when exposed to the same vapour. As described earlier, the discrepancy between the two arrays may be a result of

the different growth regimes used, and variability associated with using a PPy/Cl vapour deposited adhesion layer.

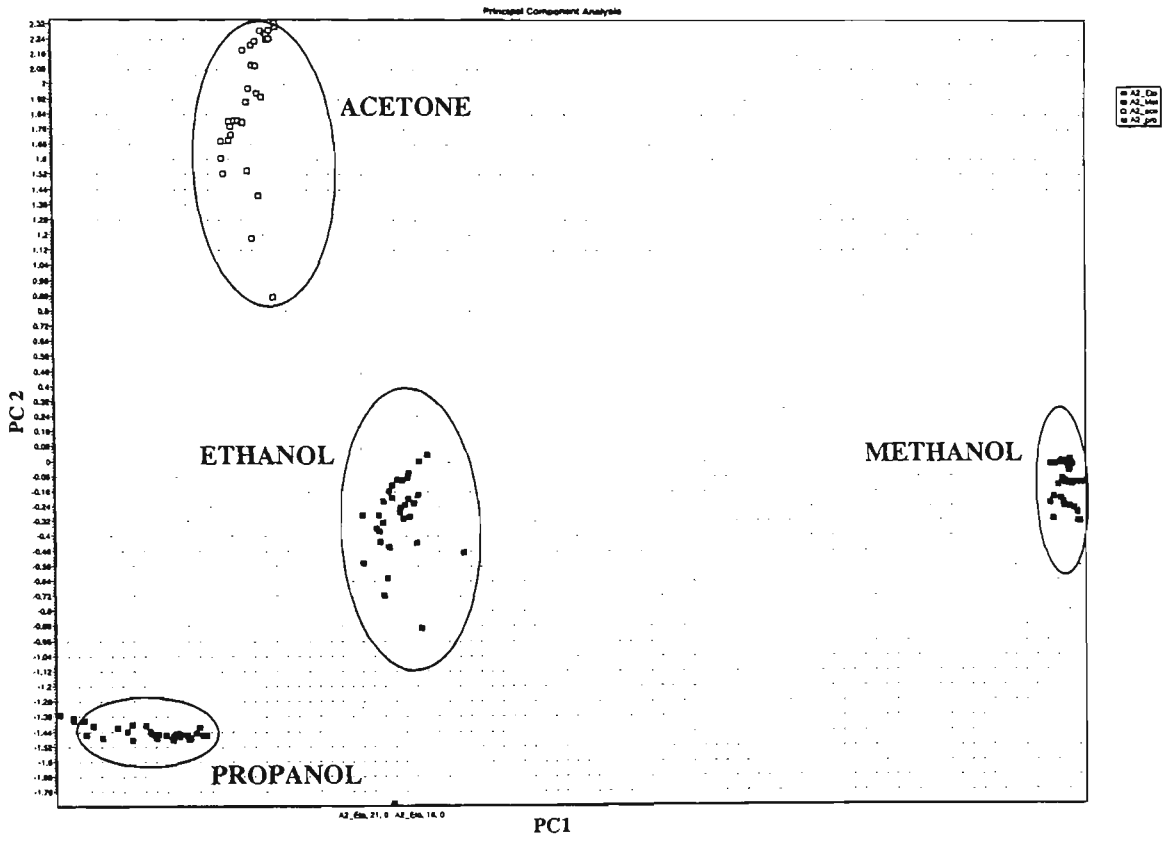

Figure 2.14 Principal component analysis of solvent responses from screen-printed array.

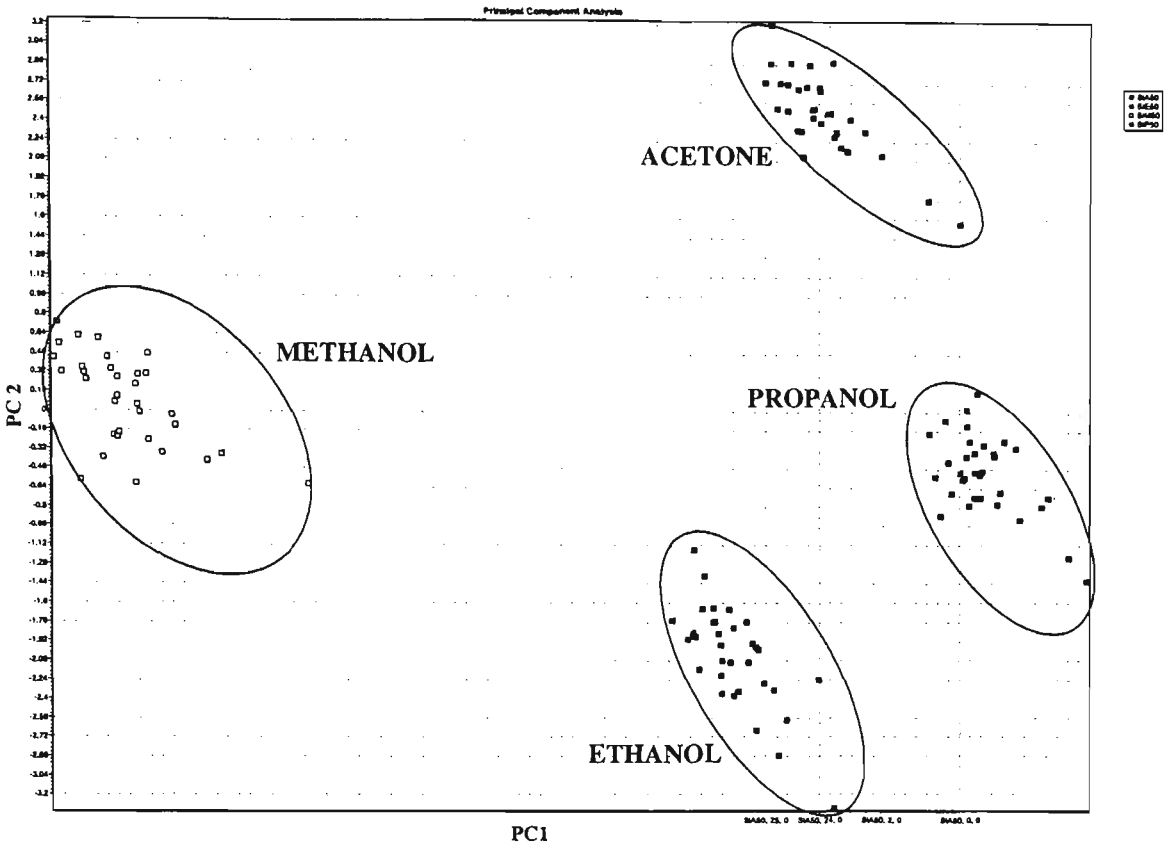

Figure 2.15 Principal component analysis of solvent responses from silicon odour chip array.

2.4 CONCLUSIONS

The performance of two arrays of PPy based gas sensors deposited on screen-printed carbon electrodes on Melinex and lithographically defined gold electrodes on silicon were evaluated. Various approaches to fabrication of the sensors on Melinex were considered, and it was found that the most effective method involved pre-treating the sensor surface with a vapour deposited PPy/Cl layer upon which the PPy sensing film was deposited. Based on the relative resistance values of the two layers and CV data it was concluded that the top polymer layer dominated the sensing properties of these sensors. Limits of detection of the two arrays were compared using methanol and it was found that both could detect this vapour at a concentration of less than 1%. The silicon based array, however, did give greater responses at lower methanol concentrations with all sensors giving a signal. In comparison only some of the sensors in the screen-printed Melinex array responded to methanol at 1%. Despite this, the two arrays exhibited the same linear ranges for methanol (1 - 10%), and it was shown by PCA that the screen-printed array could discriminate between methanol, ethanol, propanol and acetone vapours at 50% of saturation equally as well as the silicon array. The results indicate that when the issues of cost and ease of fabrication are considered, the screen-printed sensors become an attractive alternative to silicon based arrays. Obviously the issue of sensor reproducibility needs to be addressed before this can be realized, both in terms of response patterns relative to the silicon array, and between sets of screen-printed sensors. If this is to be achieved further optimization of the PPy/Cl vapour deposition process is required. Alternately, a different surface modification may overcome the problem, or indeed the use of a different polymer substrate could completely eliminate this step. Reduction of the inter-track spacing between the screen-printed electrodes may serve as another means to improving reproducibility, but will be limited by the

resolution associated with this method. One possibility for improving the PPy/Cl process could be a reduction in the oxidant ($FeCl_3$) concentration used, which may allow for better control over film conductivity. Another possibility is to use electrochemical post-deposition processing of PPy/Cl films in order to exchange the chloride ion for a different dopant.

Chapter 3

Anion Exchange Modification of PPy/Cl Vapour Deposited Gas Sensors

3.1 INTRODUCTION

One extremely useful feature of conducting polymer films is the possibility of electrochemical switching between reduced and oxidised states in a reversible manner. In solution this switching causes movement of ions in and out of the polymer to ensure that charge neutrality is maintained. This process is thought to involve a combination of anion and cation insertion/expulsion as the potential is cycled [203, 208, 209]. In the case of anion movement into and out of PPy films, at positive potentials the polymer is oxidised and anions are incorporated while at negative potentials the anion (A^-) may be expelled as the polymer is reduced to an insulating state (1).

$$PPy^0 + A^- > PPy^+A^- \qquad (1)$$

If anion movement to and from PPy is not significant as the polymer is reduced at negative potentials cations (C^+) are incorporated to balance the negative charge while at positive oxidative potentials the cations are expelled according to (2).

$$PPy\ A^-\ C^+ > PPy\ A^- + C^+ \qquad (2)$$

The movement of ions also is controlled by the mobility of both the dopant anion present in the film and the species being transported. When small dopant anions are incorporated into PPy during polymerisation, electrochemical cycling of the film in electrolyte is dominated by anion exchange [210]. This has been observed for PPy/Cl [211] and PPy/NO_3 [212]. When larger anions are employed during film preparation cation exchange dominates as the anions present are not suitably mobile to be expelled. Zhao and Wallace found that for PPy films, as the size of the sulfonated counterion

employed for doping increased so did the transport of Ca^{2+} [203]. PPy/PSS was found to exchange cations only [208, 209], as was the case for PPy/Tiron [213]. The exchange of ions in conducting polymers does not always follow these mechanisms, often both anions and cations are transported even when only one of these cases would be expected to dominate. The use of a large anion such as dodecylbenzenesulfonate (DBS) would be expected to effect mainly cation transport, however, Torresi *et al* observed anion exchange also in this case [214]. When PPy/Cl was cycled in a range of Cl^- solutions which varied in terms of the cation present, different mass changes were observed using EQCM suggesting cation exchange was significant in spite of the small Cl^- anion [209]. Departures from the expected transport mechanism may arise due the effect of PPy film microstructure, which is known to affect ion exchange [215]. Also, ion flux in and out of PPy has been shown to depend upon the affinity of anions for the polymer backbone [216]. Therefore in the case of PPy/Cl films cycled in Cl^- solutions there may not be a sufficient driving force to bring about significant anion movement. The nature of the ion exchanged in PPy has also been shown to be dependent on solution pH. At low pH anion exchange was favoured while a combination of cation and anion exchange was observed at pH > 3 - 4 [217].

Ion exchange has also been observed for PPy films soaked in electrolyte solutions without the application of a potential. Tsai *et al* soaked PPy/Tosylate films in aqueous anion solutions such as SO_4^{2-} and found that the rate of exchange depended on the nature of the anion in solution [218]. PPy/Cl and PPy/ClO_4 films were soaked in a range of anion solutions including SO_4^{2-}, Br^- and I^- with successful anion exchange observed which was again dependant on the anion in solution [219].

These properties of PPy have been used to enable ion transport through membranes, which is achieved by continually pulsing the potential [203, 220]. The type of ion exchanged can be controlled to some extent by the applied potential, and by using a dual PPy membrane system, the transport of anions and cations can be selected by applying appropriate potentials at the source and receiver sides of a transport cell. The ion exchange properties of PPy have also been used for chemical sensing of both anions and cations [e.g. 221, 222] where movement of these species brings about a measurable change in current.

The nature of the anion incorporated into PPy films is known to effect the morphology and also chemical sensing characteristics [203, 218, 223, 224]. The gas sensing properties of PPy are known to be effected by film morphology and can therefore be tailored by varying the anion present during polymerisation [101, 119, 225]. Electronic nose and systems based on CPs utilise the influence that the counter-ion has on chemical affinity to discriminate between different vapours. Serra *et al* [226] showed that polythiophene sensor responses to hexanal, a key component in the olive oil aromatic spectrum, were significantly affected by the oxidising salt used for polymer formation. Others using poly-3-methylthiophene sensors doped with different counter-ions for olive oil analysis have made this observation. The response of four sensors, each with a different dopant anion, to the same extra virgin olive oil was markedly different, providing a means of discriminating between different olive oils [154]. The same system has also been used to successfully discriminate between three different varieties of Spanish wine, ethanol and water [227].

By preparing PPy gas sensing films with small counter-anions such as chloride, anion exchange by either electrochemical pulsing or soaking should be favoured and it may be possible to incorporate other anions post-polymerisation. In the case of the PPy/Cl

vapour deposited sensing films described earlier in Chapter 2, this approach would combine the benefits of depositing very thin PPy layers onto flexible polymer substrates with the potential to vary selectivity and sensitivity to organic vapours.

3.1.1 Aims and Approach

The aim of this work was to modify PPy/Cl vapour deposited sensors, both electrochemically and by electrolyte soaking, by exchanging the Cl^- dopant with other anions. It was hoped that in doing so the advantages of the very thin PPy/Cl films would be retained, while selectivity to chemical vapours would be changed as a function of the new anion introduced. This approach could provide a means of overcoming the limited range of dopants available when preparing PPy sensors by chemical oxidation. The effect of PPy sensor ion exchange on solvent vapour discrimination was investigated using methanol, ethanol and acetone. X-ray photoelectron spectroscopy (XPS) was used to confirm that changes in gas responses were due to ion exchange within the PPy films.

3.2 EXPERIMENTAL

3.2.1 Preparation of PPy/Cl sensors

Thin films of PPy/Cl were vapour deposited onto Melinex polymer substrates, with an array of four screen-printed carbon track electrodes, using the approach detailed in Chapter 2, section 2.3.1.4. The resistance of these films was checked using a hand-held voltmeter between the outer pair of tracks. The film dimensions were defined by masking with cellulose tape to give an area of 5.0 mm × 2.0 mm.

3.2.2 Cyclic Voltammetry

The first approach employed was cycling of PPy/Cl sensors in various counter-ion solutions, between - 1000mV and + 700mV @ 100mV/s, using a standard three electrode cell with a Ag/AgCl reference, platinum auxiliary, and the sensor connected as

the working electrode. The counter-ion solutions used were KCl, $NaNO_3$, NapTS and polystyrene sulfonate (PSS), all of which were made up in Milli-Q water to a concentration of 0.1 M. The resistance of the sensors was monitored after cycling in the counter-ion solutions.

3.2.3 Soaking

Another approach examined was the use of soaking to exchange the Cl^- anion from PPy/Cl films. Solutions of 0.1 M NapTS, PSS and KCl were made up in Milli-Q water for these experiments. The sensors were placed in solution to soak initially for a period of 3 days. The R_0 of the sensors was measured before and after the soaking treatment. In later experiments the soaking time was limited to 5 minutes to ensure sensor resistances were not affected significantly.

3.2.4 Chronoamperometry

To monitor decay of electrochemical response of PPy/Cl sensors in 0.1M KCl, a constant reduction potential (-0.8V or -0.4V) was applied to the sensor versus a Ag/AgCl reference, using a platinum mesh auxiliary electrode. Chronoamperograms were recorded for a range of sensors and the corresponding resistance changes recorded. To investigate the reversibility of this reduction process, a constant oxidation potential (+ 0.7V) was subsequently applied and the resistance measured after this.

3.2.5 Potentiometry

To monitor the decay of PPy/Cl sensor potential in solution, E (mV) was measured relative to Ag/AgCl while the sensors were soaked in 0.1M KCl. The potential difference between the working and reference was simply measured using a hand-held

voltmeter over a period of 60 minutes. No current was applied during these experiments.

3.2.6 Pulsed Potential

A final approach used for electrochemically assisted anion exchange in PPy/Cl films was pulsed potential. The two potential limits were set at - 400mV and + 700mV with total pulse periods of 0.5 seconds and 1.0 second employed. The total time of each pulse potential experiment was limited to either 30 or 60 seconds.

3.2.7 X-ray Photoelectron Spectroscopy

Sensing films were analysed by XPS to determine whether anion exchange had been achieved using the techniques described above. Wide scan spectra scans were run to determine the relative amounts of nitrogen, chloride and sulfur in the sensing films.

3.2.8 Responses to Vapours

An electronic nose system was used to generate methanol vapours in nitrogen at a concentration of 50% saturation. Initial responses of the PPy/Cl sensors to this vapour were recorded before anion exchange treatments were applied. These responses were compared to those obtained after attempts were made to exchange the Cl^- counter-ion. The effect of anion exchange on vapour discrimination was also investigated using this approach with methanol, ethanol and acetone vapours at 50% saturation in nitrogen. Principal component analysis (PCA) was employed to examine any differences in separation of these three solvent vapours.

3.3 RESULTS AND DISCUSSION

3.3.1 Ion Exchange by Soaking

Four sensors were used to examine the effect of ion exchange on the resistance and gas response of PPy/Cl films. Prior to soaking the sensors were exposed to 50% methanol vapour in nitrogen and the responses monitored (results not shown). Two of the sensors were soaked in 0.1M counter-ion solutions, one in water, and a reference sensor was left in air. After a soaking period of 3 days the base resistance of all sensors placed in solution had increased significantly, while the resistance of the reference sensor remained constant (Table 3.1). Unfortunately the final resistance values of these sensors were too high to enable measurement of vapour responses on the test-rig available. The base resistance of sensor 8, which was soaked in PSS, did not increase to the same degree as the other sensors. This is most likely due to differences in film thickness, which were effected by the addition of a second PPy/Cl sensing layer. This second layer was added, only for sensor 8, in order to reduce film resistance so that vapour responses could be measured before soaking.

Table 3.1 Effect of soaking on PPy/Cl sensor base resistance values. * The initial R_0 of sensor 8 was 73.2 kΩ which was too high for measurement of methanol vapour responses. Hence a second layer of PPy/Cl was vapour deposited to reduce the R_0 thereby producing a thicker sensing film.

Sensor	R_0 (kΩ)	Soak solution	R_0 after 3 days (kΩ)
7	46.4	0.1 M NapTS	1910
8	23.1*	0.1 M NaPSS	414
9	36	Milli-Q Water	1220
10	17.7	N/A (Air)	17.8

Clearly the time period over which these sensors were soaked was too long. To assist in the selection of more appropriate times, PPy/Cl sensors were placed in KCl and the potential drop measured over time.

3.3.1.1 Potentiometry

Movement of ions to and from CP films causes changes in the resistance of these materials, and this property has been utilised for potentiometric sensing of ions in solution. CP ISEs have been developed for a range of species including H^+[40, 42], Br^- [43], DS^- [45].

The potential of a PPy/Cl sensor against a Ag/AgCl reference electrode in 0.1 M KCl was monitored over a 60 minute period after which the E (mV) had plateaued (Figure 3.1). The initial potential difference, which was 305 mV, decreased to 79 mV over the course of the experiment. The sensor resistance increased from an initial value of 158 kΩ to a final R_0 of 830 kΩ. The results obtained for duplicate PPy/Cl sensors (Table 3.2) suggest soaking times of no more than 5 minutes should be employed to ensure that sensor resistances are not significantly compromised. To investigate this further, a single PPy/Cl sensor was soaked in 0.1 M KCl for a period of 5 minutes.

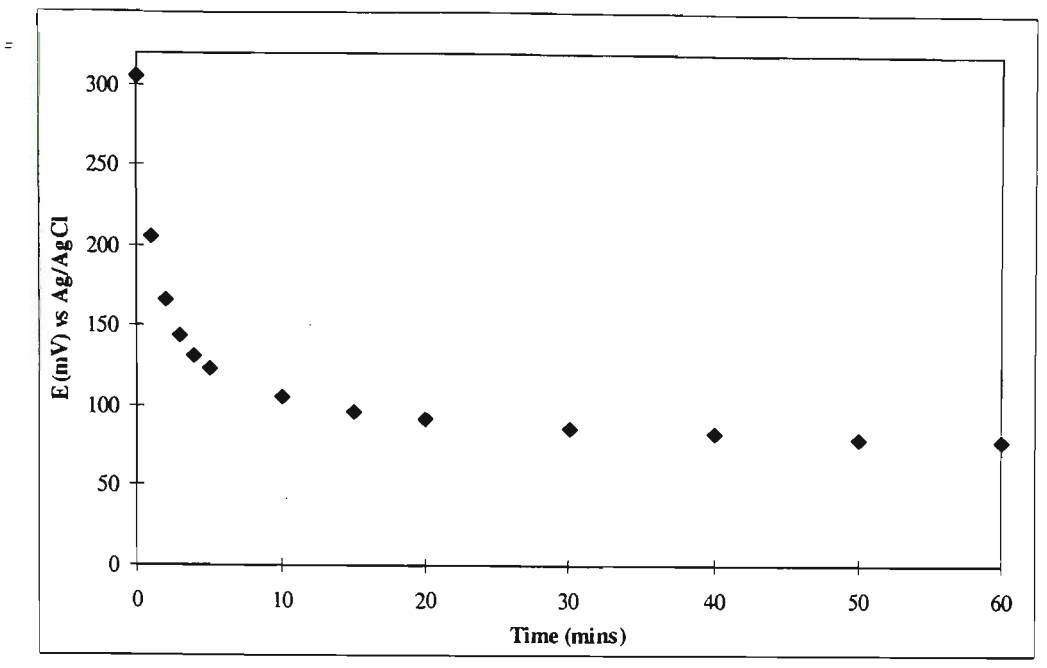

Figure 3.1 Potential drop of PPy/Cl sensor soaked in 0.1 M KCl measured against Ag/AgCl reference over a period of 60 minutes.

Table 3.2 Effect of soaking on E (mV) vs Ag/AgCl reference of duplicate PPy/Cl sensors initially (E0), after 5 minutes (E5), and after 60 minutes (E60). Base sensor resistances prior to soaking (Rinit) and after 60 minutes (Rfinal) are included.

Sensor	E0	E5	E60	Rinit	Rfinal
1	305	123	79	158	830
2	350	112	51	96	280

Sensor resistance was measured before and after this period of soaking. The resistance only changed by about 6 kΩ as a result of soaking, with an increase from 24.2 to 30.5 kΩ observed. Results obtained from pulse potential work (section 3.3.4.3) suggested that by increasing the KCl concentration to 1M, a significant reduction in R_0 increase could be achieved. A single sensor was placed in 1M KCl to soak for 5 minutes. After soaking the resistance had changed by only 0.4 kΩ (R_0 = 24.9, Rfinal = 25.3 kΩ), confirming that the use of a higher KCl concentration has a significant effect

on Rfinal. Based on these results, a soak time of 5 minutes and counter-ion concentration of 1M were selected for all future work.

3.3.1.2 Effect on PPy/Cl Gas Responses

After soaking for a period of 5 minutes the R_0 values of all sensors increased (Table 3.3) but by less than 10 kΩ. Even sensors 7 and 8, which were soaked in water, showed increased base resistance possibly due to removal of chloride anions. These changes in resistance were generally smaller when compared to the changes observed for sensors pulsed in the same counter-anion solutions (Table 3.7), but the changes caused by water were greater in the case of soaking. A comparison of responses to methanol before and after soaking (Figure 3.2) shows that the sensitivity of soaked sensors increased. The pattern of responses on the whole was similar with the exception of sensors 3 and 4, which were soaked in PSS. Prior to soaking sensor 3 gave a slightly smaller response to

Table 3.3 Base resistance values of the sensors before and after soaking.

Sensor	R_0 pre -soaking (kΩ)	Soak solution	R_0 post-soaking (kΩ)
1	15.8	pTS	24.4
2	18.5	pTS	24.6
3	16.5	PSS	24.2
4	18.6	PSS	23.0
7	16.6	Water	22.9
8	20.4	Water	27.4

methanol than sensor 4, but after soaking the response of sensor 3 increased significantly relative to sensor 4. The sensing array was also exposed to ethanol and

acetone, both before and after soaking, to examine solvent discrimination properties. PCA plots of the response data (Figure 3.3) show that separation between these compounds is similar before and after soaking. However, the data points clustered more tightly after soaking due to improvements in the sensitivity.

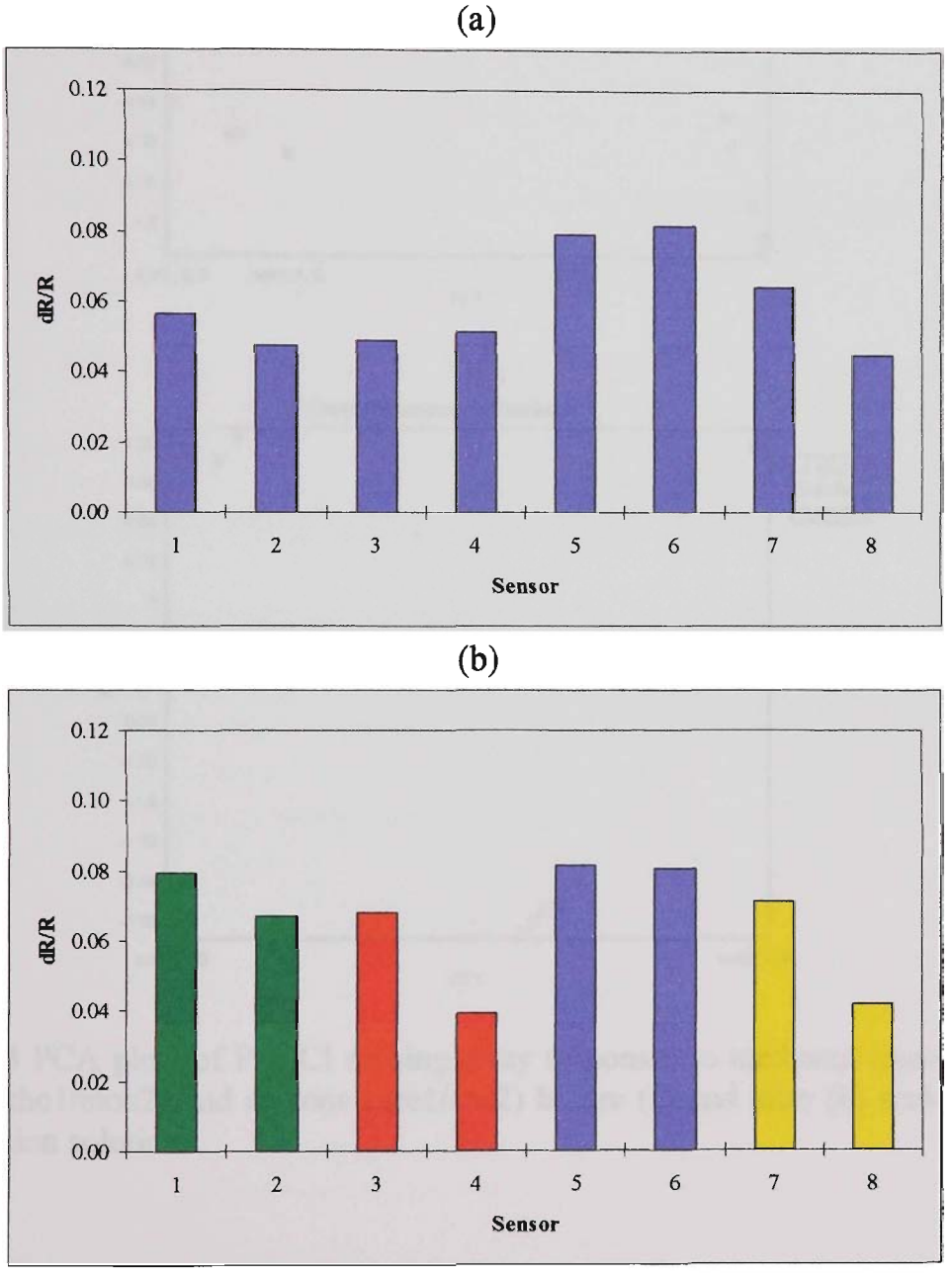

Figure 3.2 Response of PPy/Cl sensor array (a) before and (b) after soaking in 1M counter-ion solutions to 50% methanol in nitrogen. Sensors 1 - 2 were soaked in pTS, 3 - 4 in PSS and 7 - 8 in water.

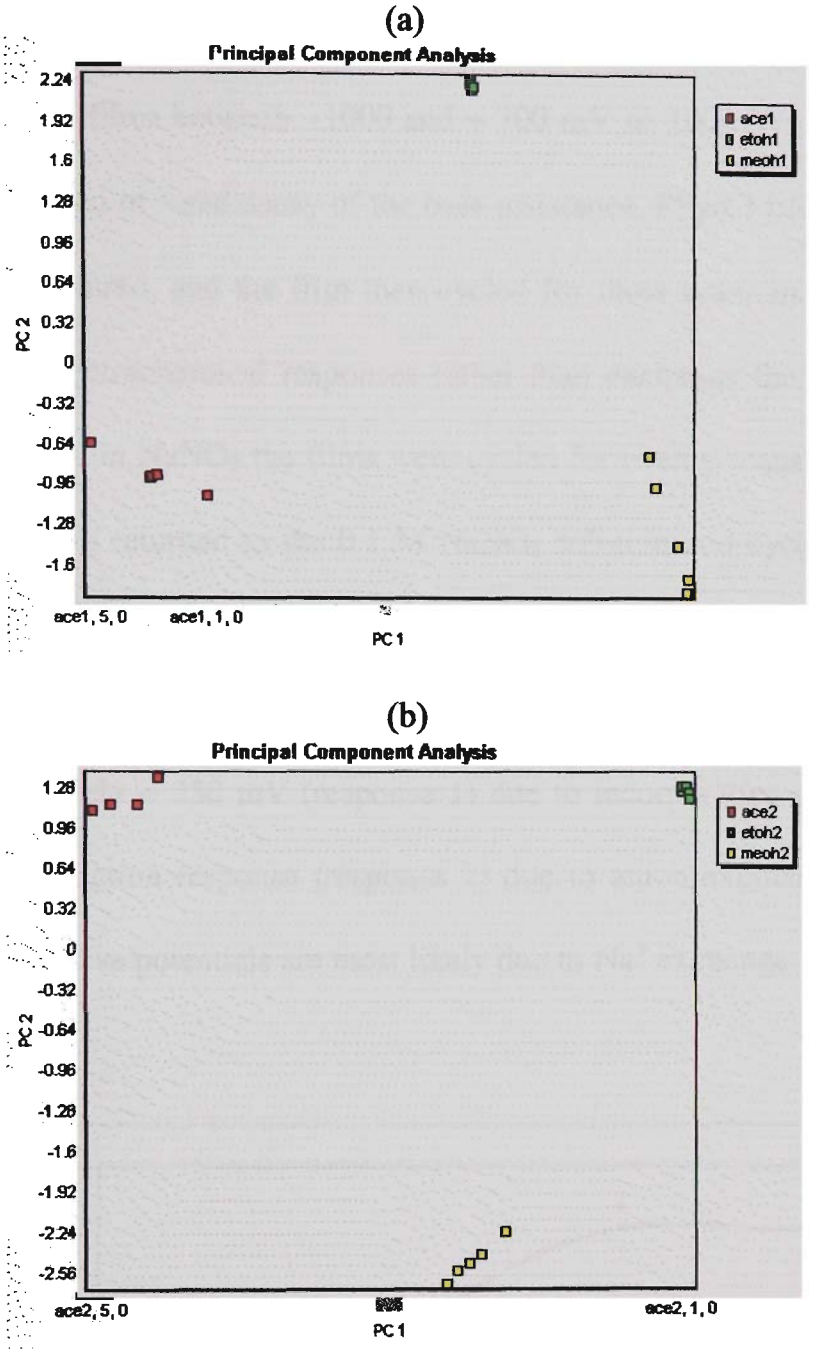

Figure 3.3 PCA plots of PPy/Cl sensing array responses to methanol (meoh1/meoh2), ethanol (etho1/etoh2) and acetone (ace1/ace2) before (a) and after (b) soaking in 1 M counter-anion solutions.

3.3.2 Cyclic Voltammetry

Cycling the PPy/Cl films between -1000 and + 700 mV @ 100mV/s in 0.1 M counter-ion solutions resulted in rapid decay of the base resistance. PPy/Cl films were prepared, the resistance measured, and the film then cycled for three scans in 0.1 M $NaNO_3$ to characterise the electrochemical responses rather than exchange the anion. After the short cycling period in $NaNO_3$ the films were cycled for twenty scans in 0.1 M NapTS. The films were then returned to the 0.1 M $NaNO_3$ solution and cycled for a further 3 scans to investigate any changes in film electrochemistry.

The CV of a PPy/Cl film (Sensor 1) in $NaNO_3$ (Figure 3.4) shows a broad oxidation peak at approximately + 250 mV (response 1) due to incorporation of the NO_3, and a poorly defined reduction response (response 2) due to anion expulsion. Responses 3 and 4 at more negative potentials are most likely due to Na^+ exchange.

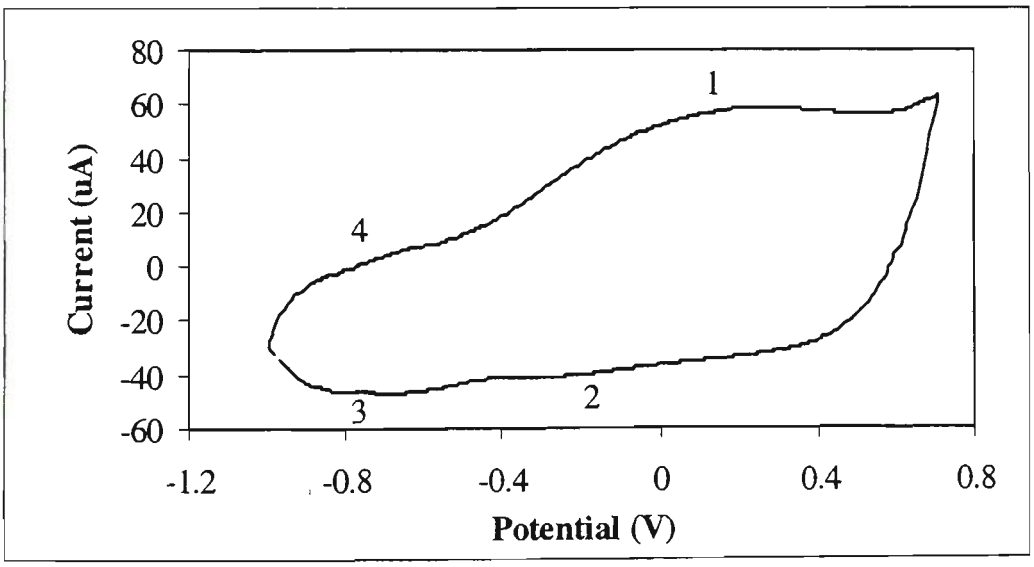

Figure 3.4 Cyclic voltammogram of PPy/Cl sensor (Sensor 1) in 0.1 M $NaNO_3$ scanned between -1000 and + 700 mV @ 100 mV/s.

The dominance of anion transport would be expected as the chloride anion is know to readily exchange from PPy films when cycled in solution [213]. Zhao *et al* observed

two sets of responses for PPy/pTS films cycled in 0.2 M KCl, but much larger responses were observed on the reduction scan at more negative potentials. The responses at positive potentials were assigned to anion exchange while the large reduction response and corresponding oxidation peak at negative potentials was attributed to preferential incorporation of the K^+ cation [203]. Cycling of the PPy/Cl sensor (Sensor 1) in 0.1 M NapTS gave rise to a much different voltammogram (Figure 3.5) with responses only at negative potentials.

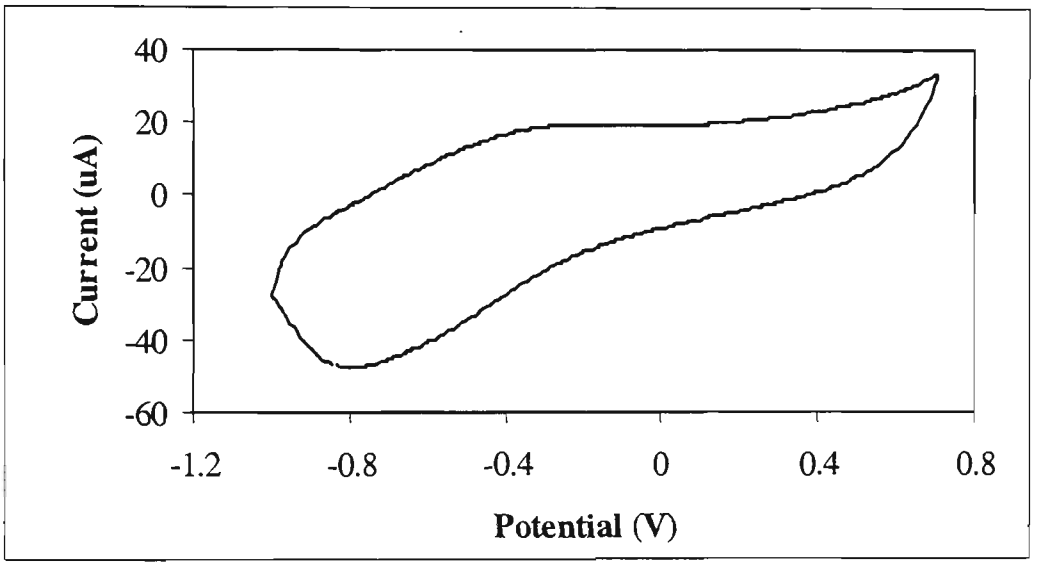

Figure 3.5 Cyclic voltammogram of a PPy/Cl sensor (Sensor 1) when cycled in 0.1 M pTS. Scan range -1000 to + 700 mV @ 100 mV/s.

The sensor was first characterised by CV in 0.1 M $NaNO_3$ before the above voltammogram was recorded. This infers that cation exchange is the dominant process in this case, which may be due to the difficulty in exchanging the larger pTS anion for the Cl^-. It has been suggested that if dopant anions are intercalated between polymer chains during PPy growth, the use of small dopants such as Cl^- leads to small interplanar spacing making it difficult for larger anions to be incorporated from solution [219, 228]. After 20 scans in NapTS, a loss of electroactivity was observed when the film was

cycled again in 0.1 M $NaNO_3$ (Figure 3.6). The CV was similar to that shown in Figure 3.5 but the oxidation response 1 was much less significant. This may also be due to the incorporation of some pTS anions, which would be expected to decrease the amount of anion exchange.

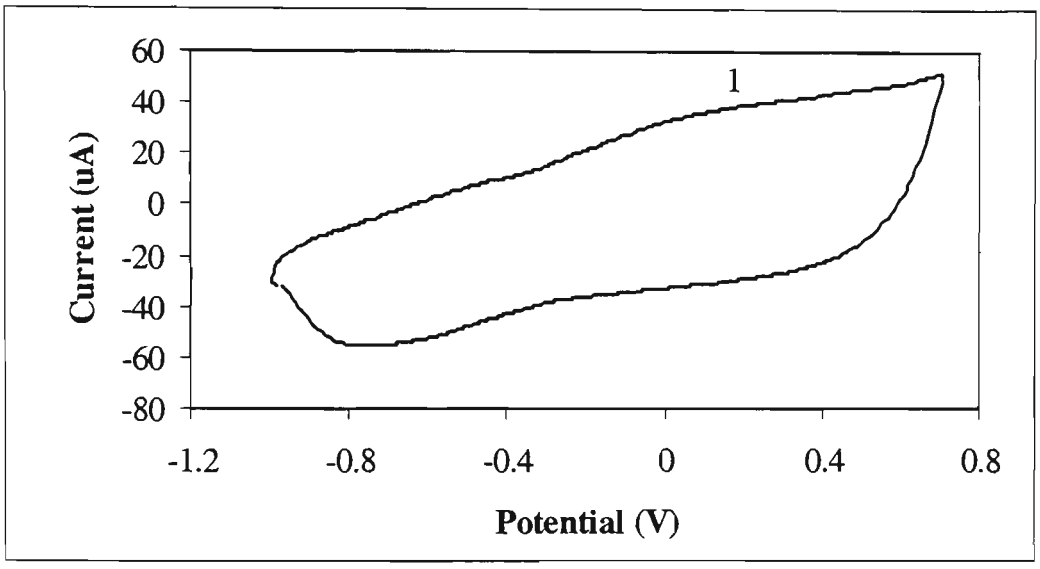

Figure 3.6 Cyclic voltammogram of PPy/Cl sensor (Sensor 1) in 0.1 M $NaNO_3$ after 20 cycles in 0.1 M pTS. Scan range -1000 to + 700 mV @ 100 mV/s.

The initial cycling of sensors in 0.1 M $NaNO_3$ led to unwanted increases in resistance so this step was omitted when attempts were made to exchange PSS with Cl^- anions. In this case PPy/Cl films were prepared and then placed directly into PSS for cycling. The CV of PPy/Cl (Sensor 3) in 0.1 M PSS (Figure 3.7) exhibited different responses when compared to PPy/Cl responses in 0.1 M NapTS (Figure 3.5), which may be related to the initial $NaNO_3$ step used prior to pTS cycling. The large oxidation response (3) observed at negative potentials may be due to either cation expulsion or incorporation of PSS into the PPy/Cl film. However, in the case of PSS, which is a much larger anion than pTS, incorporation should be even more difficult.

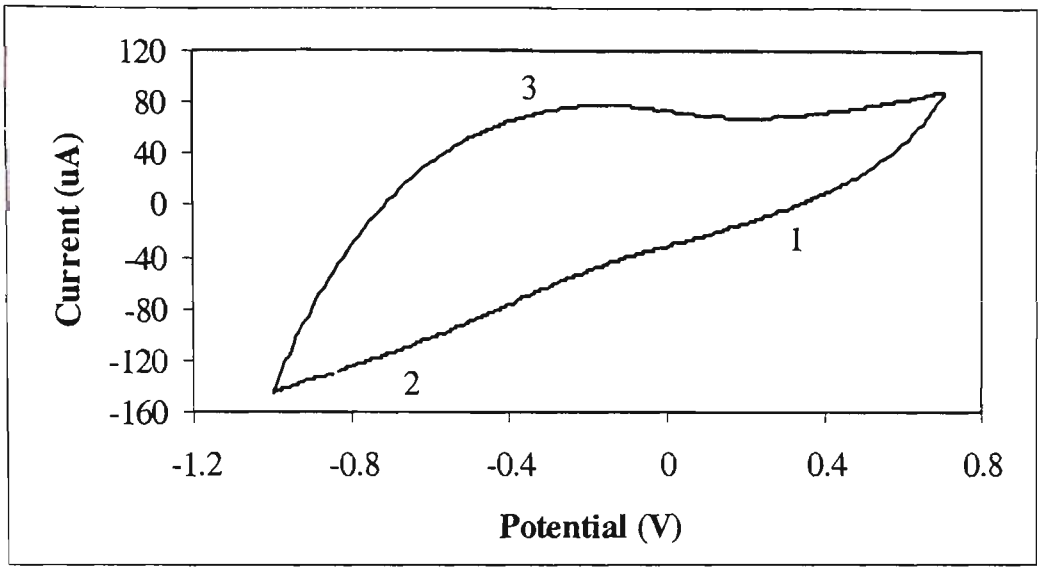

Figure 3.7 Cyclic voltammogram of PPy/Cl sensor (Sensor 3) in 0.1 M PSS. Scan range -1000 to + 700 mV @ 100 mV/s.

For comparison with the sensors cycled in pTS (Sensor 1 and 2), the sensor cycled in PSS (Sensor 3) was subsequently scanned in 0.1 M $NaNO_3$ (Figure 3.8) for three cycles. The profile of this CV was clearly different to the PPy/Cl/pTS film indicating that PSS anions may have been incorporated.

The effects of cycling PPy/Cl sensors in NO_3, pTS, and PSS counter-ion solutions on sensor resistance are summarised in Table 3.4. The resistance of the films cycled in $NaNO_3$ prior to cycling in pTS (Sensor 1 and 2) increased significantly after only three cycles, which may be due to the ease with which the thin PPy/Cl layer is overoxidised. After twenty scans in NapTS the resistance of these sensors had again increased, but more significantly. To avoid unwanted increases in sensor resistance, Sensors 3 and 4 were cycled only in PSS. After cycling in PSS the resistance of these sensors increased significantly, but not to the same extent as did the sensor exposed to both NO_3 and pTS (Sensors 1 and 2). It is possible that the process of cycling these thin films, rather than the nature of counter-ion exchange solution, may exert a significant effect on conductivity. If the films are sufficiently rigid the process of cycling may in fact break

the polymer chains apart. Unfortunately all four sensors treated by the above method were too resistive to be used as gas sensors on the test-rig available.

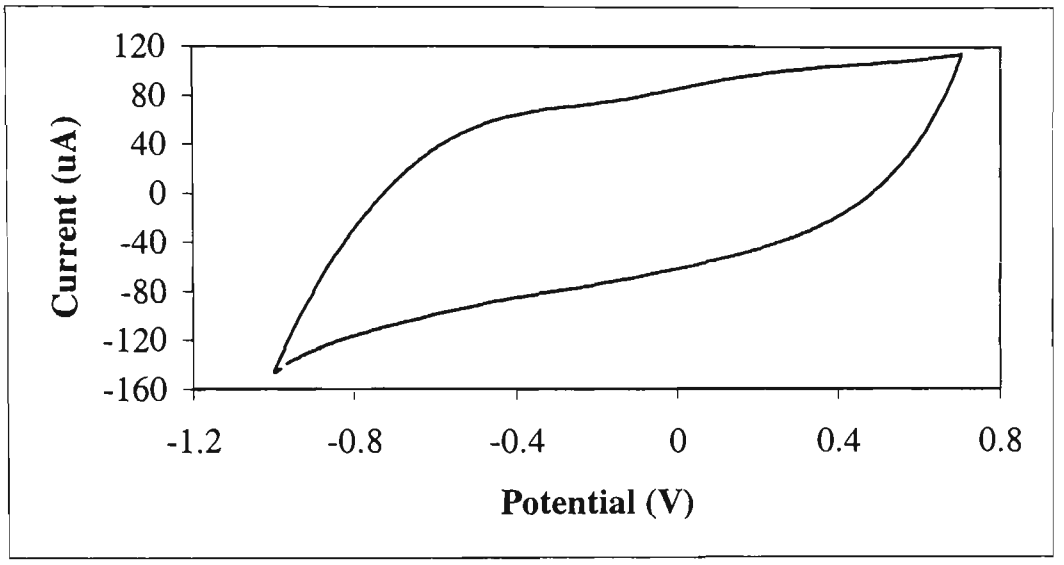

Figure 3.8 Cyclic voltammogram of PPy/Cl sensor (Sensor 3) in 0.1 M $NaNO_3$ after cycling in 0.1 M PSS. Scan range -1000 to + 700 mV @ 100 mV/s.

Table 3.4 Resistance of PPy/Cl sensors initially (R_0), after 3 cycles in NO_3^-(R_{NO3}), and after cycling for 20 scans in counter-ion solutions (R_{final}). * Sensors 3 and 4 were not cycled in NO_3^- and hence R_{NO3} values were not measured.

Sensor	R_0 (kΩ)	R_{NO3}(kΩ)	Counter-ion	R_{final} (kΩ)
1	25.0	250	pTS	2000
2	21.2	77	pTS	1700
3	22.0	*	PSS	800
4	15.7	*	PSS	500

To confirm that the observed losses of conductivity were due to the cycling process rather than the nature of counter-ion solution used, sensors were scanned in 0.1 M KCl for three cycles. The results obtained show that even in KCl a significant loss of electroactivity (Figure 3.9) occurs. The resistance of the sensor employed in this

experiment increased from 31 kΩ to 460 kΩ after the three scans. It was decided in light of these findings that the use of cyclic voltammetry was not suitable for anion exchange between PPy/Cl vapour deposited films and solutions of other counter-ions.

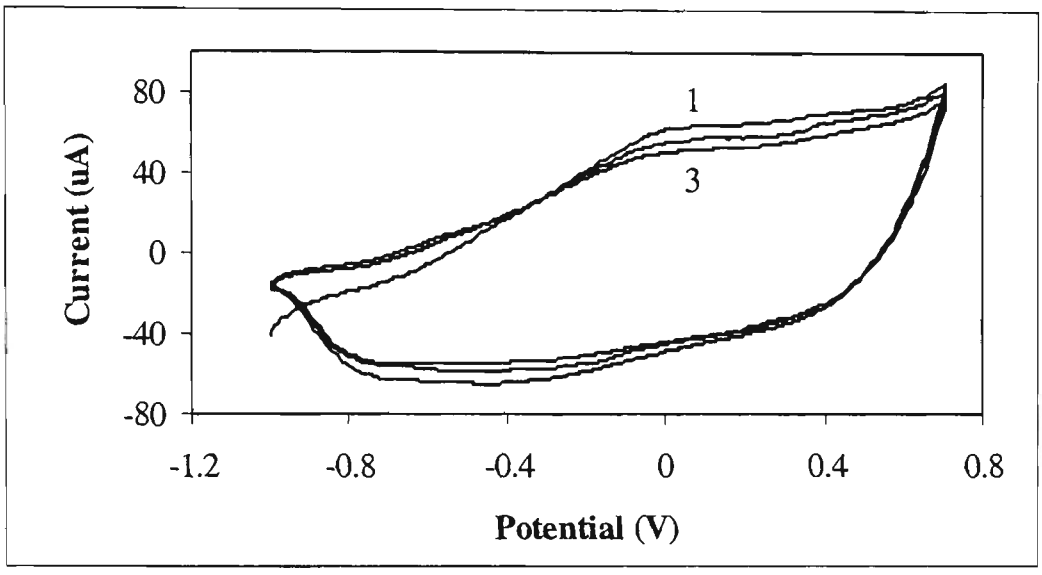

Figure 3.9 Decrease in electroactivity of PPy/Cl film after three cycles in 0.1 M KCl. Scan range -1000 to + 700 mV @ 100 mV/s.

3.3.3 Chronoamperometry

To gain some insight into the rapid decay of conductivity observed when PPy/Cl films were cycled, chronoamperometry was employed. When a PPy/Cl film was held at - 0.8 V vs Ag/AgCl in 0.1 M KCl, the current decayed to 0 μA in about 20 seconds (Figure 3.10). The film resistance was measured after this and had increased from an initial 33.3 kΩ to 1100 kΩ. Attempts to reoxidise this film by applying a potential of + 0.7 V led to further increases in resistance (1980 kΩ) indicating that these films irreversibly reduce rapidly at a potential of - 0.8 V. As was mentioned earlier, this may be related to the thickness of the PPy/Cl layer which is only a few nanometres.

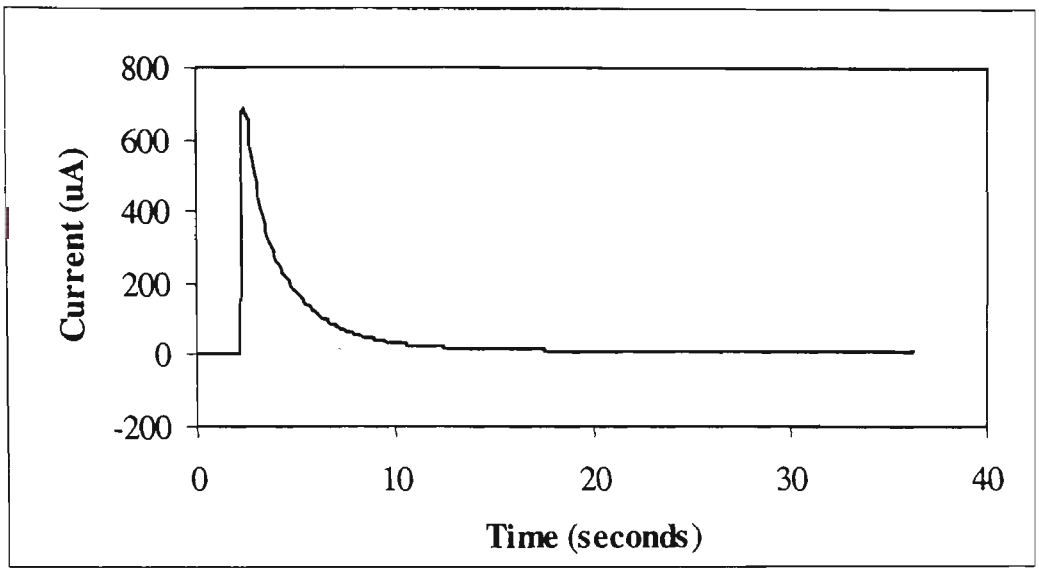

Figure 3.10 Current response of a PPy/Cl sensor held at a constant potential of - 0.8 V vs Ag/AgCl in 0.1 M KCl.

For this reason a series of chronoamperograms were run using an applied potential of - 0.4 V. The observed current decay of a PPy/Cl sensor held at this potential was not as significant when compared to the results discussed above (Figure 3.11). The corresponding resistance change of this sensor was also reduced, with a final R_0 of 670 kΩ from an initial value of 17.8 kΩ. Attempts to reoxidise this film were more successful with a marked reduction in resistance change as a result (158 kΩ). The time taken for the current to half decay was estimated from Figure 3.11 to be approximately one second. As the use of -0.4 V caused less conductivity decay in PPy/Cl films, this potential was selected for investigation in pulsed potential anion exchange. Also, the pulse period was limited to 1 second maximum to ensure some film conductivity was retained.

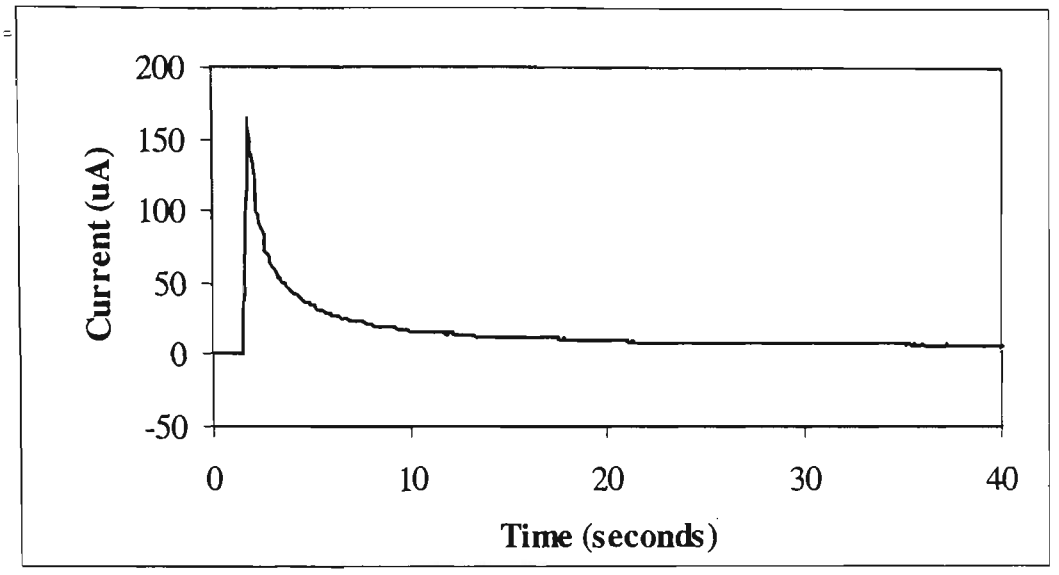

Figure 3.11 Current response of a PPy/Cl sensor held at a constant potential of - 0.4 V vs Ag/AgCl in 0.1 M KCl.

3.3.4 Pulse Potential Anion Exchange

3.3.4.1 Effect on Sensor Resistance

Initial experiments were carried out to determine the effect of applying a pulsed potential on PPy/Cl sensor resistance in 0.1 M KCl. The resulting chronoamperograms were similar for all sensors with a reproducible current response observed over time (Figure 3.12). However, R_0 values of the four sensors examined increased by a factor of two to three times as a result of pulsing (Table 3.5).

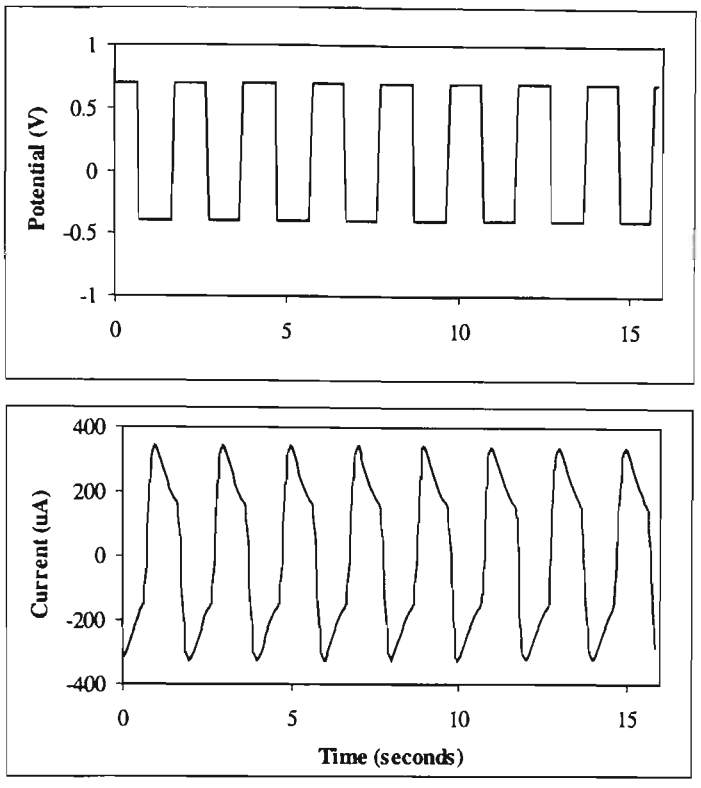

Figure 3.12 Potential wavefrom and current response of PPy/Cl sensor when pulsed between - 0.4 and + 0.7 V in 0.1 M KCl. Pulse period was 1 second.

These increases seemed to be independent of the pulse period employed with similar changes observed for both 0.5 and 1.0 second pulse times. The final sensor R_0 values were too high for the circuitry of the electronic nose system used for testing and hence the response to vapours could not be measured.

Table 3.5 Effect of applying a pulsed potential in 0.1 M KCl on PPy/Cl sensor resistance.

Sensor	R_0 (kΩ)	Pulse Period (s)	Total Pulse Time (mins)	Rfinal (kΩ)
21	32.2	0.5	1	84.5
22	24.2	0.5	1	79.0
23	22.0	1.0	1	50.0
24	29.3	1.0	1	93.0

The effect of reducing the total pulse time to 30 seconds was investigated in an attempt to overcome this problem. The resistance change observed was not as significant when sensor 23 was pulsed for a total 30 seconds in 0.1 M KCl using a 1 second pulse period. The R_0 increased from 52.4 to 76.0 kΩ, a total change of 23.6 kΩ. This improvement, while only small, suggested that limiting total pulse time to 30 seconds could overcome the problem of large final R_0 values.

3.3.4.2 Effect of Electrolyte Concentration

A PPy/Cl sensor was pulsed for 30 seconds in 1 M KCl using a pulse period of 1s and the potentials mentioned above. The change in resistance after pulsing was drastically reduced when compared to the results obtained for PPy/Cl sensors in 0.1 M KCl (Table 3.5). The R_0 increased from 60.8 kΩ to 71.6 kΩ, which was a total change of only 10.8 kΩ. This result suggested that the concentration of counter-ion in solution affects the final resistance of PPy/Cl sensors. For further pulse potential work the following conditions were selected; a pulse period of 1 second, total pulse time of 30 seconds, pulse potentials of – 400 mV and + 700 mV, and counter-ion solution concentration of 1 M.

3.3.4.3 Effect on Methanol Vapour Responses

For initial investigation of the effect pulsed potential anion exchange has on PPy/Cl sensor gas responses, 50% methanol vapour in nitrogen was employed. An array of six PPy/Cl sensors were prepared and then exposed to methanol vapour. Four of the six sensors were pulsed in solutions of 1 M counter-ion, and the remaining 2 left untreated for reference (Table 3.6). The resistances of sensors pulsed in KCl and pTS did not

increase to exceedingly high values, allowing the methanol vapour responses to be tested.

Table 3.6 Details of sensor array used for testing effect of pulsing on methanol vapour response. * Sensors 5 and 6 were kept as references and hence were not electrochemically modified by pulsing in an electrolyte solution.

Sensor	R_0 (kΩ)	Counter-ion Solution	Rfinal (kΩ)
1	15.6	1M KCl	18.1
2	15.9	1M KCl	25.5
3	15.6	1M pTS	20.2
4	18.1	1M pTS	35.2
5	17.0	*	17.0
6	22.7	*	22.7

The pattern of responses due to 50% methanol in nitrogen changed after the sensors were pulsed. Figure 3.13a shows the pattern obtained pre-pulsing, and Figure 3.13b shows responses after the sensors had been pulsed and allowed to dry for a short period. Sensors 3 and 4, which had been pulsed in pTS, showed varied response changes. The response from sensor 3 decreased slightly, while sensor 4 exhibited a large increase in sensitivity to methanol. The two sensors that were pulsed in KCl (1 and 2) both showed increased responses to methanol vapour, which were most significant for sensor 2. The reason for this increase may be related to a change in the amount of Cl^- incorporated

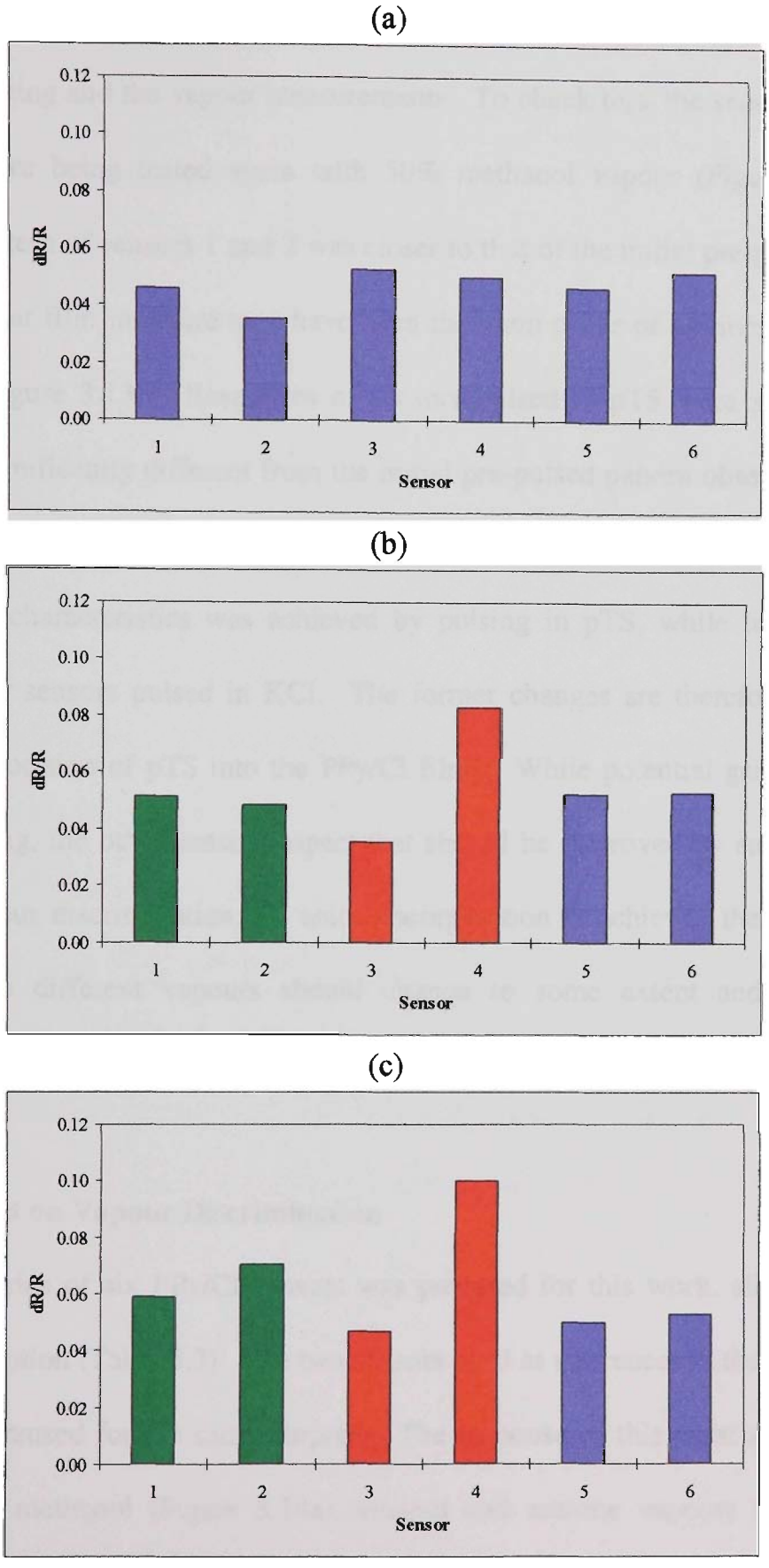

Figure 3.13 Response of PPy/Cl sensor array to 50% methanol vapour in nitrogen before (a) and after (b) sensors 1 - 4 were pulsed in 1 M counter-ion solutions. Responses of the pulsed sensor array to methanol after a period of 3 days (c) are also included. Sensors 1 and 2 were pulsed in KCl, sensors 3 and 4 in NapTS, and sensors 5 and 6 were not modified.

or a change in the R_0 value, but is more likely due to the insufficient drying time between pulsing and the vapour measurements. To check this, the sensors were left for 3 days before being tested again with 50% methanol vapour (Figure 3.13c). The response pattern of sensors 1 and 2 was closer to that of the initial pre-pulse experiment indicating that film moisture may have been the main cause of the increased responses shown in Figure 3.13b. Responses of sensors pulsed in pTS were also smaller, but remained significantly different from the initial pre-pulsed pattern observed, and sensor 4 still exhibited enhanced methanol sensitivity. These results infer that some change to the sensing characteristics was achieved by pulsing in pTS, while little change was observed for sensors pulsed in KCl. The former changes are therefore likely due to some incorporation of pTS into the PPy/Cl films. While potential gains in sensitivity are interesting, the other sensing aspect that should be improved by anion exchange is solvent vapour discrimination. If anion incorporation is achieved then the pattern of responses to different vapours should change to some extent and hence modify selectivity.

3.3.4.4 Effect on Vapour Discrimination

A second series of six PPy/Cl sensors was prepared for this work, all of which were pulsed in solution (Table 3.7). The two sensors used as references in the work described above were reused for the same purpose. The response of this eight sensor array was tested using methanol (Figure 3.14a), ethanol and acetone vapours in nitrogen at a concentration of 50% saturation, both before and after pulsing in solution. To avoid any effects of residual water in the films after pulsing, responses were obtained after the films had dried for 24 hours.

Table 3.7 Properties of sensors used to test effect of pulsing on solvent vapour discrimination.

Sensor	R_0 (kΩ)	Counter-ion Solution	Rfinal (kΩ)
1	15.3	1 M pTS	30.2
2	18.6	1 M pTS	35.1
3	28.8	1 M PSS	62.5
4	14.5	1 M PSS	20.5
5	14.2	Water	15.7
6	13.5	Water	21.1

Responses to methanol again increased for all sensors that were pulsed in solution, including the two exposed to water. The reason for the increased sensitivity to methanol after pulsing in water, or KCl as was noted above, may be due to a reordering of the polymer film in solution when pulsed. This may lead to changes in film morphology which give rise to improved gas sensing properties. The changes in response of sensors pulsed in counter-ion solutions to methanol were significant in terms of sensitivity, but the actual pattern of responses did not appear to change substantially (Figure 3.14b).

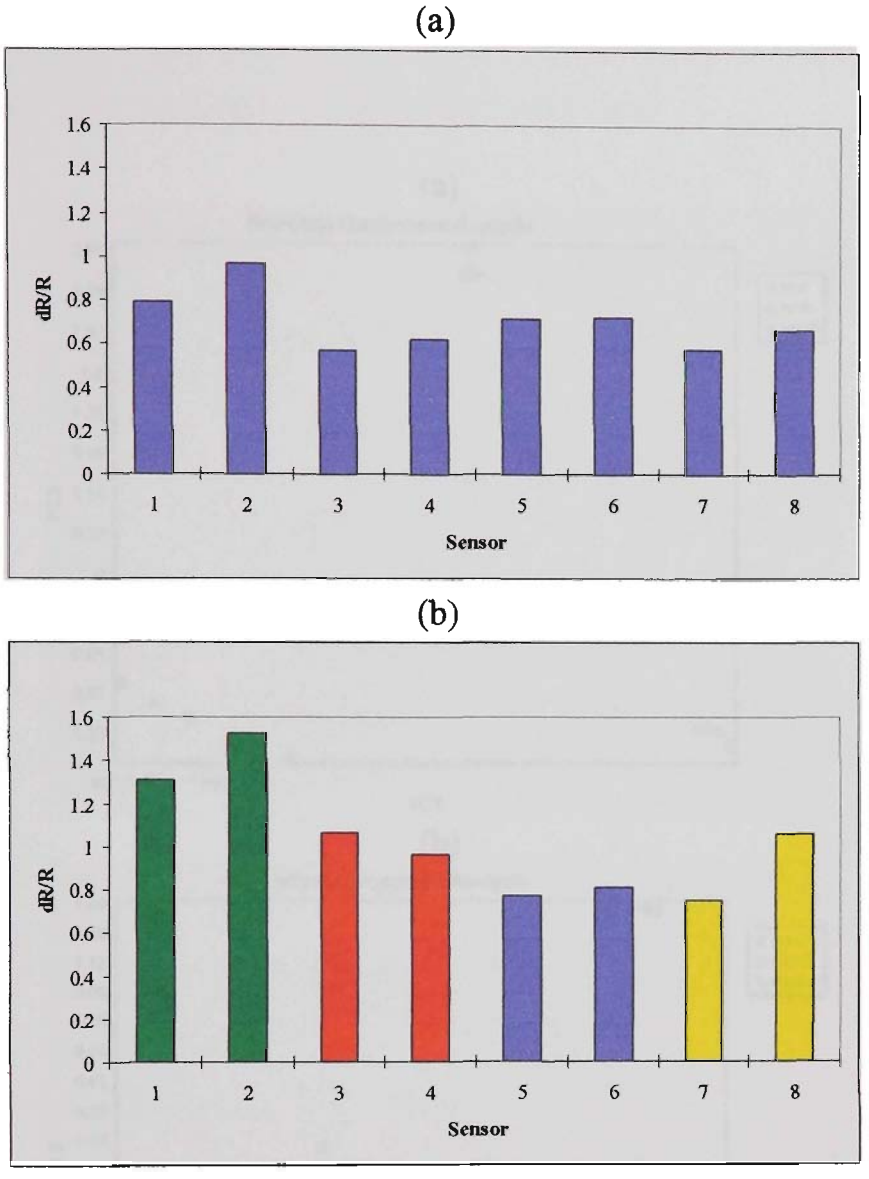

Figure 3.14 Response of PPy/Cl sensor array to 50% methanol in nitrogen before (a) and after (b) pulsing in 1 M counter-ion solutions. Sensors were pulsed in pTS (1-2), PSS (3-4) and water (7-8). Sensors 5 and 6 were untreated and used as controls.

To analyse the set of results completely for changes in response patterns, PCA was used. Figure 3.15a shows the PCA of sensor responses to the three solvent vapours pre-pulsing. Each point on the plot represents the average response of four exposures to each of the gases. The sensors were exposed to each vapour five times in total. Figure 3.15b shows the corresponding PCA of sensor responses after the six test sensors were pulsed in the various solutions. The patterns did not change significantly but the post-

pulsing plot shows tighter clustering for both methanol and ethanol as a result of the enhanced sensitivity achieved by anion exchange.

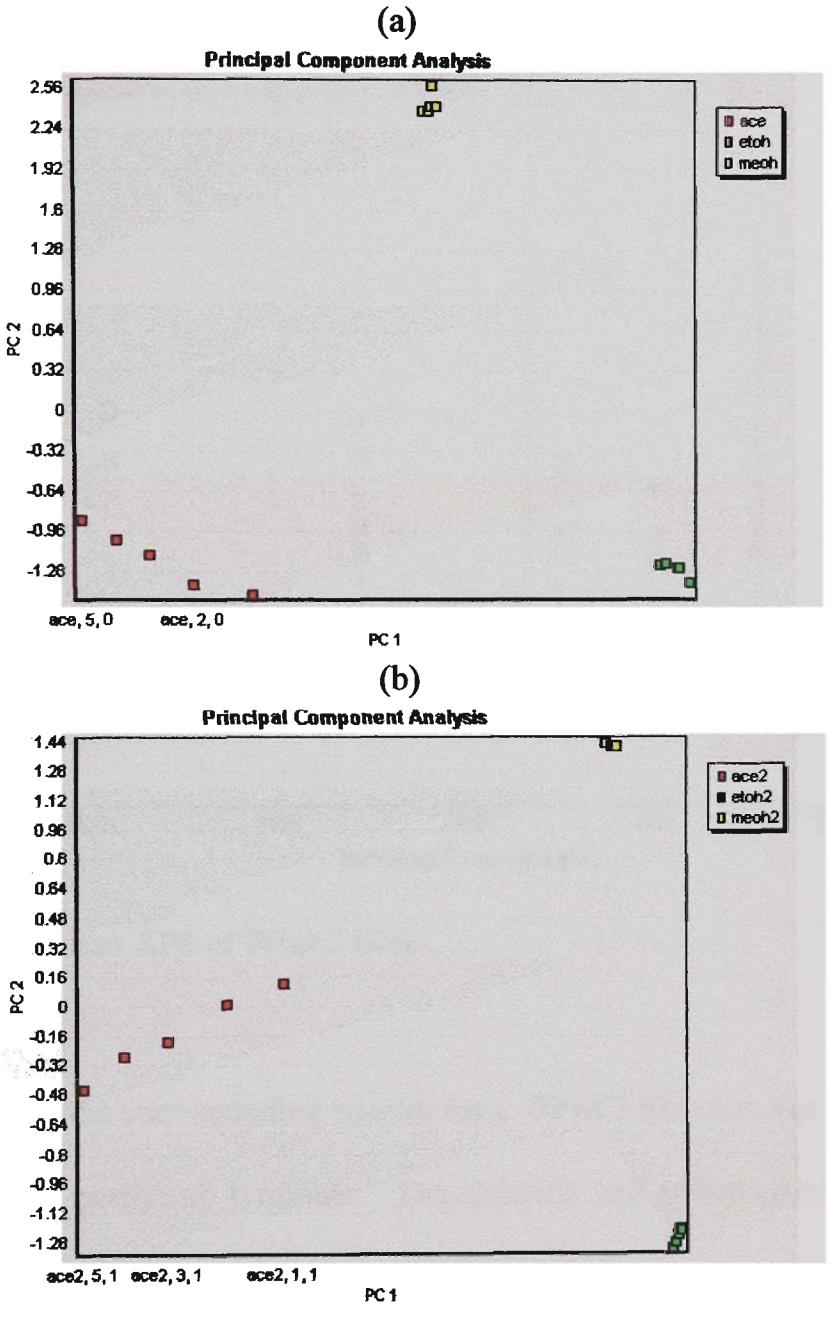

Figure 3.15 PCA plots of responses from (a) PPy/Cl sensors, and (b) PPy/Cl sensors after anion exchange solution pulsing, to 50% methanol (meoh/meoh2), ethanol (etoh/etoh2) and acetone (ace/ace2) in nitrogen.

3.3.5 X-ray Photoelectron Spectroscopy

Sensing films were characterised by XPS in order to confirm that changes in sensor response observed after pulsing or soaking in solutions were due to anion exchange.

Figure 3.16 shows a wide scan spectra for a PPy/Cl film and highlights the range of species present. The chloride peak in this case is significant, as would be expected, while the peak corresponding to sulfur is relatively small.

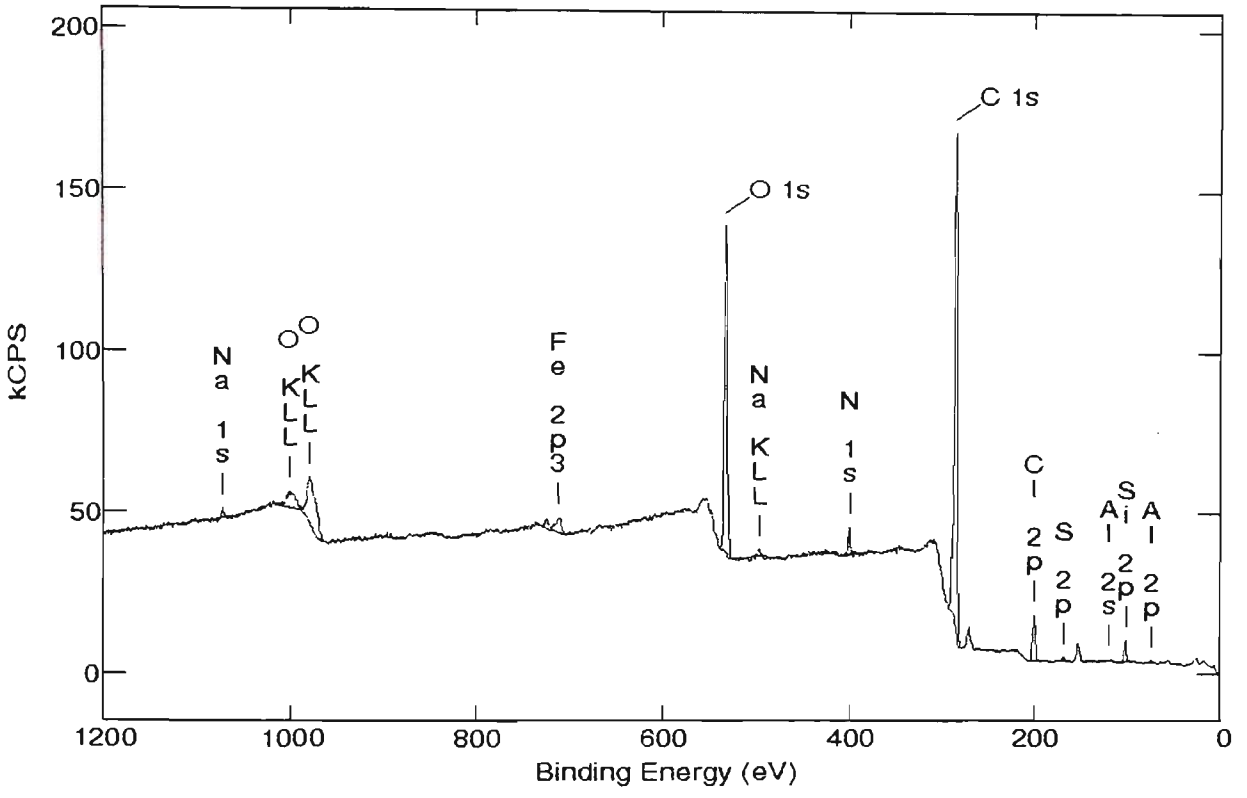

Figure 3.16 Wide scan XPS of PPy/Cl film.

Figure 3.17 shows the corresponding spectra for a PPy/Cl film that has been pulsed in 1 M NapTS for a period of 1 minute. The chloride and sulfur peaks are of similar magnitude for this film which indicates there has been some loss of Cl^- due to pulsing, and although slight, a corresponding increase in sulfur due to incorporation of the pTS anions. The results of XPS for a selection of sensors are given in Table 3.8. The S/N ratios are similar for all films but are highest for those sensors that were pulsed in

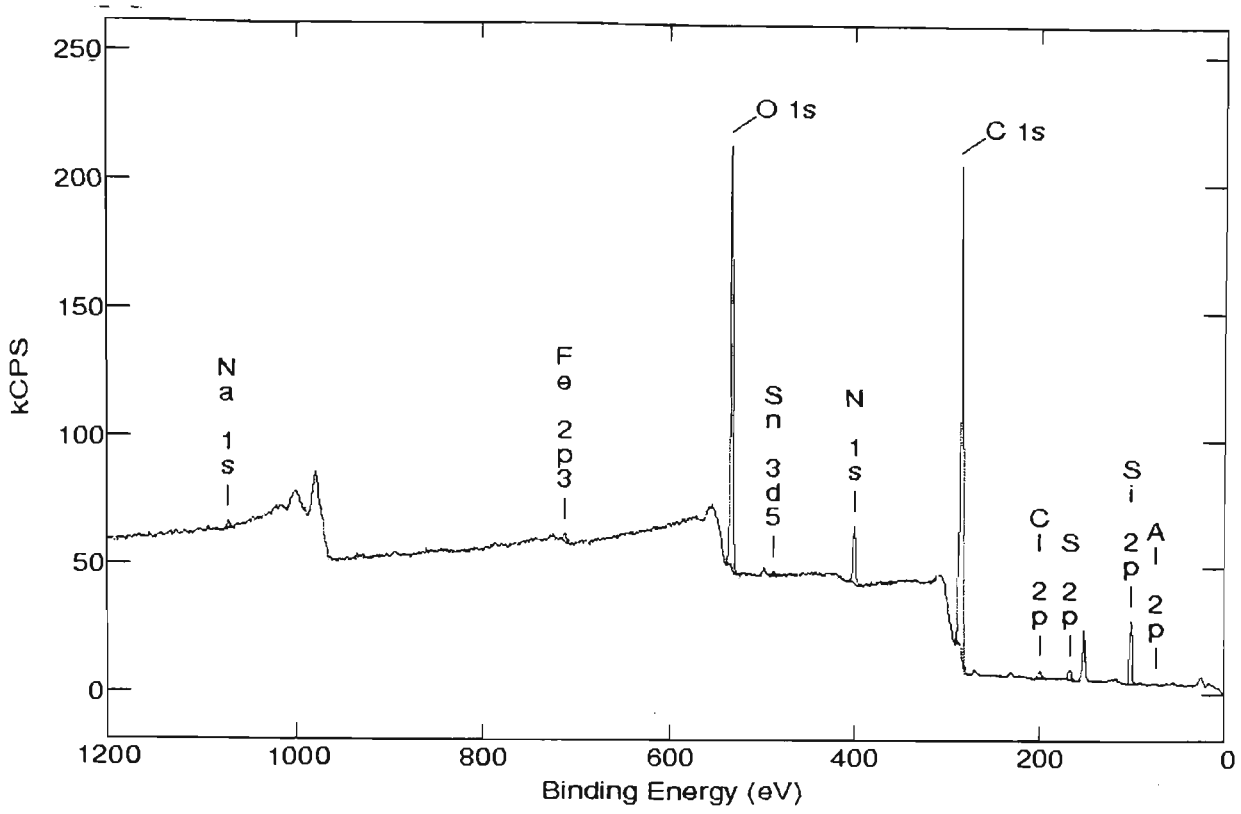

Figure 3.17 Wide scan XPS of PPy/Cl after pulsing in 1 M NapTS.

Table 3.8 XPS data for PPy/Cl sensors pulsed and soaked in 1 M pTS and PSS solutions. Figures given are as total percentage of element in each sample. The S/N and S/Cl ratios for each sensor are shown in bold.

Peak	PPy/Cl	pTS pulsed	pTS soaked	PSS pulsed	PSS soaked
N	2.049	4.007	3.787	2.254	2.510
Cl	2.972	0.579	0.731	0.369	0.745
S	0.312	1.002	0.456	0.826	0.552
S/N	**0.15**	**0.25**	**0.12**	**0.37**	**0.22**
S/Cl	**0.11**	**1.73**	**0.62**	**2.24**	**0.74**

solution. The S/Cl ratios for the films pulsed in solution are much larger than that of the control PPy/Cl sensor (15 to 20 times) confirming more clearly that anion exchange was achieved. In the case of the soaked films the S/Cl ratios were approximately five times

greater than the control which suggests this approach does bring about anion exchange but that it is not as effective as applying a pulsed potential. When the S/Cl ratios are compared for the two exchange counter-anions higher values were observed in the case of PSS. This is most likely due to a greater concentration of sulfonate groups present in the polymeric anion compared to pTS. The larger size of PSS would be expected to limit the amount of exchange, but even if this is the case, a higher S/Cl ratio is likely to be observed.

3.4 CONCLUSIONS

For anion exchange without significant loss of PPy film conductivity, it was found that either soaking in a 1 M electrolyte solution for short period or the use of pulsed potential exchange in 1 M electrolyte solution were most suitable. Although the XPS results discussed above indicate that some anion exchange may have taken place in the PPy/Cl films, the vapour response patterns observed (section 3.3.4.3) were in most cases similar after sensor modification. The main difference noted was in terms of sensitivity with only minor changes in the actual response patterns to various vapours. This is most likely related to film morphology, which in the case of these films may not be modified significantly after anion exchange. While the chloride anion is to some extent replaced by the sulfonated dopants, the film morphology obtained during chemical polymerisation of PPy/Cl remains. The enhanced responses are therefore brought about largely by stronger interactions between vapours and the different dopant rather than anion induced morphology changes in the film. There may be some effect on film structure as other workers have reported this be the case in previous studies of PPy. For example, Truong *et al* found that when thick PPy/pTS films (43 μm) were treated with

dilute sulfuric acid no changes in morphology were noted, while in the case of thin (12 μm) PPy/pTS films a more ordered structure was observed after treatment [215]. As the PPy/Cl films used in this work were thin perhaps some minor change in film order occurred, however, based on the vapour responses observed post-treatment any changes were not such that the patterns changed significantly.

As vapour responses are significantly affected by film morphology, these findings suggest that film structure is determined during polymerisation and thereafter cannot be modified significantly. If this is the case then the discriminating power of an array of PPy sensors must be tailored during film growth as a function of the counter-ion employed. The unique structural properties imparted to a polymer film by the anion are related to the polymerisation process [15].

Chapter 4

Approaches to Reducing the Humidity Response of PPy Gas Sensors

4.1 INTRODUCTION

One of the main problems with the use of PPy as a sensing material is susceptibility to interference by environmental factors, namely humidity and temperature [141, 180, 206]. The effect of temperature can be controlled with relative ease but unfortunately the humidity problem is not as easily overcome.

One possible solution to this problem is to carefully understand and monitor the humidity of a particular sampling application and thereby account for the effect of water vapour on sensor responses [229]. By incorporating a humidity sensor, PPy responses due to the real sample can be correctly calibrated by comparing these to a reference sample of known humidity. This approach is commonly employed in PPy based commercial electronic nose systems [230, 165], and has been reported to work effectively for the detection of various species in high humidity environments [161, 165]. However, this approach is not always ideal or possible, and also requires the added cost and complication of monitoring humidity with an appropriate sensor.

Another approach to address this humidity response is the use of a hydrophobic polymer membrane coating to exclude water. Reddy and Payne [181] used cast unplasticised poly(vinyl chloride) (PVC) membranes to reduce the humidity response of an array of 32 CP gas sensors. Interferences from water were minimised, but changes in sensor response to polar organic vapours were also noted. In this chapter, the utility of this approach will be investigated using solvent cast silicone membranes on screen-printed PPy sensors.

Polymeric diffusion membranes, which have been used extensively to remotely sample organic contaminants in both aqueous and high humidity vapour phases, offer another potential solution to this problem. Strakova *et al* [231] reported the use of a 0.2 mm silicone membrane in conjunction with a SnO_2 gas sensor to monitor ethanol and

butanol in water. Yano *et al* employed silicone tubing (i.d. 1 mm, thickness 0.25 mm) coupled to a GC to monitor methanol levels in a culture broth over time [232]. A series of tubes has been used in order to increase the surface area of the sampling system. Chlorinated hydrocarbons in water were monitored, and discriminated from other species such as hexane and phenol, using this device and a metal oxide gas sensor [233]. Silicone membranes have also been used to develop a core-based intrinsic fibre-optic sensing device where the polymer acts as both selective membrane and light pipe. The silicone was used to connect two quartz optical fibres and the adsorption of volatile organics monitored by Near-IR Spectroscopy [234]. LaPack *et al* used silicone hollow fibre sampling membranes connected to a mass spectrophotometer for the detection of a range of organic compounds in water [235].

The advantages of this approach for environmental monitoring are the exclusion of water, which interferes with analyte detection, pre-concentration of species at low levels, and the ability to control selectivity by simply changing the polymer tube employed. This approach, to our knowledge, has not yet been coupled with an electronic nose system as a means of minimising the effect of humidity on sensor responses. This may be related to the longer sampling times associated with vapours diffusing through the tube to the sensors. However, it should be possible to minimise this effect by careful selection of the polymer tube employed. Also, for certain applications such as long-term environmental monitoring, time delays are not problematic. The most obvious advantage for electronic nose systems with CP sensors, and the one focused on in this work, is the potential to minimise humidity effects.

4.1.1 Aims and Approach

This chapter describes the use of two different methods for reducing the humidity responses of an array of PPy gas sensors: the use of silicone membranes cast over the PPy sensing film, and diffusion tube sampling systems for delivery of low humidity vapours to the sensing array. The intention of this work was to demonstrate the utility of either silicone coating or polymer tubes for overcoming, or at least reducing the inherent humidity problems associated with PPy gas sensors.

Silicone coating involved casting membranes over PPy sensing films, which had been electrochemically deposited on PPy/Cl modified polymer substrates with screen-printed electrodes. The preparation of these sensors was described in detail in Chapter 2. The response of various PPys, to water, methanol, and methanol in water was examined, both before and after the addition of silicone membranes.

The tubing based approach initially involved the evaluation of six different tube materials by exposing each to the headspace of methanol, water, and methanol in water (50%). Permeation of each vapour through the tube walls was monitored with an array of eight PPy sensors prepared on silicon chips. From this, polyvinyl chloride (PVC) and silicone (Si) were selected for further investigation.

To test the utility of this approach for delivering humidity reduced solvent vapours to the PPy sensing array, both PVC and silicone tubes were suspended in the headspace of solutions containing organic solvents in water, and the sensor responses monitored. Methanol, ethanol, propanol and acetone were dissolved in water at 20 and 50% (v/v), and tube contents monitored with the PPy sensors, relative to a water blank.

The final section of work investigated the development of a unique PPy tube sensor comprising a PPy/Cl film coated onto the outer walls of a polymer tube. The ultimate goal was to combine this with an uncoated diffusion tube to produce a novel 'tube in

tube' (T.I.T.) sensor. It was envisaged that the outer tube would act as a diffusion membrane blocking water from the inner CP coated sensing tube.

4.2 EXPERIMENTAL

4.2.1 Chemicals and Materials

Pyrrole (Merck) was distilled prior to use. *p*-toluenesulfonate (pTS) was obtained from Merck and used as supplied. All other dopants [4,5-dihydroxy-1,3-benzenedisulfonic acid (Tiron), 4-hydroxybenzenesulfonic acid (HBS), 4-sulfobenzoic acid (SB), methanesulfonic acid (MS), 1,5 napthalenedisulfonic acid (NDS) and Polysodium-4-styrenesulfonate (PSS), 3-nitrobenzenesulfonic acid (NBS)] were obtained from Aldrich and used as received. Silicone window and glass sealant (Selleys) was used as received. A selection of tubing was purchased from Nalgene® Labware each with dimensions of 1.56 mm. (I.D.), 3.13 mm. (O.D.) and 0.78 mm (wall thickness). The tubing included; Santoprene® thermoplastic rubber (BPT, 8070), fluorinated ethylene propylene (FEP, 8050), PFA (8051), ethylene tetrafluoroethylene (ETFE, 8054), polyvinyl chloride (PVC, 8000). Also silicone (poly(dimethylsiloxane) tubing (dimensions 2 mm (O.D.) 0.5 mm (wall thickness)) from A.I. Scientific was examined. For preparation of PPy/Cl tube sensors, red polyurethane air-line tubing was obtained (Dionex 030089), with dimensions 1.59 mm i.d., 3.18 mm o.d. Milli-Q distilled water was used throughout.

An array of eight polypyrrole sensors (PPy/SB, PPy/NDS, PPy/pTS, PPy/HBS, PPy/MS, PPy/NBS, PPy/Tiron, PPy/PSS) on silicon substrates was used to monitor vapours diffusing into the tubes. Details of sensor fabrication, and the apparatus used to generate the vapours and monitor the sensor responses, have been reported in Chapter 2, section 2.2.4.3. For membrane coating, layers of silicone were applied to sensors by casting 50 μL of 7% (w/v) silicone in xylene over the sensing area. The coated area was defined by masking with electrical tape to give an area of 10×4 mm.

4.2.2 Vapour Diffusion

Diffusion of solvent vapours was measured for the 6 types of tubing; BPT, FEP, PFA, ETFE, PVC and silicone, by placing 15 cm lengths into the headspace of sealed gas bubblers containing solvent. Initial tube selection experiments made use of methanol and water as solvents with air as the blank. Subsequent testing with PVC and silicone tubes involved the use of methanol, ethanol, propanol, and acetone dissolved in water at concentrations of 20 and 50% v/v. In these later experiments a tube suspended over water was used as the blank. The contents of the tubing were successively purged with nitrogen and tested with the PPy sensor array. The testing protocol, which included a sensor flush cycle before and after the contents of each tube were analysed, resulted in a delay of approximately 90 minutes between repeat cycles. During this delay the gas inside the tube remained stationary. Each test cycle involved sampling the tube four times for 10 second intervals. The responses for the eight PPy sensors were averaged and the data analysed using an in-house principal component analysis (PCA) package.

4.2.3 Fabrication of PPy/Cl Tube Sensors

PPy/Cl tube sensors were prepared by vapour depositing PPy/Cl onto PUR tubing. The tube was first soaked in methanol before being placed in a 0.5 M $FeCl_3$/methanol solution for ten minutes to allow permeation of the oxidant. The tube was removed from the solution and suspended above neat pyrrole for a period of approximately five minutes until a satisfactory PPy/Cl coating had formed. The resulting sensor was rinsed several times with methanol and then Milli-Q water before being left to dry.

4.2.4 Response of PPy/Cl Tube sensors

PPy/Cl sensors were monitored initially in a polymer tube flow cell (Figure 4.22) to test responses to methanol in nitrogen. Resistance measurements were made using a 2-point approach with a semi-portable gas rig built by Industrial Research Limited (IRL), NZ. Subsequent to these experiments, the PPy/Cl sensors were sealed permanently into larger diameter silicone tubes (4.0 mm i.d., wall thickness 0.8 mm) and the resistance monitored using a HP 34401A multimeter over time, again using a 2-point measurement. These T.I.T. sensors were suspended in the headspace of aqueous methanol solutions or over water.

4.3 RESULTS AND DISCUSSION

4.3.1 Silicone Coating

Silicone coated sensors were tested in pairs using water, methanol and 50% methanol/water delivered to the sensors in nitrogen. Base resistance values of the sensors coated with silicone were not significantly affected by the process, with only minor increases noted (Table 4.1).

Table 4.1 Resistance values of sensors before and after coating with silicone.

Sensor	Dopant	R_0 (kΩ)	R_0 post-silicone (kΩ)
S1	SB	13.0	13.2
S2	HBS	15.2	15.4
S3	pTS	15.0	15.2
S4	PSS	29.0	29.0

Responses of both sensors S1 (PPy/SB) and S2 (PPy/HBS) to water vapour decreased after silicone coating (Figure 4.1). These decreases were significant for both coated sensors relative to the control, with changes of 75% observed for S1 responses (1.2% down to 0.3%), and 35% for S2 (2.5% down to 1.6%). The response of the control sensor (C) also decreased, but only slightly, which was most likely due to small variations in flow rate delivered by the gas rig. These results indicate clearly that the humidity responses were reduced, most significantly in the case of S1, by the silicone membrane. Differences in the effect of the silicone membrane on responses of the two sensors most likely relate to strength of binding between the CP sensing film and silicone, and possibly the morphology of the base CP layer.

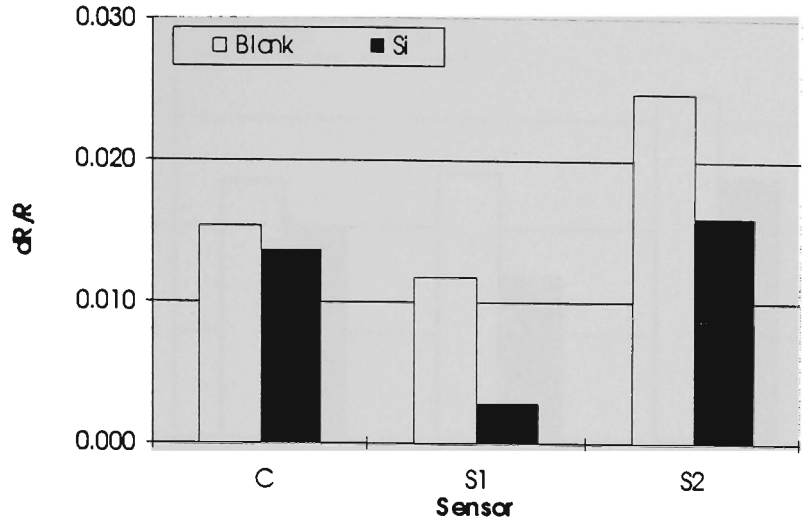

Figure 4.1 Response of PPy sensors, before (Blank) and after silicone was applied (Si), to 50% water vapour in nitrogen. Sensor C was left uncoated as a control against which the other sensor responses could be measured.

To investigate this possibility further, the effect of silicone coating on the humidity response of a second pair of different PPy sensors was tested. Again the resistance values of these sensors increased slightly after adding the silicone membrane (Table 4.1). The responses of S3 (PPy/pTS) and S4 (PPy/PSS) to 50% water vapour, before and after silicone coating, indicate again that the humidity response was suppressed to some extent (Figure 4.2). However, the control sensor response also decreased more significantly in this experiment, again most likely due to variation in gas flow rate, which suggests that the changes in S3/S4 response are not as significant. Hence the nature of the underlying PPy layer, and therefore morphology, appear to have had an effect on the uniformity of the overlying silicone coating. This was indicated by the marked differences in the effect of silicone coating on responses observed from one sensor to the next. Also, the presence of a silicone layer, while effective in blocking out water, may

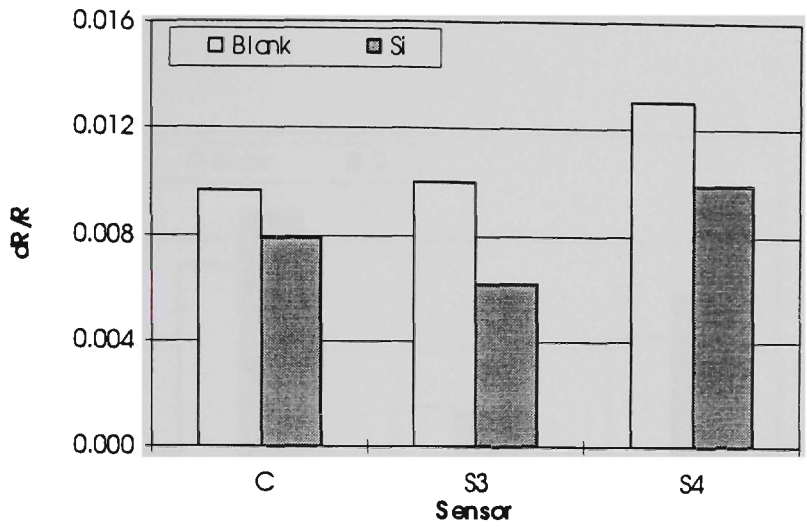

Figure 4.2 Response of sensors S3 (PPy/pTS) and S4 (PPy/PSS) to 50% water before (Blank), and after silicone coating (Si). Sensor C was used as a reference and was not coated.

induce a mechanical stress on the underlying PPy film as swelling occurs. If this process had an effect then adhesion of the silicone membrane to the underlying PPy layer would also effect the changes in response observed. Having established that the effect of humidity could be reduced, in some cases significantly, the next step taken was to investigate the effect of silicone coating on sensor response to methanol.

The response of sensors S1 and S2 to 50% methanol in nitrogen were affected to some extent by silicone coating, with an increase in S2 response being the most notable change. This increase was also observed for the control sensor, however, suggesting that it be due to some variation in gas flow rate rather than an effect of the silicone membrane. The S1 response remained virtually constant in spite of the variation observed both for the control and S2, which suggests that the actual response did decrease slightly after silicone coating. This suggests a very uniform coating of silicone, which may be due to good adhesion to the PPy/SB.

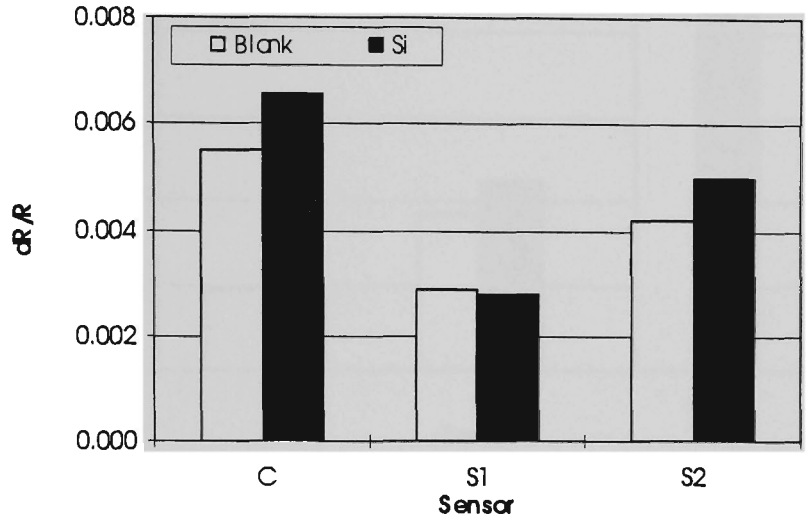

Figure 4.3 Response of PPy sensors S1 (PPy/SB) and S2 (PPy/HBS), before (Blank) and after coating with silicone (Si), to 50% methanol vapour in nitrogen. Sensor C was not coated.

The corresponding data for sensors S3 and S4 indicate that responses to methanol did not decrease in either case. In this experiment the control sensor responses remained unchanged, as did the responses from S4. Sensor S3 showed an increase in response to methanol after silicone coating, which is not clearly understood but may be due to strong absorption of methanol in the silicone membrane. In summary it was found that for all four silicone coated sensors, methanol could still be detected effectively, and hence the detection of methanol in water was evaluated as the final stage of this work.

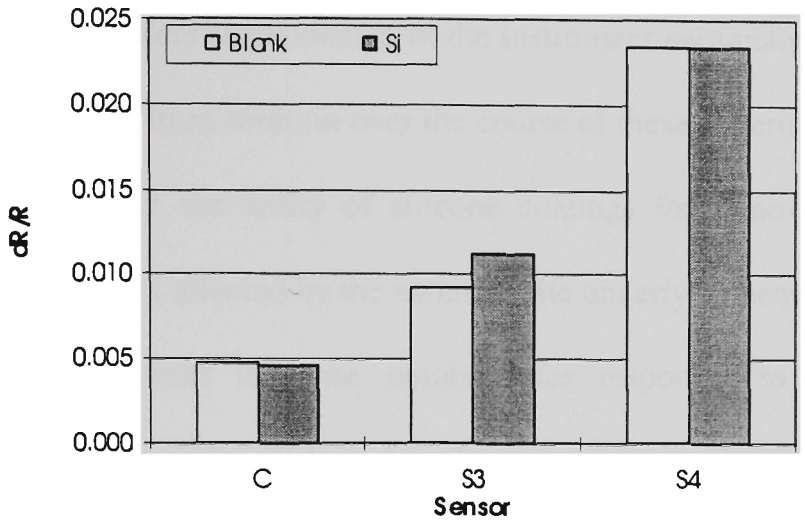

Figure 4.4 Effect of silicone coatings on PPy sensor responses to 50% methanol. Responses were measured before coating (Blank), and after silicone was applied (Si). Sensor C (PPy/NDS) was left uncoated.

The effects of silicone coating on responses to methanol in water were similar to those observed for water. Both sensors S1 and S2 showed marked decreases in response after the application of silicone layers, for S1 a decrease of 76% (1.00% down to 0.25%) and for S2 a decrease in response of 48% (Figure 4.5).

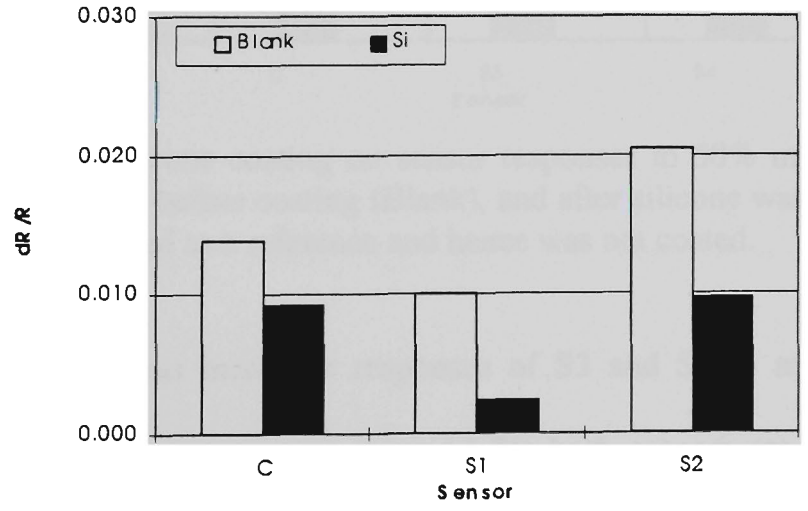

Figure 4.5 Response of silicone modified PPy sensors S1 (PPy/SB) and S2 (PPy/HBS), both before (Blank) and after coating (Si), to 50% methanol in water vapour. Sensor C was used as a reference and hence no coating was applied.

The control sensor response also decreased quite significantly (35%) and this cannot be ignored. Again this infers some change in the instrument parameters or perhaps some methanol had been lost from solution over the course of these experiments. In any case, the results confirm that the utility of silicone coatings for removing PPy humidity responses is significantly affected by the nature of the underlying sensing film. Also, as the results are so similar to those obtained for responses to water alone, the discrimination between water and methanol/water mixtures does not seem possible using this approach.

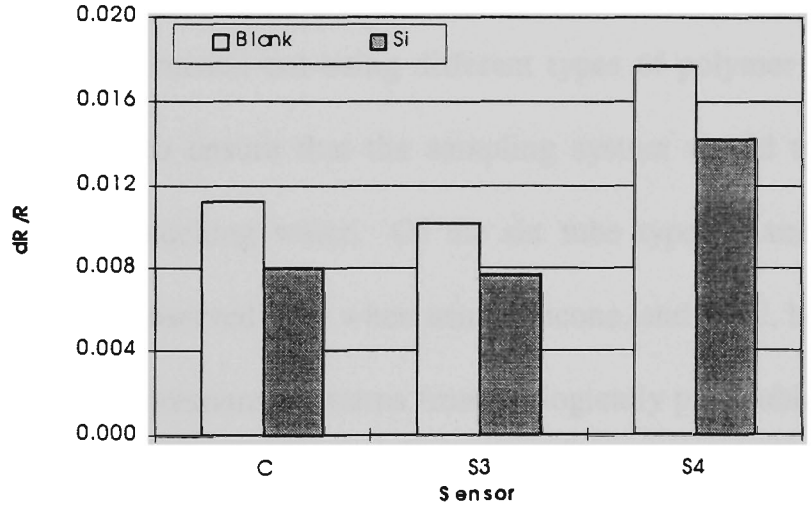

Figure 4.6 Effect of silicone coating on sensor responses to 50% methanol in water. Responses to this vapour before coating (Blank), and after silicone was applied (Si) are shown. Sensor C was used as a reference and hence was not coated.

A similar observation was made for responses of S3 and S4 to methanol in water (Figure 4.6). The response patterns observed for both sensors are not significantly different to those noted for water alone (Figure 4.2), again suggesting that while the silicone membrane removes water quite effectively, the ability to detect methanol in a high humidity background is not possible.

Attempts to use cast silicone coatings for reducing the water responses of PPy films were only partially successful. Water responses decreased after silicone coating but were not completely removed. Responses to methanol remained similar, but responses to mixtures of methanol and water, and water alone, were too similar for successful discrimination of methanol. The effect of silicone coating appears to be dependant on the underlying PPy layer. It is proposed that the silicone layer swells when in contact with water inducing a physical change in the coated PPy. As a result the utility of this approach for removing humidity responses is questionable.

4.3.2 Diffusion Tube Sampling

Initial experiments were carried out using different types of polymer tube exposed to neat methanol in order to ensure that the sampling system would transport organic vapours in addition to blocking water. Of the six tube types examined, significant methanol diffusion was observed only when using silicone, and PVC, both of which are flexible materials. Sensor response patterns from biologically pure tubing, and the rigid flouropolymer tubes (FEP, ETFE, PFA) upon exposure to methanol showed very small changes relative to the blank. This agrees with previous work on diffusion of organic chemicals through polymer tubes, which has shown that transport decreases with increasing tube rigidity [236, 237].

Response patterns obtained from the PPy sensing array to the contents purged from silicone sampling tubes show clear differences between the air blank (Figure 4.7a) and methanol (Figure 4.7b) samples. Due to the sampling arrangement of the automated system used, a period of approximately 90 minutes had elapsed by the time the first silicone tube responses were obtained. To confirm that the pattern observed after 90 minutes was due to methanol diffusion, comparison was made to the sensor response

pattern observed normally when the array is exposed directly to 20% methanol in nitrogen (Figure 4.7c). Similar results were obtained for the PVC tubing (not shown), but the change in response pattern observed for the methanol sampling tubes did not occur as rapidly as for the silicone tubes. In order to investigate these changes in sensor response due to methanol diffusion over time, response curves were prepared for selected sensors from the array.

Figure 4.8 shows the response of selected PPy sensors to gas purged from a PVC diffusion tube suspended in the headspace above neat methanol. Responses increased initially, due to methanol diffusion through the walls of the tube, until equilibrium was established at approximately 7.5 hours. The same increasing response profile was not observed for the silicone sampling tube, but rather a steady-state response appears to have been established from the first reading (Figure 4.9). This suggests that methanol diffusion through the silicone tube material is rapid, so fast in fact that equilibrium is established immediately. It should be noted that as the contents of each sample tube were completely flushed at each sampling interval, it is the rate of methanol diffusion rather than the internal tube concentration of this species that reaches equilibrium.

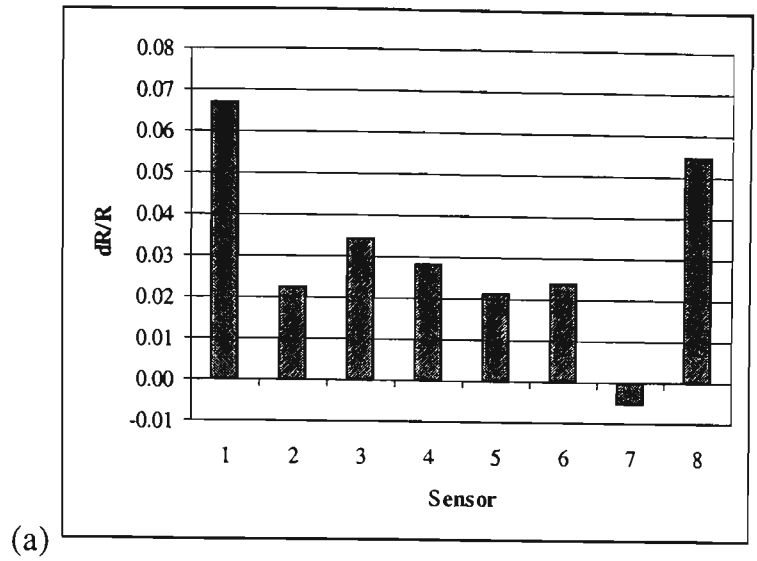

(a)

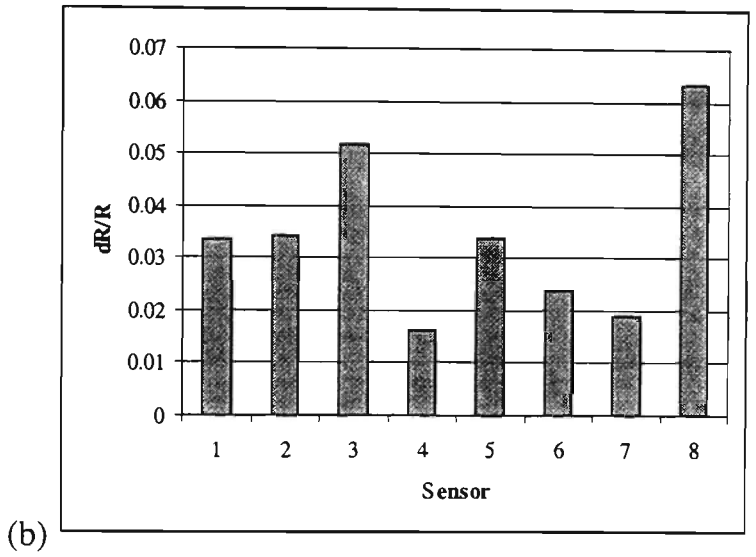

(b)

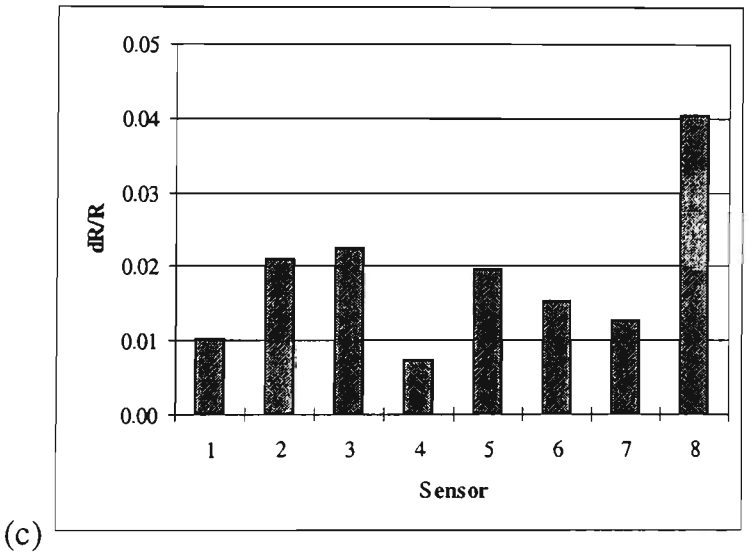

(c)

Figure 4.7 PPy sensing array response patterns for silicone tubing suspended in (a) air and (b) above neat methanol after a period of 90 minutes. For comparison the response pattern of the sensing array when exposed directly to 20% methanol vapour in nitrogen (c) is also shown.

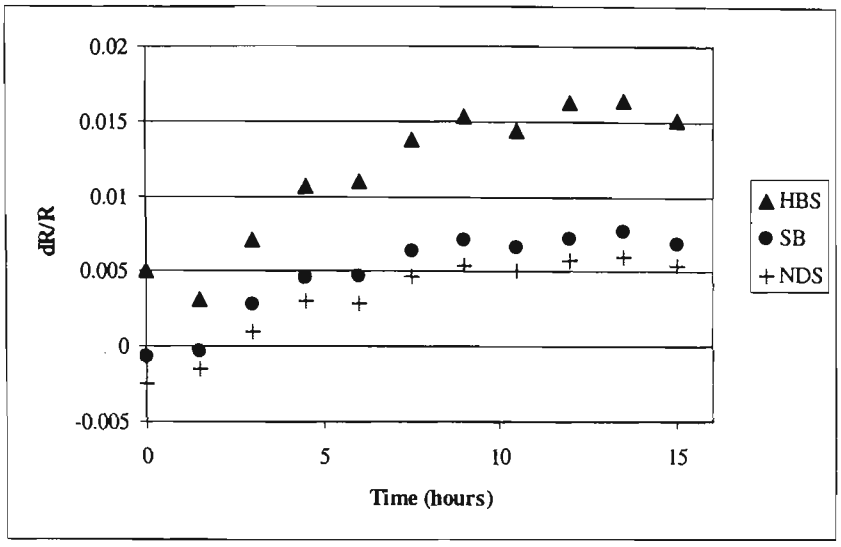

Figure 4.8 Response of selected PPy sensors (PPy/HBS, PPy/SB, PPy/NDS) to gas purged at 90 minute intervals from a PVC diffusion tube suspended above neat methanol.

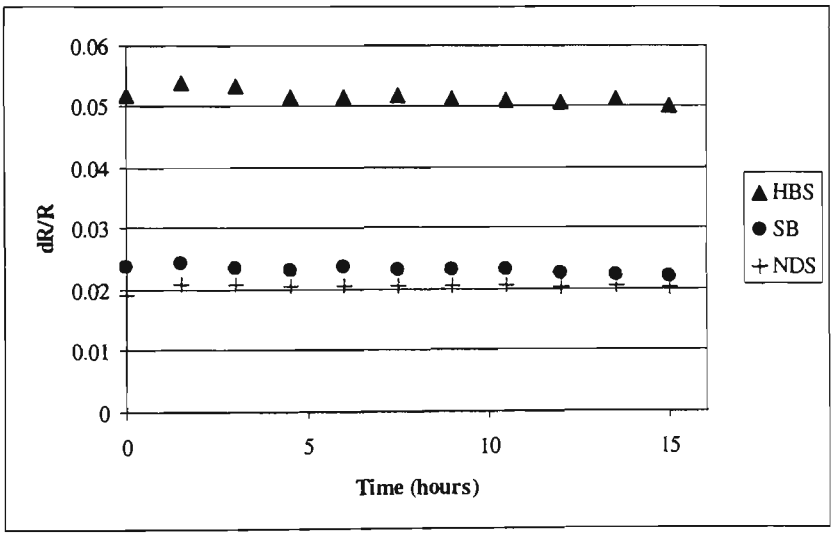

Figure 4.9 Response of selected PPy sensors (PPy/HBS, PPy/SB, PPy/NDS) to gas purged at 90 minute intervals from a silicone diffusion tube suspended above neat methanol.

Therefore, the results indicate that the final rate of methanol diffusion is reached far sooner when silicone tubing is used instead of PVC. The higher rate of transport in silicone may be due in part to differences in wall thickness, (0.50 mm for silicon, and 0.79 mm for PVC) a factor that has a significant effect on diffusion [238], and the higher permeability of silicon which is a characteristic feature of this material [239].

Diffusion of organics through polymer membranes initially involves dissolution of solvent molecules at the high concentration surface [238], a process that is controlled by solubility. So differences in the solubility of methanol in various tube materials would also have an effect on the rate of diffusion.

In order to analyse the sensor response patterns to silicone and PVC tubes completely, principal component analysis (PCA) was employed. Responses to tubes suspended above water and methanol were compared to responses to tubes in air. For both silicone (Figure 4.10) and PVC (Figure 4.11) tubes, the methanol and water data points were well separated. Air and water data points grouped in clusters, which were clearly separated in the case of PVC tubing indicating that some transport of water through the tube wall occurred. These clusters overlapped to some extent in the case of the silicone tubing, which suggests better exclusion of water. The rate of methanol diffusion is also indicated in the PCA plots by the profile of clusters formed. For silicone tubing, which as discussed earlier transports methanol rapidly, the data points begin to cluster by the second sample. This is not true for data from PVC sampling tubes, which take much longer to reach a common point. However, the final clusters formed are far more compact for PVC tubing which suggests better reproducibility may be achieved using this material.

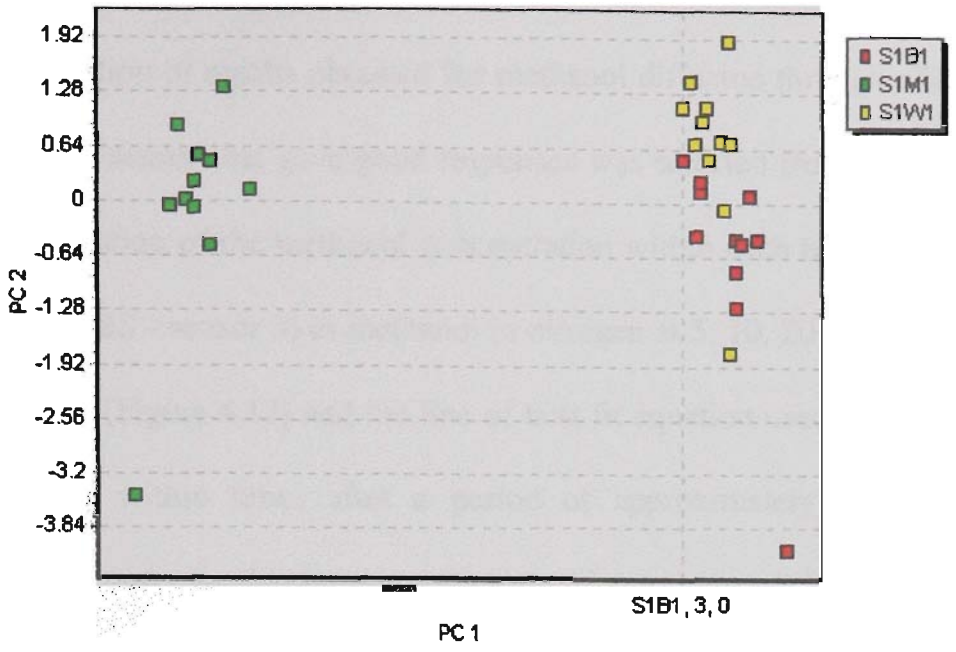

Figure 4.10 Principal component analysis of PPy sensor responses to gas purged from silicone tubes in air (S1B1), and suspended above water (S1W1) and methanol (S1M1).

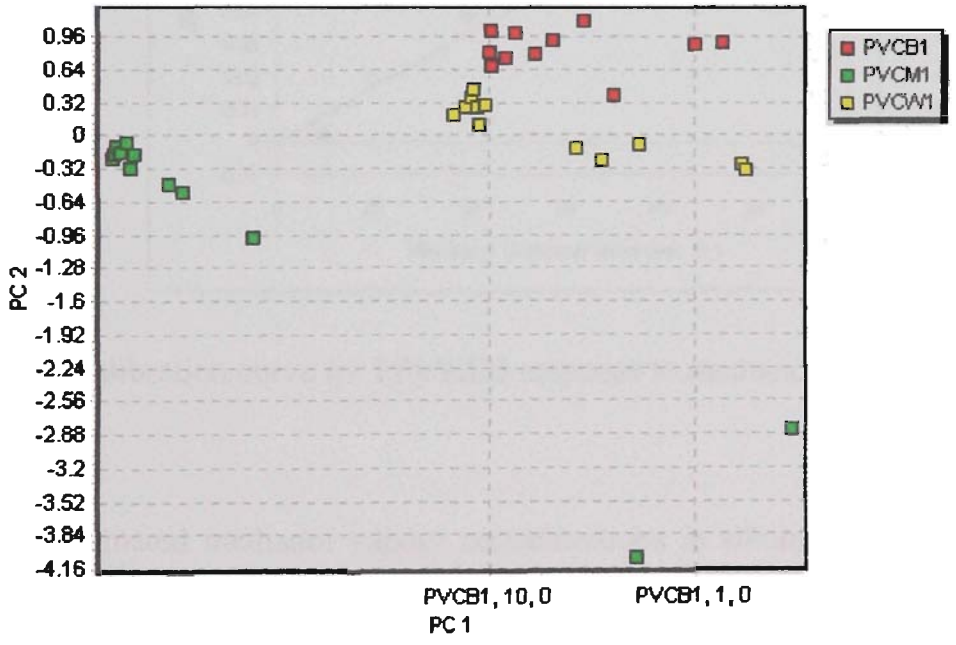

Figure 4.11 Principal component analysis of PPy sensor responses to gas purged from PVC tubes in air (PVCB1), and suspended above water (PVCW1) and methanol (PVCM1).

4.3.3 Estimating Methanol Concentration

From examination of results obtained for methanol diffusion through silicone and PVC tubes, a single sensor that gave good responses was selected from the array of eight to simplify estimation of the methanol concentration within each tube. Responses of this sensor (PPy/HBS - sensor 3) to methanol in nitrogen at 5, 10, 20, and 50% were plotted for calibration (Figure 4.13) and the line of best fit equation used to calculate methanol concentrations within tubes after a period of approximately 8 hours. Estimated concentrations refer to the amount of methanol present as a percentage of saturated vapour, and were 29.7% and 9.1% for silicone and PVC respectively (Table 4.2).

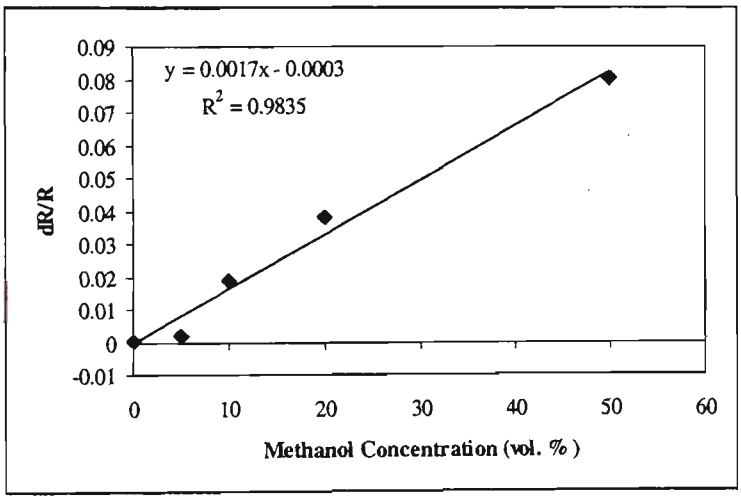

Figure 4.12 Calibration curve for PPy/HBS response to methanol in nitrogen.

Table 4.2 Estimated methanol vapour concentrations in silicone and PVC tubes after suspension over neat methanol for a period of approximately 8 hours. Sensor 3 (PPy/HBS) was used as for the calculation it gave good responses to methanol diffusion over time.

Tube	dR/R (8 hours)	[MeOH] (% vol.)
silicone	0.0502	29.7
pvc	0.0151	9.1

4.3.4 Solvent Discrimination in Solution

To test the potential of this sampling system for both discriminating between different solvents in water and reducing the humidity response, experiments were carried out using 20% and 50% solutions of methanol, ethanol, propanol, and acetone in water. These solvents were dissolved separately in Milli-Q water and analysed with reference to control tubes suspended over water. PCA of data from PVC (Figure 4.13) and silicone (4.14) tubes show that both sampling systems were successful in differentiating between water and all other solvent solutions tested. PVC tubing excluded water better than did silicone as indicated by the separation between the water cluster and methanol data points. In the case of silicone the water points clustered in close proximity to ethanol responses, but a distinct grouping was still formed.

The silicone tubes performed better in terms of solvent discrimination, with much more distinct clusters formed for all solvents. The only exceptions were the two propanol samples, which formed slightly overlapping clusters, and the 20% ethanol samples which clustered in close proximity to the 50% propanol data points. PVC tubes led to reasonable solvent discrimination, but the overlap of clusters for ethanol and propanol was such that separation was not clear for these samples. This may in part be due the greater scatter of points observed for PVC data, which relates to the slower rate of diffusion. Even the well formed clusters took some time to form, whereas data from silicone tubes grouped quickly and hence formed more distinct clusters. This can be seen most clearly for acetone, the most volatile solvent vapour examined, which was separated well from all other solvents using both PVC and silicone.

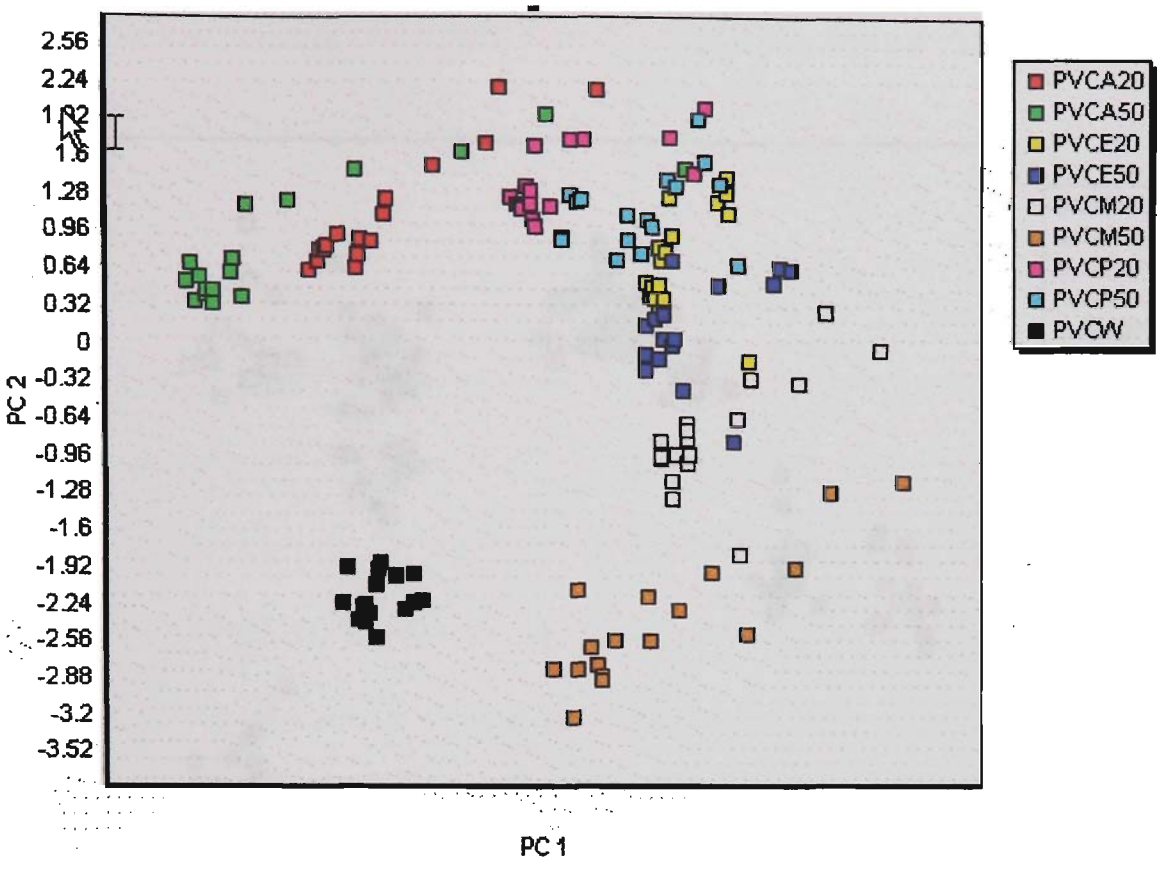

Figure 4.13 Separation achieved by using PVC tubes for the detection of methanol (M20/M50), ethanol (E20/E50), propanol (P20/P50), and acetone (A20/A50) dissolved in water at concentrations of 20% and 50% v/v. Water (W) was used as a blank.

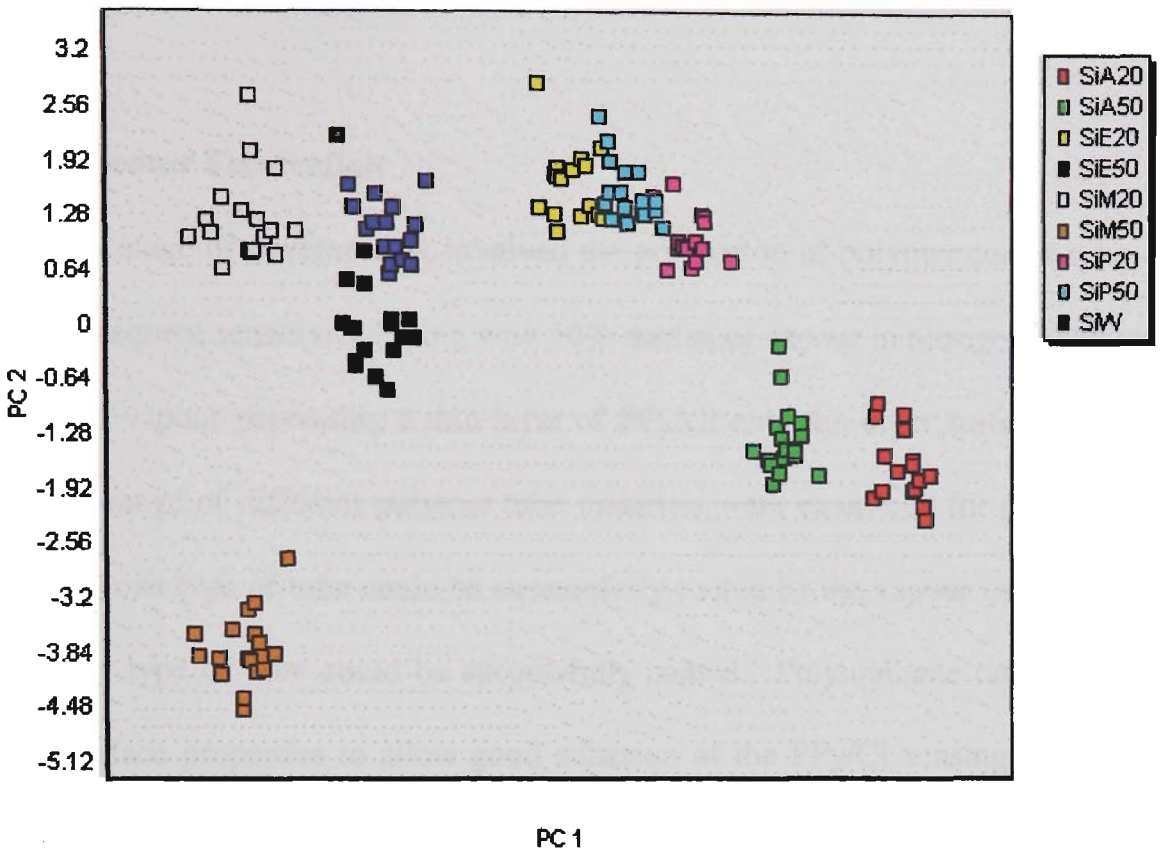

Figure 4.14 Separation achieved by using silicone tubes for detection of methanol (M20/M50), ethanol (E20/E50), propanol (P20/P50), and acetone (A20/A50) dissolved in water at concentrations of 20% and 50% v/v. A water control was used for reference.

4.3.5 PPy/Cl Tube Sensor

Having establish the potential of a diffusion tube sampling system for discrimination of alcohols and acetone in aqueous solutions using PPy gas sensors, the final objective of this work was to integrate the sampling and sensing systems into a single unit. The Tube in Tube Sensor (T.I.T) not only simplifies the process of sampling, but potentially would lead to enhanced sensitivity as a result of the cylindrical geometry of the sensing component. By using a tube design sensor the surface area to volume ratio of the device is maximised. As resistance is directly proportional to area, these tubes should offer improvements in sensitivity over conventional planar designs. Also, as the

sensing element consists of a PPy/Cl coated polymer tube, the cost of production is very low and the sensors are relatively simple to make.

4.3.5.1 Sensor Fabrication

The first stage of development involved the production of polymer coated tube sensors and subsequent sensitivity testing with 50% methanol vapour in nitrogen. The approach involved vapour depositing a thin layer of PPy/Cl onto the outer surface of a polymer tube. A range of different polymer tube materials were examined for use as the sensor but only one type of tube could be successfully coated by the vapour deposition process only one type of tube could be successfully coated. Polyurethane tube possessed the right surface properties to allow good adhesion of the PPy/Cl sensing film. Attempts were made to deposit onto both silicone and PVC tubes, as these gave good results when used as sampling tubes, but good adhesion could not be achieved. In the case of PVC this was an interesting result, as PVC polymer film was used quite successfully for the preparation of PPy/Cl sensing layers in previous sensor work (Chapter 2). The two materials are no doubt different, not only in terms of morphology, but also in terms of the surface chemistry as each would have different amounts of plasticisers, etc., added. The curved surface to be coated would have some effect on the PPy/Cl deposition process as it would cause increased solvent runoff.

4.3.5.2 Methanol Responses

In these initial experiments the sensor was exposed to vapours while housed in a polymer tube that served as a flow cell rather than a diffusion membrane (Figure 4.15). A stream of methanol in nitrogen was passed through the inside of the outer tube and subsequent changes in resistance of the inner PPy/Cl tube sensor monitored. The response of a 10 mm long PPy/Cl tube sensor to pulses of 50% methanol in nitrogen (Figure 4.16) was in the order of 2.5% (dR/R). The base resistance of this sensor (from end to end) was initially 2 kΩ, which compared to R_0 values of the planar sensors described in Chapter 3 is quite low, but drifted to approximately 10 kΩ after a few days sealed in a glass vial in air. Considering that connection to the sensor was made crudely by attaching ring-terminals to the PPy/Cl sensing layer itself, the responses were quite good. A calibration plot for methanol responses of this sensor (Figure 4.17) shows that at higher concentrations the sensor resistance changes begin to plateau inferring that a saturation point is reached. The non-linear response over this concentration range is a common feature of polypyrrole gas sensors, but this may be accentuated in this instance by methanol diffusion into the underlying PUR tube over time. When the length of the sensing tube was doubled, the % change in resistance to 50% methanol in nitrogen increased by more than a factor of two. Figure 4.18 gives a comparison of the average responses to 50% methanol for four sensors ranging in length from 5 to 20 mm. As the sensing area increases in length so does the response to methanol, confirming that by increasing the sensing surface area greater sensitivity can be achieved.

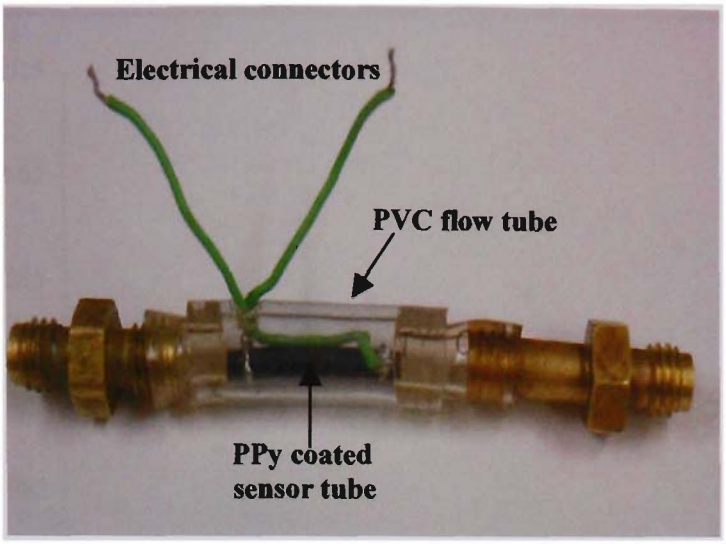

Figure 4.15 PPy/Cl tube sensor housed in a PVC flow tube for testing with methanol in nitrogen. Test vapours were purged through the PVC tube while monitoring the resistance of the PPy coated sensing tube.

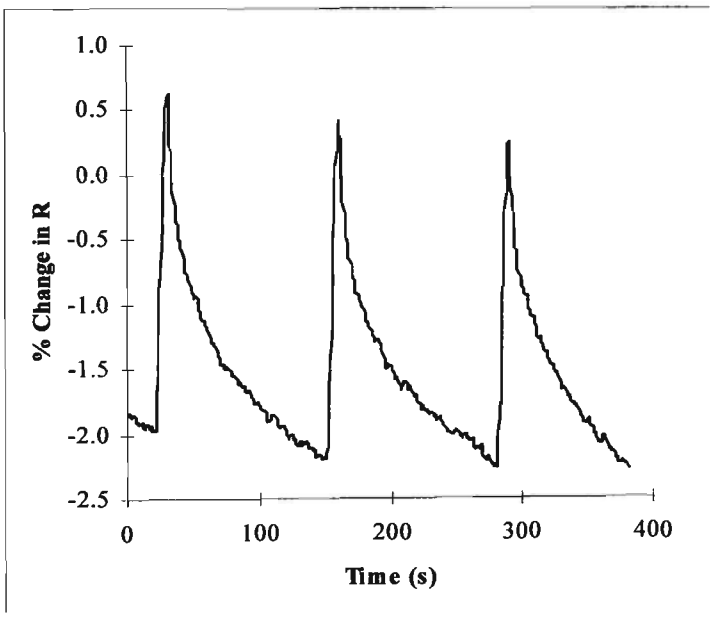

Figure 4.16 Response of a 10 mm PPy/Cl coated PUR tube to 50% methanol in nitrogen.

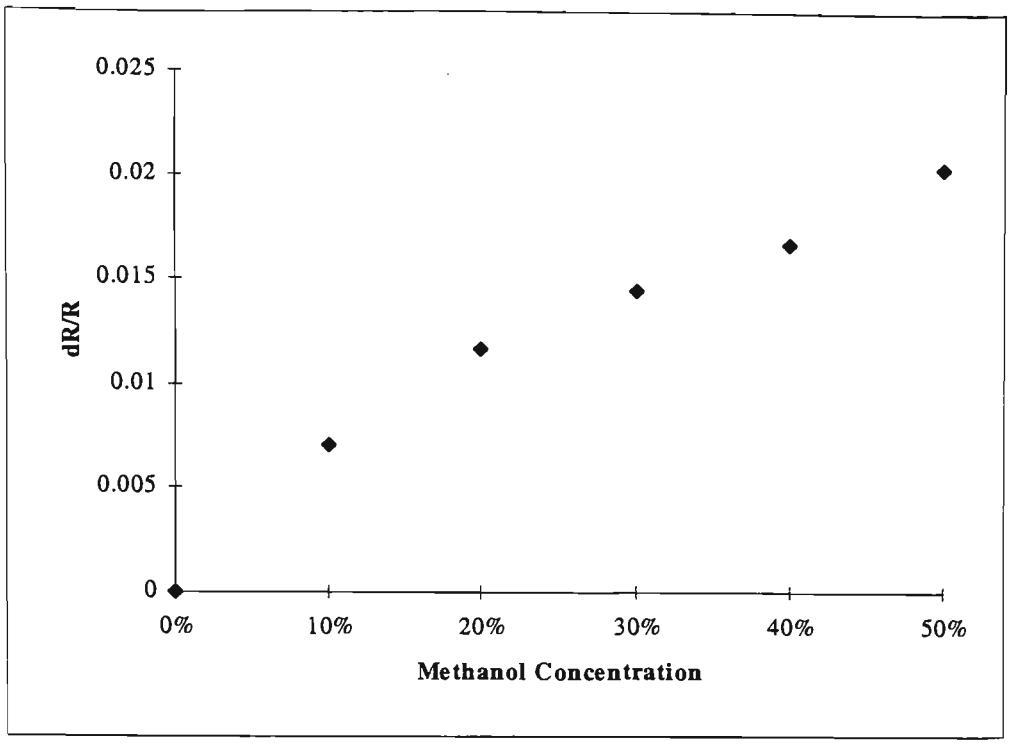

Figure 4.17 Average responses of 10 mm PPy/Cl tube sensor to methanol vapours in nitrogen at 10, 20, 30, 40 and 50% of saturation.

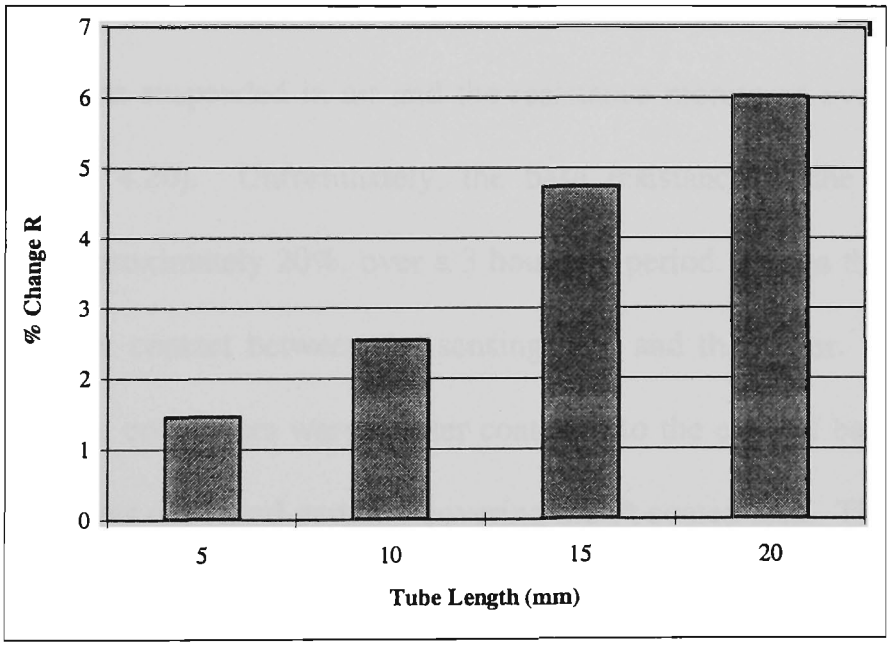

Figure 4.18 Effect of tube sensor length on sensitivity to 50% methanol in nitrogen.

4.3.6 T.I.T. Sensor

The final stage of this work was the fabrication of a tube in tube (T.I.T.) sensor and an investigation of its use to sample diffusion of methanol from water over time. The outer tube used for this was silicone (4.0 mm i.d.) with a sufficient internal volume to allow the PPy/Cl coated PUR sensing tube to be installed inside. Also, the wall thickness of the outer tube (0.8 mm) was kept as thin as possible to ensure reasonable diffusion rates. The two leads used for connection were passed through two small holes in the outer tube which were sealed with silicone sealant. Figure 4.19 shows a complete T.I.T. sensor. The ends of the tube were sealed using nylon bolts which were convenient to remove in order to change the internal sensing tube. Connection to the sensor was made by two wires, the ends of which were formed into a ring to fit tightly over the tube. These connecting rings were soldered in order to maintain the correct shape over time.

In order to check sensor stability over time, an initial experiment was conducted where the T.I.T. sensor was suspended in air and the resistance monitored over time using a multimeter (Figure 4.20). Unfortunately, the base resistance of the sensor drifted significantly, by approximately 20%, over a 3 hour test period. It was thought that this may be due to poor contact between the sensing film and the meter. To check this possibility, platinum connectors were sputter coated onto the ends of bare PUR tubing and a PPy/Cl film was deposited partially covering the Pt coated area. The very ends of the platinised area were left uncoated to allow for connection. Again a significant amount of drift in the base resistance of the sensor was observed inspite of improved electrical contact (Figure 4.21). The drift observed was most likely due to the PPy/Cl itself over time. It was hoped that this was associated with dehydration of the film after deposition, and therefore that the R_0 would stabilise after sufficient time. (See Ashton's paper about sensor initial and final R_0 values). The base resistance of the

aforementioned sensor (Figure 4.21) was checked after 2 days rest time by repeating the above experiment. After the 2 day period, the R_0 had increased to 6.20 kohm (from 2.6 kohm) and over a 3 hour period of sampling in air this changed to 8.65 kohm. It would appear from these results that the PPy/Cl tube sensors are not air stable even when sealed in a diffusion tube. The sensors were not tested with methanol as the 20% drift in R_0 values observed in air would definitely overshadow any responses caused by methanol diffusion. Prior work with these sensors showed that resistance changes of between 2.5 and 6% were obtained when 50% methanol in nitrogen was passed directly over the PPy/Cl film. The amount of methanol diffusing through the outer tube from solution over a 3 hour period would be much less than this. Unfortunately further investigative work to improve sensor stability in air was outside the scope of this work, but results obtained to this point are very promising and suggest this aspect warrants further study.

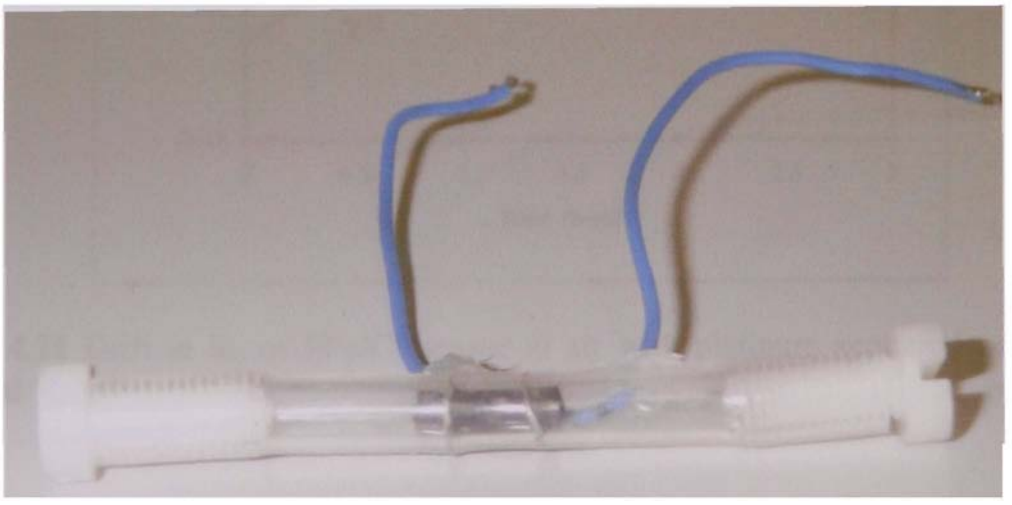

Figure 4.19 Complete T.I.T. sensor comprising a silicone outer diffusion tube (4.0 mm i.d., 0.8 mm wall) and PPy/Cl coated PUR polymer tube sensor (1.59 mm i.d., 3.18 mm o.d.) sealed within.

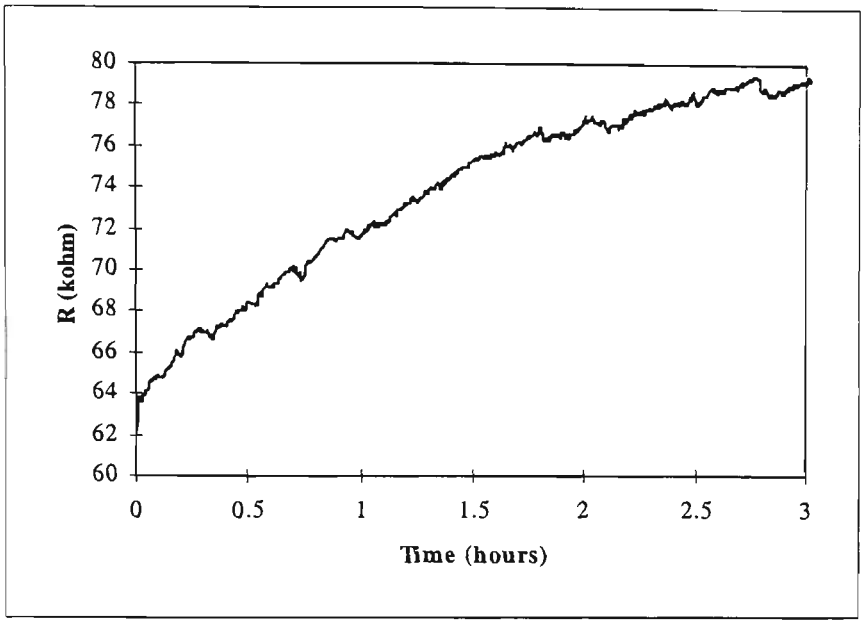

Figure 4.20 Drift of PPy/Cl sensing tube in air over a 3 hour period using direct contact to the sensing layer.

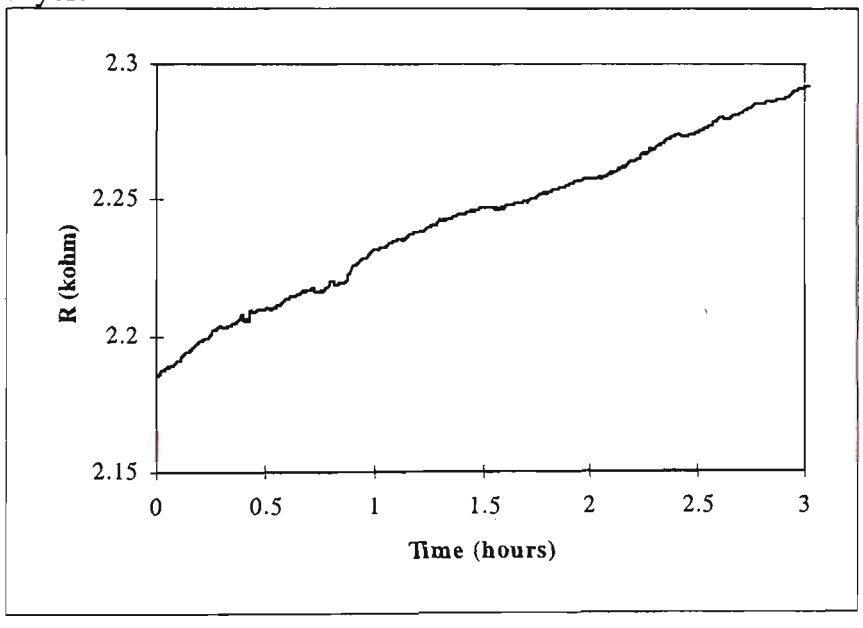

Figure 4.21 Drift in R_0 of PPy/Cl sensor in air with platinum sputtered contacts for electrical connection.

4.4 CONCLUSIONS

Detection of organic vapours from aqueous solutions using PPy gas sensors has been achieved by employing two different methods of humidity control: hydrophobic silicone membranes, and polymer diffusion tube sampling systems.

The silicone membranes were effective in significantly reducing PPy sensor responses to water vapour, but the reductions varied from one polymer to the next. This may in part relate to morphological differences and the affinity of a particular polymer for silicone. The detection of methanol vapours from an aqueous solution of methanol in water was not possible using this approach, but it is possible that other more volatile species may be successfully detected in this manner.

The polymer tube approach for reduction of humidity responses involved testing six different polymer tubing materials, of which only silicone and PVC were effective for diffusion controlled vapour sampling. Silicone and PVC tubes gave good separation between methanol and water, and hence were subsequently used to assist in differentiation between aqueous solutions containing methanol, ethanol, propanol, acetone, and a water blank. It was found that silicone tubing gave better separation between these solvents than PVC, but that both tube types were effective in blocking water. This approach offers a potential means of differentiating between a wide range of volatile organic species dissolved in water.

PPy/Cl coated PUR tubes were successfully used as conventional gas sensors for detecting methanol vapours (50%) in nitrogen, and the sensitivity of these was shown to increase when the surface area of the sensor was doubled. Attempts to encapsulate these sensors in a silicone diffusion tube for detecting organics in water were hindered by a lack of base resistance stability in air. Over a period of only a few hours the R_0 values

commonly drifted by about 20% making detection of methanol by diffusion impossible. This issue needs to be addressed before a complete T.I.T. sensor can be realised.

Chapter 5

Preliminary Investigations into the use of Vapour Deposited PPy Gas Sensors for Autonomous Robotic Plume Tracking

5.1 INTRODUCTION

Many environmental sensing tasks involve exposure to extreme conditions that are not desirable for humans, for example locating the source of hazardous or toxic chemical gas leaks. The use of autonomous robots in these situations could provide a means of overcoming this problem, and also by deploying robots in groups to enable 'swarm' like searching has the advantage of covering large areas. This principle has been described previously in the literature [240, 241].

The use of autonomous robots for chemical plume tracking has received limited attention to date with only a few examples available. Nakamoto *et al* [242] reported on the use of an ethanol tracking robot equipped with four semi-conductor tin oxide sensors. The robot, which sensed wind direction using four thermistor type anemometric sensors, was able to successfully detect and track an ethanol plume and even estimate the distance to the source at a distance of 1.5 m. Russell *et al* [243] used the RAT robot employed in this work fitted with QCM gas sensors to detect and track a camphor source. The QCM oscillators were coated with silicone OV-17, a common stationary phase used in gas chromatographic columns, and allowed the robot to successfully locate and follow a plume to the source from distances of 15 cm. Plume tracking in aqueous environments has also been demonstrated in an attempt to mimic the behaviour of lobsters [244]. In this case a robot used bilateral conductivity sensors to successfully trace a NaCl plume in fresh water over a distance of 90 cm from the source.

Gas sensors for the purpose of vapour plume tracking should be lightweight and have low power requirements as conventional batteries are commonly used to power search robots. The polypyrrole coated screen-printed sensors described in chapters 2 and 3 possess these attributes, and in addition are very easy to produce at low-cost.

Polypyrrole sensors also show remarkable sensitivity to amines and in particular ammonia, and hence provide a means of tracking these at low ppm levels.

5.1.1 Aims and Approach

This section of work sought to evaluate the use of vapour deposited polypyrrole gas sensors on an autonomous mobile robot for tracking an ammonia plume. A comparison was made between PPy/Cl sensors, and electrochemically modified PPy/Cl sensors that had been subjected to anion exchange in pTS. The effect of various environmental factors, such as wind speed and ammonia concentration, on sensor response and robot tracking was examined.

5.2 EXPERIMENTAL

A 'RAT' reactive autonomous testbed robot (Figure 5.1), developed at the Intelligent Robotics Research Centre, Monash University, Melbourne Australia, was used for all experiments. The RAT is controlled by a Motorolla 68HC11 microcontroller, the EEPROM of which can be reprogrammed in order to modify the behaviour of the robot. Whisker sensors on the front of the robot are used for obstacle detection and avoidance. Wind direction and velocity were monitored using a novel airflow sensor [245]. Real-time sensor responses were obtained by means of an RS-232 serial cable

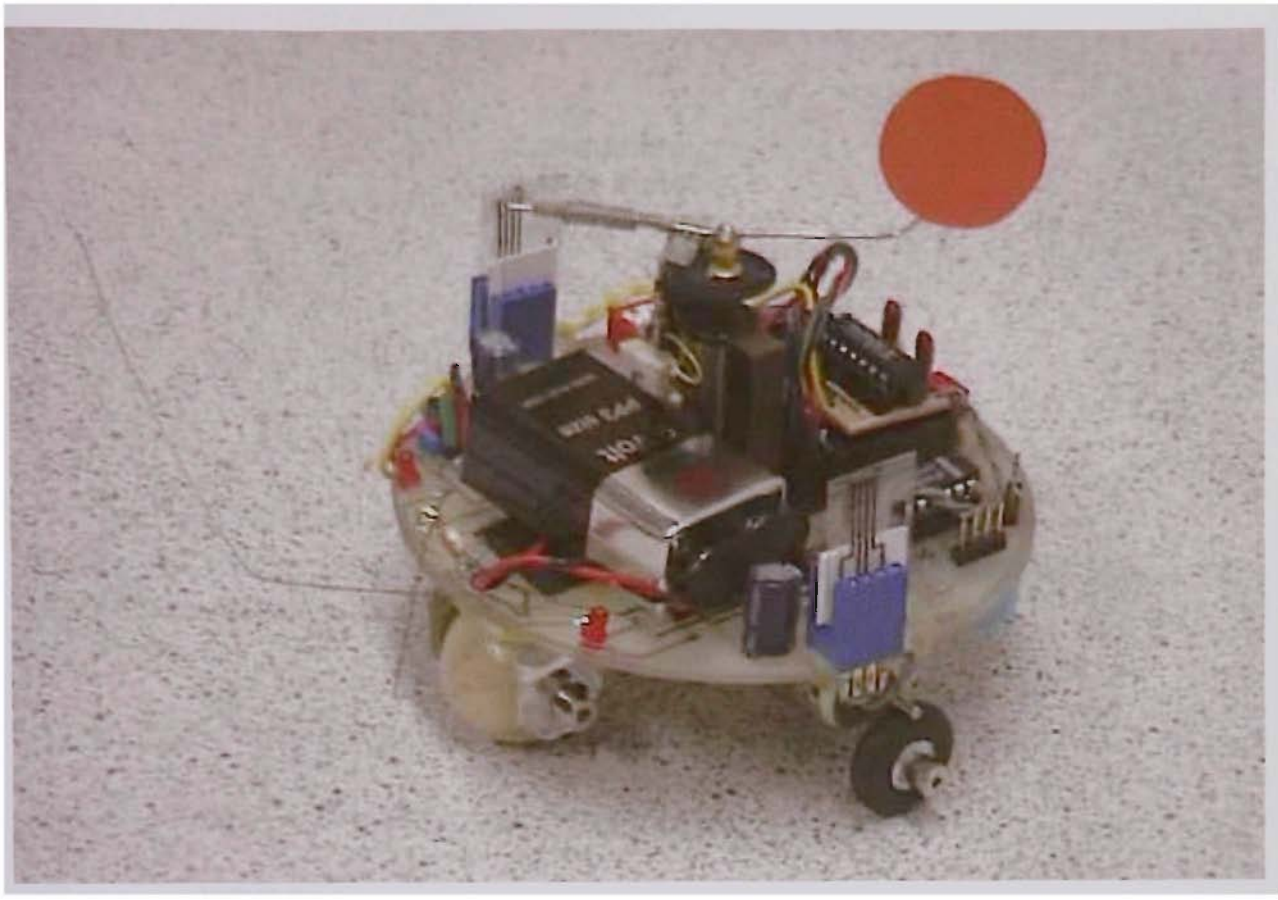

Figure 5.1 Reactive Autonomous Testbed (RAT) robot equipped with PPy screen-printed gas sensors.

linking the robot to a Macintosh computer. A pair of conducting polymer sensors was mounted on the left and right side of the RAT.

The sensors were incorporated into a simple oscillator circuit based on a Schmitt trigger (Figure 5.2) where the sensor resistance forms part of the frequency controlling RC network. The onboard 68HC11 micro-controller was used to count the number of rising edges, which changed as a function of sensor resistance. The approximate output frequency in hertz of the sensing circuit is given by (1):

$$F = 0.53\ RC \qquad (1)$$

where C = 0.01 μF and R is the resistance of the PPy sensor in ohms.

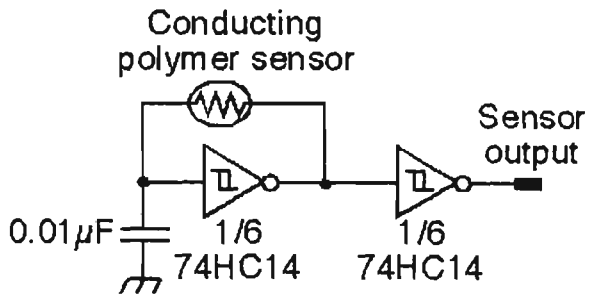

Figure 5.2 Circuit used for monitoring resistance changes of PPy gas sensors during exposure to ammonia vapour.

All ammonia source solutions used for testing were prepared on a % (w/w) basis in water. Nitrogen was bubbled through the source solution and blown toward the robot using a small DC fan.

5.3 RESULTS AND DISCUSSION

5.3.1 Static Responses

Static responses of the PPy gas sensors were monitored in real-time using a cable link from the RAT to a computer. The robot was able to detect 5% ammonia vapour source at a distance of at least 1.2 m (Figure 5.3), but the magnitude of response at this and other distances varied from one sensor to the next. The two unmodified PPy/Cl sensors gave rise to responses of different magnitudes whilst responses from the two anion exchanged sensors were similar. This may relate to the reproducibility of response obtained between sensors after they have been modified electrochemically, although due to the limited number of sensors used for comparison further testing is required before this can be confirmed. In any case, the two sensors that had undergone anion exchange processing did not show any increased sensitivity to ammonia.

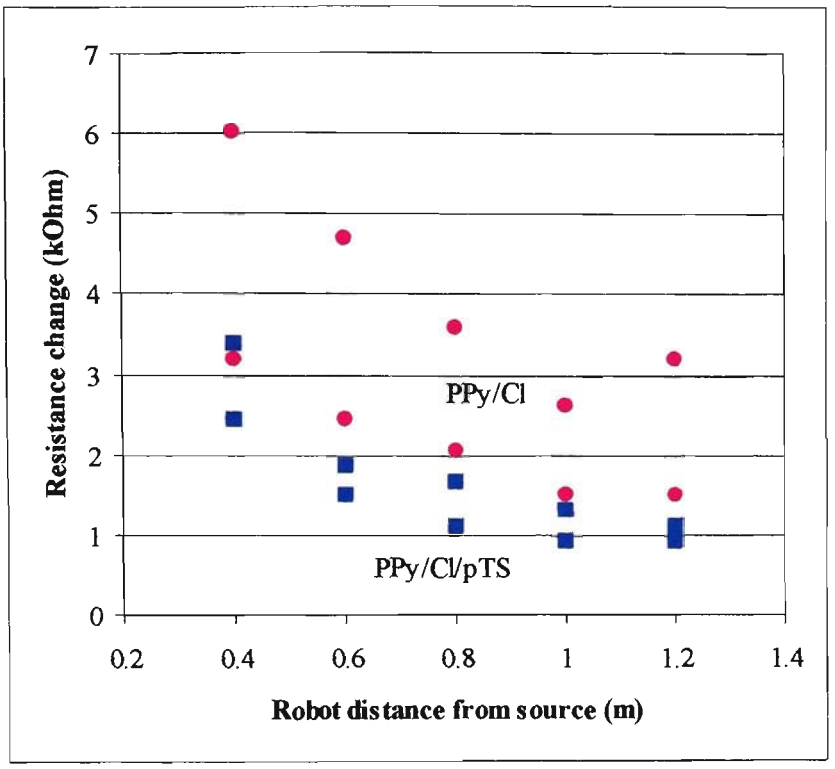

Figure 5.3 Response of PPy sensors to a 5% ammonia vapour source at various distances. The robot was in a fixed position during these experiments and the sensor reading taken after 50 seconds of exposure to the ammonia plume. Unmodified PPy/Cl sensors responses are shown in pink, anion exchanged PPy/Cl/pTS responses in blue.

5.3.1.1 Wind Velocity

The effect of wind speed on the static sensor responses was examined using a single unmodified PPy/Cl vapour deposited sensor. The voltage of a small DC fan was varied, between 3 V and 12 V to give a range of speeds, and the sensor response to ammonia measured at a fixed distance of 0.2 m from the source. As was expected responses decreased in magnitude with increased wind velocity (Figure 5.4).

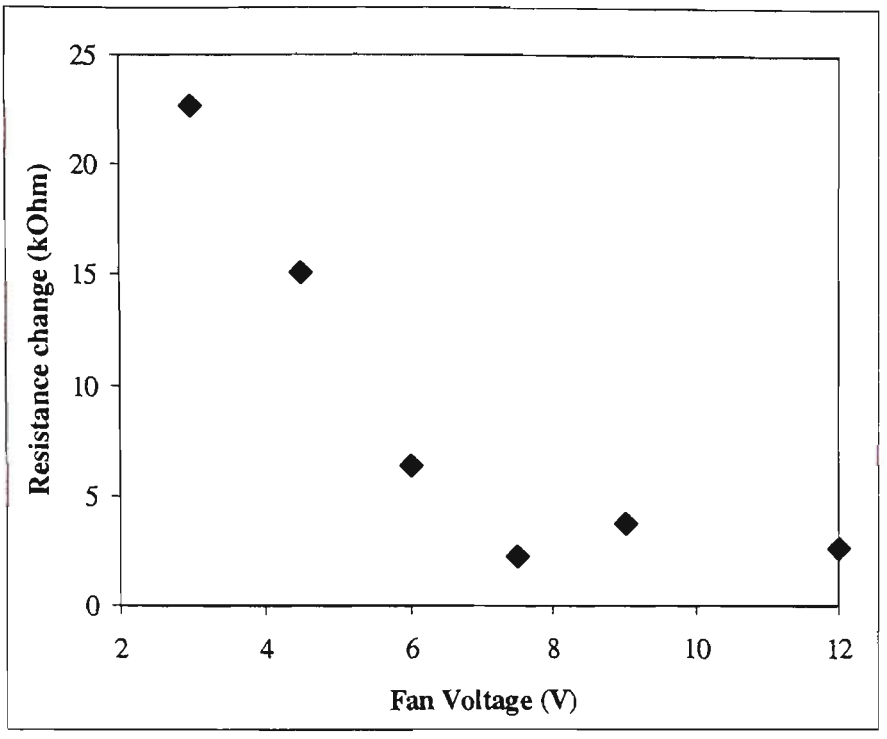

Figure 5.4 Resistance change of a PPy/Cl gas sensor to 3.5% ammonia vapour versus fan voltage at a fixed distance (0.2 m) from the source. The sensor readings were taken after 30 seconds of exposure to the vapour plume.

5.3.1.2 Ammonia Concentration

The static responses of this vapour deposited PPy/Cl sensor were also tested over a range of ammonia concentrations with the robot positioned a fixed distance of 0.2 m from the source. The R^2 co-efficient was 0.95 indicating the scatter of points around the line of best fit shown in Figure 5.5. While these responses are not perfectly linear, the results confirm that the sensor and associated circuitry function in a predictable fashion over a range of vapour concentrations.

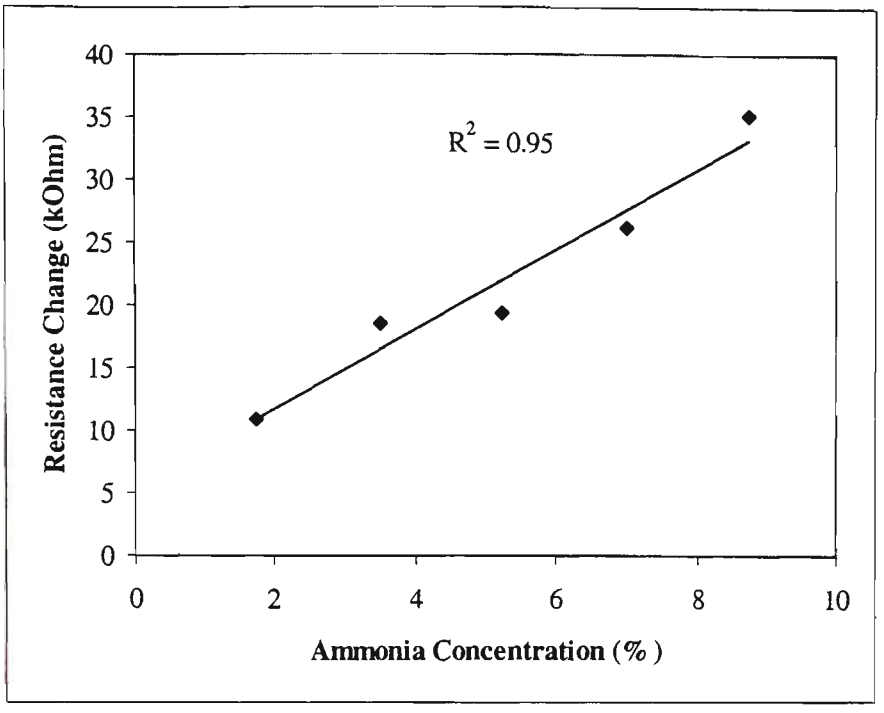

Figure 5.5 Response of PPy/Cl sensor to a range of ammonia concentrations at a fixed distance of 0.2 m from the source. A low fan speed (3V) was used and responses were measured after a 30 second exposure time.

5.3.2 Ammonia Plume Tracking

The search algorithm used by the RAT robot for plume tracking is inspired by a real biological system, the dung beetle *Geotrupes stercorarius*. This creature flies in a random pattern of ellipses until the dung plume is detected. It then moves upwind toward the source making tacking movements back and forward across the plume. The beetle flies at an angle to the source until the edge of the plume is reached and passed. It then turns back toward the plume and continues back across until the other side is reached. It moves toward the source in this zigzag pattern until it is directly above it and hence cannot detect the odour any more. At this point it stops and lands on the target [246]. The RAT tracks in a very similar fashion (Figure 5.6). Initially it moves in a roughly perpendicular direction to the wind in order to locate the odour plume. This has the advantage of allowing the human user to release the robot away from the danger

of a potentially hazardous chemical exposure. Once the robot contacts the plume it moves upwind but still moves at an angle to the source. In this way it eventually reaches the edge of the plume, moves beyond the area effected by the vapour, and then turns back toward the odour. It tacks across the plume, like the dung beetle, until the source is located. At this point it circles around the source to ensure that it has correctly located the target rather than just an obstacle obstructing the plume.

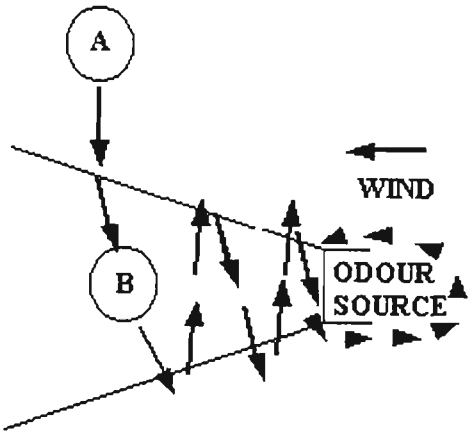

Figure 5.6 RAT robot tracking routine. From point A the robot moves perpendicular to the wind until it detects the odour plume. Once in the plume, at point B, the RAT moves toward the source.

Table 5.1 Results of RAT ammonia plume tracking using different chemical concentrations.

Ammonia Conc. (%)	Start Distance from Source (m)	Final Distance from Source (m)	Search Duration (mins)
1.75	0.7	0.7	10
1.75	0.5	0.4	10
3.5	1.0	0.1	15
5.5	1.0	0.2	13
5.5	0.5	0.3	12

The data from actual tracking experiments are summarised in Table 5.1. The results of tracking a 1.75% ammonia source indicate that at this low concentration the PPy sensors are not sufficiently sensitive. In the first experiment the robot simply circled at a distance of 0.7 m from the source and had not made progress after a period of ten minutes. A second experiment was run under these conditions but using a starting point that was closer to the source (0.5 m). In this case the robot did move slightly, but spent most of the ten minute period circling in place.

The concentration of ammonia was increased to 3.5%, and the starting point set at 1.0 m from the source. After ten minutes the robot had progressed well toward the source and hence was left for another five minutes until it started circling at a final distance of 0.1 m from the target. A second experiment was not carried out as this result was considered a successful tracking event.

The ammonia concentration was increased further to 5.5% with mixed results. The first experiment carried out used a start position 1.0 m from the odour source. The robot had again made good progress toward the target after a ten minute period and hence was left to continue. After a further three minutes the RAT began circling at a distance of 0.2 m from the odour source. In the second experiment at this ammonia concentration, the robot was started 0.5 m from the target. After ten minutes reasonable progress had been made so the RAT was allowed to continue searching. After a total of twelve minutes the robot began circling at a distance of 0.3 m from the source.

The results suggest that at low concentrations the RAT robot equipped with PPy gas sensors is unable to locate and trace the odour plume. At higher concentrations the robot was able to track toward the source quite effectively, but the final distances

reached did not always lead the robot to the exact target position. This is illustrated most clearly by the results obtained at the highest concentration (5.5%) of ammonia. The reason for this may relate to the shape and dimensions of the odour plume produced by the experimental set-up used for this work. As the plume is not visible to the human eye it was not possible to ensure that a fan shaped odour trail was produced. This may be due to fluctuations in airflow caused by drafts in the experimental area, which were of a magnitude to strong for the small fan to counter. Another possible problem may be that the experimental area, which was in a fairly narrow corridor, was too narrow. This would lead to the entire area becoming saturated with ammonia, and hence the robot would not be able to move completely out of the plume. The RAT may have been simply tracking in and out of lower concentration areas toward the edge of the plume, rather than according to the intended algorithm. In spite of these potential problems, the RAT robot did successfully track to within an acceptable distance from the target, from a distance of 1m, using screen-printed PPy gas sensors.

5.4 CONCLUSIONS

PPy gas sensors were employed on an autonomous mobile robot for successful tracking of an ammonia odour plume source. Static responses at a fixed distance from the source were used to compare the performance of different PPy/Cl sensors. Unmodified PPy/Cl sensors were more sensitive to ammonia than were anion exchanged PPy/Cl/pTS devices, and the response of all decreased with increasing distance from the source. The effect of varying wind velocity on sensor responses was investigated simply by varying the speed of a small DC fan used to generate the odour plume. The largest sensor frequency changes were observed at the minimum fan speed, and sensor responses decreased significantly as the fan speed was increased. At a fixed distance from the

ammonia source, the PPy/Cl sensor response was reasonably linear over a range of ammonia source concentrations.

Robot tracking experiments established that a minimum source concentration of 3.5% ammonia could be successfully located when the RAT commenced 1 m from the source and the wind velocity was low. When a 1.75% ammonia source was used under the same conditions the robot was not able to detect the odour plume.

While this approach to the detection of vapour plumes and location of odour sources is only in the fundamental stages of development, in the future it could prove a very useful tool for many environmental and hazardous gas leak monitoring tasks. The conducting polymer gas sensors used in this work are simple to prepare, lightweight and have low power requirements making them ideal for use on battery driven tracking robots.

Chapter 6

Factors Influencing the Electrochemistry of Poly-methoxyaniline sulfonate (PMAS) and the Effect on *Listeria* Detection

6.1 INTRODUCTION

The detection of microorganisms in solution using a soluble mediator to enhance electron transfer to an electrode has been demonstrated [247, 248] and forms the basis of commercial systems, for example Biocheck [249] and CellSense [250]. The mediator, a low molecular weight redox compound, is reduced by the microorganism and then diffuses to the working electrode where it is reoxidised [251]. Common mediators that have been employed include ferrocyanide, phenazine ethosulfate, and dichlorophenol indophenol [249].

The use of conducting polymers for microorganism detection in solution has primarily been limited to modified polymer electrode films, which are often impregnated with a redox mediator to enhance detection. These films are usually modified by incorporating some biological component such as an enzyme or antibody, and a common mediator such as ferrocene [252] that serves to reduce overpotential by speeding up electron flow to the electrode [253]. CPs have also been used as a substrate to which mediators are attached covalently [254], an approach which avoids diffusion of the mediator from the CP film [253]. The use of soluble CPs as conventional solution mediators for the detection of microorganisms has not yet been reported, possibly due to the limited availability of these materials in the past.

More recently the range of water soluble conducting polymers has increased due to a growing interest in the processing of these materials. One such conducting polymer, poly-methoxyaniline sulfonate (PMAS), has been noted as having some very interesting electrochemical and optical properties [255]. PMAS is a fully sulfonated, self-doped polyaniline that is soluble in water up to a concentration of about 20% w/w [256]. Recently we have been investigating the potential use of this polymer as a soluble biomediator for the detection of microorganisms including *Listeria monocytogenes.*

The addition of live *Listeria* to solutions of PMAS caused notable decreases in polymer oxidation currents observed using cyclic voltammetry (CV) or differential pulse voltammetry (DPV). Using this approach, low levels of *Listeria* were detectable (10 - 10^2 *Listeria*/mL) and the technique gave linear responses over a wide range of microorganism concentrations [257]. However, the mechanism of detection at this stage is not well understood and variations in the electrochemical stability of PMAS from batch to batch interfere with the detection of *Listeria.*

Characterisation of PMAS in our laboratories by gel permeation chromatography (GPC) has shown that the polymer consists of a range of different molecular weight fractions. It is possible to separate these using GPC and subsequently investigate the electrochemical and spectral properties of each. The detection mechanism is possibly dependent on molecular weight and hence particular fractions of the PMAS may give rise to the responses observed. It is also plausible that the ratio of these fractions vary from one batch of polymer to the next, which could lead to significant changes in the electrochemical stability of the polymer and also may affect detection performance.

6.1.1 Aims and Approach

The main aim of this section was to investigate the electrochemical and optical properties of the constituent molecular weight fractions of PMAS, and to determine which if any of these in particular give rise to interactions between *Listeria* and the polymer. It was hoped that the findings of this work would help understand the stability variation observed between batches of PMAS. The effect of electrolyte concentration on PMAS responses will also be discussed briefly.

6.2 EXPERIMENTAL

6.2.1 Chemicals and Materials

Water soluble poly(methoxyaniline sulfonic acid) (PMAS) was obtained from Mitsubishi Rayon, Japan, and was used as received. Two batches of PMAS were used, Lot No. 951205 and Lot No. 980306, and will be referred to as Batch A and Batch B respectively. Methoyxaniline sulfonic acid (MAS) was obtained from Mitsubishi Rayon, Japan, and was first cleaned by dialysis in Milli-Q water before use. KCl was obtained from BDH and used as received. Cultures of *Listeria monocytogenes* were supplied by Tecra Diagnostics, Sydney, in a Triptose Soy Broth/0.5% Yeast Extract (TSB/YE) medium at concentrations of approximately 10^9 mo/mL. These solutions were diluted in 0.1 M KCl for detection using PMAS.

6.2.2 Instruments and Apparatus

All voltammetry was carried out using a standard three-electrode cell with a BAS Ag/AgCl reference electrode and platinum mesh auxiliary electrode. A BAS glassy carbon disc (3 mm diameter) working electrode was used exclusively. Voltammetry was carried out using a MacLab potentiostat (ADI, Australia) coupled to a Macintosh computer via a MacLab (ADI). The system was controlled and voltammograms recorded using Echem software (ADI). UV-visible spectroscopy was carried out using a Shimadzu UV-1601 spectrophotometer operating in absorbance mode. A Waters GPC system interfaced to a PC with Millenium^{32} software was employed for all gel permeation chromatography. A PL aquagel-OH 30 prep-column (Polymer Laboratories) was used both for separation and characterisation of polymer fractions. The mobile phase used was 20% methanol/80% $NaNO_3$ (0.2 M), Na_2HPO_4 (0.01 M), which was filtered by vacuum though a 0.45 μm Nylon 66 membrane filter (Alltech) prior to use.

All dialysis post-GPC was carried out using cellulose acetate dialysis tubing with a molecular weight exclusion of 12000 (Sigma Aldrich) in tap water, then R_0 water (Waters) in the final stages. The fractions were concentrated using a Bucci rotavap at 60 degrees C. All pH measurements were made using a Denver Model 20 pH/conductivity meter.

6.2.3 Post-GPC Processing

To allow for proper electrochemical characterisation, the fractions were concentrated down from volumes of 200 - 600 mL to approximately 5 mL by rotavap at 60 degrees C. Prior to this, the samples were dialysed for a period of 5 days in R_0 water to remove the mobile phase electrolyte (methanol, $NaNO_3/Na_2HPO_4$). A small volume of 4 M KCl was added to the final reduced volume of each fraction to give a KCl concentration of 0.1 M. After dialysis and concentration, the pH of each fraction was measured to be approximately 9. This was adjusted using HCl to give a pH of 2.6.

6.3 RESULTS AND DISCUSSION

The detection of *Listeria* in solution containing PMAS involved scanning the potential between - 400 mV and +1000 mV and measuring changes in the oxidation peak current response at approximately 0.80 V (vs Ag/AgCl). In a typical experiment the polymer was first cycled between these potentials for 3 scans, then an aliquot of *Listeria* was added and a further 3 scans recorded. The effect of *Listeria* on the peak current at 0.80 V was determined by comparing data from the 3rd and 6th scans. Figure 6.1 shows a typical result when *Listeria* (10^2 mo/mL) was added to a 1% (w/v) solution of PMAS in 0.1 M KCl. The observed decrease in peak current, the magnitude of which relates to

the concentration of *Listeria* added, appeared to hold promise as a means of rapidly detecting this microorganism over a range of concentrations.

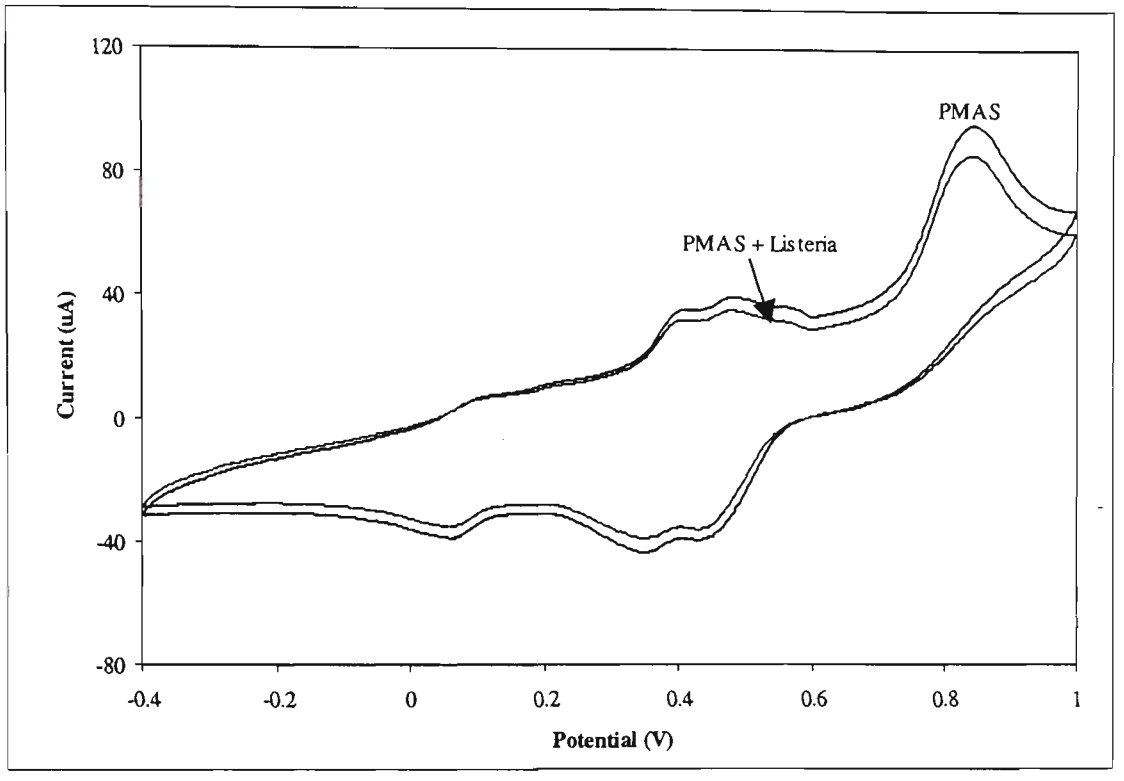

Figure 6.1 Change in current response of 1% (w/v) PMAS in 0.1 M KCl at 0.80V upon the addition of 10^2 *Listeria*/mL. Scan range was – 400 to + 1000 mV at 100 mV/sec.

6.3.1 PMAS Electrochemical Stability

The peak current of the 0.80 V oxidation response of PMAS (Batch A) was not completely stable, with decreases observed as the potential was continually scanned, but the changes were only slight (Figure 6.2) and hence did not interfere with the detection of *Listeria*. When a different batch of PMAS (Batch B) was received from Mitsubishi Rayon and tested, peak current stability problems were noted. In the absence of *Listeria*, repeated cycling of PMAS caused a continual decrease in the current response at the potential of interest (0.80 V) (Figure 6.3). The response of PMAS Batch A at this potential was more stable over successive scans (Figure 6.2) making the detection of *Listeria* due to decreases in peak current more reliable. While it was still possible to

detect *Listeria* using PMAS Batch B, significant peak current decay in the absence of *Listeria* made differentiation between microorganism concentrations difficult. The peak current observed at 0.80 V on the initial scan of PMAS Batch B was much higher than Batch A, suggesting some difference in the conductivity, and hence electrochemistry of the two samples. Table 6.1 shows peak current responses at 0.80 V from CVs of this PMAS Batch B, before and after the addition of 10^2 and 10^5 *Listeria*/mL. Decreases in peak current observed for the PMAS alone from scan to scan give some idea of the instability described above. There are clear decreases in peak current due to the addition of microorganisms; however, similar changes in response were observed for two concentrations of *Listeria* in spite of the fact that these samples differed by three orders of magnitude.

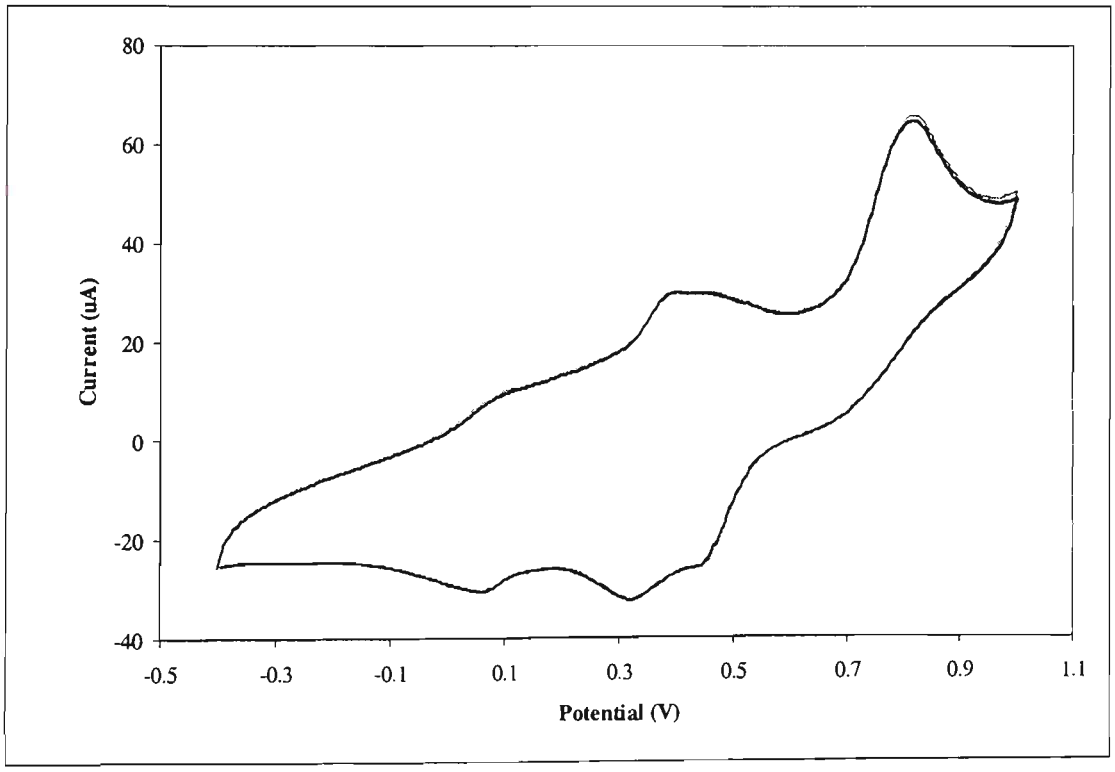

Figure 6.2 Peak current variation observed over 5 scans for 1% (w/v) PMAS in, Batch A, 0.1 M KCl at 0.80 V vs Ag/AgCl. Scan range was - 400 to + 1000 mV at 100 mV/sec.

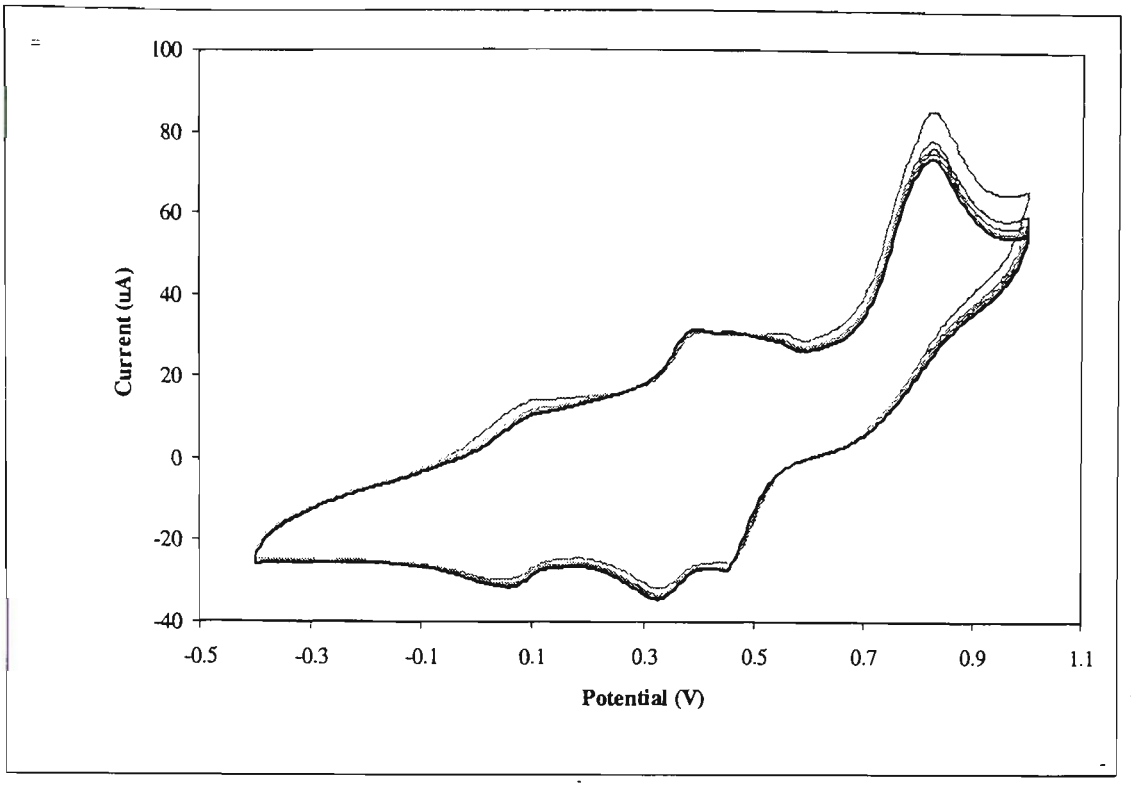

Figure 6.3 Peak current variation observed over 5 scans for 1% (w/v) PMAS, Batch B, in 0.1 M KCl at 0.80V vs Ag/AgCl. Scan range was - 400 to + 1000 mV at 100 mV/sec. The 5th scan is shown in bold.

Table 6.1 Variation in peak current (μA) response (0.8 V) of 1% (w/v) PMAS in 0.1 M KCl before and after the addition of live *Listeria* in 0.1 M KCl. The potential was cycled between -400 and + 1000 mV (vs Ag/AgCl) at 100 mV/s.

Scan	PMAS	PMAS + 10^2 *Listeria*/mL	PMAS	PMAS + 10^5 *Listeria*/mL
1	112.3	95.1	110.1	98.1
2	102.6	87.1	100.6	90.1
3	98.9	84.5	97.3	86.8
4	97.2	83.4	95.6	84.9
5	96.1	83	94.6	83.9
6	95.2	82.8	93.8	83.2

The current decay of the polymer alone masks the expected changes after adding microorganisms, and made it difficult to determine whether decreases in peak current were due to the polymer itself or due to some interaction with the *Listeria*. One possible explanation for these variations in polymer response is that the molecular weight

distribution varies between batches of PMAS having some effect on the electrochemistry. In order to investigate this possibility, GPC analysis was performed on different batches of PMAS.

6.3.2 GPC Characterisation of PMAS

A typical GPC chromatogram of saturated (ca 10% w/v) PMAS in water as obtained is shown in Figure 6.4. The large peak (A) is due to the high molecular weight components of PMAS (ca 20000), while the shoulder region (B) relates to the mid-weight material (ca 9000). The small peak (C), which elutes at approximately 22 minutes, corresponds to the lower molecular weight fractions (ca 2000), and the final peak (D) is due to residual monomer in the PMAS. Figure 6.5 shows a GPC of MAS in water, the elution time of the peak being 26 minutes, confirming that peak (D) observed for PMAS is due to the presence of residual monomer. A comparison of four batches of PMAS using GPC (Figure 6.6.) shows differences between them. The mid-weight shoulder appearing at approximately 18.5 minutes is well resolved for sample 3 compared to the other samples indicating a higher mid-weight fraction component. The low weight fraction peak present at approximately 22 minutes is much larger for sample 2, as is the monomer content as indicated by the peak at approximately 27 minutes. These examples indicate that there are some variations between PMAS batches in terms of molecular weight distribution, and hence it would be expected that this would lead to some differences in electrochemical properties. According to the GPC results, the two batches used for *Listeria* detection (1 and 2) varied in terms of the amount of low weight and monomeric material present. Sample 2, which had a higher concentration of these components, showed greater electrochemical instability as was noted in the proceeding section.

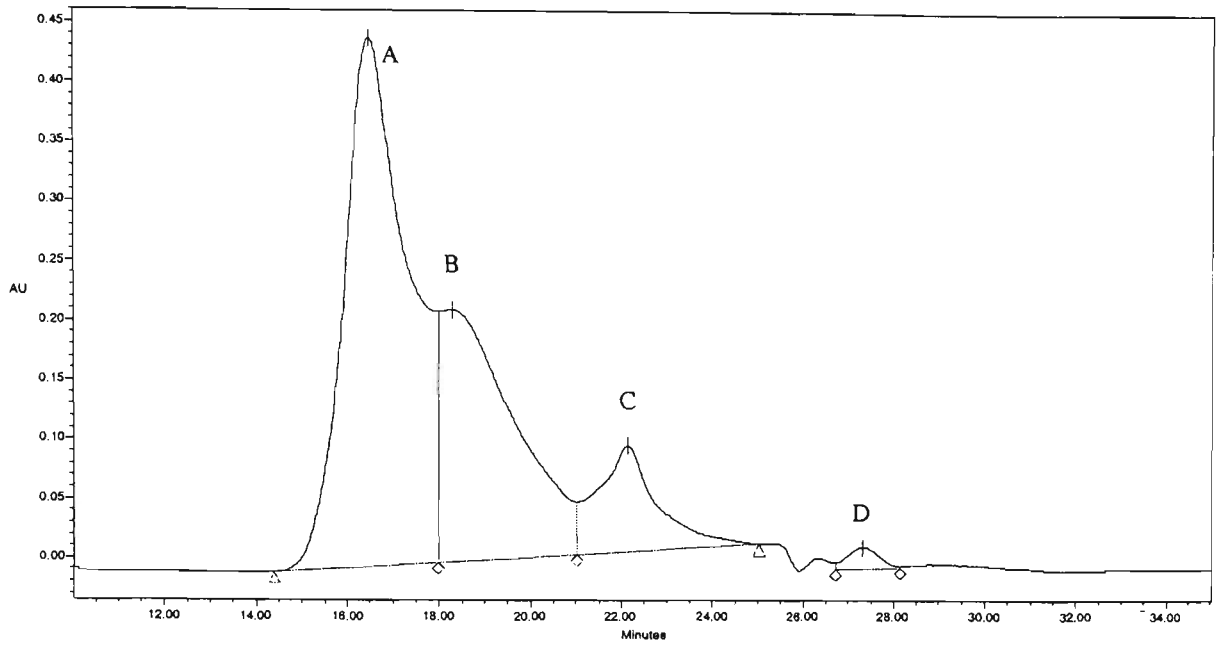

Figure 6.4 GPC chromatogram of saturated PMAS (ca 10% w/v) in water, Batch B (Lot No.980306) as obtained from Mitsubishi Rayon (Japan).

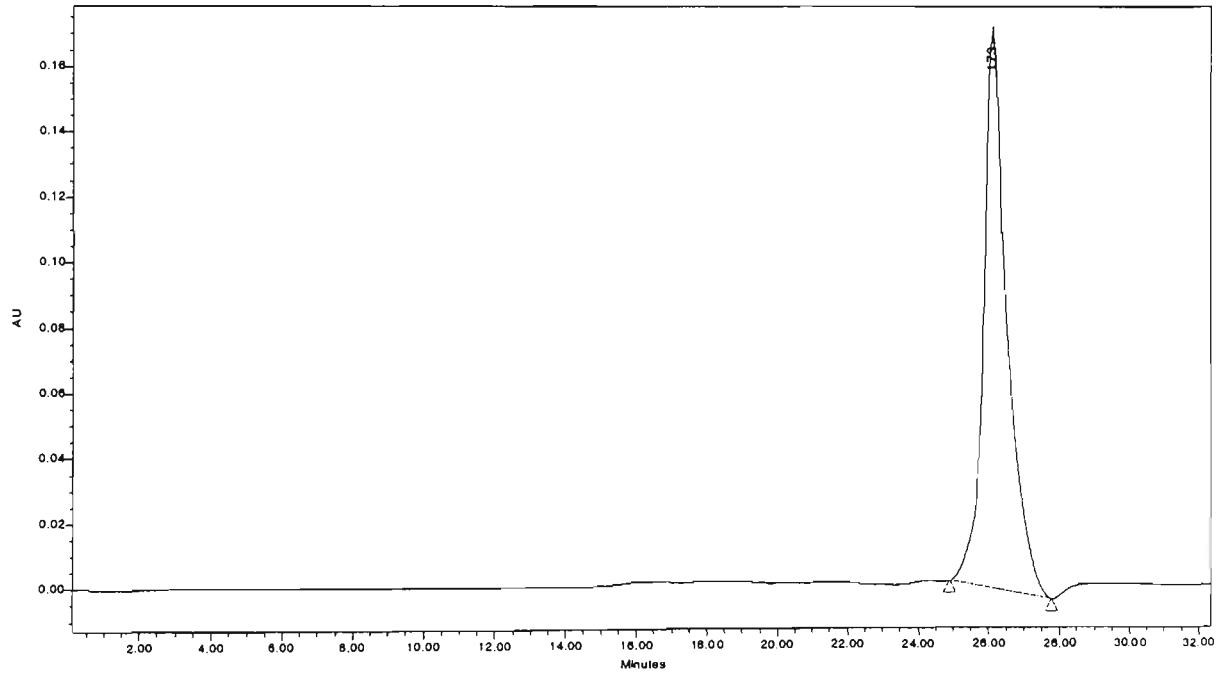

Figure 6.5 GPC analysis of MAS monomer in water.

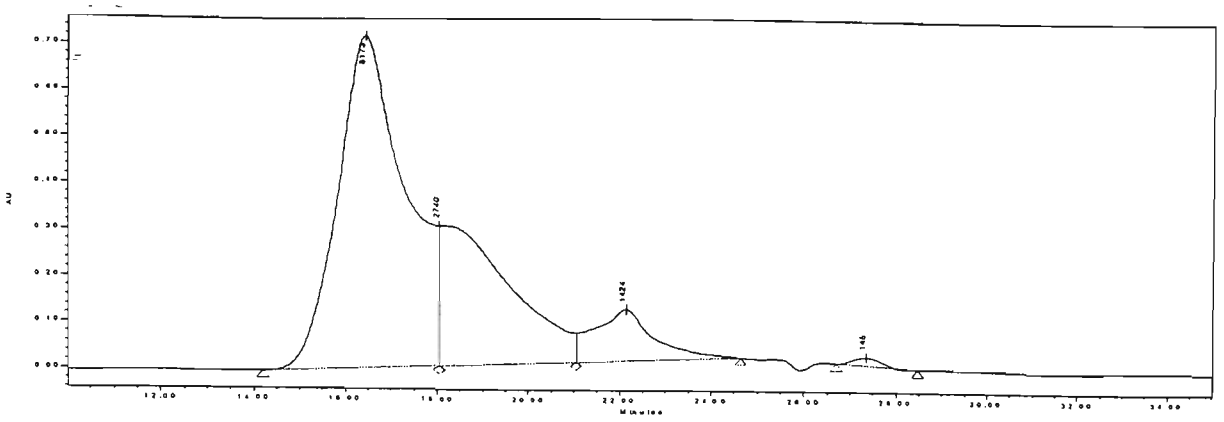

1 - PMAS 951205

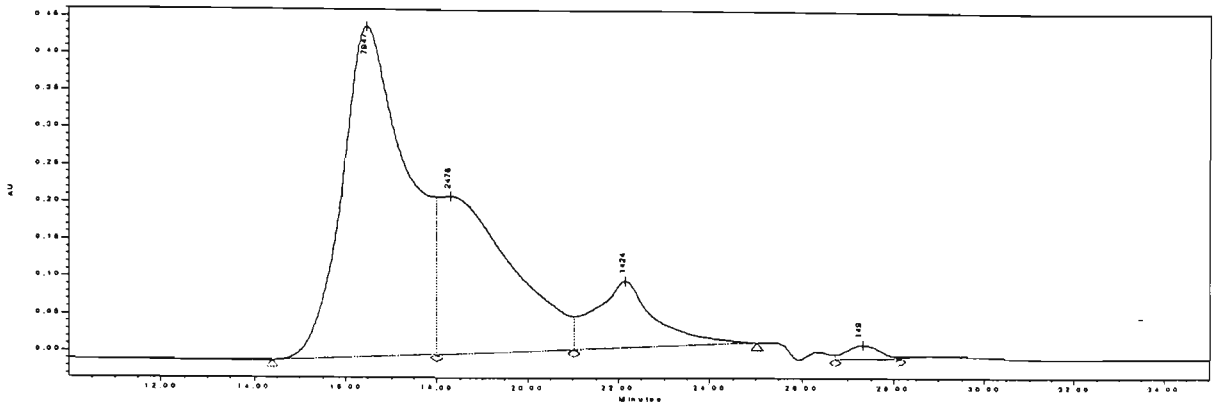

2 - PMAS 980306

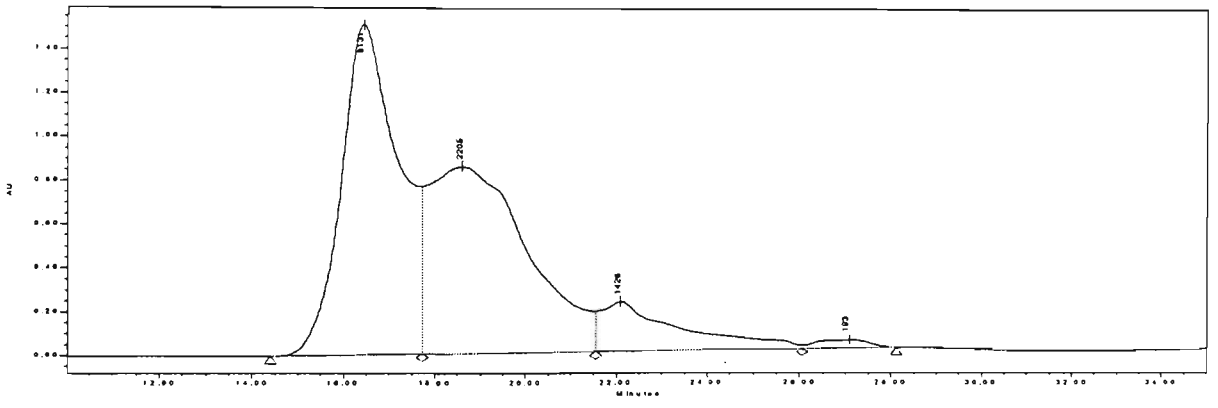

3 - PMAS MU23-57

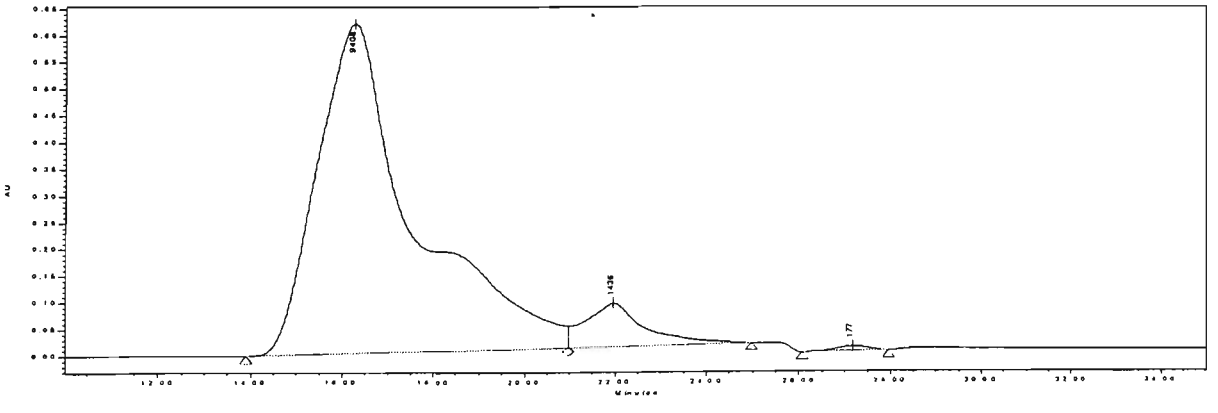

4- PMAS 1B-1

Figure 6.6 GPC chromatograms of four different batches of PMAS obtained from Mitsubishi Rayon (Japan).

6.3.3 Characterisation of Fractions

6.3.3.1 GPC

Five separate components of PMAS were collected to ensure a range of molecular weight materials were obtained. Post-fractionation samples of each component were kept for subsequent GPC molecular weight analysis, the results of which are given in Table 6.2. The average molecular weights, which are quoted on the basis of mass (Mw), in this case are an approximation as indicated by the relatively high polydispersity values obtained. Two values are included for fraction 5 as a mix of lower weight material was present. Chromatograms (Figure 6.7) show that there was also a significant amount of monomer present in fraction 5, as indicated by the large peak at 26 minutes, and some monomer present in fraction 1. The higher monomer presence in fraction 1 would be due to the fact that it is the major component in the whole PMAS sample, and hence has more monomer associated with it.

Table 6.2 Average molecular weights (Mw) and associated polydispersity figures obtained for GPC analysis of fractions after separation.

Fraction	Average Molecular Weight (Mw)	Polydispersity
1	25388	2.9
2	16906	1.8
3	11158	1.5
4	9307	1.4
5	8772/2149	1.3/1.0

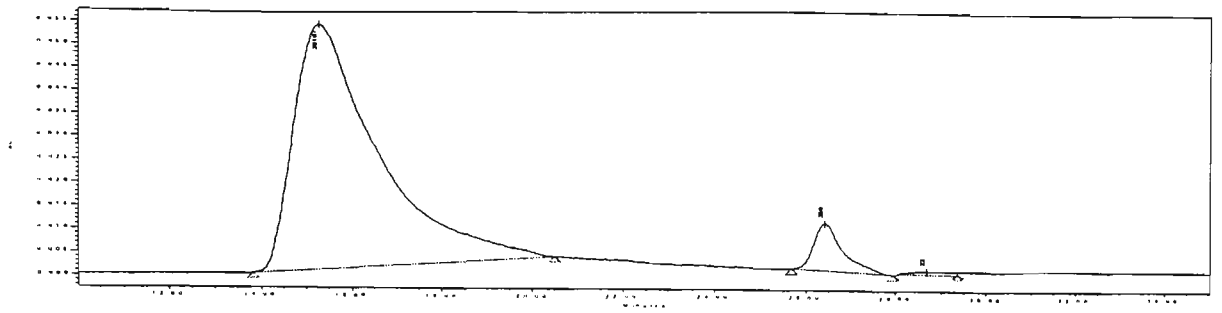

Fraction 1

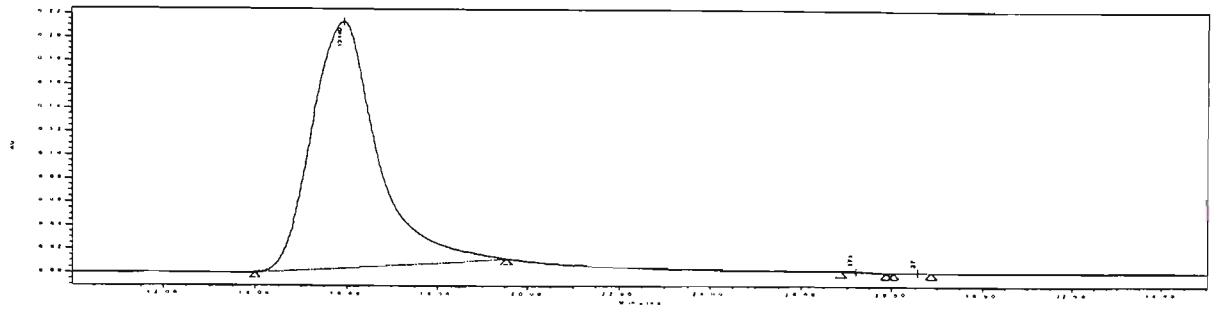

Fraction 2

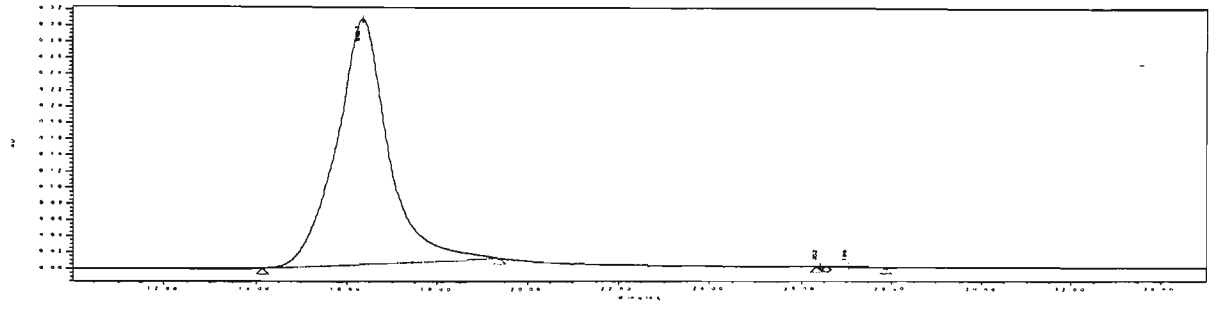

Fraction 3

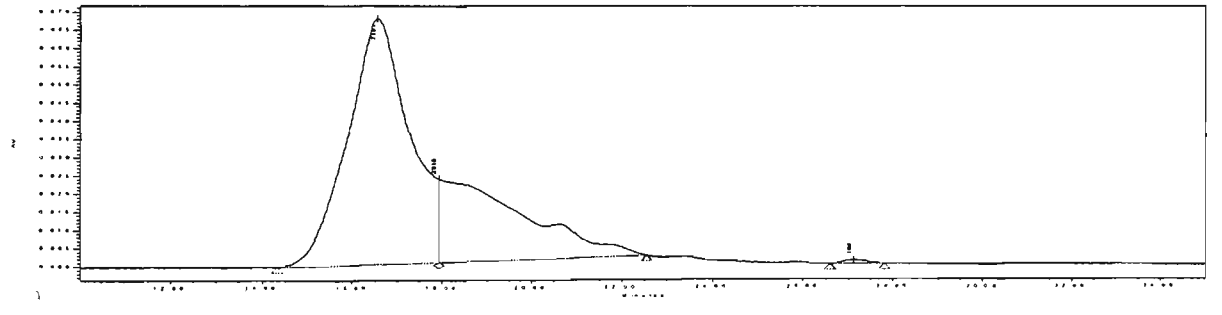

Fraction 4

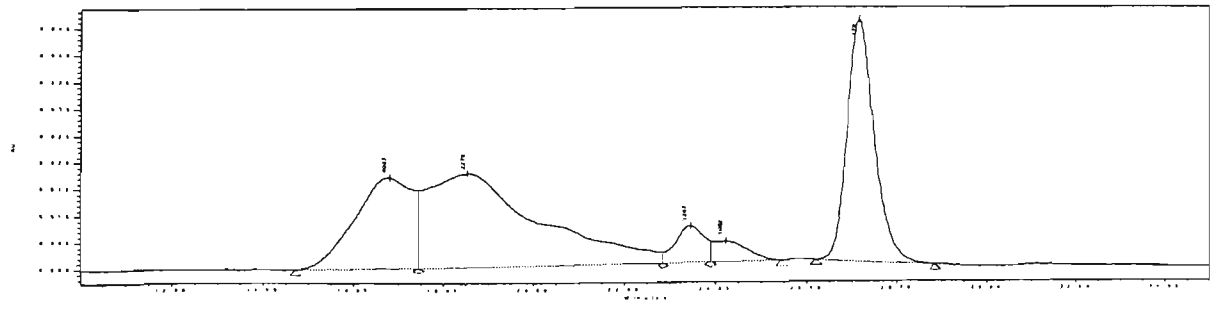

Fraction 5

Figure 6.7 GPC analysis of the five fractions in 20% methanol/ 80% 0.2 M $NaNO_3$,0.01 M Na_2HPO_4 obtained from PMAS Batch B.

6.3.3.2 UV-visible Spectroscopy

The UV-vis spectra of the five fractions (Figure 6.8) at pH 9 were similar with three absorption bands at 350 - 360 nm, 463 - 470 nm and 778 - 806 nm. The spectra are similar to those reported previously for sulfonated polyanilines [258,259], however, the absorption maxima are all red shifted to slightly higher wavelengths. The first band at 350 - 360 nm may relate to the π-π^* transition of the benzenoid ring, but this peak usually appears at shorter wavelengths around 310-320 nm [260,261]. The poorly defined shape of this band infers that there is superposition of peaks in this region of the spectra as has been suggested is sometimes the case for polyaniline [262]. It is more likely that this absorption is a combination of the π-π^* transition and a second absorption at approximately 360 nm, which has been reported previously for polyaniline as being related to the protonated emeraldine salt [263]. While these samples were analysed at pH 9, and hence should be deprotonated, the fractions may remain partially protonated under the conditions used due to the inherent self-doping nature of the polymer. The second band observed (463 - 470 nm) can be assigned to a polaron transition that is red shifted when compared to fully sulfonated SPANI [259], most likely due to a lower level of sulfonation. The presence of sulfonate groups is thought to cause blue shifts in the spectra due to increases in the band gap caused by the strong electron withdrawing nature of these groups [258]. The presence of these groups is also associated with increased strain on the polymer backbone causing distortions in the structure and hence increases in the band gap. [264]. The third band (778 - 806 nm) arises due to the presence of localised polarons [260], the position of which varies from 750 nm to NIR depending on the conditions employed [262].

Molecular weight did have an effect on the spectra with differences between the fractions observed in terms of relative absorption band magnitudes (Table 6.3). For example, the spectrum obtained for fraction 1 shows strong absorption in the 770-800 nm band relative to the other peaks and only minor absorption at 470 nm. Fractions 2 and 3 show less significant absorption in the 770-800 nm region but well defined polaron peaks at 470 nm. This may be due to differences in the concentration of polarons and bipolarons as a function of molecular weight, with a greater level of bipolaron species present in the high molecular weight material (fraction 1) giving rise to the stronger 770-800 nm band absorption.

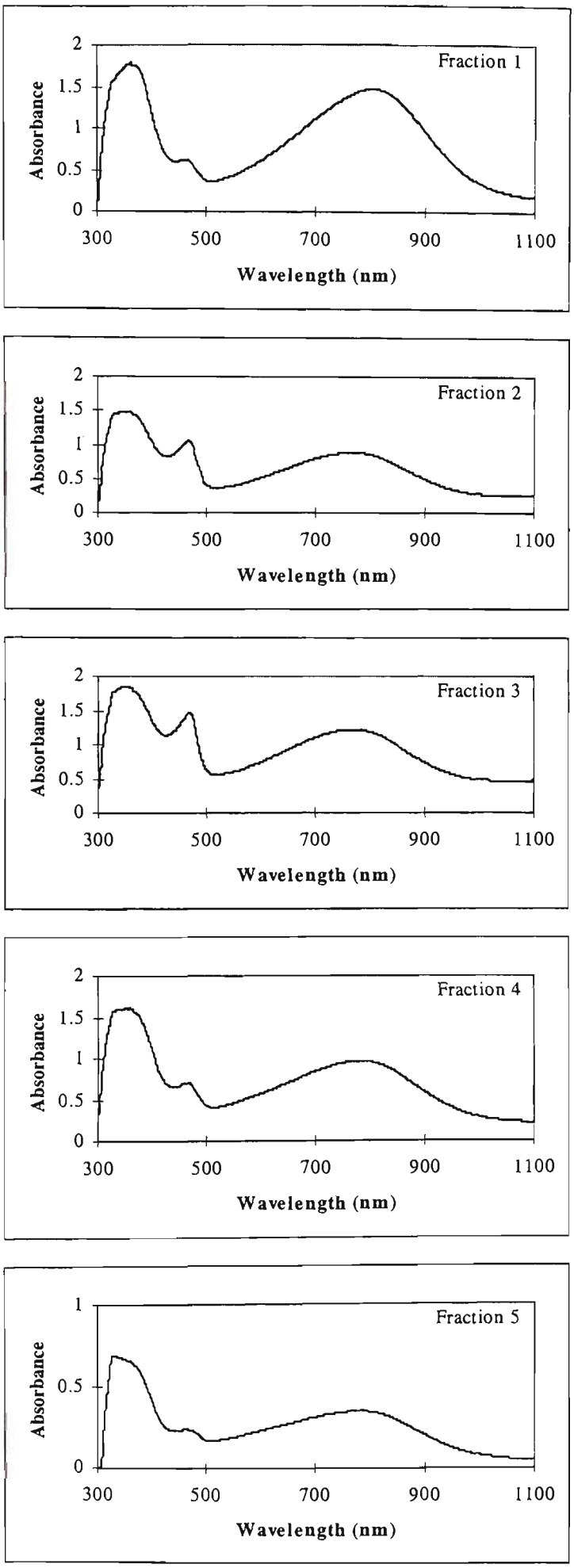

Figure 6.8 UV-visible spectra of the five PMAS fractions at pH 9 in water.

Table 6.3 Absorbance maxima and associated wavelengths of these bands from UV-visible spectra of PMAS fractions.

Fraction	λ_{max} nm	ABS	λ_{max} nm	ABS	λ_{max} nm	ABS
1	364	1.78	463	0.63	806	1.47
2	350	1.49	467	1.06	767	0.88
3	350	1.85	469	1.46	767	1.22
4	353	1.61	464	0.70	780	0.96
5	329	0.69	470	0.24	778	0.35

These two fractions were the most concentrated (Table 6.4) after post-GPC processing which may also explain the stronger absorption at 470 nm. The spectrum of fraction 4 shows that absorption for both the 470 and 770-800 nm bands was less significant relative to the 350-360 nm peak. Fraction 5 gave rise to a similar spectrum for which the overall absorbances relative to the other fractions were lower due to concentration differences (Table 6.4).

To compare spectra of the fractions and PMAS, the pH of the former were adjusted to 2.6. The spectra obtained for the fractions (Figure 6.9) were similar to a typical PMAS spectrum (Figure 6.10), with a characteristic peak in the 480 nm region, which based upon assignments made above is due to the polaron band. The absorbance band present at 300 nm may be due to the combined effects of π-π^* transitions and the emeraldine salt as discussed above, and the free-carrier tail extending out beyond 700 nm indicates that the fractions are conducting. The presence of the band at approximately 480 nm in spectra of the fractions at both pH 9 and 2.6 infers that this peak relates to the level of doping. Therefore, differences in spectra discussed above may relate to the extent to

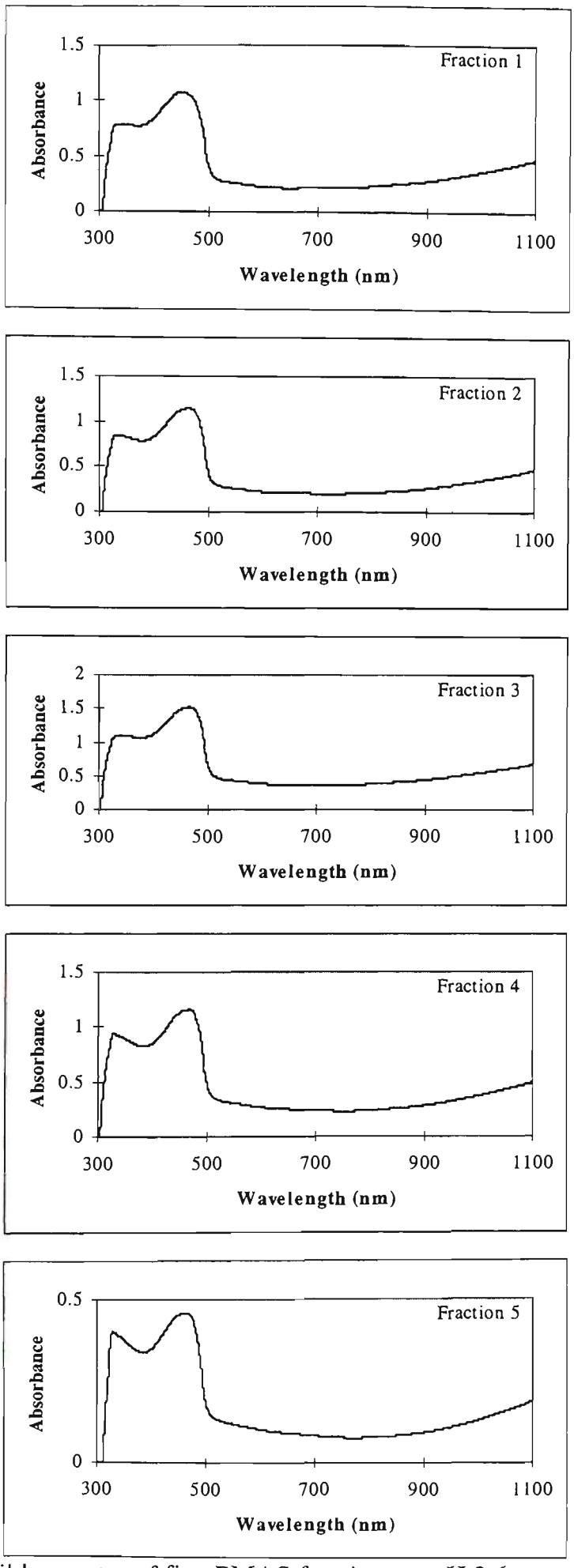

Figure 6.9 UV-visible spectra of five PMAS fractions at pH 2.6.

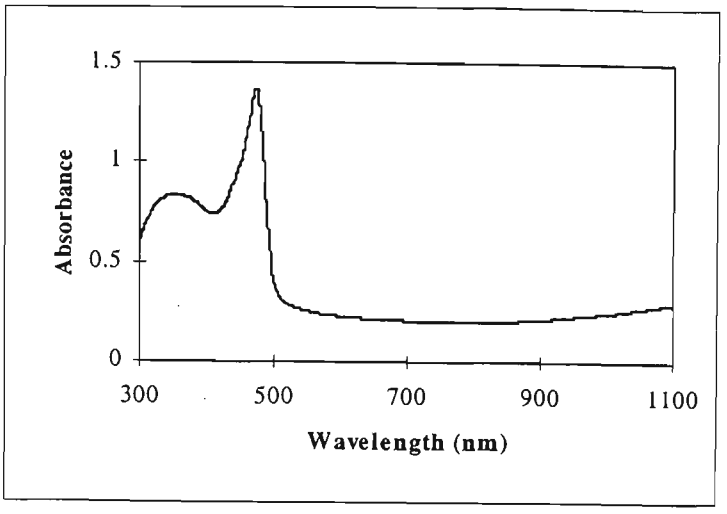

Figure 6.10 UV-visible spectrum of 0.005% PMAS.

which different molecular weight fractions de-dope at pH 9. Chan *et al* observed a significant decrease in the absorption band of fully sulfonated SPANI at 448-450 nm after adding base to dedope the polymer [259]. The band at 778 - 806 nm observed for fractions at pH 9 is no longer present after adjusting the pH to 2.6, which infers in the case of PMAS that this peak relates to the presence of the emeraldine base form.

Again differences between fractions were observed in terms of absorbance band magnitudes. The higher molecular weight fractions (1 - 3) absorbed more strongly in the polaron band region (480 nm) than fractions 4 and 5. For the two lower weight fractions, the peak at approximately 480 nm was smaller relative to the peak in the 300-330 nm region when compared to spectra of the other fractions, which most likely relates to a lower concentration of polarons in the low weight materials. Spectra of the higher molecular weight fractions bare most similarity to the PMAS spectrum, which shows even larger differences between the absorption bands at 480 nm and 330 nm (Figure 6.10). The magnitude of the 480 nm peak in this spectrum suggests a very high

concentration of polarons in the PMAS that probably arises due to the polymer being self-doping.

6.3.3.3 Estimation of Fraction Concentration

As the UV-vis spectra of the acidified fractions and PMAS are similar, the concentration of each fraction after rotavaping (% w/v) was estimated by preparing a UV-vis calibration for PMAS. A 1% (w/v) PMAS solution was prepared and diluted to give a range of PMAS samples at concentrations suitable for UV-vis calibration. The absorbance maximum at 480 nm was obtained for each concentration and a calibration plot prepared (Figure 6.11). Using a least squares linear regression an equation describing the line of best fit was calculated (Equation 1). The fractions were then diluted to appropriate concentrations and the peak maxima at 480 nm measured. Table 6.4 lists the estimated concentration of each fraction, after rotavap, obtained by substituting the measured absorbance into Equation 1.

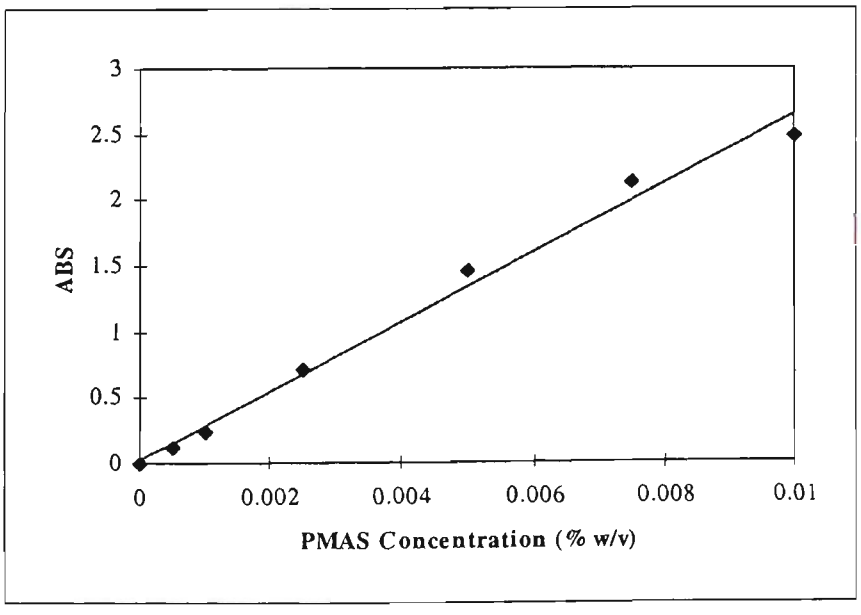

Figure 6.11 UV-vis calibration curve for PMAS obtained using the polaron absorption band at 480 nm.

Equation 1. $$\text{Concentration} = \frac{(\text{Absorbance} - 0.028)}{261.47}$$

Table 6.4 Estimated concentrations of the five PMAS fractions based upon UV-vis calibration of diluted PMAS. Fraction dilution ratios required for measurement of spectra within the linear range of the spectrophotometer and the corresponding absorbances are included.

Fraction	Dilution	UV-vis Absorbance (471 nm)	Estimated Concentration (% w/v)
1	1 : 100	0.8076	0.30
2	1 : 100	1.2734	0.48
3	1 : 100	1.0035	0.37
4	1 : 100	0.8478	0.31
5	1 : 10	0.2395	0.04

With the exception of fraction 5, the estimated concentration of the fractions was in the range 0.3 - 0.5% w/v. The estimated concentration of fraction 5 was significantly lower than the others (0.04% w/v) as a result of this component being present at low levels in the PMAS parent material. These differences in concentration were considered when analysing results of comparisons between the fractions.

6.3.3.4 Cyclic Voltammetry

CVs of each fraction at pH 9 were recorded but no responses were observed. After pH adjustment to 2.6 better CV responses were observed which varied from one fraction to the next (Figure 6.12). The responses obtained for all fractions were similar to the voltammograms obtained for PMAS (Figure 6.1) with the exception of the oxidation

peak at + 0.80 V. As the fractions were dialysed before analysis this suggests that the 0.80 V oxidation response may be due to the presence of low weight material or monomer in the PMAS. CVs of Fractions 2 and 3 are similar, having well defined oxidation peaks at 0.40 and 0.55 V. Usually these peaks are not as clearly resolved in CVs of PMAS. Fraction 1 also gave rise to good signals but the peak at 0.40 V is much larger than the peak at 0.55 V. Fractions 4 and 5 gave poorly resolved responses with the oxidation peaks at 0.40 and 0.55 V merged. Fraction 5 was still quite dilute after concentration (Table 6.4), a factor which would have some effect on the electrochemical responses. Differences in these voltammograms suggest that molecular weight does have an effect on electrochemical responses with the higher weight materials having better defined peaks. Previous studies of conducting polymers have shown the electronic properties to be dependent on chain length and hence molecular weight. Zotti *et al* investigated the electrochemical properties of pyrrole oligomers using CV and found that as chain length increased so did the number of oxidation responses observed. For bipyrrole and terpyrrole only one oxidation peak was observed, whereas for pentapyrrole and heptapyrrole two oxidation responses were noted [265]. Wei *et al* noted that for polyaniline oligomers the electronic conductivity was higher for longer chain molecules [266].

In order to investigate the electrochemical differences between PMAS fractions further DPV was employed as it allowed for the oxidation responses to be examined in more detail.

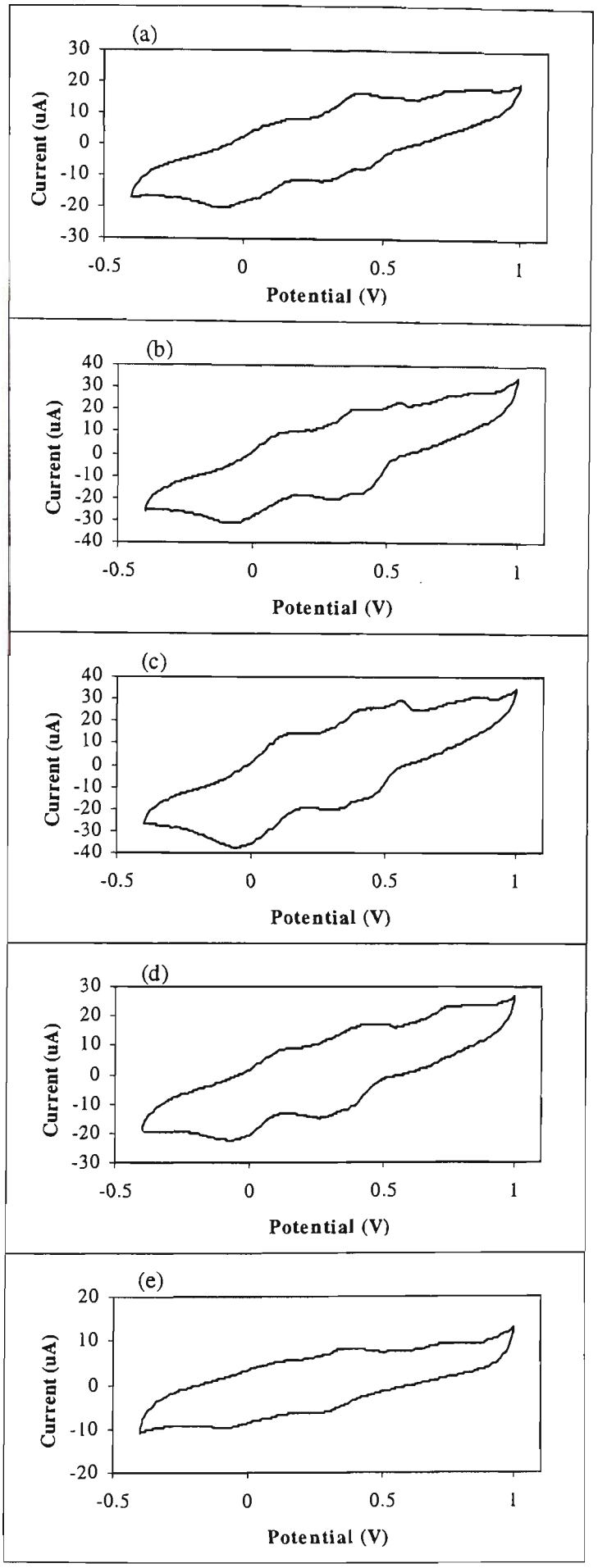

Figure 6.12 CVs of concentrated PMAS fractions 1(a) - 5(e) in 0.1 M KCl after dialysis. Scan range was - 400 mV to + 1000 mV at 100 mV/sec.

6.3.3.5 Differential Pulse Voltammetry

The differences in response for each of the 5 fractions are shown more clearly in the DPVs (Figure 6.13, Table 6.5). Again fractions 2 (b) and 3 (c) gave similar voltammograms having well defined peaks at 0.35 and 0.55 V and three smaller peaks at 0.05, 0.70 and 0.80 V, which were more clearly defined in the case of fraction 3. A total of seven oxidation peaks were observed for fraction 1 (Figure 6.13a), the most significant of these at 0.35 V. The presence of this number of peaks is most likely related to the high molecular weight of this component. Fraction 4 (d) shows only 3 peaks at potentials of 0.10, 0.35 and 0.70 V, and a shoulder at 0.80 V. The three oxidation peaks while broad are clearly defined, with the most significant response at 0.35 V. The reason for fewer peaks in this case may again relate to molecular weight, which is much lower for this fraction (approximately 9000 amu). The lowest weight fraction responses (Figure 6.13e) are somewhat smaller than those observed for the other fractions. This is due to fraction 5 being approximately ten times more dilute than the other four fractions after GPC separation and subsequent concentration (Table 6.4). In all five peaks were observed for this component with the oxidation response at 0.35 V again being most significant. Due to the greater sensitivity achieved using DPV, the 0.80 V oxidation peak was observed for fractions 1 to 3, and a shoulder in this region is present for fraction 4. This infers even after dialysis that some low weight material/monomer remains or that the oxidation peak at 0.80 V is in some way related to the polymer as well. For comparison a DPV of as received PMAS is shown in Figure 6.14. The most prominent peak lies at a potential of 0.75 V, with other broad oxidation responses at 0.00, 0.30 and 0.60 V. The main difference between the parent polymer and the fractions is the magnitude of the oxidation response at approximately 0.80 V. This peak is quite large for PMAS (0.75 V) while being only small for all the fractions

which is most likely due to the fact that the fractions were dialysed while the PMAS was not. Also the oxidation responses observed for PMAS at 0.00 and 0.30 V were broad compared to the higher weight fractions. This may be due to overlapping of the oxidation responses from the fractions that are present in the polymer.

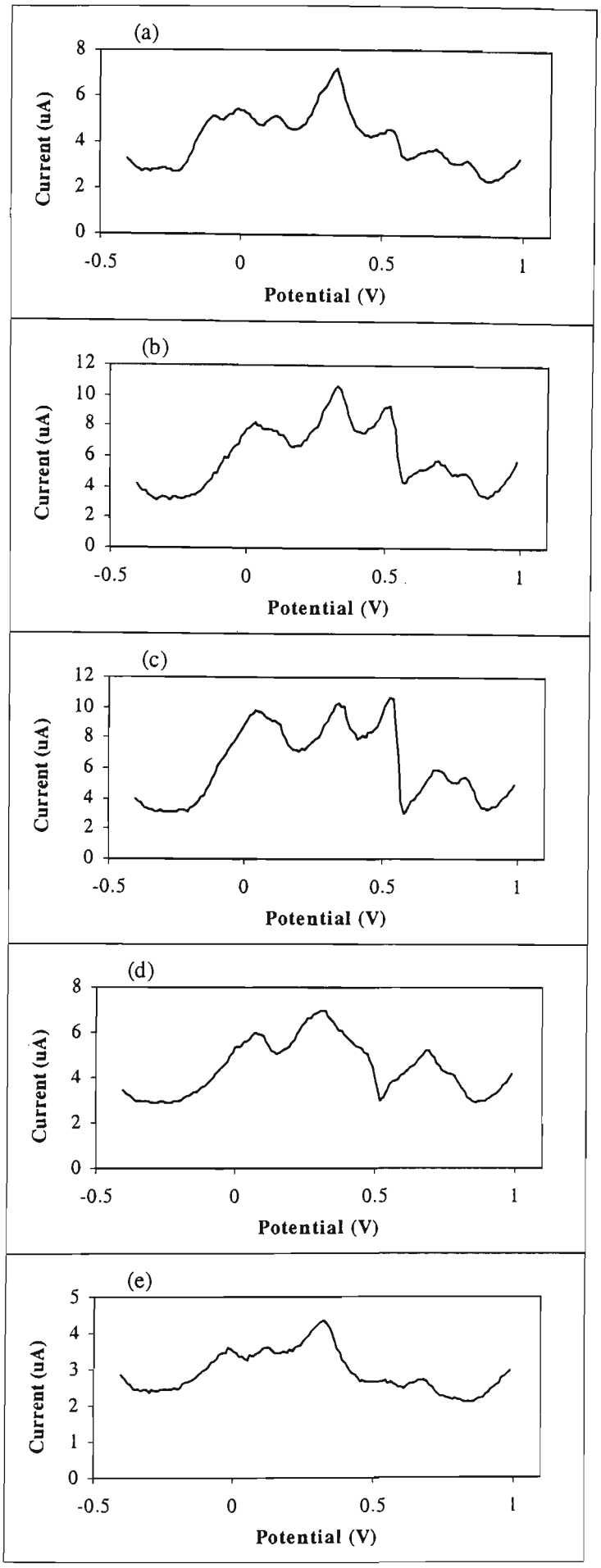

Figure 6.13 DPVs of PMAS fractions 1 (a) - 5 (e) in 0.1 M KCl at pH 2.6. Scan range was –400mV to + 1000 mV at 20 mV/sec.

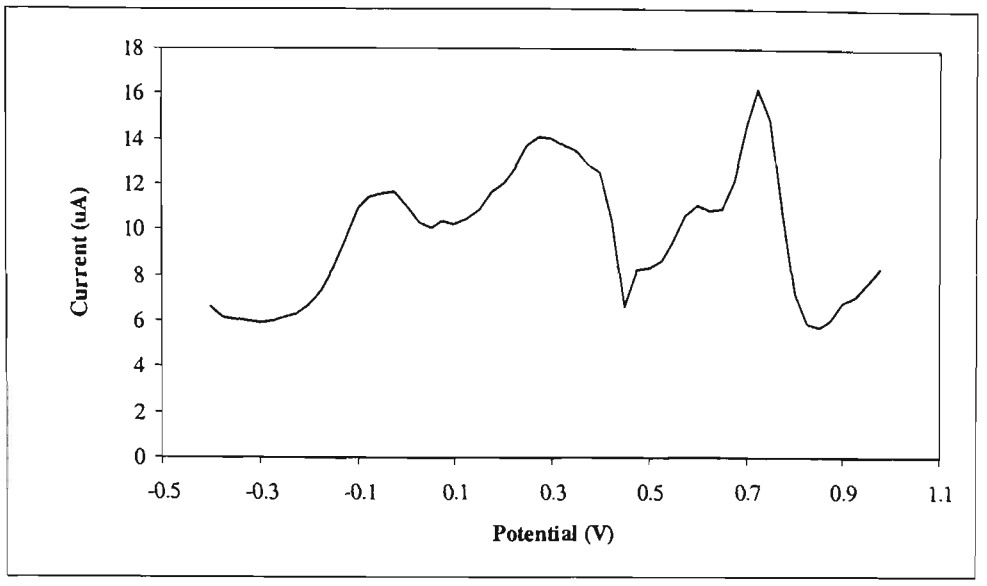

Figure 6.14 DPV of 1% PMAS in 0.1 M KCl. Scan range was – 400 mV to + 1000 mV at 20 mV/sec.

Table 6.5 Oxidation potentials of peaks present in DPVs of the five fractions shown in Figure 6.15.

Peak	Fraction 1	Fraction 2	Fraction 3	Fraction 4	Fraction 5
1	- 0.10	-	-	-	-0.05
2	0.00	0.05	0.05	0.10	-
3	0.10	0.10	0.10	-	0.10
4	0.35	0.35	0.35	0.30	0.35
5	0.55	0.55	0.55	-	0.60
6	0.70	0.70	0.70	0.70	0.70
7	0.80	0.80	0.80	0.80	-

6.3.4 Electrochemical Properties of the Monomer

The presence of MAS was noted in both PMAS and the fractions during GPC analysis, and the main difference between CVs and DPVs of the as received polymer and dialysed fractions was the presence or absence of an oxidation response at + 0.80 V. The monomer in 0.1 M KCl at pH 2.6 was characterised by CV to establish the oxidation potential of this system using a glassy carbon electrode. A well defined oxidation response was observed at 0.80 V vs Ag/AgCl on the initial scan, as were small oxidation peaks at 0.35 and 0.45 V. With successive scans the Ipa at 0.80 V decreased significantly and the peaks at 0.35 and 0.45 V increased (Figure 6.15). Single scan CVs were recorded for a series of MAS solutions with concentrations ranging from 0.005 to 0.05% (w/v) (Figure 6.16). No oxidation response was observed at 0.35 or 0.45 V while large responses that increased with MAS concentration were observed at 0.77 V. A calibration plot of the oxidation peak currents at this potential shows a linear relationship between current response and MAS concentration (Figure 6.17). On the reverse potential sweep reduction peaks were noted at 0.36 and 0.26 V which also increased in magnitude as the MAS concentration increased. The results clearly show that the oxidation response at 0.77 V arises due to the monomer (MAS) while the other peaks present are due to formation of PMAS. On the forward scan the monomer is oxidised forming polymer at the working electrode which is subsequently reduced on the reverse potential sweep. This also explains why on successive scans at a fixed MAS concentration the 0.80 V oxidation peak current continually decreases while the redox couples at 0.35 and 0.45 V increase.

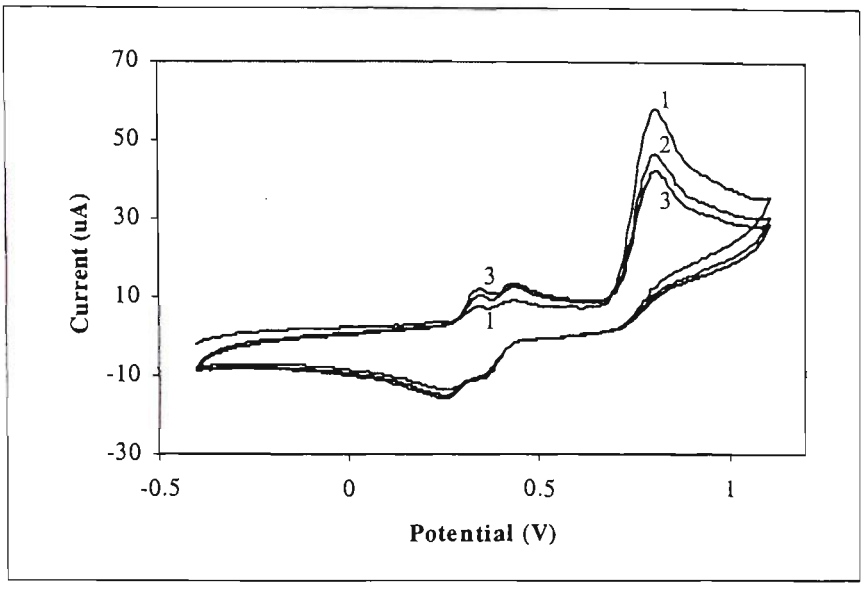

Figure 6.15 CV of 0.05% MAS in 0.1 M KCl. Scan range was – 400 to + 1000 mV at 100 mV/sec. Annotations indicate scan number.

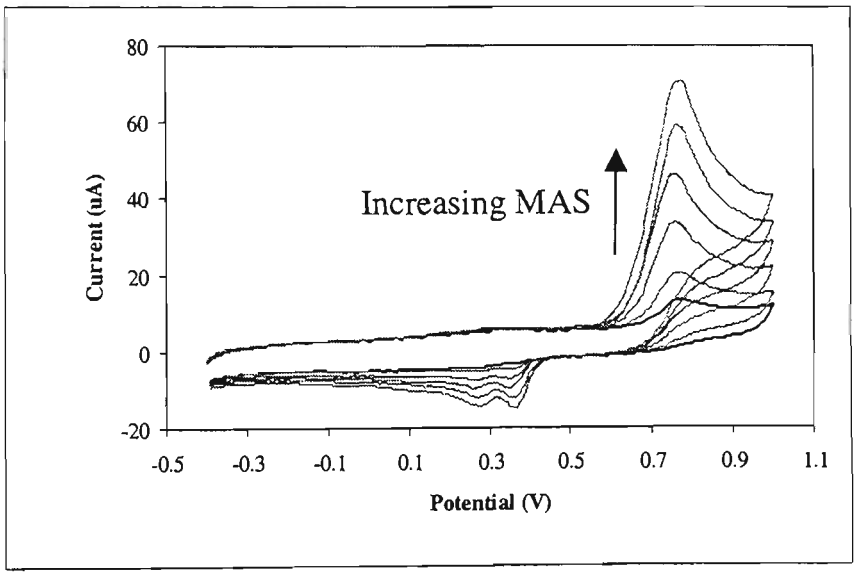

Figure 6.16 Effect of varying concentration on the cyclic voltammetric responses of MAS. Concentrations ranged from 0.005 to 0.05% (w/v) and the supporting electrolyte was 0.1 M KCl. The 0.005% scan is shown in bold. Scan range was – 400 to + 1000 mV at 100 mV/sec.

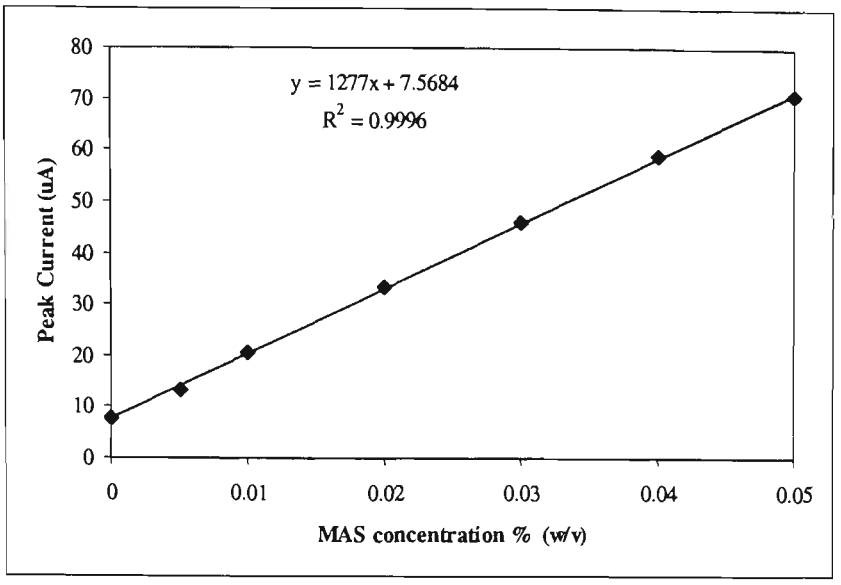

Figure 6.17 Calibration for MAS peak current response at 0.77 V obtained from CVs carried out in 0.1 M KCl in the range – 400 to + 1000 mV at 100 mV/sec.

6.3.5 Effect of MAS on PMAS Response

The effect of adding MAS to as received PMAS on the 0.80 V oxidation response was examined by standard addition. Figure 6.18 shows CVs of PMAS before and after the addition of aliquots (100 μL) of 0.025% (w/v) MAS. With each addition the peak current at 0.85 V increased while the oxidation peaks at lower potentials did not change significantly. After the last two additions of MAS the other oxidation responses where slightly higher which is most likely due to the formation of polymeric species near the electrode. The glassy carbon electrode was not removed in between additions of MAS. Also, on these later scans the corresponding reduction peaks are slighter larger indicating the formation of more polymer. The peak current response at 0.85 V increased linearly as the concentration of MAS increased (Figure 6.19). These findings provide further evidence that the oxidation peak used thus far for the detection of *Listeria* is directly related to the presence of monomer in PMAS. Dialysis was used in an attempt to completely remove this oxidation response.

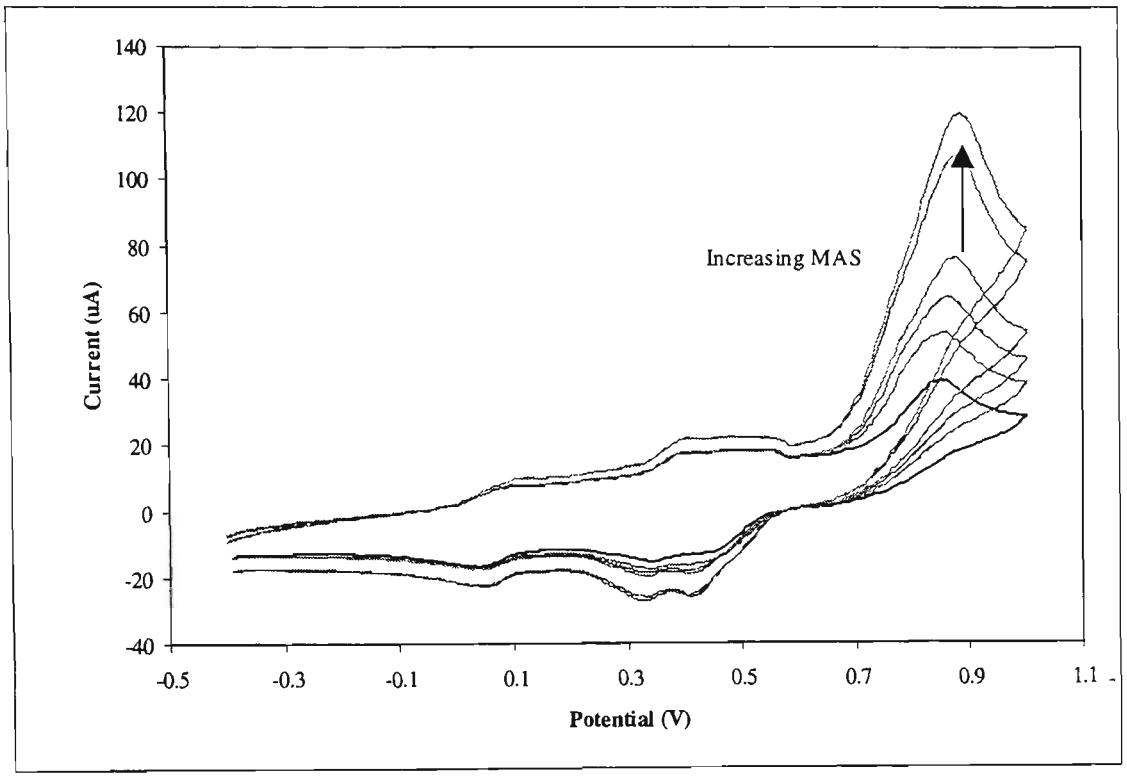

Figure 6.18 Cyclic voltametric response of 1% PMAS (w/v) in 0.1 M KCl before and after the addition of 0.025% (w/v) MAS in 0.1 M KCl. The initial PMAS response is shown in bold. Potential range was - 400 mV to + 1000 mV, scan rate 100 mV/sec.

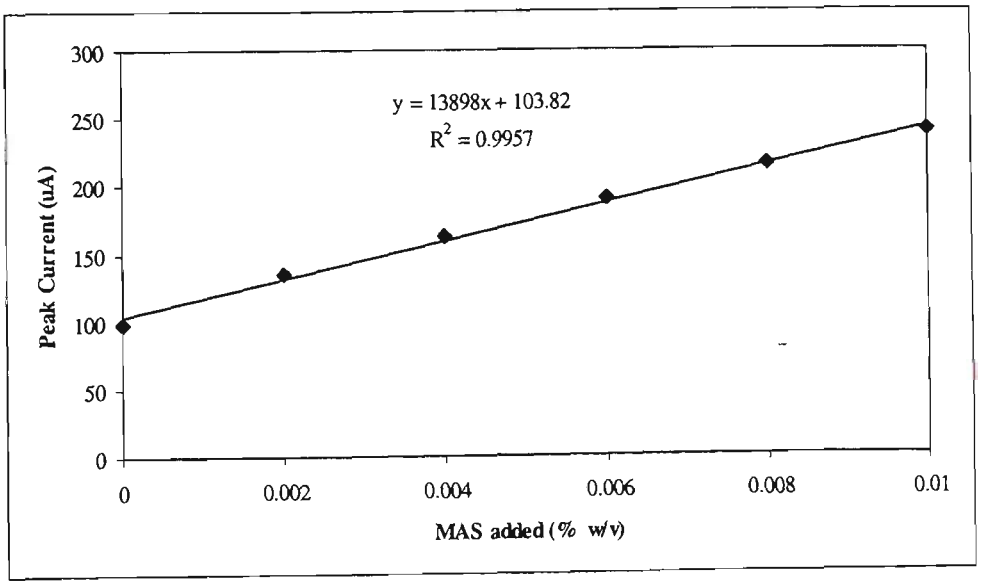

Figure 6.19 Peak current response of PMAS at 0.85 V after 100µL additions of 0.025% (w/v) MAS from CVs in 0.1 M KCl. Scan range was – 400 to + 1000 mV at 100 mV/sec.

6.3.6 Dialysis of PMAS

To confirm that the 0.80 V peak observed in CVs of PMAS was due to the presence of monomer, a solution of the polymer was dialysed before characterisation. After dialysis the concentration of monomer should be greatly reduced, and the oxidation peak at 0.80 V if related should also decrease. The concentration of PMAS used in solution for dialysis was high (ca 5% w/v) to ensure that a sufficient amount was still present after the process. A sample of the dialysed material was taken and diluted for UV-vis analysis. This allowed an estimate of the final PMAS concentration post-dialysis to be made using the observed absorption band at 480 nm and Equation 1 (section 6.3.3.3). The calculated concentration was 0.97% (w/v). A comparison of CVs of as prepared 1% w/v PMAS (Figure 6.20a) and the dialysed material (Figure 6.20b) reveal that after dialysis the oxidation peak at 0.80 V is not present. After dialysis, the oxidation peaks normally present at about 0.35 and 0.45 V shifted to higher potentials as did the corresponding reduction peaks indicating that the polymer is more difficult to oxidise (Table 6.6). It is clear that the presence of monomer has an effect on the electrochemical properties of PMAS, and hence must be involved in the process of *Listeria* detection.

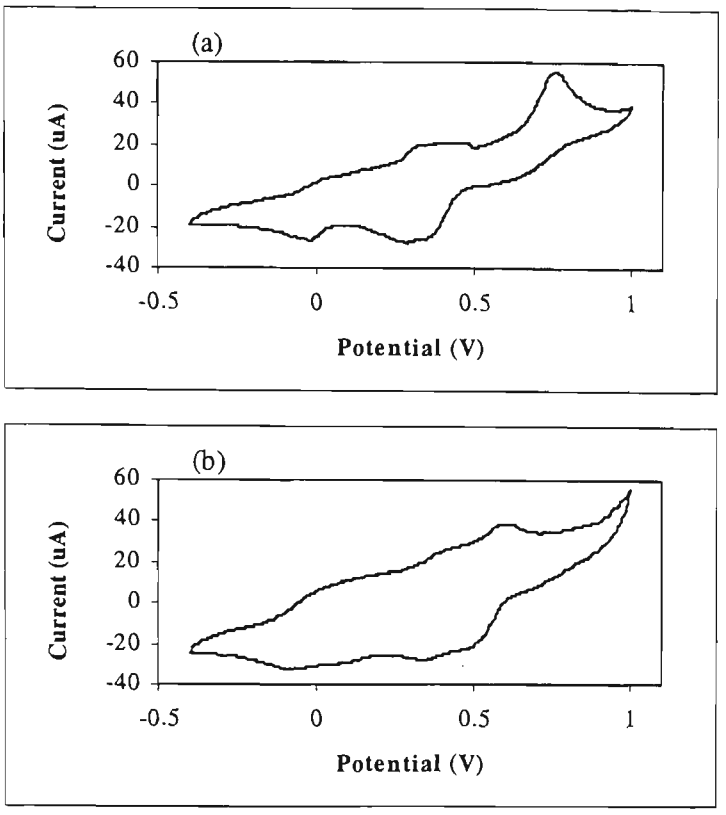

Figure 6.20 CVs of (a) 1% (w/v) PMAS Batch A as obtained in 0.1 M KCl and (b) dialysed PMAS Batch A (0.97% w/v) in 0.1 M KCl. Scan range was – 400 to + 1000 mV at 100 mV/sec.

Table 6.6 Peak potential change after dialysis of PMAS as recorded in CVs.

Solution	Epa1	Epa2	Epc1	Epc2
PMAS	0.32	0.46	0.35	0.28
Dialysed PMAS	0.41	0.61	0.49	0.33

6.3.6.1 Effect of Monomer on PMAS Response Stability

If residual monomer is present in PMAS, the mechanism observed for oxidation of MAS described above may have a significant effect on the peak current reproducibility of the polymer from scan to scan. The oxidation peak current of the polymer at 0.80 V tends to decrease if continually scanned which is consistent with this suggestion. Also, there is some variation in peak current reproducibility at this potential between batches

of PMAS, which is most likely due to varied amounts of residual monomer as indicated by GPC analysis of different PMAS samples. If this instability arises only in the presence of monomer then peak currents should be more reproducible when dialysed PMAS is cycled repeatedly. This was the case (Figure 6.21), with much more reproducible responses from scan to scan observed for this material (a) when compared to as received PMAS (b). The peak current response of the dialysed material is not completely reproducible with some drift observed from scan to scan, however, the larger drift in response observed for as received PMAS confirms that residual monomer is the main cause of instability. For this reason the performance of dialysed PMAS for *Listeria* detection was evaluated in subsequent work.

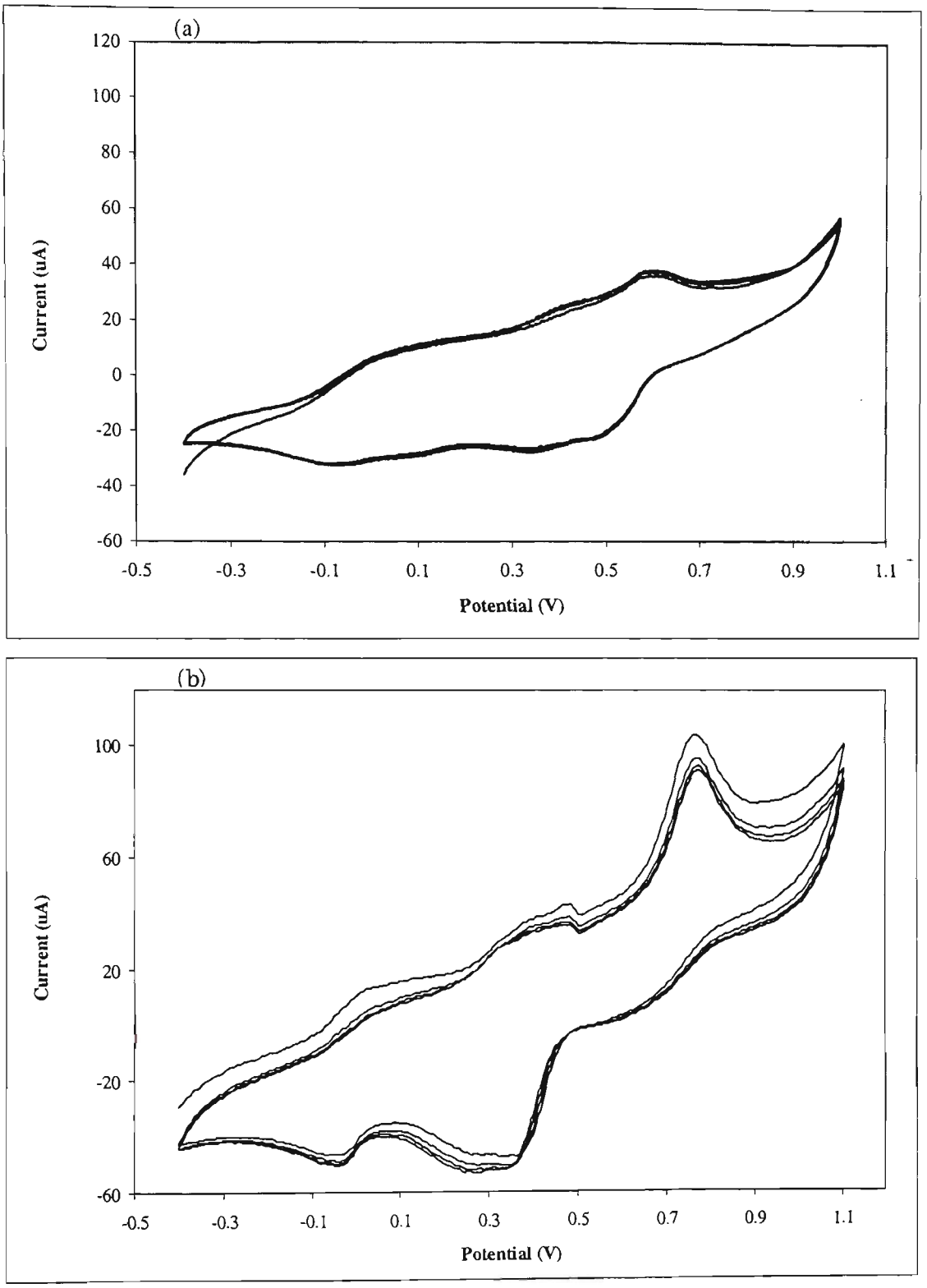

Figure 6.21 CVs of (a) dialysed PMAS Batch B and (b) as received PMAS Batch B scanned for four cycles in 0.1 M KCl. Scan range was – 400 to + 1000 mV at 100 mV/sec.

6.3.6.2 Stability of Dialysed PMAS over Time

PMAS was not completely stable after dialysis, with the appearance of an oxidation peak at 0.94 V after a period of two weeks (Figure 6.22b). This suggests that over time monomeric or small polymeric units may be cleaved from the polymer chains by some oxidative process, perhaps as a result of exposure to light. This peak corresponds to the main oxidation response of as received PMAS normally seen at 0.80 V, simply shifted to a higher potential after dialysis. The oxidation peak originally observed at 0.61 V was sharper after this period and had also shifted further to a higher potential of 0.68 V. It was noted in section 6.4.5 that after dialysis of PMAS, potentials of both the oxidation and reduction peaks had increased. The higher potentials observed suggest that once the monomer is removed, PMAS becomes more difficult to oxidise. However, even though the peak associated with the monomer reappeared at 0.94 V after two weeks (Figure 6.22b), the other peak potentials did not shift back to lower values. This infers that the increases in peak potentials observed after dialysis are not just due to the removal of monomer. To investigate these observations further, solutions of dialysed PMAS were stored, both in the presence and absence of light, and the CV responses monitored over time (Figure 6.23). After a 17 day period the monomer oxidation response had returned in both cases. There was no appreciable difference between responses obtained from the sample stored in darkness and of that stored in light, indicating that degradation process is independent of exposure to light.

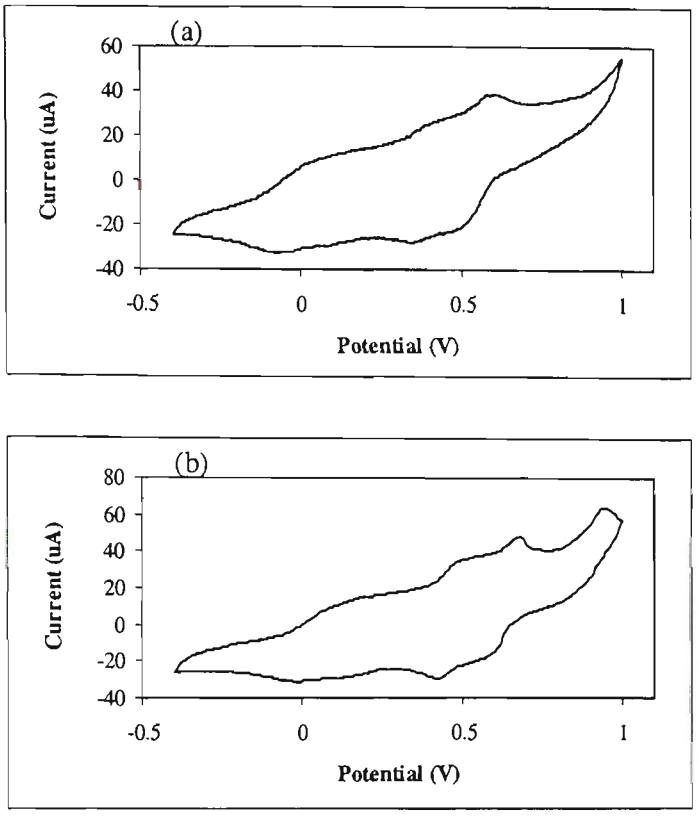

Figure 6.22 Voltammetric response of dialysed PMAS in 0.1 M KCl (a) initially and (b) after a period of two weeks. Scan range was – 400 to + 1000 mV at 100 mV/sec.

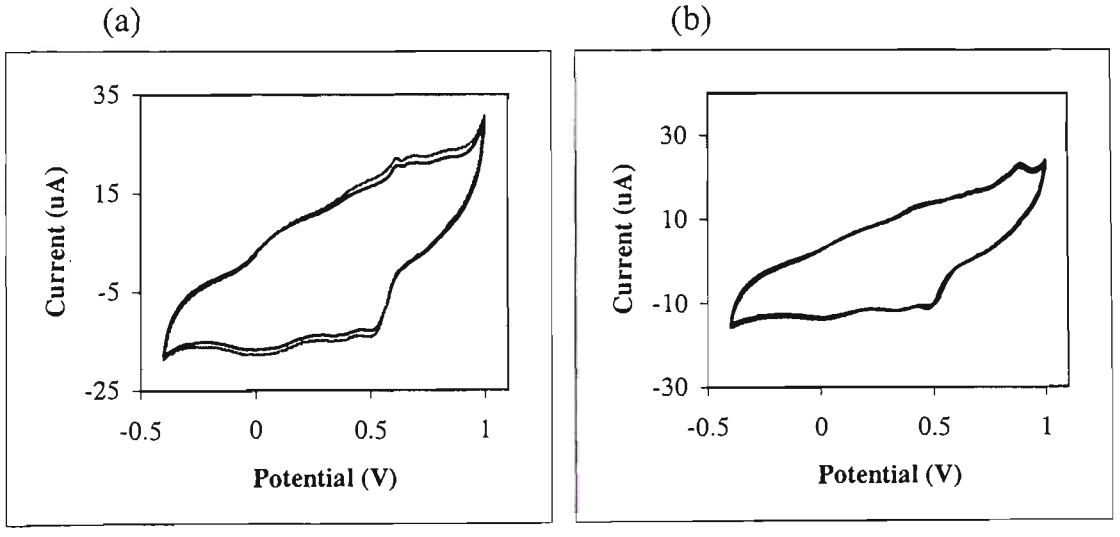

Figure 6.23 CVs of dialysed PMAS samples in 0.1 M KCl (a) immediately after dialysis and (b) after 17 days of storage. Samples were prepared in duplicate and sealed in screw cap vials, one in darkness, the other in light. Scan range was – 400 to + 1000 mV at 100 mV/sec.

6.3.7 *Listeria* Detection

6.3.7.1 MAS

Having established that the presence of MAS in the polymer contributes to the oxidation peak used previously for *Listeria* detection with PMAS, the interaction between the monomer and *Listeria* was investigated as a possible alternative approach. Both CV and DPV were employed for this work. When using CV a single scan was run before and after the addition of *Listeria*, and the scan rate employed was reasonably high (100 mV/s), to minimise the effect of polymerisation products forming. CVs of MAS before and after the addition of live *Listeria* at a concentration of 10^6 mo/mL (Figure 6.24) showed little difference in peak current at 0.84 V. The change in Ipa observed is similar to changes noted when scanning MAS monomer alone (Figure 6.15), and was most likely due to oxidation (depletion) of the monomer rather than any interaction with the microorganisms. DPVs of MAS before and after addition of *Listeria* (Figure 6.25) show no difference at all in peak current at 0.79 V, confirming that the changes observed using CV were due to MAS polymerisation, not *Listeria* interaction. However, at a potential of 0.29 V an increase in peak current of 1.20 μA was observed after *Listeria* were added. The peak at this potential corresponds to the formation or presence of polymer as was noted earlier. As the electrode was not polished in between the two scans, this small increase was most likely due to polymer formed at the electrode after the initial scan. Also, when PMAS was used for live *Listeria* detection decreases in peak current were observed, not increases, which further suggests the changes observed for MAS were not due to interactions with the microorganisms.

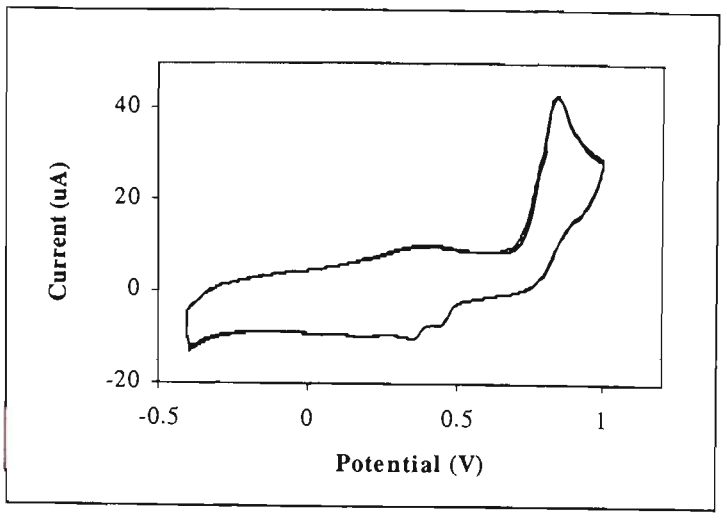

Figure 6.24 Effect of *Listeria* on CV response of glassy carbon electrode in 0.025% MAS in 0.1 M KCl. Scan range was – 400 to + 1000 mV at 100 mV/sec.

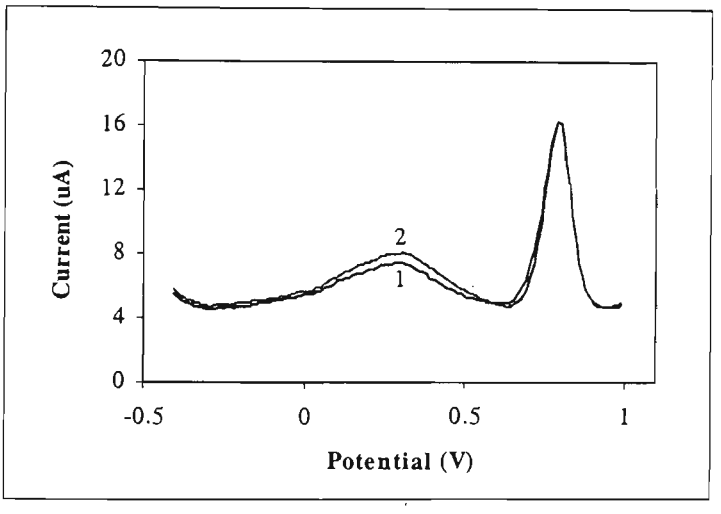

Figure 6.25 DPVs of 0.025% MAS in 0.1 M KCl before (1) and after (2) the addition of 10^8 live *Listeria/mL*. Scan range was – 400 to + 1000 mV at 20 mV/sec.

These results suggest that the interaction between *Listeria* and PMAS is not simply due to the presence of monomer. It was thought that the monomer unit may be acting as an electron transfer mediator, due to its small dimensions and mobility relative to the polymer, but it would seem that the mechanism involved is far more complex involving both the monomer and polymer. It is not clear whether the monomer or polymer gives rise to the *Listeria* signal, or if the mechanism involves some combined interaction with

both components. What has been shown is that the monomer alone, in the absence of PMAS, does not generate a detectable signal in the presence of live *Listeria.*

6.3.7.2 Dialysed PMAS

To investigate the interaction mechanism further, the effect of live *Listeria* on the electrochemical responses of dialysed PMAS was examined using both CV and DPV. As the oxidation peak at 0.80 V is removed after dialysis of the polymer, the peak at 0.50 V was monitored for changes in current after adding *Listeria.* CVs of the PMAS solution before and after the addition of 10^6 live *Listeria*/mL (Figure 6.26) exhibited only small changes in peak current at this potential. The decrease observed was just over 1μA, which when compared to changes in current at this potential for undialysed PMAS (7.6 μA, [257]), is small. The corresponding DPV experiment gave rise to even smaller changes in peak current after the addition of *Listeria* (Figure 6.27). A comparison of this change, which was only 0.5 μA, with results obtained for undialysed PMAS under the same conditions (9.6 μA, [257]), again suggests that the removal of monomer by dialysis significantly affects the detection of *Listeria.*

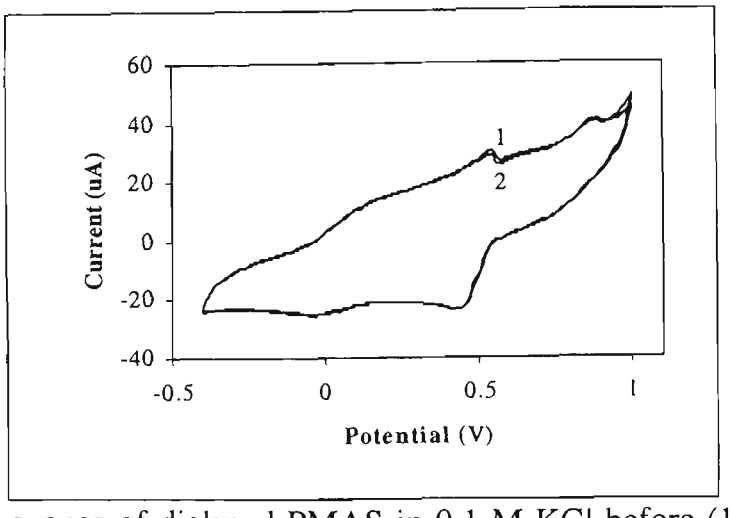

Figure 6.26 CV response of dialysed PMAS in 0.1 M KCl before (1) and after (2) the addition of 10^6 live *Listeria/mL.* Scan range was – 400 to + 1000 mV at 100 mV/sec.

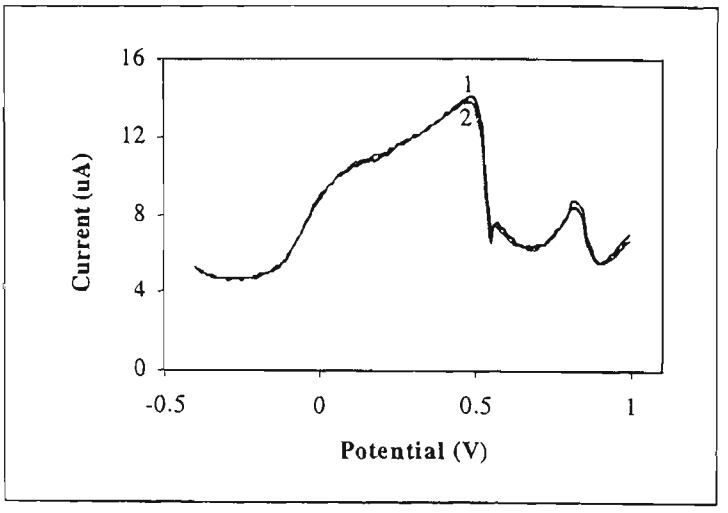

Figure 6.27 DPV response of dialysed PMAS in 0.1 M KCl before (1) and after (2) the addition of 10^6 live *Listeria*/mL. Scan range was – 400 to + 1000 mV at 20 mV/sec.

After dialysis with 12000 Mw membranes, both monomer and to a lesser extent low molecular weight fractions will have been removed. The results suggest that these materials have a significant effect on the interaction between PMAS and *Listeria*, and in fact the mechanism may rely solely on these components. If *Listeria* detection using PMAS does involve some form of conventional electron mediation the smaller molecules would be expected to play an important role. The detection mechanism may involve interaction between the microorganisms and the higher weight materials followed by shuttling of electrons to or from the electrode by the lower molecular weight fractions and possibly monomer units. To examine the effect of molecular weight on *Listeria* detection, experiments were carried out using a range of PMAS fractions.

6.3.7.3 PMAS Fractions

The five different PMAS fractions, which were separated by GPC, dialysed and concentrated by rotavap, were characterised by both CV and DPV before and after the addition of live *Listeria*. These fractions, which were characterised two weeks prior (section 6.3.3.5), had undergone significant electrochemical changes (Figure 6.28). The most obvious change was a significant decrease in peak current at 0.34 V. For all fractions this peak was no longer present in DPVs after a period of two weeks which suggests these materials degrade in solution over time. As this was the main oxidation peak present in DPVs of all fractions, interactions with *Listeria* were to be examined at this potential. The decreases in electroactivity observed, which were significant, may have been such that the detection of *Listeria* was no longer possible.

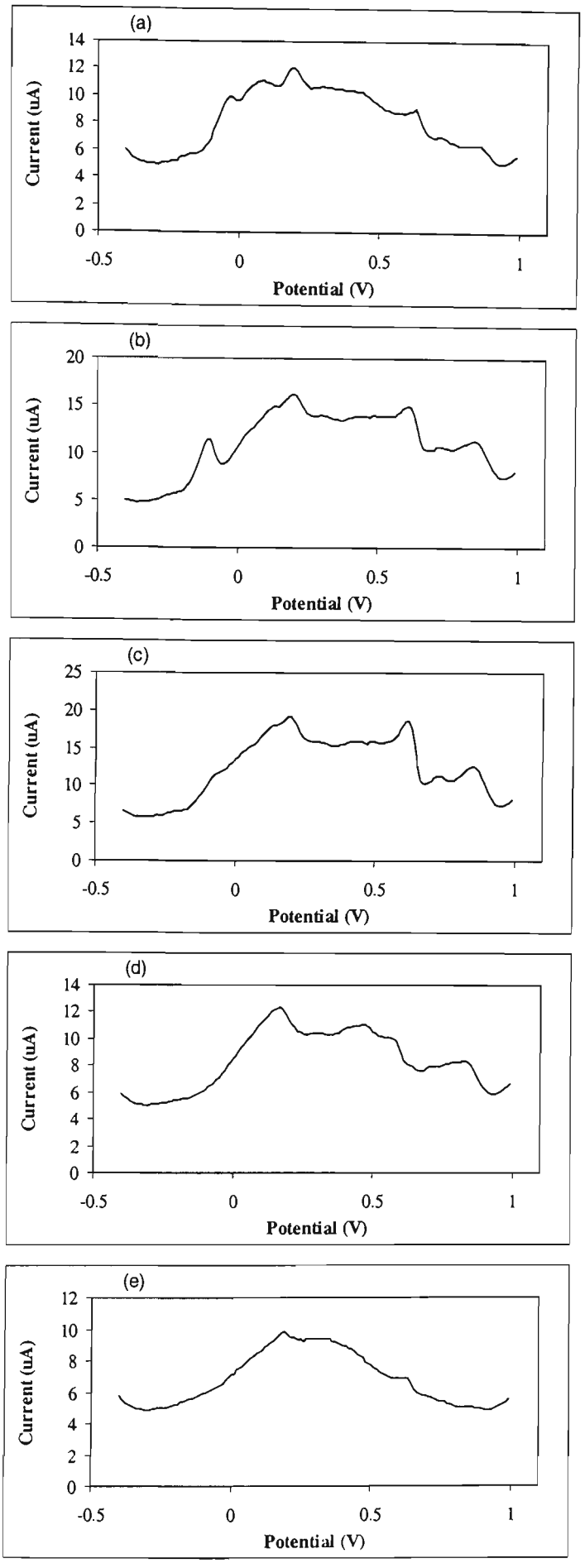

Figure 6.28 DPV responses of five PMAS Batch B fractions in 0.1 M KCl after a period of two weeks. Scan range was – 400 to + 1000 mV at 20 mV/sec.

All fractions were characterised by CV and DPV before adding 10^6/mL live *Listeria*. Only fraction 2 gave significant changes after the addition of microorganisms with the CV response at 0.65 V decreasing by 1.75 μA (Figure 6.29a), and the corresponding DPV peak current change at 0.61 V being -2.25 μA (Figure 6.29b). The change in cyclic voltammetric response of fraction 4 at 0.65V was the only other notable result with a decrease of 1.20 μA after the addition of *Listeria*. However, the corresponding DPV current change for this fraction was relatively small (0.75 μA). The other fractions gave little or no changes (Table 6.7), possibly as a result of the low concentrations used. In previous work on *Listeria* detection using PMAS it was found that electrochemical responses are effected once the concentration is less than 0.7% w/v [257]. Also, as was mentioned above, the electrochemical responses of the fractions decreased over time making *Listeria* detection more difficult.

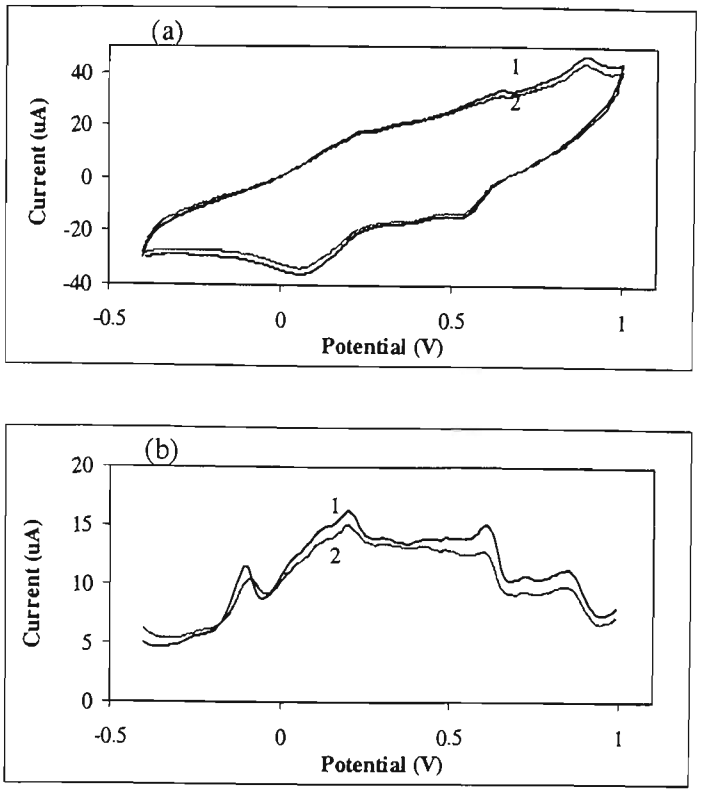

Figure 6.29 Effect of *Listeria* on (a) CV and (b) DPV of PMAS Batch B fraction 2. Responses before (1) and after (2) the addition of 10^6 /mL live *Listeria* in 0.1 M KCl. Scan range was – 400 to + 1000 mV at 100 mV/sec for CV and 20 mV/sec for DPV.

Table 6.7 Cyclic and differential pulse voltammetric responses (μA) at potentials of 0.65 V and 0.61 V respectively, before and after the addition of 10^6/mL *Listeria*.

Fraction	CV	CV/*Listeria*	DPV	DPV/*Listeria*
1	21.00	20.85	9.15	8.60
2	33.60	31.85	15.10	12.85
3	39.10	39.30	18.65	17.95
4	23.25	22.05	11.05	10.75
5	13.10	12.90	6.85	6.70

These two factors combined are likely to have effected the detection of *Listeria*. While it was not possible to obtain responses for the lower molecular weight fractions, the fact that fraction 2 (Mw = 16906 Da) gave responses to *Listeria* casts doubt on the theory

discussed earlier. While it is possible that the presence of lower molecular weight materials may improve responses, from this result it is clear that the higher molecular weight fractions are required for electron transfer between the organism and electrode. Also, the lack of electrochemical stability of these fractions in solution may be a problem if they are to be used for *Listeria* detection.

6.3.8 Effect of KCl Concentration on Dialysed PMAS Response

The effect of the concentration of supporting electrolyte (KCl) on the response of dialysed PMAS was investigated after it was noted that better electrochemical signals were observed at higher KCl levels. The CV response of dialysed PMAS in 2.0 M KCl (Figure 6.30b) at 0.60 V was significantly greater when compared to the corresponding oxidation peak of dialysed PMAS in 0.1 M KCl (Figure 6.30a). The effect of increased KCl concentration on dialysed PMAS response is made even clearer when DPV is employed (Figure 6.31). The increases in peak current observed in CVs plateau once the KCl concentration is increased beyond 0.5 M (Table 6.8, Figure 6.32), the data points described well by a logarithmic curve fit. Peak currents observed in DPVs continued to increase with KCl concentration in a linear fashion (Figure 6.31). the improvements in signal obtained by increased KCl concentration were examined as a means to potentially improve *Listeria* detection.

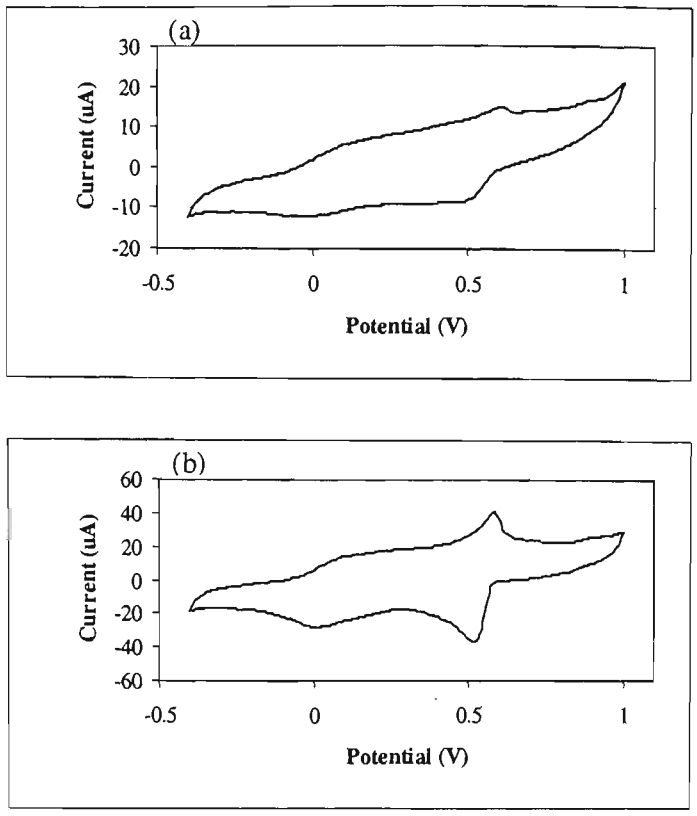

Figure 6.30 Effect of KCl concentration on CV response of dialysed PMAS : (a) 0.1 M KCl and (b) 2.0 M KCl. Scan range was – 400 to + 1000 mV at 100 mV/sec.

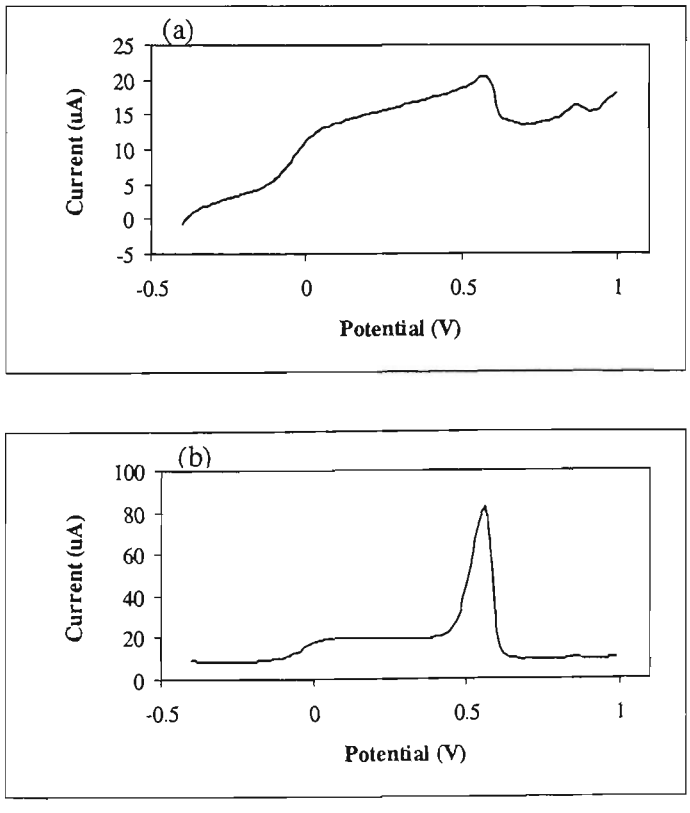

Figure 6.31 Effect of KCl concentration on DPV response of PMAS : (a) 0.1 M KCl and (b) 2.0 M KCl. Scan range was – 400 to + 1000 mV at 20 mV/sec.

Table 6.8 Effect of varying KCl concentration on CV and DPV responses (μA) of 0.97% (w/v) dialysed PMAS.

KCl Concentration (M)	CV	DPV
0.1	29.80	14.70
0.5	37.30	28.30
1.0	38.30	49.65
2.0	40.45	81.90

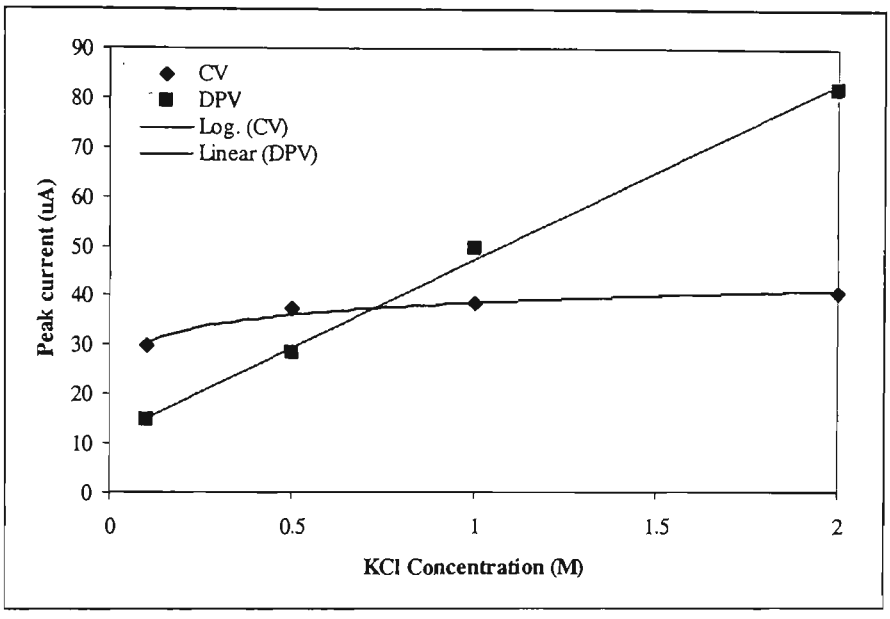

Figure 6.32 Peak current response profiles obtained from CVs and DPVs of dialysed PMAS with varied concentrations of KCl. CV responses were fitted to a logarithmic curve (Log (CV)) while DPV responses were described well by a linear regression (Linear (DPV)).

6.3.8.1 *Listeria* Detection at Elevated KCl Concentrations

The changes in peak current of dialysed PMAS in 0.1 M KCl after the addition of 10^6/mL *Listeria* were similar to results obtained previously, with a decrease of 1.15 μA observed in the CV and a small change of 0.30 μA for DPV. After the KCl concentration was increased to 0.5 M, the changes in peak current responses due to the addition of *Listeria* were much greater (Table 6.9). For CV a decrease of 2.7 μA was observed, and for DPV an even larger change of - 4.50 μA was brought about. The changes in peak current of PMAS observed after *Listeria* addition at higher KCl concentrations did not continue to increase. Changes of 0.750 - 0.800 μA in CVs of PMAS were observed in the presence of 1 M and 2 M KCl. As the responses obtained in 0.5 M KCl were significantly higher, a repeat experiment was carried out at this concentration. The changes after *Listeria* addition were not as great but were still larger than those observed for PMAS in 1 M and 2 M KCl. The reasons for these results are not clear but relate to the peak current profile observed for CVs (Figure 6.32) which suggests not much improvement in signal is gained when KCl concentration increases beyond 0.5 M.

Table 6.9 Effect of KCl concentration on *Listeria* detection with dialysed PMAS. Peak currents given are in microamps.

KCl Conc. (M)	CV PMAS	CV PMAS/List.	DPV PMAS	DPV PMAS/List.
0.1	29.700	28.550	14.050	13.750
0.5	37.300	34.600	28.300	23.800
0.5	36.050	34.500	25.35	24.15
1.0	37.050	36.300	30.300	29.200
2.0	38.650	37.850	40.250	38.000

6.4 CONCLUSIONS

GPC analysis of PMAS showed that the molecular weight distribution varies from batch to batch of polymer, and in particular that the amount of monomer changes quite significantly. The amount of MAS monomer present was correlated with stability of the oxidation peak current at approximately 0.80 V in CVs of PMAS. A comparison of two batches of PMAS showed that a less stable response from scan to scan is observed at this potential when the MAS component is higher.

Five different molecular weight fractions ranging from 2000 - 25000 amu were collected from PMAS using GPC. UV-vis of the fractions at pH 9 showed differences due to molecular weight in terms of relative band absorbance magnitudes but on the whole the spectra observed were comparable to those previously reported for sulfonated polyanilines. When acidified to pH 2.6 the fractions gave similar spectra to PMAS with a characteristic polaron peak at approximately 480 nm. This peak was present at both pH 2.6 and 9 suggesting that these materials are not fully dedoped at high pHs and that

differences observed under basic conditions may relate to differences in the extent of de-doping. Comparison of spectra from the fractions and PMAS at pH 2.6 revealed that the higher weight materials were most similar to the parent polymer.

CV and DPV characterisation of the fractions confirmed that molecular weight effects the electrochemical properties of these materials with different responses observed for each. Again the higher molecular weight fractions gave the most pronounced responses and bore most similarity to PMAS responses.

Studies of the monomer confirmed that the oxidation response observed at 0.80 V for PMAS in CVs is due to the presence of residual MAS. Standard addition of MAS to as received PMAS caused linear increases in the peak current at this potential. Further to this, dialysed PMAS showed little or no oxidation response at 0.80 V. The peak current stability from scan to scan of the dialysed polymer improved confirming that the presence of MAS in as received PMAS effects the electrochemical responses. After dialysis the oxidation response at 0.80 V reappeared over time suggesting that monomeric units may be cleaved from the polymer in solution due to oxidative degradation. It was found that this process in dialysed PMAS is not caused by exposure to light.

Detection of *Listeria* was attempted using the MAS monomer alone but responses were insignificant, inferring that the interaction involves the polymer, or some combination of the two. Dialysed PMAS was employed for *Listeria* detection and changes were observed in the presence of *Listeria*, however, these were small when compared to those observed for as received PMAS. While the removal of monomer by dialysis improved stability, it seems that both the monomer and polymer play a role in the detection mechanism of *Listeria* and hence this step may introduce additional problems. The PMAS fractions were also used to detect *Listeria* but after GPC separation the

electrochemical responses of these materials had decayed rapidly over time. Only fraction 2 (high Mw) gave reasonable changes when both DPV and CV were employed while fraction 4 (low Mw) gave a small change upon addition of *Listeria* that was only observed in the CV. For effective detection of *Listeria* using PMAS fractions the materials should be stored as solids prior to use to avoid any loss of response of time.

The effect of supporting electrolyte concentration on the electrochemical responses of dialysed PMAS was significant which much larger oxidation peak currents at 0.60 V observed at higher concentrations of KCl. As changes in peak current of dialysed PMAS after addition of *Listeria* were slight, the use of higher KCl concentrations was investigated as a means to improve detection. Larger responses to *Listeria* were noted at higher KCl concentrations suggesting that dialysed PMAS could be used for microorganism detection under appropriate conditions.

Chapter 7

Conclusions And Future Work

7.1 General Conclusions

As was pointed out in Chapter 1, CPs are extremely versatile materials for chemical sensing due to their inherent conductivity, the ease of preparation and control over final properties through the chosen fabrication method, the possibility of incorporating biomolecules and the fact that they are ion exchangers. As a consequence CP sensors have been employed for a range of environmental monitoring tasks. The main focus of this thesis is on the development of novel CP gas sensors, based on inexpensive polymer substrates with screen-printed carbon electrodes, for monitoring organic vapours. Solution based electrochemistry of CPs was also considered for post-polymerisation modification of these gas sensors, and for the study of a water soluble CP used as an electron mediator/sensor for *Listeria Monocytogenes*.

7.2 Chapter 2

A comprehensive study of CP gas sensors, based on polymer substrates with screen-printed electrodes, was reported in Chapter 2. The CP sensors developed in this work were based on pristine ICP (inherently conducting polymer) films, rather than on insulating polymer matrices rendered conductive by the addition of conductive particles such as carbon or the presence of an ICP. This approach has the advantages of direct electrodeposition, which gives greater control over film thickness during sensor preparation, and the possibility of post-fabrication electrochemical modification of the devices as a means to vary specificity as required. Considerable effort was spent optimising the deposition process in order to achieve sufficient sensitivity and discrimination power. Both direct electrodeposition and electrodeposition in concert with a chemical vapour deposited PPy/Cl layer were employed to prepare these sensors. It was found that the direct electrodeposition process involved lengthy growth times,

leading to the formation of very thick sensing layers. The effect of the underlying substrate was examined in an attempt to reduce deposition times, and although improvements were noted, these were not sufficient. The use of a thin vapour deposited PPy/Cl layer to aid electrodeposition allowed for the use of much shorter electrodeposition times. Based on CV characterisation of these films, it is suggested that the top electrodeposited layer dominates the sensing properties of such devices. The performance of these sensors was compared to that of the same PPy films electrodeposited onto silicon substrates with lithographically defined gold electrodes. The limits of detection were similar for the two sensor configurations, however, the silicon based devices gave more reliable responses at low concentrations. This is attributed to variation in the resistance of the underlying PPy/Cl vapour deposited layer used with the polymer substrate sensors, which was difficult to control exactly. The performance of arrays of both sensor types were also compared for the discrimination of organic vapours (methanol, ethanol, propanol, and acetone) in nitrogen. The sensors based on screen-printed polymer substrates performed equally as well as the silicon based devices when differentiating between the test vapours. Although there are some obvious problems with reproducibility, the sensors developed could prove to be an attractive alternative to far more expensive methods of gas sensor fabrication such as lithography.

Before this can occur, the issue of sensor reproducibility must be addressed, both in terms of response patterns relative to the silicon array, and between sets of screen-printed sensors. This may be achieved by further optimisation of the PPy/Cl vapour deposition process, perhaps by modifying the solvent used, and ensuring that a controlled volume of oxidant is placed on the sensor surface each time. Alternately, a different surface modification to improve CP adhesion may overcome the problem, or

indeed the use of a different polymer substrate could completely eliminate the need for the PPy/Cl layer. One potential substrate that could prove useful in addition to those investigated in this work is polyurethane, which is already used in the preparation of conducting polymer colloids. Another approach to improve upon these sensors is reduction of the inter-track spacing between the screen-printed electrodes. Narrower inter-track spacing would significantly reduce electrodeposition times, and hence should mean that the PPy/Cl layer is not required. However, this approach will be limited by the resolution associated with screen-printing, which is of the order of 100 – 200 μm. Another possibility is to increase the conductivity of the electrode tracks. In this work carbon based ink was used, which gives rise to fairly resistive layers. This may in fact hinder, to some extent, the deposition process. By printing with a more conductive ink, for example platinum/carbon, or by printing a highly conductive silver track with a carbon contact layer on top, the deposition process may be more efficient.

7.3 Chapter 3

An alternative approach to electrodeposition of the required PPy film over a vapour deposited PPy/Cl layer was considered in Chapter 3. In this section of work, the ion exchange properties of CPs were exploited in attempts to exchange the chloride anion of PPy/Cl for a different dopant. It was hoped that by using this process the sensing properties of the PPy films would be altered. Various chemical and electrochemical solution based treatments were applied to PPy/Cl sensors, but as these films are reasonably thin, significant increases in resistance were observed. It was found that using a higher concentration of electrolyte (1 M), and shorter treatment times overcame this problem. The response patterns of modified sensor arrays were not significantly affected by the solution treatments, however, sensitivity increased notably which may be

a result of reordering within the films after treatment. XPS analysis of treated sensors suggest that some anion exchange occurred, however, as the response to organic vapours was not altered significantly, it would appear that the sensing properties of these films are determined at polymerisation time. Even though some exchange may be possible, this process is not likely to effect film morphology, and hence sensor selectivity is largely unaffected. Any changes to sensing properties therefore are most likely due to interactions between the newly incorporated anion, rather than with the polymer itself.

There are a number of different ideas well worth investigating to further improve the performance and selectivity of these sensors. By simply varying the oxidant used for vapour deposition, different anions can be incorporated during polymerisation. For example, ferric nitrate could be used in place of ferric chloride to produce PPy/NO_3 sensors. This approach may also lead to better anion exchange during post-polymerisation solution modification, as if slightly larger anions are incorporated during PPy formation more it will be slightly easier for anions to be incorporated from solution. An alternative approach would be to use a mixed oxidant solution for polymerisation, containing both the chemical oxidising species and a second anion to be incorporated during polymerisation. For example, a methanol solution containing ferric chloride and nitrate ions could be used. While this is likely to produce films with a mix of the two anions, the sensing properties may be suitably altered when compared to the case where only a single anion is incorporated during polymerisation.

It may also be of use to investigate a wider range of monomers, in particular substitution of the same base monomer could be used as a simple means of imparting different selectivity. Another approach that could be examined is the use of mixed monomer solutions for vapour deposition. This approach may produce films with mixed sensing

properties also, but as a result of the monomers present rather than the incorporated anions.

7.4 Chapter 4

The presence of water vapour is a significant problem when using CP gas sensors for the detection of volatile species, and often causes the response of interest to be lost. Chapter 4 reports on the results of two different approaches used to overcome this problem; casting of hydrophobic silicone membranes over the PPy film, and the use of polymer diffusive sampling tubes to deliver moisture free sample to the PPy sensors. The intention of this work was to enable the detection of volatile organic species present in water.

Cast silicone membranes were effective in significantly reducing PPy sensor responses to water vapour, but the effects varied from one polymer to the next. This may in part relate to morphological differences and the affinity of a particular polymer for silicone. The detection of methanol vapours from an aqueous solution of methanol in water was not possible using this approach, but it is possible that other more volatile species may be successfully detected in this manner. Other polymers that adhere more strongly to the CP layer may be more suitable for casting over PPy. Again, as was mentioned above in section 7.2, polyurethane may be a suitable material for this purpose due to the favourable adhesive properties of this polymer.

The other approach employed for the reduction of PPy humidity responses was polymer diffusion tubes for sampling organics. A range of different materials were evaluated but only PVC and silicone tubing blocked water but still allowed transport of organic volatiles. The tubes were placed in the headspace of solutions containing various organic species, and the internal contents of the tube monitored by an array of PPy sensors periodically. Discrimination between water samples containing methanol,

ethanol, propanol, acetone, relative to a water blank was successfully achieved. It was found that silicone tubing gave better separation between these solvents than PVC, but both tube types were effective in blocking water. This approach offers a potential means of differentiating between a wide range of volatile organic species dissolved in water.

Further evaluation of such as system should be carried out using a wider range of polymer tube materials. Also, the tests carried out in this work were limited to only a few organic species, most of which were not extremely volatile. Further investigations may reveal that the use of diffusive sampling tubes with CP gas sensors are of particular use for more volatile pollutants such as BTEX vapours.

Novel PPy/Cl coated PUR polymer tubes were also tested as potential gas sensing elements. Methanol vapours (50%) in nitrogen were successfully detected with these devices, the sensitivity of which was shown to increase in relation to surface area. Attempts to encapsulate these sensors in a silicone diffusion tube for detecting organics in water were hindered by a lack of base resistance stability in air.

Future work in this area could be carried out developing polymer tube sensors that are coated on the interior surface, rather than on the outer tube walls as was the case here. This may help to reduce the effect of resistance instability, and also provides a novel approach to sensing whereby the sample, either in the gas or solution phase, is passed through a sealed unit in direct contact with the sensing film. This approach also has the advantage of maximising the surface to volume ratio, and results already obtained suggest that this will lead to increased sensitivity.

7.5 Chapter 5

PPy/Cl vapour deposited gas sensors were used on a small autonomous mobile robot for

successful tracking of an ammonia odour plume source. Sensors that had been modified by solution treatment, as discussed above in section 7.3, were less sensitive to ammonia than the pristine PPy/Cl sensors. The effect of wind velocity was examined, and it was found that the best responses were observed at low flow rates. At a fixed distance from the ammonia source, the PPy/Cl sensor response was reasonably linear over a range of ammonia source concentrations.

Robot tracking experiments established that a minimum source concentration of 3.5% ammonia could be successfully located when the RAT commenced 1 m from the source and the wind velocity was low. When a 1.75% ammonia source was used under the same conditions the robot was not able to detect the odour plume.

While this approach to the detection of vapour plumes and location of odour sources is only in the fundamental stages of development, in the future it could prove a very useful tool for many environmental and hazardous gas leak monitoring tasks. The conducting polymer gas sensors used in this work are simple to prepare, lightweight and have low power requirements making them ideal for use on battery driven tracking robots.

The next stage of development for a system of this nature is odour or gas identification. Using arrays of CP gas sensors and some form of discriminate analysis, it should be possible for a small search robot to differentiate between hazardous and acceptable substances in a search area.

7.6 Chapter 6

Electrochemical and spectral studies of the water soluble CP PMAS revealed that there is significant variation between batches of the same material. This was shown to be related to the amount of unreacted MAS monomer in the polymer material, which varies from one production run to the next. As the presence of this species was a cause of

irreproducibility in terms of electrochemical response, dialysis was used to remove any residual monomer from the PMAS before subsequent characterisation.

As the PMAS system has been developed by IPRI as a *Listeria* detection tool, it was of interest to investigate the effect of removing the MAS on microorganism detection. It was found that in the absence of MAS, the signals observed in the presence of *Listeria* were much smaller, indicating that both the PMAS and monomer play a role in the detection mechanism. It is proposed that the MAS acts as an electron mediator shuttling electrons from the microorganism to an electrode where a detectable signal is measured. The problem with this system is that during electrochemical analysis of *Listeria*, the monomer is oxidised to form more PMAS, which interferes with the detection signal.

It may be possible to overcome these problems by first dialysing the PMAS to remove and residual monomer, and then adding in a more conventional mediator, such as ferricyanide, that will transfer electrons without being consumed at the electrode surface. This approach would have the advantage of reducing electrochemical instability caused by MAS, but would potentially still allow for the detection of *Listeria*.

The PMAS was also separated into a range of molecular weight fractions ranging from 2000 - 25000 amu using GPC. UV-vis of the fractions at both pH 9 and pH 2.6 were similar to the parent PMAS. However, at both pHs the fractions showed a peak at approximately 480 nm due to the presence of polarons. The fact that this peak was present at both pH 2.6 and 9 suggests that these materials do not fully dedoped at high pHs. The higher weight fractions were most similar to PMAS.

Electrochemical characterisation of the fractions confirmed that molecular weight affects the electrochemical properties of these materials with different responses observed for each. Again the higher molecular weight fractions gave the most pronounced responses and bore most similarity to PMAS responses. Attempts to use

the fractions for *Listeria* detection were not successful, as over only a short period of time the electrochemical properties of these materials decayed significantly. There may be ways to overcome this, and due to the promise already shown by the PMAS system for microorganism detection, further study of the effect of molecular weight on detection should be carried out.

References

[1] Shirakawa, H., Louis, E.J., MacDiarmid, A.G., Chiang, C.K., and Heeger, A.J., *J.Chem. Soc. Chem. Commun.*, (1977) 578.

[2] Lonergan, M.C., Severin, E.J., Doleman, B.J., Beaber, S.A., Grubb, R.H., and Lewis, N.S., *Chem. Mater.*, 8 (1996) 2298.

[3] Doleman, B.J., Sanner, E.J., Severin, R.H., Vaid, T.P., and Lewis, N.S, *Anal. Chem.*, 70 (1998) 4177.

[4] Severin, E.J., Doleman, B.J., and Lewis, N.S., *Anal. Chem.*, 72 (2000) 658.

[5] Freund, M.S., and Lewis, N.S., *Proc. Natl. Acad. Sci. U.S.A.*, 92 (1995) 2652.

[6] Honeybourne, C.L., *Journal of Chemical Education*, 77 (2000) 338.

[7] Pfluger, P., Weiser, G., Scott, J. C., and Street, C.B., *Handbook of Conducting Polymers*, Skotheim, T.A. Ed., Vol. 2, pp 1369 - 1381, Marcel Dekker, New York, 1986.

[8] Heinze, J. *Synthetic Metals*, 41-43 (1991) 2805.

[9] Reynolds, J.R., *Chemtech*, July (1988) 440.

[10] Albert, K.J., Lewis, N.S., Schauer, C.L., Sortzing, G.A., Stitzel, S.E., Vaid, T.P., and Walt, D.R., *Chemical Reviews*, 100 (2000) 2595.

[11] Trojanowicz, M., Krawczynski vel Krawczyk, T., and Alexander, P.W., *Chem. Anal. (Warsaw)*, 42 (1997) 199.

[12] Zotti, G., *Handbook of Organic Conductive Molecules and Polymers*, Nalwa, H.S. Ed., Vol 2., pp 137 - 170, John Wiley & Sons, Chichester, 1997.

[13] Imisides, M.D., John, R., Riley, P.J., and Wallace, G.G., *Electroanalysis*, 3 (1991) 879.

[14] Kaufman, J.H., Melroy, O.R., Abraham, F.F., Nazzal, A.I., and Kapituluik, *Synthetic Metals*, 18 (1987) 89.

[15] Teasdale, P.R., and Wallace, G.G., *Chimicaoggi*, October (1992) 19.

[16] Suu, B., Jones, J.J., Burford, R.P., and Skyllas-Kazacos, M., *J. Electrochem. Soc.*, 136 (1989) 698.

[17] Lin, Y., and Wallace, G.G., *Electrochimica Acta*, 39 (1994) 1409.

[18] John, R., Talaie, A., Wallace, G.G., *J. Electroanal. Chem.*, 319 (1991) 365.

[19] John, R., and Wallace, G.G., *J. Electroanal. Chem.*, 354 (1993) 145.

[20] Michalska, A.J., and Hall, E.A.H., *Electroanalysis*, 11 (1999) 756.

[21] Talaie, A., and Wallace, G.G., *Synthetic Metals*, 63 (1994) 83.

[22] Adeloju, S.B., Barisci, J.N., and Wallace, G.G., *Anal. Chim. Acta*, 332 (1996) 145.

[23] Umana, M., and Waller, J., *Anal. Chem.*, 58 (1986) 2979.

[24] Adeloju, S.B., Shaw, S.J., and Wallace, G.G., *Electroanalysis*, 6 (1994) 865.

[25] Sangodkar, H., Sukeerthi, S., Srinivasa, R.S., Lal, R., and Contractor, A.Q., *Anal. Chem.*, 68 (1996) 779.

[26] Barnett, D., Sadik, O.A., John, M.J., and Wallace, G.G., *Analyst*, 119 (1994) 1997.

[27] Sadik, O.A., and Wallace, G.G., *Anal. Chim. Acta*, 279 (1993) 209.

[28] Hodgson, A.J., John, M.J., Campbell, T., Georgevich, A., Woodhouse, S., and Wallace, G.G., *Proc. SPIE Smart Mater. Technol. Biomimetics,* 2716 (1996) 164.

[29] Reiter, R., Habermuller, K., and Schuhmann, W., *Sensors and Actuators B*, 79 (2001) 150.

[30] Cooper, T.C, Hammerle, M., Schuhmann, W., and Schmidt, H.-L., *Biosensors and Bioelectronics*, 8 (1993) 65.

[31] Dobay., R., Harsanyi, G., and Visy, G., *Analytica Chimica Acta*, 385 (1999) 187.
[32] Wang, J., Jiang, M., Fortes, A., and Mukherjee, B., *Analytica Chimica Acta*, 402 (1999) 7.
[33] Hendrickson, S.M., Krejcik, M., and Elliot, C.M., *Analytical Chemistry*, 69 (1997) 718.
[34] Barnett, D., Laing, D.G., Skopec, S., Sadik, O., and Wallace, G.G., Analytical Letters, 27 (1994) 2417.
[35] Besombes, J-L., Cosnier, S., Labbe, P., Reverdy, G., *Anal. Chim. Acta*, 311 (1995) 1157.
[36] Liu, A., and Wang, E., *Analytica Chimica Acta*, 282 (1993) 497.
[37] Lvovich, V., and Scheeline, A., *Anal. Chem.*, 69 (1997) 454.
[38] Nguyen, T.A., Kokot, S., Ongarato, D.M., and Wallace, G.G., *Electroanalysis*, 11 (1999) 1327.
[39] Vinokurov, I.A., *Sensors and Actuators B*, 10 (1992) 31.
[40] Lindino, C.A., and Bulhoes, L.O.S., *Analytica Chimica Acta*, 334 (1996) 317.
[41] Pei, Q., and Qian, R., *Electrochim. Acta*, 37 (1992) 1075.
[42] Jovanovic, V.M., Dekanski, A., Vlajnic, G., and Jovanvic, M.S., *Electroanalysis*, 9 (1997) 564.
[43] Wang, Z., Zhang, H.S., Mark, H.B., and Rubinson, J.F., *Analytical Letters*, 30 (1997) 1.
[44] Galal, A., Wang, Z., Karogozler, H., Mark, H.B., and Bishop, P.L., *Analytica Chimica Acta*, 299 (1994) 145.
[45] Alizadeh, N., and Mahmodian, M., *Electroanalysis*, 12 (2000) 509.
[46] Alizadeh, N., and Khodaei-Tazekendi, H., *Sensors and Actuators B*, 75 (2001) 5.
[47] Karyakin, A.A., Bobrova, O.A., Lukachova, L.V., and Karyakina, E.E., *Sensors and Actuators B*, 33 (1996) 34.
[48] Shim, Y.B., Stilwell, D.E., and Park, S.M., *Electroanalysis*, 3 (1991) 31.
[49] Hutchins, R., and Bachas, L.G., *Analytical Chemistry*, 67 (1995) 1654.
[50] Atta, N.F., Galal, A., Mark Jr., H.B., Yu, T., and Bishop, P.L., *Talanta*, 47 (1998) 987.
[51] Lindfors, T., Sjoberg, P., Bobacka, J., Lewenstam, A., and Ivaska, A., *Analytica Chimica Acta*, 385 (1999) 163.
[52] Gyurcsanyi, R.E., Nyback, A.-S., Toth, K., Nagy, G., Ivaska, A., *Analyst*, 123 (1998) 1339.
[53] Bobacka, J., Lindfors, T., McCarrick, M., Ivaska, A., Lewenstam, A., *Analytical Chemistry*, 67 (1995) 3819.
[54] Cadogan, A., Gao, Z., Lewenstam, A., Ivaska, A., and Diamond, D., *Analytical Chemistry*, 64 (1992) 2496.
[55] Lindfors, T., and Ivaska, A., *Analytica Chimica Acta*, 437 (2001) 171.
[56] Bobacka, J., Ivaska, A., and Lewenstam, A., *Analytica Chimica Acta*, 385 (1999) 195.
[57] Lindfors, T., and Ivaska, A., *Analytica Chimica Acta*, 404 (2000) 111.
[58] Sjoberg, P., Bobacka, J., Lewenstam, A., Ivaska, A., *Electroanalysis*, 11 (1999) 821.
[59] Wallace, G.G., and Lin, Y.P., *Journal of Electroanalytical Chemistry*, 247 (1988) 144.
[60] Song, F., and Shiu, K., *Journal of Electroanalytical Chemistry*, 498 (2001) 161.

[61] Nguyen, T.A., Kokot, S., Ongarato, D.M., and Wallace, G.G., *Electroanalysis*, 12 (2000) 89.
[62] Nicolas, M., and Fabre, B., and Simonet, J., *Journal of Electroanalytical Chemistry*, 509 (2001) 73.
[63] Nicolas, M., and Fabre, B., and Simonet, J., *Chem. Commun.*, (1999) 1881.
[64] Tsai, Y.C., Davis, J., Compton, R.G., Ito, S., and Ono, N., *Electroanalysis*, 13 (2001) 7.
[65] Dam, M.E.R, Thomsen, K.N., Pickup, P.G., and Schroder, K.H., *Electroanalysis*, 7 (1995) 70.
[66] Ram, M.K, Bertoncello, P., and Nicolini, C., *Electroanalysis*, 13 (2001) 574.
[67] Koul, S., Chandra, R., and Dhawan, S.K., *Sensors and Actuators B*, 75 (2001) 151.
[68] Hailin, G., and Yucheng, L., *Sensors and Actuators B*, 21 (1994) 57.
[69] Talie, A., *Polymer*, 38 (1997) 1145.
[70] Talaie, A., Lee, J-Y, Adachi, K., Taguchi, T., and Romagnoli, J., *Journal of Electroanalytical Chemistry*, 468 (1999) 19.
[71] Palmqvist, E., Berggren Kriz, C., Khayyami, M., Danielsson, B., Larsson, P-O., Mosbach, K., and Kriz, D., *Biosensors and Bioelectronics*, 9 (1994) 551.
[72] Koncki, R., and Wolfbeis, O.S., *Analytical Chemistry*, 70 (1998) 2544.
[73] de Marcos, S., and Wolfbeis, O.S., *Analytica Chimica Acta*, 334 (1996) 149.
[74] Pringsheim, E., Terpetschnig, E., and Wolfbeis, O.S., *Analytica Chimica Acta*, 357 (1997) 247.
[75] Sotomayor, P.T., Raimundo, I.M., Zarbin, A.J.G., Rohwedder, J.J.R., Oliveira Neto, G., and Alves, O.L., *Sensors and Actuators B*, 74 (2001) 157.
[76] Grummt, U-W., Pron, A., Zagorska, M., and Lefrant, S., *Analytica Chimica Acta*, 357 (1997) 253.
[77] Wu, J., and Pawliszyn, J., *Analytical Chemistry*, 73 (2001) 55.
[78] Wu, J., Mester, Z., and Pawliszyn, J., *Analytica Chimica Acta*, 424 (2000) 211.
[79] Wu, J.,Yu, X., Lord, H., and Pawliszyn, J., *Analyst*, 125 (2000) 391.
[80] Rodriguez, F.J., Gutierrez, S., Ibanez, J.G., Bravo, J.L., and Batina, N., *Environ. Sci. Technol.*, 34 (2000) 2018.
[81] Lokhande, T.N., Anuse, M.A., and Chavan, M.B., *Talanta*, 47 (1998) 823.
[82] Desimoni, E., and Bassani, I., *Anal. Commun.*, 36 (1999) 45.
[83] McCullough, R.D, and Ewbank, P.C., *Synthetic Metals*, 84 (1997) 311.
[84] Pan, J.J, and Charych, D., *Langmuir*, 13 (1997) 1365.
[85] Sergeyeva, T.A., Lavrik, N.V., Piletsky, S.A., Rachkov, A.E., El'skaya, A.V., *Sensors and Actuators B*, 34 (1996) 283.
[86] Slater, J.M., and Watt, E.J., *Analyst*, 116 (1991) 1125.
[87] Ratcliffe, N.M., *Analytica Chimica Acta*, 239 (1990) 257.
[88] Li, D., Jiang, Y., Wu, Z., Chen, X., Li, Y., *Sensors and Actuators B*, 66 (2000) 125.
[89] Agbor, N.E., Petty, M.C., and Monkman, A.P., *Sensors and Actuators B*, 28 (1995) 173.
[90] Selampinar, F., Toppare, L., Akbulut, U., Yalcin, T., and Suzer, S., *Synthetic Metals*, 68 (1995) 109.
[91] Krivan, E., Visy, C., Dobay, R., Harsanyi, G., and Berkesi, O., *Electroanalysis*, 12 (2000) 1195.
[92] Kukla, A.L., Shirshov, Y.M., and Piletsky, S.A., *Sensors and Actuators B*, 37 (1996) 135.

[93] Tan, C.K., and Blackwood, D.J., *Sensors and Actuators B*, 71 (2000) 184.
[94] Hanawa, T., and Yoneyama, H., *Synthetic Metals*, 30 (1989) 341.
[95] Slater, J.M., Watt, E.J., Freeman, N.J., May, I.P., and Weir, D.J., *Analyst*, 117 (1992) 1265.
[96] Slater, J.M., Paynter, J., and Watt, E.J., *Analyst*, 118 (1993) 379.
[97] de Lacy Costello, B.P.J., Evans, P., Guernion, N., Ratcliffe, N.M., Sivanand, P.S., and Teare, G.C., *Synthetic Metals*, 114 (2000) 181.
[98] Josowicz, M., Janata, J., Ashley, K., and Pons, S., *Anal.Chem.*, 59 (1987) 253.
[99] Collins, G.E., and Buckley, L.J., *Synthetic Metals*, 78 (1996) 93.
[100] Topart, P. and Josowicz, M., *Journal of Physical Chemistry*, 96 (1992) 7824.
[101] MacDiarmid, A.G., *Synthetic Metals*, 84 (1997) 27.
[102] Kunugi, Y., Nigorikawa, K., Harima, Y., and Yamashita, K., *J. Chem. Soc., Chem. Commun.*, (1994) 873.
[103] Blackwood, D., and Josowicz, M., *J. Phys. Chem.*, 95 (1991) 493.
[104] Feng, J., and MacDiarmid, A.G., *Synthetic Metals*, 102 (1999) 1304.
[105] Lin, C.W., Liu, S.S., and Hwang, B.J., *Journal of Applied Polymer Science*, 82 (2001) 954.
[106] Misra, S.C.K., Suri, A., Chandra, S., and Bhattacharya, R., *Indian Journal of Pure & Applied Physics*, 38 (2000) 545.
[107] Hosseini, S.H., Entezami, A.A., *Iranian Polymer Journal*, 8 (1999) 205.
[108] Li, J., Petelenz, D., and Janata, J., *Electroanalysis*, 5 (1993) 791.
[109] de Souza, J.E.G., dos Santos, F.L., Barros-NetoB., dos Santos, C.G., and de Melo, C.P. *Synthetic Metals*, 119 (2001) 383.
[110] Sata, T., *Sensors and Actuators B*, 23 (1995) 63.
[111] Ogura, K., Shiigi, H., Nakayama, M., *J. Electrochem. Soc.*, 143 (1996) 2925.
[112] Wu, S., Zeng, F., Li, F., and Zhu, Y., *European Polymer Journal*, 36 (2000) 679.
[113] Hirata, M., and Sun, L., *Sensors and Actuators A*, 40 (1994) 159.
[114] Przyluski, J., and Budrowski, C., *Synthetic Metals*, 41 (1991) 1163.
[115] Chabukswar, V.V., Pethkar, S., and Athawale, A.A., *Sensors and Actuators B*, 77 (2001) 657.
[116] Nylander, C., Armgarth, M., and Lundstrom, I., *Anal. Chem. Symp. Ser.*, 17 (1983) 203.
[117] Miasik, J., Hooper, A., and Tofield, B., *J. Chem. Soc. Faraday Trans.* I, 82 (1986) 1117.
[118] Gustafsson, G., and Lundstrom, I., *Synth. Met.*, 21 (1987) 203.
[119] Brie, M., Turcu, R., Neamtu, C., and Pruneanu, S., *Sensors and Actuators B*, 37 (1996) 119.
[120] Penza, M., Milella, E., Alba, M.B., Quirini, A., and Vasanelli, L., *Sensors and Actuators B*, 40 (1997) 205.
[121] Assadi, A., Spetz, A., Willander, M., Svensson, C., Lundstrom, I., and Inganas, O., *Sensors and Actuators B*, 20 (1994) 71.
[122] Domansky, K., Baldwin, D.L., Grate, J.W., Hall, T.B., Li, J., Josowicz, M., and Janata, J., *Anal. Chem.*, 70 (1998) 473.
[123] Dogan, S., Akbulut, U., Yalcin, T., Suzer, S., and Toppare, L., *Synthetic Metals*, 60 (1993) 27.
[124] de Lacy Costello, B.P.J., Evans, P., and Ratcliffe, N.M., *Analyst*, 121 (1996) 793.
[125] Gangopadhyay, R., and De, A., *Sensors and Actuators B*, 77 (2001) 326.

[126] Barker, P.S., Di Bartolomeo, C., Monkman, A.P., Petty, M.C., and Pride, R., *Sensors and Actuators B*, 24-25 (1995) 451.
[127] Barker, P.S., Monkman, A.P., Petty, M.C., and Pride, R., *IEE Proceedings: Circuits, Devices & Systems*, 144 (1997) 111.
[128] Prissanaroon, W., Ruangchuay, L., Sirivat, A., and Schwank, J., *Synthetic Metals*, 114 (2000) 65.
[129] Takeda, S., *Thin Solid Films*, 344 (1999) 313.
[130] Liu, D.M., Aguilar-Hernandez, J., Potje-Kamloth, K., and Liess, H.D., *Sensors and Actuators B*, 41 (1997) 203.
[131] Nguyen Van, C., and Potje-Kamloth, K., *Thin Solid Films*, 338 (1999) 142.
[132] Nguyen Van, C., and Potje-Kamloth, K., *Thin Solid Films*, 392 (2001) 113.
[133] Torsi, L., Pezzuto, M., Siciliano, P., Rella, R., Sabbatini, L., Valli, L., and Zambonin, P.G., *Sensors and Actuators B*, 48 (1998) 362.
[134] Krutovertsev, S.A., Sorokin, S.I., Zorin, A.V., Letuchy, Y.A., and Antonova, O.Y., *Sensors and Actuators B*, 7 (1992) 492.
[135] Unde, S., Ganu, J., Radhakrishnan, S., *Advanced Materials for Optics and Electronics*, 6 (1996) 151.
[136] Lin, C.W., Hwang, B.J., Lee, C.R., *Journal of Applied Polymer Science*, 73 (1999) 2079.
[137] de Souza, J.E.G., Neto, B.B., dos Santos, F.L., de Melo, C.P., Santos, M.S., and Ludermir, T.B., *Synthetic Metals*, 102 (1999) 1296.
[138] Gardener, J.W., Vidic, M., Ingleby, P., Pike, A.C., Brignell, J.E., Scivier, P., Bartlett, P.N., Duke, A.J., and Elliot, J.M., *Sensors and Actuators B*, 48 (1998) 289.
[139] Meijerink, M.G.H., Strike, D.J., de Rooij, N.F., and Koudelka-Hep, M., *Sensors and Actuators*, 68 (2000) 331.
[140] Meijerink, M.G.H., Koudelka-Hep, M., de Rooij, N.F., Strike, D.J., Hendrikse, J., Olthuis, W., and Bergveld, P., *Electrochemical and Solid State Letters*, 2 (1999) 138.
[141] van de Leur, R.H.M., and van der Waal, A., *Synthetic Metals*, 102 (1999) 1330.
[142] Cabala, R., Meister, V., and Potje-Kamloth, K., *J. Chem. Soc., Faraday Trans.*, 93 (1997) 131.
[143] Slater, J.M., and Watt, E.J., *Analyst*, 116 (1991) 1125.
[144] Syritski, V., Reut, J., Opik, A., and Idla, K., *Synthetic Metals*, 102 (1999) 1326.
[145] Henkel, K., Oprea, A., Paloumpa, I., Appel, G., Schmeiber, D., and Kamieth, P., *Sensors and Actuators B*, 76 (2001) 124.
[146] Cui et al, *Sensors and Actuators B*, 66 (2000) 94.
[147] Hwang, B.J., Yang, Y.J., and Lin, C.W., *Sensors and Actuators B*, 75 (2001) 67.
[148] Milella, E., and Penza, M., *Thin Solid Films*, 327 – 329 (1998) 694.
[149] Milella, E., Musio, F., and Alba, M.B., *Thin Solid Films*, 284-285 (1996) 908.
[150] Jin, Z., Su, Y., and Duan, Y, *Sensors and Actuators B*, 72 (2001) 75.
[151] Nicho, M.E., Trejo, M., Garcia-Valenzuela, A., Saniger, J.M., Palacios, J., and Hu, H., *Sensors and Actuators B*, 76 (2001) 18.
[152] Agbor, N.E., Cresswell, J.P., Petty, M.C., and Monkman, A.P., *Sensors and Actuators B*, 41 (1997) 137.
[153] Stella, R., Barisci, J.N., Serra, G., Wallace, G.G., and De Rossi, D., *Sensors and Actuators B*, 63 (2001) 1.

[154] Guadarrama, A., Rodriguez-Mendez, M.L., de Saja, J.A., Rios, J.L., and Olias, J.M., *Sensors and Actuators B*, 69 (2000) 276.
[155] Baldacci, S., Matsuno, T., Toko, K., Stella, R., and De Rossi, D., *Sensors and Materials*, 10 (1998) 185.
[156] Coghlan, A., *New Scientist*, (1993) 18.
[157] Annor-Frempong, I.E., Nute, G.R., Wood, J.D., Whittington, F.W., and West, A., *Meat Science*, 50 (1998) 139.
[158] Oshita, S., Shima, K., Haruta, T., Seo, Y., Kawagoe, Y., Nakayama, S., and Takahara, H., *Computers and Electronics in Agriculture*, 26 (2000) 209.
[159] Ridgway, C., Chambers, J., Portero-Larragueta, E., and Prosser, O., *Journal of the Science of Food and Agriculture*, 79 (1999) 2067.
[160] Persaud, K.C., Pisanelli, A.M., Szyszko, S., Reichl, M., Horner, G., Rakow, W., Keding, H.J., and Wessels, H., *Sensors and Actuators B*, 55 (1999) 118.
[161] Stuetz, R.M., Fenner, R.A., and Engin, G., *Wat. Res.*, 33 (1999), 442.
[162] Stuetz, R.M., White, M., and Fenner, R.A., *Journal of Water Services Research and Technology-Aqua*, 47 (1998) 223.
[163] Stuetz, R.M., Fenner, R.A., and Engin, G., *Wat. Res.*, 33 (1999), 453.
[164] Di Francesco, F., Lazzerini, B., Marcelloni, F., and Pioggia, G., *Atmospheric Environment*, 35 (2001) 1225.
[165] Hodgins, D., *Sensors and Actuators B*, 26-27 (1995) 255.
[166] Byun, H.G., Persaud, K.C., Khaffaf, S.M., and Hobbs, P.J., Misselbrook, T.H., *Computers and Electronics in Agriculture*, 17 (1997) 233.
[167] Misselbrook, T.H., Hobbs, P.J., and Persaud, K.C., *J. Agr. Eng. Res.*, 66 (1997) 213.
[168] Masila, M., Sargent, A., and Sadik, O.A., *Electroanalysis*, 10 (1998) 312.
[169] Hudon, G., Guy, C., and Hermia, J., *Journal of the Air & Waste Management Association*, 50 (2000) 1750.
[170] Sotzing, G.A., Briglin, S.M., Grubbs, R.H., and Lewis, N.S., *Analytical Chemistry*, 72 (2000) 3181.
[171] Sotzing, G.A., Phend, J.N., Grubbs, R.H., and Lewis, N.S., *Chemistry of Materials*, 12 (2000) 593.
[172] Ogura, K., and Shiigi, H., *Electrochemical and Solid-State Letters*, 2 (1999) 478.
[173] Conn, C., Sestak, S., Baker, A.T., and Unsworth, J., *Electroanalysis*, 10 (1998) 1137.
[174] Persaud, K., *Trends in Analytical Chemistry*, 11 (1992) 61.
[175] Namdev, P.K., Alroy, Y. and Singh, V., *Biotechnol. Prog.*, 14 (1998) 75.
[176] Stat, T., *Laboratory Medicine*, 29 (1998) 206.
[177] Gibson, T.D., Prosser, O., Hulbert, J.N., Marshall, R.W., Corcoran, P., Lowery, P., Ruck-Keene, E.A. and Heron, S., *Sensors and Actuators B*, 44 (1997) 413.
[178] Magan, N., Pavlou, A., and Chrysanthakis, I., *Sensors and Actuators B*, 72 (2001) 28. [179] Schaller, E., Bosset, J.O., and Escher, F., *Lebensm-Wiss. U.-Technol.*, 31 (1998) 305.
[180] Partridge A.C., Harris P. and Andrews M.K, *Analyst*, 121 (1996) 1349.
[181] Reddy, S.M. and Payne, P.A., *Sensors and Actuators B*, 58 (1999) 536.
[182] Hart, J.P, and Wring, S.A., *Trends in Analytical Chemistry*, 16 (1997) 89.
[183] Koopal, C.G.J., Bos, A.A.C.M. and Nolte, R.J.M., *Sensors and Actuators B*, 18-19 (1994) 166.

[184] Goldberg, H.D., Brown, R.B., Liu, D.P. and Meyerhoff, M.E., *Sensors and Actuators B*, 21 (1994) 171.
[185] Wang, J., Tian, B., Nascimento, V.B., and Angnes, L., *Electrochimica Acta*, 43 (1998) 3459.
[186] Bagel, O., Limoges, B., Schollhorn, B., and Degrand, C., *Analytical Chemistry*, 69 (1997) 4688.
[187] Walsh,S., Diamond, D., McLaughlin, J., McAdams, E., Woolfson, D., Jones, D., and Bonner, M., *Electroanalysis*, 9 (1997) 1318.
[188] Kawahara, A., Katsuki, H., and Egashira, M., *Sensors and Actuators B*, 49 (1998) 273.
[189] Solis, J.L., and Lantto, V. *Physica Scripta*, T69 (1997) 281.
[190] Hitch, T.J.A.R., and Honeybourne, C.L., *Journal of Materials Chemistry*, 6 (1996) 285.
[191] Menil, F., Lucat, C., and Debeda, H., *Sensors and Actuators B*, 25 (1995) 415.
[192] Ferrari, V., Marioli, D.,Taroni, A., and Ranucci, E., *Sensors and Actuators B*, 68 (2000) 81.
[193] Martinelli, G., Carotta, M.C., Ferroni, M., Sadaoka, Y., and Traversa, E., *Sensors and Actuators B*, 55(1999) 99.
[194] Napier, A and Hart, J.P., *Electroanalysis*, 8 (1996) 1006.
[195] Brignell, J.E., White, N.M., and Cranny, A.W.J., *IEE Proceedings*, 135 (1988) 77.
[196] Golovanov, V., Solis, J.L., Lantto, V., and Leppavuori, S., *Sensors and Actuators B*, 34, (1996) 401.
[197] Dobay, R., Harsanyi, G. and Visy, C., *Electroanalysis*, 11 (1999) 804.
[198] Alvarez-Icaza, M., and Bilitewski, U., *Analytical Chemistry*, 65 (1993) 525A.
[199] White, N.M. and Ko, V.T.K., *Electronics Letters*, 29 (1993) 1807.
[200] Zinger, B., *Synthetic Metals*, 28 (1989) C37.
[201] Pearce, T.C., Gardener, J.W., Friel, S., Bartlett, P.N., and Blair, N., *Analyst*, 118 (1993) 371.
[202] Ingleby, P. Gardner, J.W., and Bartlett, P.N., *Sensors and Actuators B*, 57 (1999) 17.
[203] Zhao, H., Price, W.E., and Wallace, G.G., *Journal of Membrane Science,* 87 (1994) 47.
[204] Yuan, C., Li, P., Shan, J., and Zhang, H., *Supramolecular Science*, 5 (1998) 751.
[205] Neaves, P.I., and Hatfield, J.V., *Sensors and Actuators B*, 26-27 (1995) 223.
[206] Mielle, P., *Trends in Food Science and Technology*, 7 (1996) 432.
[207] Skoog, D.A., Holler, F.J., and Nieman, T.A, *Principles of Instrumental Analysis 5th Ed.,* pp12-13, Harcourt Brace College Publishers, Philadelphia, 1998.
[208] Naoi, K., Lien, M., and Smyrl, W.H., *J. Electrochem. Soc.*, 138 (1991) 440.
[209] Lim, J.Y., Paik, W., and Yeo, I., *Synth. Met.*, 69 (1995) 451.
[210] Bruckenstein, S., Brzezinska, K., and Hillman, A.R., *Electrochimica Acta*, 45 (2000) 3801.
[211] Bose, C .S.C., Basak, S., Rajeshwar, K.J., *J. Phys.Chem.*, 96 (1992) 9899.
[212] Yang, H., and Kwak, J., *J. Phys. Chem. B*, 101 (1997) 4656.
[213] Petit, M.A., Plichon, V., and Colin, C., *Electrochimica Acta*, 45 (2000) 1953.
[214] Torresi, R.M., Cordoba de Torresi, S.I., Matencio, T., and De Paoli, M.-A., *Synth. Met.*, 72 (1995) 283.
[215] Truong, V.-T., Ennis, B.C., and Forsyth, M., *Polymer*, 36 (1995) 1933.

[216] Yamaura, M., Sato, K., Hagiwara, T., and Iwata, K., *Synth. Met.*, 48 (1992) 337.
[217] Xie, Q., Kuwabata, S., Yoneyama, H., *J. Electroanal. Chem.*, 420 (1997) 219.
[218] Tsai, E.W., Pajkossy, T., Rajeshwar, K., and Reynolds, J.R., *J. Phys. Chem.*, 92 (1988) 3560.
[219] Ge, H., and Wallace, G.G., *React. Polym.*, 18 (1992) 133.
[220] Mirmohseni, A., Price, W.E., and Wallace, G.G., *Journal of Membrane Science*, 100 (1995) 239.
[221] Sadik, O.A., and Wallace, G.G., *Electoranalysis*, 6 (1994) 860.
[222] Martinez, R.C., Dominguez, F.B., Gonzalez, F.M., Mendez, J.H., and Orellana, R. C., *Anal. Chim. Acta*, 279 (1993) 299.
[223] Warren, L.F., Walker, J.A., Anderson, D.P., and Rhodes, C.G., *J. Electrochem. Soc.*, 136 (1989) 2286.
[224] Gandhi, M., Spinks, G. M., Burford, R. P., and Wallace, G.G., *Polymer*, 36 (1995) 4761.
[225] Nagase, H., Wakabayashi, K., and Imanaka, T., *Sensors and Actuators B*, 13-14 (1993) 596.
[226] Serra, G., Stella, R., and De Rossi, D. *Material Science and Engineering C*, 5 (1998) 259.
[227] Guadarrama, A., Fernandez, J.A., Iniguez, M., Souto, J., and de Saja, J.A, *Analytica Chimica Acta*, 411 (2000) 193.
[228] Josowicz, M., *Analyst*, 120 (1995) 1019.
[229] Zubritsky, E., *Anal. Chem.*, June (2000) 421A.
[230] Ouellette, J., *The Industrial Physicist*, February (1999) 26.
[231] Strakova, M., Matisova, E., Simon, P., Annus, J., and Lisy, J.M., Sensors and Actuators B, 52 (1998) 274.
[232] Yano, T., Kobayashi, T., and Shimizu, S., J. Ferment. Technol., 56 (1978) 421.
[233] Stetter, J.R., and Cao, Z., *Anal. Chem.*, 62 (1990) 182.
[234] Klunder, G.L., and Russo, R.E., *Applied Spectroscopy*, 49 (1995) 379.
[235] LaPack, M.A., Tou, J.C., and Enke, C.G., *Anal.Chem.*, 62 (1990) 1265.
[236] Reynolds, G.W., Hoff, J.T., and Gillham, R.W., *Environ. Sci. Technol.*, 24 (1990) 135.
[237] Barcelona, M.J., Helfrich, J.A., and Garske, E.E., *Anal. Chem.*, 57 (1985) 460.
[238] Henis, J.M.S., and Tripodi, M.K., Science, 220 (1983) 11.
[239] Watson, J.M., and Payne, P.A., 49 (1990) 171.
[240] Genovese, V. *et al*, *Proceedings of the IEEE/RSJ International Conference on Intelligent Robots and Systems*, (1992) 1575.
[241] Flam, F., *Science*, 257 (1992) 1621.
[242] Nakamoto, T., Ishida, H., and Moriizumi, T., *Analytical Chemistry News & Features*, (1999) 531.
[243] Russell, R.A., Thiel, D., Deveza, R., and Mackay-Sim, A., *IEEE International Conference on Robotics and Automation*, (1995) 556.
[244] Consi, T.R., Grasso, F., Mountain, D., and Aterna, J., *Biol. Bull.*, 189 (1995) 231.
[245] Russell, R.A., and Kennedy, S., *Mechatronics*, 00 (2000) 1.
[246] Burkhardt, D., Schleidt, W., and Altner, H., *Signals in the Animal World*, George Allen & Unwin Ltd, London, 1967, p48.
[247] Turner, A.P.F., Ramsey, G., and Higgins, I.J.H., *Biochem. Soc. Trans.*, 11 (1983) 445.

[248] Nishikawa, S., Sakai, S., Karube, I., Matsunaga, T., and Suzuki, S., *J. Appl. Environ. Microbiol.*, 43 (1982) 814.
[249] Swain, A., Allen, M., Schneider, B.H., Taylor, F., and Turner, A.P.F., *Rapid Microbiological Methods for Foods, Beverages and Pharmaceuticals*, pp 213 - 225.
[250] Terra Nova Systems Limited, *CellSense Rapid Toxicity Assessment,* York.
[251] Hobson, N.S., Tothill, I., and Turner, A.P.F., *Biosensors & Bioelectronics*, 11 (1996) 455.
[252] Cass, A.E., Davis, G., Francis, G.D., Hill, H.A.O., Alton, W.J., Higgins, I.J., Plotkin, E.V., Scott, L.D.L., and Turner, P.F., *Anal.Chem.*, 56 (1984) 667.
[253] Guiseppi-Elie, A., Wallace, G.G., and Matsue, T, in *Handbook of Conducting Polymers 2nd Ed*, (Skothiem, T.A., Elsenbaumer, R.L., and Reynolds, J.R. eds.), Marcel Dekker, New York, 1998, pp 968 - 969.
[254] Foulds, N.C., and Lowe, C.R., *Anal.Chem.*, 60 (1988) 2473.
[255] Tallman, D.E., and Wallace, G.G., *Synth. Met.*, 90 (1997) 13.
[256] Guo, R., Barisci, J.N., Innis, P.I., Too, C.O., Wallace, G.G., and Zhou, D., *Synth. Met.*, 114 (2000) 267.
[257] Minett, A.I., Electrochemical Detection of Microorganisms using Conducting Polymers, *PhD Thesis*, 2000, University of Wollongong, Australia.
[258] Wei, X.-L., Wang, Y.Z., Long, S.M., Bobeczko, C., and Epstein, A.J., *J. Am. Chem. Soc.*, 118 (1996) 2545.
[259] Chan, H.S.O., Neuendorf, A.J., Siu-Choon, N., Wong, P.M., and Young, D.J., *Chem. Commun.*, 13 (1998) 1327.
[260] Fan, J., Wan, M., and Zhu, D., *Solid State Commun.*, 110 (1999) 57.
[261] Planes, G.A., Morales, G.M., Miras, M.C., and Barbero, C., *Synth. Met.*, 97 (1998) 223.
[262] Nekrasov, A., Ivanov, V.F., and Vannikov, A.V., *J. Electroanal. Chem.*, 482 (2000) 11.
[263] Kulszewicz-Bayer, I., Wielgus, I., Pron, A., and Rannou, P., *Macromolecules*, 30 (1997) 7091.
[264] Prevost, V., Petit, A., and Pla, F., *Synth. Met.*, 104 (1999) 79.
[265] Zotti, G., Martina, S., Wegner, G., and Schluter, A-D., *Adv. Mater.*, 4 (1992) 798.
[266] Wei, Y., Yang, C., Wei. G., and Feng, G., *Synth. Met.*, 84 (1997) 289.